JOURNAL OF ENERGY IN SOUTHERN AFRICA

Volume 25 Number 4 • November 2014

CONTENTS

The sensitivity of the South African industrial sector's electricity consumption to electricity price fluctuations

Roula Inglesi-Lotz
Department of Economics, University of Pretoria, Pretoria, South Africa

Abstract
Numerous studies assume that the price elasticity of electricity demand remains constant through the years. This, in turn, means that these studies assume that industrial consumers react in the same way to price fluctuations regardless of the actual price level. This paper proposes that the price elasticity of industrial electricity demand varies over time. The Kalman filter methodology is employed in an effort to provide policy-makers with more information on the behaviour of the industrial sector with regards to electricity price changes, focusing on the period 1970 to 2007. Other factors affecting electricity consumption, such as real output and employment, are also captured. The findings of this paper show that price sensitivity has changed since the 1970s. It has decreased in absolute values from -1 in 1980 to -0.953 in 1990 and then stabilised at approximately -0.95 which indicates that the industrial sector has experienced an inelastic demand. In other words, the behaviour of industrial consumers did not vary significantly during the 2000s. In the long run and as the prices increase, probably reaching the levels of the 1970s or even before, the industrial sector's behaviour might change and the elasticity might end up at levels higher than one (elastic).

Keywords: electricity consumption; Kalman filter; price elasticity; industrial sector

1. Introduction

In South Africa, choosing the correct and appropriate electricity price regime has been under discussion during the last decade. During March 2012, the National Energy Regulator South Africa (NERSA) re-evaluated and reduced the agreed rate of increase of the electricity price for 2012. Eskom has also expressed its intentions for further application on price rises for two main reasons: first, Eskom argues that the current prices are not cost-reflective, and second, its capacity expansion plans include investing in two new power plants that will increase the company's operating costs. Before the next electricity price restructure, it is imperative for policy-makers to understand, and in a way, 'predict' the reactions of consumers to price changes. Even more important, the national electricity consumption trends do not necessarily represent each sector's individual behaviour. Different price structures as well as different electricity profiles are the main reasons why different economic sectors should be examined separately and treated accordingly.

Energy (and more specifically electricity) plays an essential role in the production capacity of a country. It is a crucial role, specifically for the manufacturing sector where energy is considered an irreplaceable input. In South Africa, the industrial sector is responsible for an average of 47% of the total electricity consumption (DoE, 2009), which makes this sector one of the most important ones from an energy consumption point of view. Ziramba (2009) studied the energy consumption of the industrial sector in South Africa and its interaction with other variables such as industrial output and employment (but not electricity prices). More recently, Inglesi-Lotz and Blignaut (2011a) found that, among various economic sectors such as agriculture and transport, the industrial sector was the only one whose electricity consumption behaviour is sensitive to price fluctuations during the period 1993 to 2006.

Following Inglesi-Lotz (2011), this paper proposes that the sensitivity of the industrial sector's electricity consumption to price fluctuations (price elasticity) has been changing through the years. As Inglesi-Lotz (2011) also points out, 'focus on variation is more important than only examining the level of change' – especially for the South African case after the price restructuring of 2009/10. The fluctuations are so drastic that one has to take into account changes in behaviour. Thus, the purpose of

this paper is to estimate the time-varying sensitivity of the industrial sector's electricity consumption to price changes, using the Kalman filter econometric methodology for the period 1970 to 2007. (See Section 3 for a discussion on the reasons for the selection of the time period).

This paper combines and extends the results by Inglesi-Lotz (2011) and Inglesi-Lotz and Blignaut (2011a) in an effort to provide policy-makers with more information on the behaviour of the industrial sector with regards to electricity price changes. The findings will assist regulators and policy-makers in future decisions on price changes, a topic extremely relevant and crucial to the current South African case.

This paper is structured as follows: Section 2 provides a brief overview of studies that deal with the industrial sector's energy or electricity consumption, as well as a summary of the South African studies that deal with electricity prices and their effect on the economy either in its entirety or specific sectors. Section 3 presents the methodology and the data used. Section 4 presents the empirical results, and Section 5 summarises the findings and concludes by discussing some possible policy implications.

2. Literature review

During the last few decades, literature has paid special attention to price elasticities of energy demand. A possible reason for this is concerns regarding the environmental effects of the rising energy demand internationally, and the ever-increasing need to find appropriate instruments (if existing) to control it. The industrial sector, specifically, attracted more attention since it currently consumes approximately 37% of the world's total delivered energy (Abdelaziz *et al*., 2011).

Many studies have been conducted on the energy (electricity) demand of the industrial sectors in various countries within different geographical regions and with different economic backgrounds. These studies also use numerous methods. Different variables are used as factors other than prices affecting the demand depending on the specific region and the time period. But all-in-all, the major determinants of the industrial sector's energy (electricity) demand in the majority of the studies are output, price of electricity and employment (Al-Ghandoor *et al*., 2008; Jamil & Ahmad, 2011).

Table 1 presents a summary of international and local studies and their findings (in chronological order) that deal with the industrial energy (electricity) demand. This collection of studies, although by no means exhaustive of the literature, is indicative of the focus on a variety of countries (developed and developing) for different time periods. A variety of numerical estimations of the price elasticity, depending on the country and more importantly the period of the sample, is also observed.

For South Africa, only one study that sheds some light on the reaction of the industrial sector (among others) to the changes of prices is identified (Inglesi-Lotz & Blignaut, 2011a). Ziramba (2009) also studies the industrial sector's electricity demand reactions but excluded price from the factors affecting it. Another recent study by Inglesi-Lotz and Blignaut (2011b) looks at the different economic sectors and the factors that affect their increasing electricity consumption. However, due the nature of the method used (decomposition techniques), the effects of price fluctuations were not studied. Other studies also look at electricity demand trends in South Africa (Odhiambo, 2009; Amusa *et al.,* 2010; Inglesi, 2010; Inglesi-Lotz, 2011) but focus on the aggregate demand of the

Table 1: Summary of selected international and local studies on price elasticity of energy (electricity) demand in the industrial sector

Authors	*Country/region*	*Sector*	*Price elasticity*
Pindcyck (1979)	Group of countries	Industrial & commercial	-0.07 to -0.16
Lynk (1989)	UK	Industrial	-0.69
Caloghirou *et al.* (1997)	Greece	Industrial	-0.90
Beenstock *et al*. (1999)	Israel	Industrial	0.123
Hunt *et al*. (2003)	UK	Manufacturing	-0.20
or 0.16 to 0.323			
Kamerschen & Porter (2004)	Oman	Industrial	-0.34 to -0.55
Dimitropoulos *et al. (*2005)	UK	Manufacturing	-0.159
Roy *et al.* (2006)	Country panel	Industrial	-0.80 to -1.76
Enevoldsen *et al*. (2007)	Denmark, Norway and Sweden	Industrial	-0.35 to -0.44
Agnolucci (2007)	UK	Industrial	-0.60
Agnolucci (2009)	UK and Germany	Industrial	-0.64
Inglesi-Lotz and Blignaut (2011a)	South Africa	Industrial	-0.869
He *et al.* (2011)	China	Industrial & commercial	-0.018

economy. Furthermore, Ziramba (2009) finds that price was an insignificant factor for the residential demand of electricity in South Africa for the period 1978–2005.

3. Methodology and data

3.1 Econometric method

Econometric methods used in the analysis of energy vary in complexity from simple to relatively complicated and have been applied to temporal, spatial and sectoral data (Greening *et al*., 2007). More specifically, co-integration techniques have been used internationally (Engle & Granger, 1987; Johansen, 1991; Hendry and Juselius, 2000; Hendry and Juselius, 2001) and locally (Inglesi, 2010) to estimate the determinants of energy and electricity consumption. However, the common constraint in all these studies is the assumption that the relationship between electricity prices and consumption has remained constant through the years. Consequently, to take this a step further, Inglesi-Lotz (2011) employs the Kalman filter technique and proposes that price elasticity has evolved during the years and should not be treated as stable. Therefore, an average elasticity through the years is not assumed and different behaviour from electricity consumers under various price regimes and during various time periods is shown with this method.

It is therefore important to test for the general stability of parameters before selecting the Kalman filter as the method of preference. To test the stability of parameters, Hansen (1992) proposes a version of past approaches to cover general models with stochastic and deterministic trends. In this paper, this test is used to statistically confirm or reject the assumption of time-varying price elasticity before proceeding with the estimation.

There are two main types of models that can be represented by the Kalman filter: a) unobservable components models; and b) time-varying parameter models (Cuthbertson *et al.,* 1992). In this study, the state-space model is applied with stochastically time-varying parameters to a linear regression in which coefficients representing elasticities are allowed to change over time.

Firstly,[1] the formal representation of a dynamic system written in state-space form suitable for the Kalman filter should be described. The following system of equations presents the state-space model of the dynamics of a n x 1 vector, y_t.

Observation (or measurement) equation:

$$y_t = Ax_t + H\xi_t + w_t \quad (1)$$

State (or transition) equation:

$$\xi_{t+1} = F\xi_t + \upsilon_{t+1} \quad (2)$$

where A, H and F are matrices of parameters of dimension (n x k), (n x r), (r x r), respectively, and x_t is a (k x 1) vector of exogenous or predetermined variables. ξ_t is a (r x 1) vector of possibly unobserved state variables, known as the state vector.

In the observation equation, the factor x_t is considered to be predetermined or exogenous which does not provide information about ξ_{t+s} or w_{t+s} for s = 0,1,2,… beyond what is given by the sequence $y_{t-1}, y_{t-2},\ldots,y_1$. Thus, x_t could include lagged values of y or variables which are uncorrelated with ξ_T and w_T for all T.

The overall system of equations is used to explain a finite series of observations $\{y_1, y_2,\ldots,y_T\}$ for which assumptions about the initial value of the state vector ξ_t are needed. With the assumption that the parameter matrices (F, Q, A, H or R) are functions of time, then the state-space representation (equations (1) and (2)) become:

$$y_t = a(x_t) + [H(x_t)]' \xi_t + w_t \quad (3)$$

$$\xi_{t+1} = F(x_t)\xi_t + \upsilon_{t+1} \quad (4)$$

Where F(xt) is a (r x r) matrix whose elements are functions of x_t; $a(x_t)$is a (n x 1) vector-valued function; and $H(x_t)$ is a (r x n) matrix –valued function.

Equations (3) and (4) allow for stochastically varying parameters, but are more restrictive in the sense that a Gaussian distribution is assumed.

With regards to the specific application to the electricity model of this paper, the dependent variable is the electricity consumption of the industrial sector (cons) while standard variables used in the international and local literature (Ziramba, 2009; Inglesi, 2010; Nakajima & Hamori, 2010; Dilaver & Hunt, 2010) are considered as independent: price of electricity (p), real output of the industrial sector (y) and employment (n). All the variables are in natural log denoted by l.

$$lcons = a_0 + a_1 l_p + a_2 ly + a_3 ln + \varepsilon_t \quad (5)$$

In equation (5), all the parameters α are considered constant over time. However, after using the Hansen (1992) test, they will either be identified as time-varying or remain constant. An indication of this will be given even before the statistical test by the graphical representation of the data. The time-varying parameters will then also have a suffix t to denote the fluctuations over time to be estimated.

3.2 Data

Local sources of data were primarily used for this exercise. Average electricity consumption is derived from the following different sources: *South African Energy Statistics 1950–1989* by the National Energy Council (NEC, 1990) for 1970–1989 and the *Aggregate Energy Balances* by the Department of Energy (DoE, various issues). The series for average nominal prices of electricity for the industrial

sector is obtained from the *Energy Price Report 2009* also by the Department of Energy (DoE, 2009). Finally, the data series for the real economic output and employment of the industrial sector is obtained from the *Quantec databases* (Quantec, n.d.). The economic output figures are presented in real terms with 2005 being the base year. In order to transform, the nominal prices of electricity into constant with 2005 base year, the Consumer Price Index (CPI) figures from *StatsSA* is employed.

The electricity consumption was measured in kWh; the electricity prices (after the transformation) in South African Rand (ZAR) cents/ kWh (constant prices 2005); the economic output of the industrial sector in ZAR (constant prices 2005) and the employment in absolute number of employees.

Table 2 summarises the descriptive statistics of all the variables (in their linearised version) used in the analysis. These primary statistics are only presented as an indication of the nature of the raw data.

Figure 1 illustrates electricity consumption and prices as well as the real economic output and employment of the South African industrial sector for the period 1970–2008. The industrial economic output and its electricity consumption showed an upward trend for the entire period examined. This trend became more intense during the 1990s, when the sanctions against South Africa were lifted and the country's trade opened to the rest of the world. Since then the real economic production of the country rose with increasing rates to match the rising electricity consumption of the sector.

Employment showed a general upward trend until the end of approximately the 1980s and then its variation relatively stabilised until the end of the sample. This can be attributed to the industrialisation of the economy. It can be argued that the growth of the industrial sector during this period led to the substitution of labour with capital, especially after opening to international markets and gaining opportunities to import capital infrastructure and know-how. Although this was indeed a reality, the labour market also opened to all previously disadvantaged South Africans and, consequently, more employment opportunities were available. The lower labour costs of unskilled or semi-skilled workers also played a role in the higher number of people employed. From the graphical representation of employment in the industrial sector, it can be assumed that these two factors drove employment in opposite directions and, especially for the period 1985 to the beginning of 2000s, the range of employment change was relatively marginal (2.4–2.8 million). Overall, the increasing trend matches the trend of the output of the industrial sector and the electricity consumed.

Electricity prices increased drastically during the first half of the 1970s, reaching a peak in the beginning of the 1980s. However, prices started declining rapidly from the 1980s until the 2000s. Looking at the steep increase in prices from 1975 to 1976, it was decided to proceed with an estimation excluding the first five years of the sample and only start from 1976. Also, data for most of the variables is available until 2010/11; however, the latest information on sectoral electricity consumption from the *Energy Balances* was released in 2009 and on prices for 2008/09. Usually, the latest reports of energy data are re-evaluated as soon as more information becomes available and hence, the latest most accurate year of energy data is 2007. Also, the international crisis affected the output of the economy after 2008/09 and the decision was made to

Table 2: Data descriptive statistics

Source: DoE (various issues), DoE (2009), Quantec (n.d.)

Variable	*Electricity consumption of the industrial sector*	*Average electricity price of industrial sector*	*Real economic output of industrial sector*	*Employment of the industrial sector*
Unit of measurement	*kWh (in natural log)*	*ZAR cents per kWh (in natural log)*	*ZAR (in natural log)*	*Number (in natural log)*
Mean	24.38	2.92	34.20	14.64
Median	24.46	2.85	34.18	14.69
Maximum	25.34	3.28	34.86	14.81
Minimum	23.16	2.61	33.64	14.21
Std. dev.	0.59	0.22	0.33	0.15
Skewness	-0.31	0.21	0.29	-1.17
Kurtosis	2.22	1.60	2.41	3.60
Jarque-Bera	1.55	3.41	1.10	9.20
Probability	0.46	0.18	0.58	0.01
Sum	926.36	110.83	1299.68	556.28
Sum sq.dev.	12.91	1.86	3.91	0.88
Observations	38	38	38	38

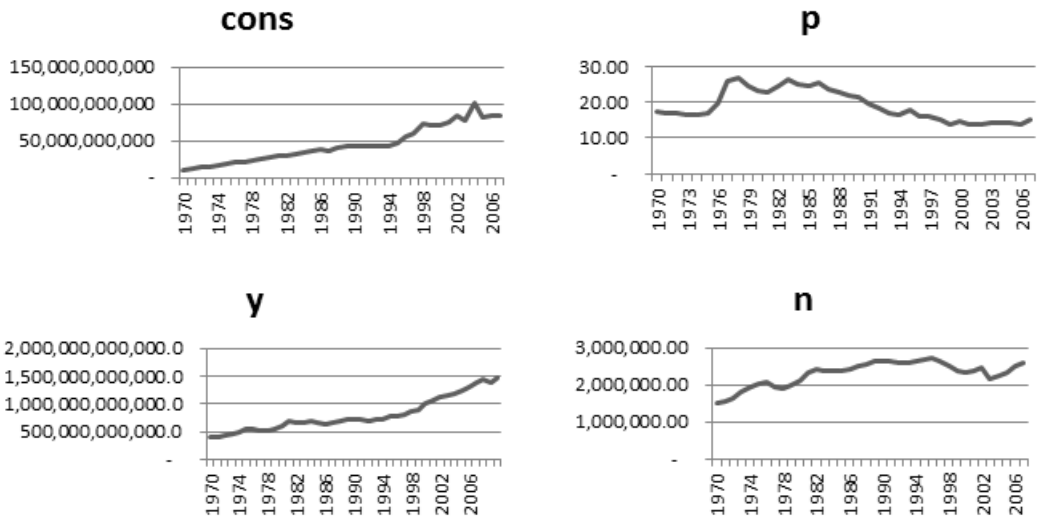

Note: Electricity consumption (cons) is measured in kWh; employment (n) in numbers; electricity prices (p) in ZAR cents /kWh; and real output (y) in ZAR.

Figure 1: Electricity consumption (cons), employment (n), electricity prices (p) and eeal output (y) of the South African industrial sector (1970–2007)
Source: DoE (various issues), DoE (2009), Quantec databases (n.d.)

exclude the years after 2008 from the estimated sample. In the future, when information becomes available for the years after the crisis, this period can be treated as a structural break in any economic analysis of data.

From Figure 1, it can also be observed that the overall real output and employment both had a constant positive correlation with electricity consumption; while the price variation is more intense over the years and might show a more changeable relationship with electricity consumption on an annual basis. These observations might be an indication of the *a priori* expectations of the Hansen test results.

4. Empirical results

As discussed in Section 3, before proceeding with the estimation using the Kalman filter, the Hansen test is performed to either confirm or reject the parameter instability. From the graphical representation of the data, a more stable coefficient is expected for output and employment while the relationship between price and consumption of electricity is expected to vary over the years, represented in an unstable parameter. The null hypothesis of the Hansen test is parameter stability and an Lc statistic is used (Lagrange Multiplier tests family). If even one of the coefficients is confirmed statistically to be unstable, the Kalman filter will produce better results than a least squares estimation.

Table 3 presents the results of the Hansen test. The test statistic for output and employment is 0.192 with p-value higher than 0.2. Because the p-value is greater than the 10% level of significance, the null hypothesis of parameter stability cannot be rejected. Hence, the parameters for output and employment are found to be constant. The results of the Hansen test for the price coefficient indicated the test statistic is 0.4 and its p-value is 0.077. Since the p-value is less than the 10% level of significance, the null hypothesis of the test can be rejected. The conclusion is that the price coefficient is not constant through the years. Overall, based on the Hansen test results, the coefficients for output and employment should be considered as constant while the coefficient for price should be considered as time-varying in the Kalman filter estimation.

Table 3: Hansen test results for parameter stability

	Lc statistic	*p-value*	*Conclusion*
ly, ln	0.192	>0.2	The null hypothesis (H_0: parameter stability) cannot be rejected **The parameters are constant**
lp	0.400	0.077	The null hypothesis (H_0: parameter stability) can be rejected **Parameter is not constant**

Note: ly denotes the natural logarithm of real output (y); ln denotes the natural logarithm of employment (n); and lp denotes the natural logarithm of electricity prices (p)

Table 4 presents the Kalman filter estimation results, and c(1) and c(2) (constant coefficients) show the output and employment coefficients respectively, while c(3) is the constant parameter of the equation. The coefficients are both positive and statistically significant: any positive change in the output or employment will result in an increase in electricity consumption.

Table 4: Kalman filter estimation results

Space model		
	Sample	*1976-2007**
	Included observations	32
	Number of iterations to convergence	9
Variables	*Estimated coefficients*	*p-values*
c(1) (output coefficient)	0.690	0.000
c(2) (employment coefficient)	0.252	0.061
c(3)	-4.065	0.000
	Final state	*p-values*
sv1 (price coefficient)	-0.952	0.000
Goodness of fit		
Log likelihood	8.502	
Akaike info criterion	-0.344	
Schwarz criterion	-0.206	
Hannan-Quinn criterion	-0.298	

* As can be seen, the sample was reduced to start from 1976 and not 1970. This was needed due to the fact that the sharp increase in the beginning of the 1970s might be due to a structural break or an anomaly of the data. Hence, the focus of the analysis is from the middle of 1970s.

Sv1 is the average of the price elasticity over the period 1976–2007 and it is negative as expected. (Law of demand: the higher the price of a good, the lower the quantity consumed of the good). Overall it is statistically significant with a p-value of zero. Both output and price coefficients are very close to the average coefficients reported in Inglesi-Lotz and Blignaut (2011) for the industrial sector. The price coefficient for the examined period (1993–2006) was -0.869 (here, -0.952) and the output elasticity was 0.712 (here, 0.690).

Figure 2 illustrates the evolution of price elasticity. In the beginning of 1980s, price elasticity of electricity demand was close to unit elastic. Since then, it has decreased in absolute values from -1 in 1980 to -0.953 in 1990. Thereafter, the elasticity stabilised at approximately -0.95 indicating that the industrial sector has experienced an inelastic demand. In other words, the behaviour of the industrial consumers did not vary significantly during the 2000s. That might explain why, in some studies, researchers assume that price has not played a significant role in the fluctuations of electricity consumption in the industrial sector and therefore not include prices in the estimations, for example, Ziramba (2009).

This result also confirms the main conclusion of Inglesi-Lotz (2011) that the sensitivity of consumers to price fluctuations became smaller in absolute terms, while the real prices of electricity declined over the last half of the sample examined. It can be seen in Figure 3 that, from 1977 until the beginning of 1990s, the electricity prices decreased in real terms and the price elasticity became lower in absolute terms. However, from the 1990s until the end of the sample period, prices stabilised at much lower rates than in the 1970s and 1980s, and the sensitivity of the consumers did not change drastically.

5. Conclusion

As the main electricity user, the industrial sector of South African plays an important role in the path of electricity consumption. Knowing and understand-

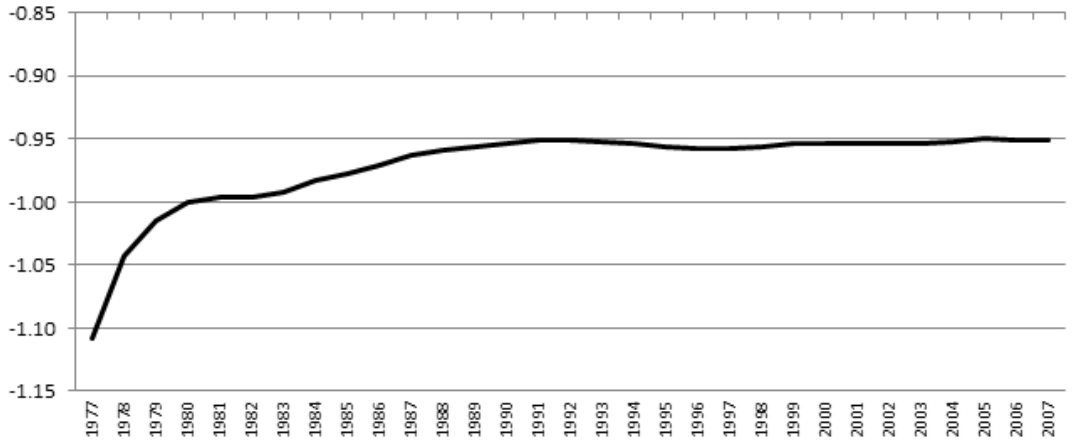

Figure 2: Estimated price elasticity from 1976 to 2007

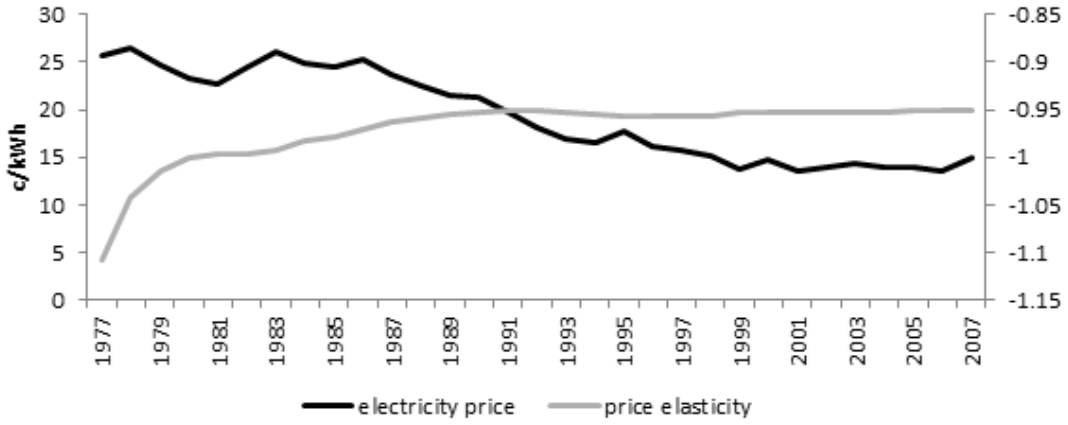

Figure 3: Electricity prices and estimated price elasticity for the industrial sector 1977–2007

ing the behaviour of this sector regarding electricity consumption will assist policy-makers in implementing appropriate policies. The sector's electricity performance has recently attracted attention. Ziramba (2009) studied the energy consumption of the industrial sector in South Africa and its interaction with other variables such as industrial output and employment (but not electricity prices). Later, Inglesi-Lotz and Blignaut (2011a) using panel data techniques, found that the industrial sector's electricity consumption was sensitive to price and output fluctuations on average during the period 1993 to 2006.

Most studies assume that the price elasticity of electricity demand remains constant through the years, that is industrial consumers behave the same way to price fluctuations regardless the economy's conditions or the actual level of prices. In South Africa, electricity prices have been low for a long period of time, which means that the economy as a whole did not react to price changes (Inglesi-Lotz, 2011). This paper follows Inglesi-Lotz (2011), who did an analysis for economy-wide electricity consumption, and uses the Kalman filter methodology to allow the price elasticity of industrial electricity demand to be time-varying. To capture other factors affecting electricity consumption, real output and employment are also included in the specification.

The findings show that price sensitivity has indeed changed since the 1970s: it has decreased in absolute values from -1 in 1980 to -0.953 in 1990. The elasticity stabilised at approximately -0.95 showing that the industrial sector has experienced an inelastic demand. In other words, the behaviour of industrial consumers did not vary significantly during the 2000s. This also confirms the main conclusion of Inglesi-Lotz (2011) that sensitivity of consumers to price fluctuations becomes smaller in absolute terms, while the real prices of electricity declined over the last half of the sample period. In addition, both papers show that the price elasticity of the electricity demand in the industrial sector or the economy as a whole has remained relatively constant, while prices were not fluctuating significantly. In other words, the sensitivity and behaviour of the consumers had remained unchanged; however, as soon as prices start varying it should be expected that the consumer's reaction to these changes will also alter.

These results also enable policy-makers to speculate about the effect of further electricity price increases planned by Eskom and NERSA for the next couple of years. An immediate change in the industrial sector's behaviour with the increase of prices should not be expected. However, in the long run and as the prices increase, probably reaching the levels of the 1970s or even before, the industrial sector's behaviour might change and the elasticity might end up at levels higher than one (elastic).

Note

1. The detailed discussion on the Kalman filter methodology is adopted directly from Inglesi-Lotz (2011).

Acknowledgements

The author wishes to extend her gratitude to participants of the South African Energy Regulators Conference for their valuable comments and suggestions.

References

Abdelaziz, E.A., Saidur, R. and Mekhilef, S. (2011). A review of energy saving strategies in industrial sector. *Renewable and Sustainable Energy Reviews*, 15, 150–168.

Agnolucci, P. (2007). Non-transport energy consumption in the UK: a comparison of alternative approaches, mimeo. Cambridge: University of Cambridge.

Agnolucci, P. (2009). The energy demand in the British and German industrial sectors: Heterogeneity and common factors. *Energy Economics*, 31, 175–187.

Al-Ghandoor, A., Al-Hinti, I. and Sawalha, S.A. (2008). Electricity consumption and associated GHG emissions of the Jordanian industrial sector: empirical analysis and future projection. *Energy Policy*, 36, 258–267.

Amusa, H., Amusa, K. and Mabugu, R. (2009). Aggregate demand for electricity in South Africa: an analysis using the bounds testing approach to cointegration. *Energy Policy*, 37, 4167–4175.

Beenstock, M., Goldin, E. and Nabot, D. (1999). The demand for electricity in Israel. *Energy Economics*, 21, 168–183.

Caloghirou, Y.D., Mourelatos, A.G. and Thompson, H. (1997). Industrial energy substitution during the 1980s in the Greek economy. *Energy economics*, 19, 476–491.

Cuthbertson, K., Hall, S. and Taylor, M.P. (1992). Applied Econometric Techniques. New York: Harvester Wheatsheaf.

Department of Energy (DoE) (2009). Energy Price Report 2009. Pretoria: Department of Energy.

Department of Energy (DoE). Various issues. Aggregate energy balances. Pretoria: Department of Energy.

Dilaver, Z. and Hunt, L.C. (2010). Industrial electricity demand for Turkey: a structural time series analysis. *Energy Economics*, 33, 426–436.

Dimitropoulos, J., Hunt, L.C. and Judge, G. (2005). Estimating underlying energy demand trends using UK annual data. *Applied Economic Letters*, 12, 239–244.

Enevoldsen, M.K., Ryelund, A.V. and Andersen, M.S. (2007). Decoupling of industrial energy consumption and CO_2 emissions in energy intensive industries in Scandinavia. *Energy Economics*, 29, 665–692.

Engle, R.F. and Granger, C.W.J. (1987). Co-integration and error correction: representation estimation and testing. *Econometrica*, 55, 251–267.

Greening, L.A., Boyd, G. and Roop, J.M. (2007). Modelling of industrial energy consumption: An introduction and context. *Energy Economics*, 29, 599–608.

Hansen, B.E. (1992). Tests for parameter instability in regressions with I(1) processes. *Journal of Business and Economic Statistics*, 10, 321–335.

He, Y.X., Yang, L.F., He, H.Y., Luo, T. and Wang, Y.J. (2011). Electricity demand price elasticity in China based on computable general equilibrium model analysis. *Energy*, 36, 1115–1123.

Hendry, D. and Juselius, K. (2000). Explaining cointegration analysis: part I. *Energy Journal*, 21, 1–42.

Hendry, D. and Juselius, K. (2001). Explaining cointegration analysis: part II. *Energy Journal,* 22, 75–120.

Hunt, L.C., Judge, G. and Ninomiya, Y. (2003). Underlying trends and seasonality in UK energy demand: a sectoral analysis. *Energy Economics*, 25, 93–118.

Inglesi, R. (2010). Aggregate electricity demand in South Africa: conditional forecasts to 2030. *Applied Energy*, 87, 197–204.

Inglesi-Lotz, R. (2011). The evolution of price elasticity of electricity demand in South Africa: A Kalman filter application. *Energy Policy*, 39, 3690–3696.

Inglesi-Lotz, R. and Blignaut, J.N. (2011a). Estimating the price elasticity of demand for electricity by sector in South Africa. *South African Journal of Economic and Management Sciences*, 14, 449–465.

Inglesi-Lotz, R. and Blignaut, J.N. (2011b). South Africa's electricity consumption: A sectoral decomposition analysis. *Applied Energy*, 88, 4779–4784.

Jamil, F. and Ahmad, E. (2011). Income and price elasticities of electricity demand: Aggregate and sectorwise analyses. *Energy Policy*, 39, 5519–5527.

Johansen, S. (1991). Estimation and hypothesis testing of cointegration vectors in gaussian vector autoregressive models. *Econometrica*, 59, 1551–1580.

Kamerschen, D.R. and Porter, D.V. (2004). The demand for residential, industrial and total electricity, 1973-1998. *Energy Economics*, 26, 87–100.

Lynk, E.L. (1989). The demand for energy by UK manufacturing industry. Manchester School of Economic and Social studies, 57, 1–16.

Nakajima, T. and Hamori, S. (2010). Change in consumer sensitivity to electricity prices in response to retail deregulation: a panel empirical analysis of the residential demand for electricity in the United States. *Energy Policy*, 38, 2470–2476.

National Energy Council (NEC). (1990). South African Energy Statistics 1950–1989. Pretoria: National Energy Council.

Odhiambo, N.M. (2009). Electricity consumption and economic growth in South Africa: A trivariate causality test. *Energy Economics*, 31, 635–640.

Pindcyck, R. (1979). Interfuel Substitution and the Industrial Demand for Energy: An International Comparison. *Review of Economics & Statistics*, 61, 169–179.

Quantec. n.d. Quantec databases. Pretoria: Quantec.

Roy, J., Sanstad, A.H., Sathaye, J.A. and Khadariia, R. (2006). Substitution and price elasticity estimates using inter pooled data in a translog cost model. *Energy economics*, 28, 706–719.

Ziramba, E. (2009). Disaggregate energy consumption and industrial production in South Africa. *Energy Policy*, 37, 2214–2220.

Appendix on following page

Appendix: Data

Source	*NEC (1990) and DoE (various issues)*	*DoE (2009)*	*Quantec (n.d)*	*Quantec (n.d)*
Variable	*Electricity consumption of the industrial sector*	*Average electricity price of industrial sector (2005=100)*	*Real economic output of industrial sector*	*Employment*
Unit of measurement	*kWh*	*ZAR cents per kWh*	*ZAR*	*Number*
1970	11,437,198,074.4	17.5	407,579,700,000.0	1,490,016.0
1971	12,351,060,507.8	17.0	409,910,300,000.0	1,569,278.7
1972	14,076,379,729.7	16.8	430,142,100,000.0	1,654,393.4
1973	15,928,682,563.9	16.4	469,797,200,000.0	1,799,111.2
1974	17,385,874,576.1	16.3	487,468,600,000.0	1,953,699.5
1975	19,396,045,044.7	16.6	538,344,400,000.0	2,047,988.8
1976	21,180,655,751.3	19.3	537,548,800,000.0	2,062,257.5
1977	21,735,630,111.7	25.6	508,994,900,000.0	1,955,811.7
1978	22,948,799,150.3	26.5	522,236,600,000.0	1,912,488.0
1979	25,846,573,660.7	24.6	537,636,500,000.0	1,969,115.9
1980	28,240,586,781.3	23.2	597,951,700,000.0	2,132,894.4
1981	30,618,678,400.9	22.6	683,286,300,000.0	2,321,714.9
1982	30,827,067,618.8	24.5	656,502,300,000.0	2,415,166.6
1983	32,709,323,916.2	26.1	661,211,800,000.0	2,380,162.2
1984	34,338,415,810.2	24.9	691,218,700,000.0	2,396,527.3
1985	36,290,778,094.6	24.5	654,709,600,000.0	2,382,966.0
1986	38,207,712,371.6	25.2	629,326,800,000.0	2,411,862.4
1987	37,406,124,690.1	23.6	649,062,900,000.0	2,489,743.5
1988	40,851,349,812.2	22.5	686,182,900,000.0	2,568,084.0
1989	43,070,289,785.9	21.6	707,251,100,000.0	2,622,583.1
1990	43,222,941,451.0	21.4	725,978,600,000.0	2,644,664.0
1991	43,375,593,116.0	19.7	711,345,700,000.0	2,616,287.3
1992	43,528,244,781.0	18.2	702,482,500,000.0	2,587,787.4
1993	43,680,896,446.0	16.9	709,118,900,000.0	2,596,795.6
1994	43,013,872,000.0	16.6	728,422,800,000.0	2,630,996.0
1995	47,481,281,000.0	17.8	775,522,300,000.0	2,681,508.1
1996	55,072,548,370.0	16.1	788,989,500,000.0	2,705,824.5
1997	61,069,678,450.0	15.8	810,489,000,000.0	2,644,922.1
1998	72,663,627,000.0	15.1	851,319,600,000.0	2,516,819.6
1999	70,796,010,000.0	13.8	892,966,300,000.0	2,388,759.2
2000	70,664,869,000.0	14.8	1,007,855,400,000.0	2,326,731.6
2001	74,778,010,000.0	13.5	1,060,504,200,000.0	2,371,413.0
2002	83,581,150,000.0	13.9	1,116,408,000,000.0	2,467,226.9
2003	78,795,790,000.0	14.4	1,140,144,000,000.0	2,174,423.9
2004	101,557,231,000.0	14.0	1,190,726,000,000.0	2,231,433.1
2005	81,521,448,000.0	14.0	1,242,088,500,000.0	2,316,355.4
2006	85,127,404,000.0	13.6	1,309,430,400,000.0	2,500,722.6
2007	83,457,753,781.3	14.9	1,378,976,000,000.0	2,584,890.4

Received 23 July 2013; revised 10 September 2014

ANN-based evaluation of wind power generation: A case study in Kutahya, Turkey

Mustafa Arif Özgür
Department of Mechanical Engineering, Engineering Faculty, Dumlupinar University, Kutahya, Turkey

Abstract
Wind energy is one of the most signi□cant and rapidly developing renewable energy sources in the world and it provides a clean energy resource, which is a promising alternative in the short term in Turkey. The wind energy potential in various parts of Turkey is becoming economical due to reductions in wind turbine costs, and in fossil fuel atmospheric pollution. This paper is to present, in brief, wind potential in Turkey and to perform an investigation on the wind energy potential of the Kutahya region. A wind measurement station was established at Dumlupinar University Main Campus in order to □gure out the wind energy potential in the province. This study analyses the electricity generation capacity of the Kutahya region, Turkey, which uses the wind power system. In the study, the wind data collected from wind measurement stations between July 2001 and June 2004 (36 months) were evaluated to determine the energy potential of the region. Using this energy potential value, the power generation capacity of Kutahya was investigated for 17 different wind turbines. In this analysis, an ANN-based model and Weibull and Rayleigh distribution models were used to determine the power generation. In the ANN model, different feed-forward back propagation learning algorithms, namely Pola-Ribiere Conjugate Gradient, Levenberg–Marquardt and Scaled Conjugate Gradient were applied. The best appropriate model was determined as Levenberg–Marquardt with 15 neurons in a single hidden layer. Using the best ANN topology, it was determined that all the turbines were profitable except turbine type 1. The system with the turbine type 3 was decisively the most profitable case as determined at the end of the study according to Net Present Value concept.

Keywords: Levenberg–Marquardt; Net Present Value; Pola-Ribiere Conjugate Gradient; Rayleigh distribution; Scaled Conjugate Gradient; Weibull distribution

1. Introduction

The most important issue of today is to use natural energy sources in an efficient way which will not pollute the environment. The energy producers have an obligation to solve the environmental problems caused while producing energy for humanity's need today as well as tomorrow. There is a relation between energy and the environment. Environmental pollution increases with energy production and consumption; therefore, both the subjects must be handled together. In this regard, energy resources are necessary to be evaluated in terms of reserves, geographic distribution, production rates, pricing stability, business conditions, source credibility, and environmental interaction. Under these conditions, a sustainable and environmentally clean use of energy sources is urgently needed.

The wind potential assessment of a site requires the knowledge of the distribution law of the wind speed measured on the site. The statistical treatment of these measurements makes it possible to have a discrete distribution law. However, to obtain a more accurate analysis of the wind potential, a continuous distribution law is essential. For this purpose, the Weibull and Rayleigh models are often used (Thiaw, 2010). Previous studies have proven that the Weibull distribution function has its merits in wind resource assessment due to its great flexibility and simplicity, but particularly, it has been found to fit a wide collection of recorded wind data (Ulgen and Hepbasli, 2002; Dorvlo, 2002; Karsli and Gecit, 2003; Sulaiman *et al.,* 2002; Celik, 2004; Keyhani *et al.,* 2010; Arslan, 2010; Ouammi *et al*., 2010; Ozgur and Kose, 2006; Jaramillo and Borja, 2004; Chang *et al.,* 2003).

Wind energy potential is not easily estimated because, contrary to solar energy, it depends on the site characteristics and topography to a large degree, as wind speeds are influenced strongly by local topographical features. The classification and characterization of an area as having high- or low-wind potential requires significant effort, as wind

speed and direction present extreme transitions at most sites and demand a detailed study of spatial and temporal variations of wind speed values. Before determining the wind farm site, the hourly and monthly mean wind speed, wind speed distributions as well as the wind power densities should be analysed carefully (Keyhani *et al.,* 2010).

In the literature, several studies dealing with artificial neural networks (ANNs) are available. One such example is the work of Dombaycı and Gölcü (2009). They developed an ANN model to predict the ambient temperature for Denizli, another city in Turkey. The results show that the ANN approach is a reliable model for ambient temperature prediction. Kalogirou *et al.* (1999) programmed an ANN to learn to predict the performance of a thermosiphon solar domestic water heating system. An ANN was conditioned to use performance data for four types of systems, all employing the same collector panel under varying weather conditions. Li and Shi (2010) investigated three different ANNs namely adaptive linear element, back propagation, and radial basis function to predict wind speeds. The results show that even for the same wind data set, no single neural network model outperforms other universally in terms of all evaluation metrics. Moreover, the selection of the type of neural networks for best performance is also dependent upon the data sources. Mohandes *et al*. (1998) in their study used neural networks technique for wind speed prediction and compared its performance with that of an autoregressive model. Results on testing data indicate that the neural network approach outperforms the autoregressive model as indicated by the prediction graph and by the root mean square errors. Öztopal (2006) in his study presented the necessary weighting factors of surrounding stations to predict about a pivot using an ANN technique. The developed ANN model was found to predict the wind speeds for the winter season very accurately. Çam *et al.* (2005) in their study developed an ANN model to predict the average wind speed and wind energy values for the seven regions of Turkey. The network has successfully predicted the required output values for the test data; the mean error levels for the regions differed between 3% and 6%. Determining a distribution law for the speeds can be considered as a nonlinear regression problem, in which the distribution law (Weibull and Rayleigh) is identified so as to get nearer the discrete law. As regards function approximation, the techniques based on the ANN approach have, however, shown that they can deliver very good performances (Thiaw, 2010; Carolin and Fernandez, 2008; Jafarian and Ranjbar, 2010).

In this study, the wind data collected between July 2001 and June 2004 (36 months) was evaluated to determine the energy potential of the region. Using this potential, the power generation capacity of Kutahya was investigated for 17 different wind turbines. For this purpose, an ANN-based model was used besides Weibull and Rayleigh distribution models. In the ANN model, different feed-forward back propagation learning algorithms, namely Pola-Ribiere Conjugate Gradient (CGP), Levenberg–Marquardt (LM) and Scaled Conjugate (SCG) Gradient, were applied. Finally, the models were evaluated using the net present value (NPV) analysis.

2. Materials and methods

2.1. Study area

2.1.1. Site description

The study area is the city of Kutahya, which is surrounded by mountains from the east and south, is located at an altitude of 969 m and has a population of 200 000. Situated at 39°42′ latitude and 29°93′ longitude, it lies on the Western Central part of the Aegean Region and therefore displays geographical properties similar to those of the Aegean, Marmara and Central Anatolia regions. The main campus of Dumlupinar University is the site of the study; it is situated at 39°29′6,34″ latitude and 29°54′4,04″ longitude and located at an altitude of 1094 m as shown in Figure 1 (Kose *et al.,* 2004; Ozgur *et al.,* 2009).

2.1.2. Wind characteristics of the region

According to data obtained between the years 1975 and 2010, average annual temperature, average sunshine duration time and average rainfall in the Kutahya province are measured as 10.8 °C, 5.8 hours and 45.4 kg/m^2, respectively (DMI, 2011). Kutahya has a transition climate (otherwise known as a semi-continental climate). In general, Kutahya has low wind speeds and therefore, limited wind energy potential. However, there may be specific sites and applications where wind is a cost-effective option.

As seen in Figure.2a, average wind speed, blowing from the direction of North (N) and South-South-West (SSW) is 6.24 m/s and 6.00 m/s, respectively. In this study, the prevailing wind direction was determined as East (E) with a frequency distribution rate of 18.15% (see Figure.2b) (Ozgur, 2006).

The wind data used in the study was collected between July 2001 and June 2004 in 10 minute intervals and from various parts of the region (for detailed information see reference (Kose *et al..,* 2004; Ozgur *et al..,* 2009; Ozgur, 2006; Ozgur and Kose, 2006). The maximum monthly average wind speed was recorded as 5.3 m/s in February, when the minimum wind speed was recorded as 3.9 m/s in September. The wind data used in the study is as given in Figure 3.

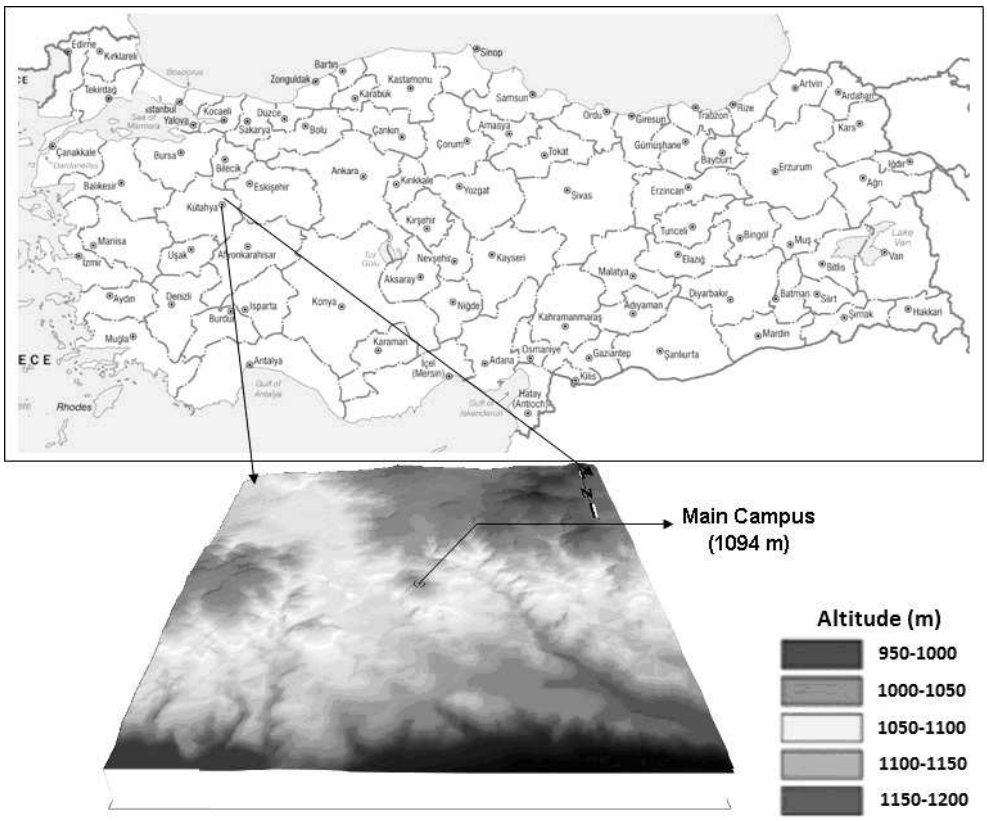

Figure.1: The main campus of Dumlupinar University, Kutahya

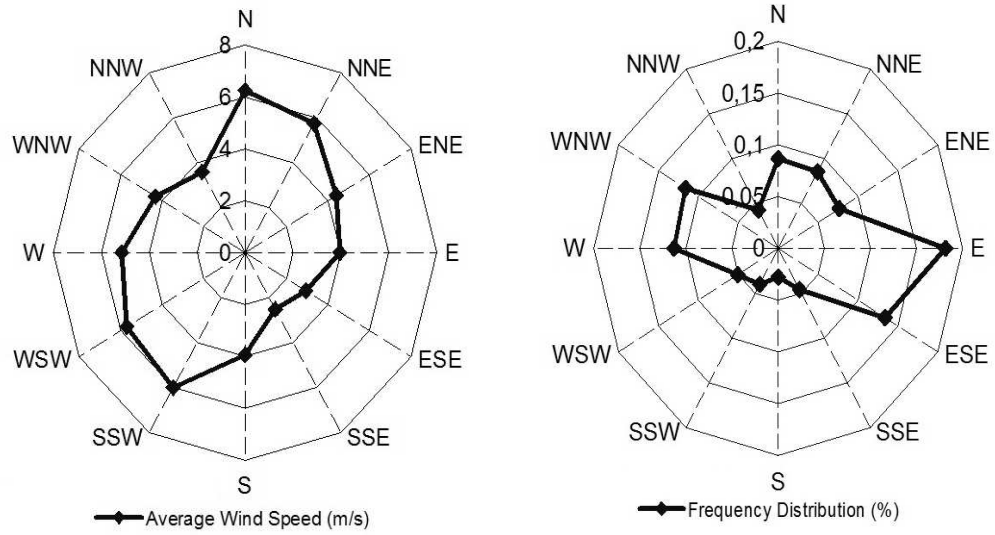

Figure 2: The wind characteristics on the main campus of Dumlupinar University; a) Average wind speed; b) Frequency distribution

2.2. Selected wind turbines

In the study, 17 different turbine models fabricated by four different manufacturers were selected to determine the power generation capacity of the study area. The installed capacities (*IC*) of these turbines range between 200 and 1650 kW, where the hub heights range between 36 and 85 m. The technical characteristics of related turbines are given in Table 1 (Ammonit, 2011).

2.3. Classical method for wind potential and energy generation

2.3.1. Weibull distribution function

Weibull probability density function (PDF) is a special case of the generalized two-parameter gamma distribution. The Weibull distribution can be characterized by *f(V)* of PDF and *F(V)* of cumulative distribution function (Bury, 1975; Fawzan, 2000). The PDF of the two-parameter Weibull distribution

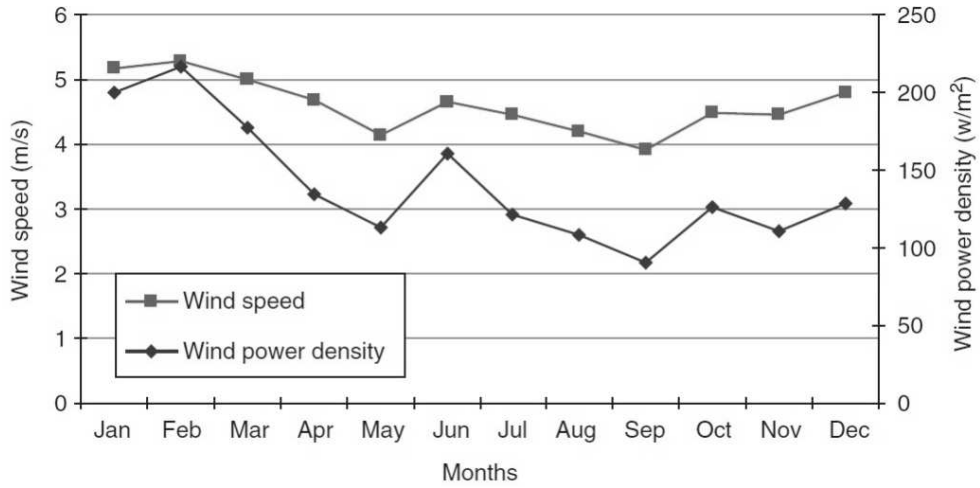

Figure 3: Monthly mean values of wind speed

Table 1: Technical specifications of wind turbines

Turbine type	*Turbine model*	*Hub height (m)*	*IC (kW)*	*Cut-in speed (m/s)*	*Cut-out speed (m/s)*	*Rated speed (m/s)*	*N (years)*
1	NEG Micon NM750/44	55	750	4	24	17	20
2	NEG Micon NM750/48	60	750	4	24	16	20
3	Enercon E-30/200kWNH50m	50	200	3	25	12	20
4	Enercon E-30/200kWNH36m	36	200	3	25	12	20
5	Enercon E-40/200kW55m	55	500	3	30	19.5	20
6	NEG Micon NM600/48	60	600	3	20	17	20
7	NEG Micon NM1500/64	80	1500	4	24	17	20
8	NEG Micon NM900/52	70	900	4	24	16	20
9	Nordex N54/1000	68.5	1000	4	24	16	20
10	Nordex N60/1300	70	1300	4	24	16	20
11	Vestas V44/600	55	600	4.50	20	17	20
12	Vestas V47/660	55	660	4	24	17	20
13	Vestas V66-1.65MW	67	1650	4	24	18	20
14	Nordex N43/600	55	600	3	24	18	20
15	Enercon E-40/600kW78m	78	600	3	25	14	20
16	Enercon E-58/1000kW70.5m	70.5	1000	3	25	14	20
17	Enercon E-66/1500kW85m	85	1500	3	25	14	20

is given by the following equation:

$$f(V)=\left(\frac{k}{c}\right)\left(\frac{V}{c}\right)^{k-1}\exp\left[-\left(\frac{V}{c}\right)^{k}\right],\quad 0<V<\infty \qquad (1)$$

where *c, k* and *V* are the scale parameter, shape parameter, and wind speed, respectively. The cumulative distribution function is given by the equation (Hennesey, 1977; Stevens and Smulders, 1979; Garcia *et al.,* 1997):

$$F(V)=1-e^{-(V/c)^{k}} \qquad (2)$$

Here, the relation between c and k is as follows:

$$\frac{\overline{V}}{c}=\Gamma\left(1+\frac{1}{k}\right) \qquad (3)$$

where $\overline{V}$ is the average wind speed. $\Gamma(...)$ is the Gamma function, and is given as

$$\Gamma(t)=\int_{0}^{\infty}e^{-x}x^{t-1}dx \qquad (4)$$

The standard deviation of the wind speed (σ) is determined by the following equation:

$$\frac{\sigma}{V}=\frac{\sqrt{\Gamma(1+2/k)-\Gamma^{2}(1+1/k)}}{\Gamma(1+1/k)} \qquad (5)$$

After calculating the parameters c and k, the most frequent wind speed and the maximum energetic wind speed are given by Eq. (6) and (7),

where $\bar{V}$ is the average wind speed. $\Gamma(...)$ is the Gamma function, and is given as

$$\Gamma(t) = \int_0^\infty e^{-x} x^{t-1} dx \tag{4}$$

The standard deviation of the wind speed (σ) is determined by the following equation:

$$\frac{\sigma}{V} = \frac{\sqrt{\Gamma(1+2/k) - \Gamma^2(1+1/k)}}{\Gamma(1+1/k)} \tag{5}$$

After calculating the parameters c and k, the most frequent wind speed and the maximum energetic wind speed are given by Eq. (6) and (7), respectively, which are as follows:

$$V_{MP} = c\left(\frac{k-1}{k}\right)^{1/k} \tag{6}$$

$$V_{\max E} = c\left(\frac{k+2}{k}\right)^{1/k} \tag{7}$$

The shape parameter, k, commonly ranges between 1.5 and 3.0. When it assumes the value 2.0, it is called the Rayleigh distribution, and the PDF for the Rayleigh distribution can then be simplified as shown in Eq. (8).

$$f(V) = \frac{2V}{c^2} \exp\left[\left(-\frac{V}{c}\right)^k\right] \tag{8}$$

2.3.2. Power extracted from wind

The kinetic energy in air of mass 'm' moving with speed V is given by the following in SI units:

$$Kinetic\ \ energy = \frac{1}{2} mV^2 \text{ joules.} \tag{9}$$

The volumetric flow rate is A·V, the mass flow rate of the air in kilograms per second is ρAV, and the power is given by the following (Patel, 1942):

$$P = \frac{1}{2}(\rho AV)V^2 = \frac{1}{2}\rho AV^3 \text{ watts.} \tag{10}$$

Here, ρ and A, respectively, define the density in kg/m^3 and the area swept by the rotor in m^2. Therefore, the wind-power density is given by the Eq. (11) in terms of the Weibull PDF, and the wind energy density is given by Eq. (12) for a period T.

$$\frac{P}{A} = \int_0^\infty P(V) f(V) dV = \frac{1}{2}\rho c^3 \Gamma\left(\frac{k+3}{k}\right) \tag{11}$$

$$\frac{E}{A} = \frac{1}{2}\rho c^3 \Gamma\left(\frac{k+3}{k}\right) T \tag{12}$$

From the technological point of view, a wind turbine that converts the kinetic energy of the wind to electrical energy, starts to generate power at a cut-in wind speed (V_1), and this process continues until a wind speed of V_R, at which the nominal power generation P_R is obtained. After this nominal point, the turbine starts to decelerate itself in a controlled manner until a speed of V_0, called the cut-out wind speed, is reached. With reference to these benchmarks, the energy achieved from an ideal turbine is given as follows:

$$E_{TW} = T\int_0^\infty P(V) f(V) dV = T\left(\int_{V_1}^{V_R} P(V) f(V) dV + \int_{V_R}^{V_0} P_R f(V) dV\right) \tag{13}$$

Substituting the Eq. (10) in Eq. (13), it can be rewritten as

$$E_{TW} = \frac{\rho}{2} TA\left(\int_{V_1}^{V_R} V^3 \frac{k}{c}\left(\frac{V}{c}\right)^{k-1} e^{-(V/c)^k} dV + V_R^3 \int_{V_R}^{V_0} \frac{k}{c}\left(\frac{V}{c}\right)^{k-1} e^{-(V/c)^k} dV\right) \tag{14}*$$

Because of the several losses occurring during the transmission mechanisms of the wind turbine, all the power carried by the wind can never be converted to electricity. In this regard, the actual power achieved from the turbine (P_T) is calculated from the turbine-performance curve described by Eq. (15).

$$P_T(V) = \begin{cases} 0 & , V < V_I \\ \left(a_1 V^3 + a_2 V^2 + a_3 V + a_4\right) P_R, & V_1 \le V < V_R \\ P_R & , V_R \le V < V_0 \\ 0 & , V \ge V_0 \end{cases} \tag{15}$$

where a_1, a_2, a_3, and a_4 are the regression constants of the turbine-performance curves (Arslan, 2010; Wu, 2002). Combining the Eqs. (1), (10), and (15), Eq. (16) gives the actual energy released from a wind turbine.

$$E_{TA} = T\int_{V_1}^{V_0} P_T(V) f(V) dV = TP_R \int_{V_1}^{V_R} (a_1 V^3 + a_2 V^2 + a_3 V + a_4) \frac{k}{c}\left(\frac{V}{c}\right)^{k-1} e^{-(V/c)^k} dV + TP_R \int_{V_R}^{V_0} \frac{k}{c}\left(\frac{V}{c}\right)^{k-1} e^{-(V/c)^k} dV \tag{16}$$

* *Equations 14, 16 and 19 have been shrunk in order to fit the column. They are given in their full size at the end of the paper.*

Therefore, the efficiency of the turbine (η) is the ratio of the real to the ideal energy-generation processes and is given by the following equation:

$$\eta = \frac{E_{TA}}{E_{TW}} \tag{17}$$

As observed from Eqs. (15)–(17), the turbine efficiency is a function of not only the wind characteristics but also wind distribution. In 1926, Betz first discovered that the wind power theoretically decreased with the wind speed. According to Betz, neglecting the transmission losses, the obtainable power from wind is approximately 59% of the total carried by it. In other words, the turbine efficiency cannot exceed the value of 59% (Golding, 1955; Considine, 1977).

For the period T, the generated nominal wind energy from a turbine operating with full capacity is given by Eq. (18).

$$E_{TR} = TP_R \tag{18}$$

After this classification, two important parameters – capacity and availability factor – should be defined for the estimation of power generated from a wind turbine. The capacity factor is defined as the ratio of the real-energy generation to nominal-energy generation and is given as follows (Ozgur, 2006; Decher, 1994):

$$C_F = \frac{E_{TA}}{E_{TR}} = \int_{V_I}^{V_R} \left(a_1 V^3 + a_2 V^2 + a_3 V + a_4\right) \frac{k}{c}\left(\frac{V}{c}\right)^{k-1} e^{-(V/c)^k} dV + \int_{V_R}^{V_0} \frac{k}{c}\left(\frac{V}{c}\right)^{k-1} e^{-(V/c)^k} dV \tag{19}$$

The availability factor is the operating percentage of a turbine and is given by the following equation:

$$A_F = P(V_I \le V < V_0) = \int_{V_I}^{V_0} \frac{k}{c}\left(\frac{V}{c}\right)^{k-1} e^{-(V/c)^k} dV \tag{20}$$

If the wind speed measurement has been made from a height of H_1 above the ground, it is possible to assess the wind speeds at a height H_2 by the relation:

$$V_e = V_m \left(\frac{H_2}{H_1}\right)^{\alpha} \tag{21}$$

where α is a parameter that depends on the soil roughness (Thiaw, 2010; Ozgur et al., 2009; Ozgur, 2006; Patel, 1942).

2.4. ANN modelling of wind power generation

Artificial neural networks are examples of the way that the biological neural system works. Nerve cells contain neurons. Neurons are interconnected in various ways and create a network. Likewise, ANN is a network applied successfully in a number of application areas such as medicine, economics, engineering, neurology, meteorology, etc. The ANN modelling is carried out in two steps: the first step is to train the network whereas the second is to test the network with data, which are not used for training. The unit element of an ANN is the neuron. As in nature, the network function is determined largely by the connections between the elements (Fu, 1994; Tsoukalas and Uhrig, 1997; Oztemel, 2003).

In an ANN, each unit is a basic unit of information process. Units are interconnected via links that contain weight values. Weight values help the neural network to express knowledge. There are several neural architectures. One of these architectures, widely used in engineering applications, is multilayer neural network (MLNN).

The MLNN consists of three layers at least: an input layer, an output layer and one hidden layer. The input and output layers represent the input and output variables of the model and the hidden layers hold the network's ability to learn the non-linear relationships between the input and output (Oztemel, 2003; Kalogirou, 2000). To obtain these relationships, several learning algorithms are available, one of which can be used. The most widely used algorithm is the feed-forward back propagation learning algorithm. It is a gradient descent algorithm. The most widely used algorithms are Levenberg-Marguardt (LM), Pola-Ribiere Conjugate Gradient (CGP) and Scaled Conjugate Gradient (SCG) in the field of energy. LM algorithm appears to be the fastest method for feed forward neural networks. CGP and SCG algorithms are a version of the Conjugate Gradient algorithm. Each of the conjugate gradient algorithms that have been discussed so far requires a line search. This line search is computationally expensive, since it requires that the network response to all training inputs be computed several times for each search (Hagan and Menjah, 1994; Fletcher and Reeves, 1964; Moller, 1993). ANN with a feed-forward back propagation algorithm learns by changing the connection weights, and these changes are stored as knowledge. The performance of the configured model is determined using some statistical methods such as the percent root mean square error (*PRMSE*), covariance (*Cov*) and the coefficient of multiple determinations (R^2). These statistical parameters are formulated in terms of output value (y_{output}), target value (y_{actual}), average of target ($\bar{y}_{actual}$) and pattern (n) as follows (Arslan, 2011):

$$PRMSE = \sqrt{\frac{\sum_{m=1}^{n}\left(\frac{y_{output} - y_{actual}}{y_{output}}\right)^2}{n}} \times 100 \quad (22)$$

$$Cov = \frac{\sqrt{\frac{\sum_{m=1}^{n}\left(y_{output} - y_{actual}\right)^2}{n}}}{\left|\overline{y}_{actual}\right|} \times 100 \quad (23)$$

$$R^2 = 1 - \frac{\sum_{m=1}^{n}\left(y_{output} - y_{actual}\right)^2}{\sum_{m=1}^{n} y_{actual}^{\ 2}} \quad (24)$$

In this study, different feed-forward back propagation learning algorithms, namely Pola-Ribiere Conjugate Gradient (CGP), Levenberg–Marquardt (LM) and Scaled Conjugate Gradient (SCG) were applied. Inputs and outputs were normalized in the (0–1) range depending on the non-linear transfer function; logarithmic sigmoid (logsig), was used as given:

$$f(z) = \frac{1}{1 + e^{-z}} \quad (25)$$

where z is the weighted sum, and given in terms of bias (b), weight (w) and output (y),

$$z_j = \sum_{i=1}^{n} w_{ij} y_i + b_j \quad (26)$$

2.5 Economic analysis

The wind power plants handled herein have been evaluated economically using net present value (*NPV*) analysis. NPV is a powerful tool for the feasibility studies and can be determined with the following equation (Ozerdem *et al.*, 2006; Zheng, 2009):

$$NPV = \sum_{t=0}^{N} \frac{B_t - C_t}{(1+r)^t} \quad (27)$$

Where B_t and C_t are the benefit and cost in the t^{th} year respectively during the program, r represents the discount rate and N is the timescale of the plant.

To this end, the cost parameters selected for the on-grid configuration were the wind turbine (C_{WT}) including installation and commissioning, and salvage (C_{sal}) where the benefits were greenhouse gases (C_{CO2}), repair and maintenance ($C_{O\&M}$), and the electricity sale (C_e). Accordingly, the general cost (C) and the benefit (B) of the system are as given in Equations (28) and (29).

$$C = C_{WT} - C_{sal} \quad (28)$$

$$B = C_{CO2} + C_e - C_{O\&M} \quad (29)$$

In this study, the unit costs used in the study were taken as 88 US$/MWh for electricity sale (C_e), 1250 US$/kW for wind turbine including installation and commissioning (C_{WT}), %5 of c_{WT} (C_{sal}), 17.5 US$/MWh for operating and maintenance ($c_{O\&M}$) and 93.2 US$/MWh for greenhouse gases (C_{CO2}) (Arslan, 2010; Green Economy, 2010; Blanco, 2009).

3. Results and discussion

In the ANN modelling of a wind power plant, the values of three inputs, turbine type, hub height and wind speed, were used. Generated power of the system was obtained as output. Different models were performed by using the software MATLAB. These models were built up using a dataset including 314 patterns. In the training step, 220 of these patterns (70% of total) were used. The remaining patterns, randomly selected from a number of 94, were used for testing. An increased number of neurons (from 6 to 16) were used to define the output accurately in a single hidden layer for 2000 epochs in the training algorithms. According to statistical performance evaluation, the summarized results are given in Table 2.

According to Table 2, all the studied ANN models are very satisfactory and can be used for the pre-feasibility of a wind power plant with an acceptable accuracy. The LM training algorithm with 15 neurons in a single hidden layer was determined as the best model. Different models with more hidden layers were also tested but none was as much accurate as LM 15. The architecture of LM 15 is shown in Figure 4.

In the training step of this topology, *PRMSE* was determined as 0.4908% when the values of *Cov* and R^2 obtained were 0.5074 and 0.9995. These values were respectively 0.6475, 0.9606 and 0.9991 in the testing step. The statistical evaluation shows that the trained ANN model can be used for the designing of a wind power plant considered suitable for Kutahya, since it has high accuracy. The comparisons of the actual and ANN outputs are shown in Figure 5.

In this study, the wind data, appropriate to World Meteorology Organization (WMO) standards, collected between July 2001 and June 2004 in 10-minute intervals were evaluated to determine the energy potential of the region. This data was used to determine the power generation capacity taking 17 different turbine models into consideration in Weibull and Rayleigh distribution models. Besides these, technical characteristics of these turbines were also modelled using ANN to give the power generation capacity. The results are given in

Table 2: A comparison of error values for studied ANN topologies

Algorithm	*Train*			*Test*		
	CoV	*PRMSE*	R^2	*CoV*	*PRMSE*	R^2
CGP 14	4.1213	3.8952	0.9694	5.2604	3.7239	0.9737
CGP 15	2.7089	2.6564	0.9867	3.6979	2.7567	0.9868
CGP 16	2.7272	2.7586	0.9865	3.9002	2.8213	0.9855
LM 14	0.6085	0.6000	0.9993	0.9963	0.6831	0.9990
LM 15	*0.5074*	*0.4908*	*0.9995*	*0.9606*	*0.6475*	*0.9991*
LM 16	0.5909	0.5630	0.9993	0.9472	0.6475	0.9991
SCG 14	3.1010	3.3463	0.9826	4.4538	3.4445	0.9816
SCG 15	2.9901	3.0489	0.9838	3.8324	2.7796	0.9868
SCG 16	2.2494	2.2151	0.9908	3.1519	2.2317	0.9905

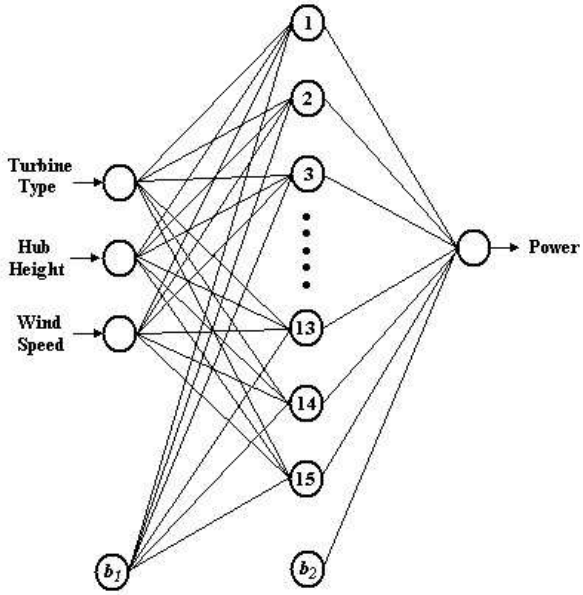

Figure 4: The architecture of the best ANN topology

Table 3: *NPV* results for a discount rate of 0.14

Turbine type	Capacity (kW)	NPV ($)	Payback period (year)
1	750	-68,979	>20
2	750	128,959	12.69
3	200	225,893	4.93
4	200	23,737	14.14
5	500	121,815	11.21
6	600	255,349	8.77
7	1,500	257,747	12.69
8	900	245,386	10.72
9	1,000	90,493	15.10
10	1,300	170,083	13.77
11	600	52,811	15.19
12	660	191,450	10.45
13	1,650	17,548	19.19
14	600	111,447	12.37
15	600	212,654	9.57
16	1,000	422,187	8.80
17	1,500	398,898	10.82

Figures 6–8. According to these figures, the results of the ANN model are more accurate than those of Weibull and Rayleigh (Arslan, 2010; Ozgur *et al.*, 2009; Ozgur, 2006; Ozgur and Kose, 2006).

For the economic evaluation of cost and benefit, the *NPV* concept was used, which included the greenhouse gas emission criteria. The calculations were based on the average energy generation of three years. The NPV results ratified for a discount rate of 0.14 (TCMB, 2010) are given in Table 3.

According to Table 3, the wind power generation is profitable for the existing turbine type 1. *NPV* values oscillate between US$ –68,979 and 422,187. Since the greater *NPV* means the more profitable, the most appropriate case seems to be the system with the turbine type 16. However, the least payback period is obtained for type 3 with an *NPV* value of US$ 225,893. So, this means that the most appropriate case is actually the system with the turbine type 3, when the capacities of the turbines are taken into consideration.

4. Conclusion

A highly unique flexible ANN algorithm was proposed to evaluate the wind power generation systems because of nonlinearity of the neural networks. The results analytically obtained were used to train the several ANN algorithms such as CGP, LM and SCG. The trained algorithms were then tested and evaluated by the statistical methods such as *Cov*, *RMS* and R^2. These statistical values showed that the best algorithm was LM. The degree of accuracy, between the real data and training data, is 99.95% for ANN algorithms, whereas the degree of accuracy, between the real data and testing data, is 99.91% for LM 15.

In this paper, the trained algorithms also show that the predicted values can be used to install a wind system with less data and high accuracy. Besides these, the best ANN topology gives more sensitive results in comparison to Weibull and

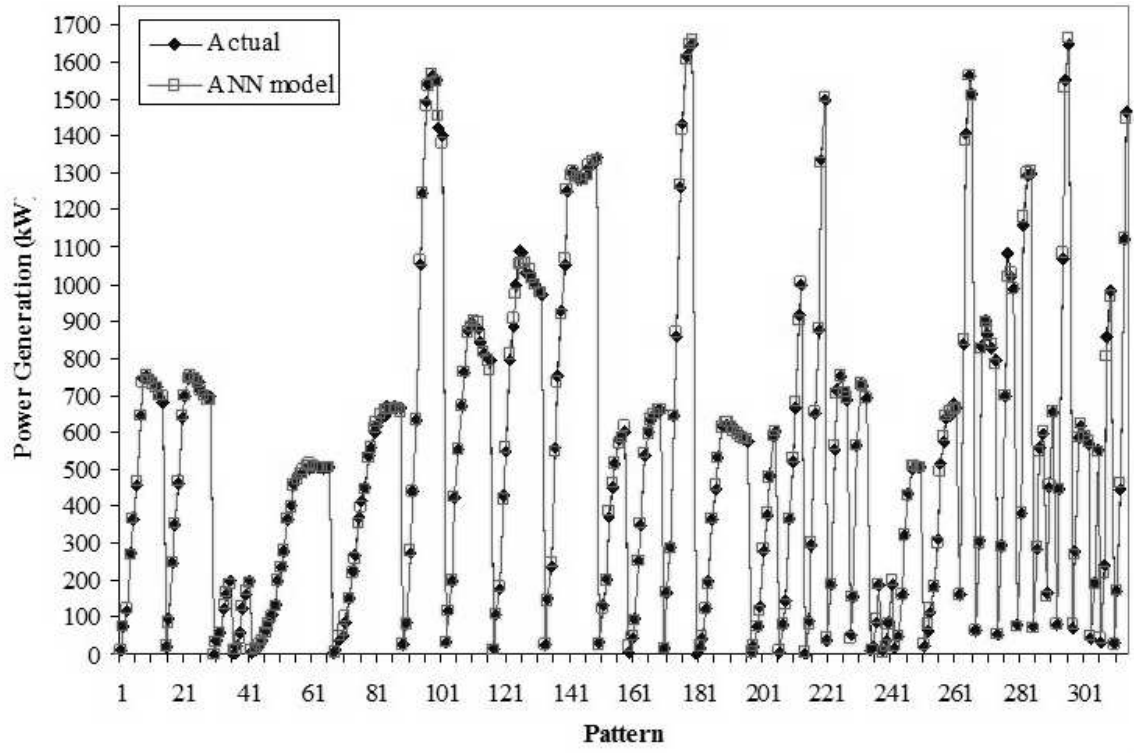

Figure 5: A comparison of ANN prediction and analytic design results for LM 15

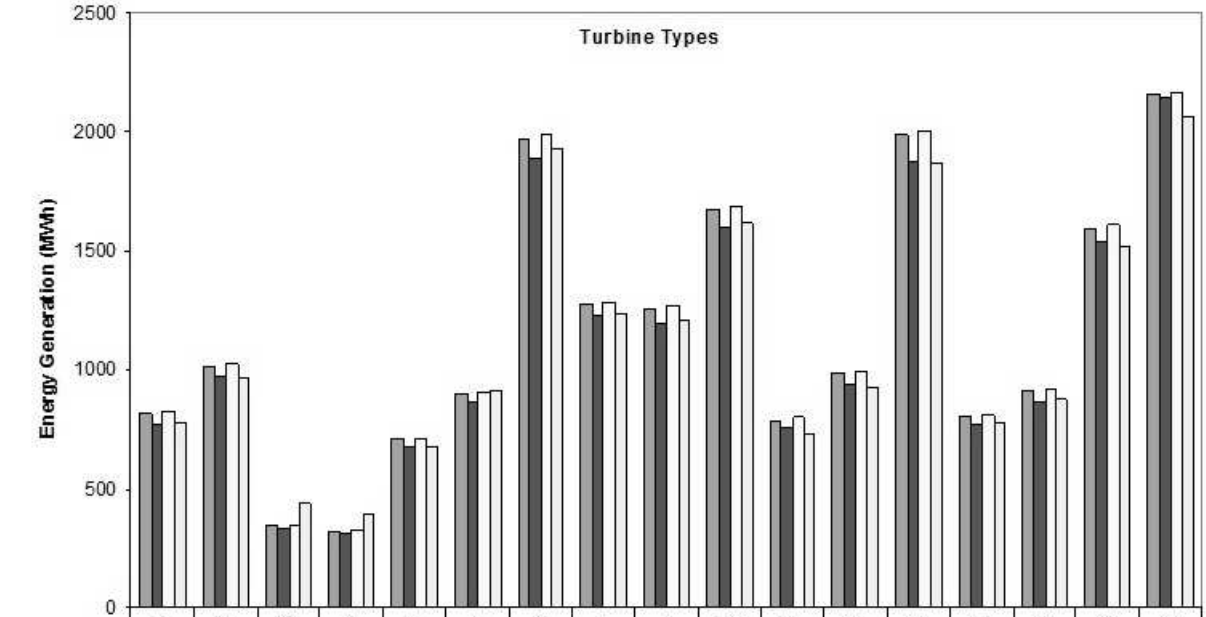

	1	2	3	4	5	6	7	8	9	10	11	12	13	14	15	16	17
Actual	817.2	1014.1	345.7	321.9	710.8	900.3	1972.4	1275.4	1256.0	1673.3	789.6	984.1	1988.2	802.8	909.4	1597.6	2161.2
Rayleigh	772.1	975.0	333.8	310.1	674.6	870.8	1891.8	1234.7	1197.7	1603.1	756.5	944.6	1880.4	767.9	871.2	1537.8	2143.5
Weibull	821.9	1020.3	347.4	324.7	713.9	908.5	1991.4	1285.2	1266.2	1685.2	799.9	991.3	2003.4	807.5	916.3	1607.9	2164.4
ANN model	776.3	964.4	435.8	396.4	675.8	913.5	1929.1	1241.3	1208.7	1620.7	724.9	923.8	1869.6	778.7	875.6	1521.5	2063.3

Figure 6: A comparison of the values of electricity production (July 2001 – June 2002)

Rayleigh distribution models. So, the neural network topology can be used for the feasibility studies of wind power projects. In this study, the *NPV* analysis-based ANN topology shows that the wind power systems for different 16 turbine types are profitable in Kutahya.

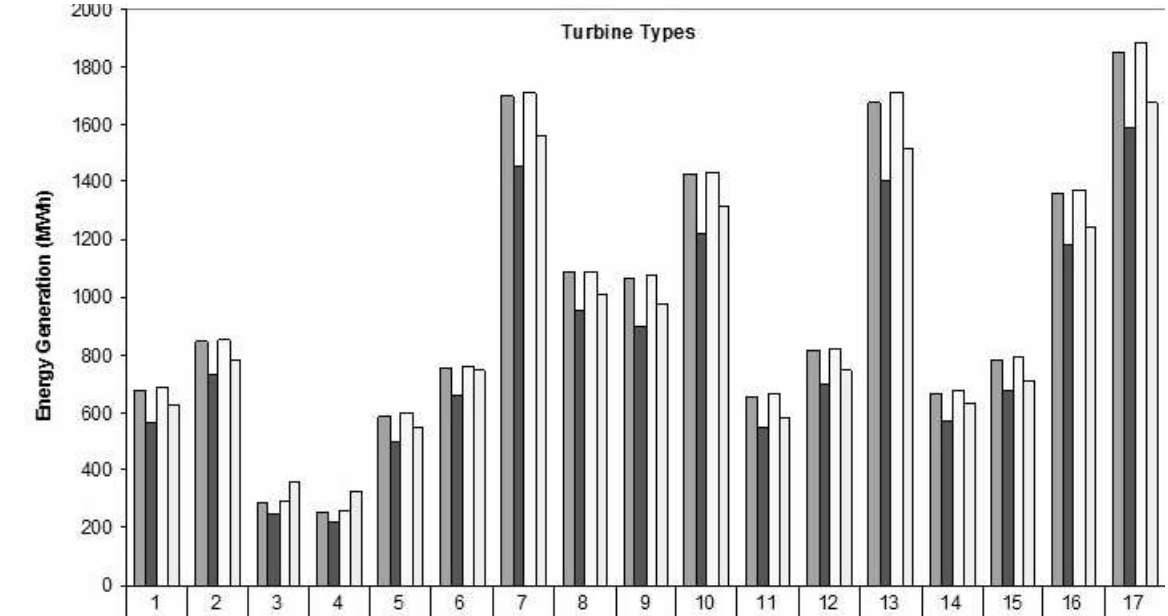

	1	2	3	4	5	6	7	8	9	10	11	12	13	14	15	16	17
Actual	673.1	847.3	286.6	257.1	588.7	753.8	1697.0	1086.3	1063.5	1423.7	650.9	815.5	1674.4	665.0	781.4	1358.5	1852.5
Rayleigh	564.7	734.1	249.2	220.8	498.0	658.4	1457.0	953.8	901.3	1218.9	548.5	697.9	1402.4	570.4	673.9	1184.7	1584.2
Weibull	687.2	853.4	287.4	260.4	598.7	757.9	1711.2	1088.4	1075.5	1431.1	662.4	824.5	1712.2	672.3	790.9	1372.1	1882.1
ANN model	630.1	781.1	359.3	325.1	551.4	747.2	1562.6	1010.5	978.4	1314.2	582.8	745.9	1513.2	634.0	711.8	1240.1	1673.1

Figure 7: A comparison of the values of electricity production (July 2002 – June 2003)

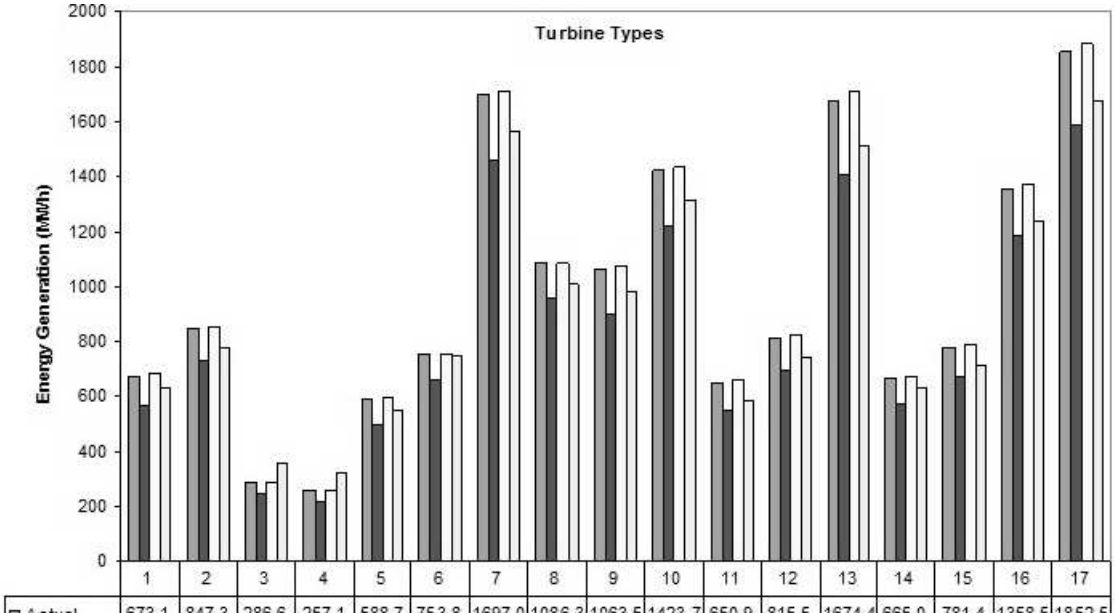

	1	2	3	4	5	6	7	8	9	10	11	12	13	14	15	16	17
Actual	673.1	847.3	286.6	257.1	588.7	753.8	1697.0	1086.3	1063.5	1423.7	650.9	815.5	1674.4	665.0	781.4	1358.5	1852.5
Rayleigh	564.7	734.1	249.2	220.8	498.0	658.4	1457.0	953.8	901.3	1218.9	548.5	697.9	1402.4	570.4	673.9	1184.7	1584.2
Weibull	687.2	853.4	287.4	260.4	598.7	757.9	1711.2	1088.4	1075.5	1431.1	662.4	824.5	1712.2	672.3	790.9	1372.1	1882.1
ANN model	630.1	781.1	359.3	325.1	551.4	747.2	1562.6	1010.5	978.4	1314.2	582.8	745.9	1513.2	634.0	711.8	1240.1	1673.1

Figure 8: A comparison of the values of electricity production (July 2003 – June 2004)

Equations 14, 16 and 19 repeated

$$E_{TW} = \frac{\rho}{2} TA \left(\int_{V_I}^{V_R} V^3 \frac{k}{c} \left(\frac{V}{c} \right)^{k-1} e^{-(V/c)^k} dV + {V_R}^3 \int_{V_R}^{V_0} \frac{k}{c} \left(\frac{V}{c} \right)^{k-1} e^{-(V/c)^k} dV \right) \quad (14)$$

$$E_{TA} = T\int_{V_1}^{V_0} P_T(V) f(V) dV = TP_R \int_{V_1}^{V_R} (a_1 V^3 + a_2 V^2 + a_3 V + a_4) \frac{k}{c}\left(\frac{V}{c}\right)^{k-1} e^{-(V/c)^k} dV + TP_R \int_{V_R}^{V_0} \frac{k}{c}\left(\frac{V}{c}\right)^{k-1} e^{-(V/c)^k} dV \quad (16)$$

$$C_F = \frac{E_{TA}}{E_{TR}} = \int_{V_1}^{V_R} \left(a_1 V^3 + a_2 V^2 + a_3 V + a_4\right) \frac{k}{c}\left(\frac{V}{c}\right)^{k-1} e^{-(V/c)^k} dV + \int_{V_R}^{V_0} \frac{k}{c}\left(\frac{V}{c}\right)^{k-1} e^{-(V/c)^k} dV \quad (19)$$

Nomenclature

A	area swept by the rotor (m^2)
ANN	artificial neural network
A_F	availability factor
B	benefit (US$)
b	bias number
C	general cost (US$)
c	scale parameter (m/s)
CF	capacity factor
CGP	Pola-Ribiere conjugate gradient
Cov	covariance
C_{CO2}	cost of greenhouse gases (US$)
C_e	cost of electricity sale (US$)
C_{sal}	cost of salvage (US$)
$C_{O\&M}$	cost of operation and maintenance (US$)
C_{WT}	cost of wind turbine (US$)
c_{CO2}	unit cost of greenhouse gases (US$/MWh)
c_e	unit cost of electricity sale (US$/MWh)
c_{sal}	unit cost of salvage (US$/MW)
$c_{O\&M}$	unit cost of operation and maintenance (US$/MWh)
c_{WT}	unit cost of wind turbine (US$/MW)
E_{TA}	actual energy released from turbine (kWh)
E_{TW}	energy achieved from an ideal turbine (kWh)
$F(V)$	cumulative distribution function
f(V)	Weibull distribution function
IC	installed capacity (kW)
k	shape parameter
LM	Levenberg–Marquardt
m	air of mass (kg)
MLNN	multi-layer neural network
N	lifetime of the plant (year)
NPV	net present value (US$)
n	pattern
PDF	probability density function
PRMSE	percent root mean square error
P_R	nominal power generation (kW)
P_T	actual power achieved from the turbine (kW)
r	discount rate (%)
SCG	scaled conjugate gradient
V	wind speed (m/s)
V_e	wind speed estimated at height H_2 (m/s)
V_{MP}	most frequent wind speed (m/s)
$V_{max\,E}$	the maximum energetic wind speed (m/s)
V_m	wind speed measured at the reference height H_1 (m/s)
V_R	rated wind speed (m/s)
V_1	cut-in wind speed (m/s)
V_0	cut-out wind speed (m/s)
y	output
y_{output}	output value
y_{actual}	target value
$\overline{y}_{actual}$	average of target
z	weighted sum
Γ(...)	gamma function
σ	standard deviation of wind speed
η	efficiency of turbine (%)
α	ground surface friction coefficient
ρ	air density (kg/m^3)

References

Ammonit. (2011). Alwin software; WEC-Catalog. <http://www.ammonit.com/images/stories/software/AmmonitALWIN/alwin_zip.zip> (access January 2011).

Arslan, O. (2010). Technoeconomic analysis of electricity generation from wind energy in Kutahya, Turkey. *Energy* 35:120-131.

Arslan, O. (2011). Power generation from medium temperature geothermal resources: ANN-based optimization of Kalina cycle system-34. Energy 36:2528-2534.

Blanco, M.I. (2009). The economics of wind energy. *Renewable and Sustainable Energy Reviews* 13:1372-1382.

Bury, K.V. (1975). Statistical models in applied science. John –Wiley Science. pp.405-437.

Çam, E., Arcaklıoğlu, E., Çavuşoğlu, A., and Akbıyık, B. (2005). A classification mechanism for determining average wind speed and power in several regions of Turkey using artificial neural networks. *Renewable Energy* 30:227-239.

Carolin, M., and Fernandez, E. 2008. Analysis of wind power generation and prediction using ANN: A case study. *Renewable Energy* 33:986-992.

Celik, A.N. (2004). A statistical analysis of wind power density based on the Weibull and Rayleigh models at the southern region of Turkey. *Renewable Energy* 29:593-604.

Chang, T.J., Wu, Y.T., Hsu, H.Y., Chu, C.R., and Liao, C.M. (2003). Assessment of wind characteristics and wind turbine characteristics in Taiwan. *Renewable Energy* 28:851-871.

Considine, D.M. (1977). Energy technology handbook. New York: McGraw Hill.

Decher, R. (1994). Energy conversion. New York: Oxford University Press. pp.454-475.

Dombaycı, Ö.A., and Gölcü, M. (2009). Daily means ambient temperature prediction using artificial neural network method: A case study of Turkey. *Renewable*

Energy 34:1158-1161.

Dorvlo, A.S. (2002). Estimating wind speed distribution. *Energy Conversion and Management* 43:2311-2318.

Fawzan, M.A. (2000). Methods for estimating the parameters of the Weibull distribution. Saudi Arabia: King Abdul-Aziz City for Science and Technology. p.1-11.

Fletcher, R., and Reeves, C.M. (1993). Function minimization by conjugate gradients. *Computer Journal* 7:149-154.

Fu, L M. (1994). Neural network in computer intelligence. Int. ed. New York: McGraw-Hill.

Garcia, A., Torres, J.L, Prieto, E., and Francisco, A. (1997). Fitting wind speed distributions: a case study. *Solar Energy* 62:139-144.

Golding, E.W. (1955). The generation of electricity by wind power. New York: Philosophical Library. p.318.

Green Economy. (2010). Objection to the draft renewable energy law from wind investors. <http://www.yesilekonomi.com/haberdetay.asp?id=NDI3> (access June 2010).

Hagan, M.T., and Menhaj, M. (1994). Training feedforward networks with the Marquardt algorithm, IEEE *Transactions on Neural Networks* 5:989-993.

Hennesey, J.P. (1977). Some aspects of wind power statistics. *Journal of Applied Meteorology* 16(2):119-128.

Jafarian, M., and Ranjbar, A.M. (2010). Fuzzy modelling techniques and artificial neural networks to estimate annual energy output of a wind turbine. *Renewable Energy* 35:2008-2014.

Jaramillo, A.O., and Borja, M.A. (2004). Wind speed analysis in La Ventosa, Mexico: a bimodal probability case. *Renewable Energy* 29:1613-1630.

Kalogirou, S.A. (2000). Applications of artificial neural networks for energy systems. *Applied Energy* 67;17-35.

Kalogirou, S.A., Panteliou, S., and Dentsoras, A. (1999). Artificial neural networks used for the performance prediction of a thermosiphon solar water heater. *Renewable Energy* 18:87-99.

Karsli, V.M., and Gecit, C. (2003). An investigation on wind power potential of Nurdagi-Gaziantep, Turkey. *Renewable Energy* 28:823-830.

Keyhani, A., Ghasemi, M.G., Khanali, M., and Abbaszadeh, R. (2010). An assessment of wind energy potential as a power generation source in the capital of Iran, Tehran. *Energy* 35:188-201.

Kose, R., Ozgur, M.A., Erbas, O., and Tugcu, A. (2004). The analysis of wind data and wind energy potential in Kutahya, Turkey. *Renewable and Sustainable Energy Reviews* 8:277-288.

Li, G., and Shi, J. (2010). On comparing three artificial neural networks for wind speed forecasting. *Applied Energy* 87: 2312-2320.

Mohandes, M.A., Rehman, S., and Halawani, T.O. (1998). A neural networks approach for wind speed prediction. *Renewable Energy* 13(3):345-354.

Moller, M.F. (1993). A scaled conjugate gradient algorithm for fast supervised learning. *Neural Networks* 6:525-533.

Öztopal, A. (2006). Artificial neural network approach to spatial estimation of wind velocity data. *Energy Conversion and Management* 47:395-406.

Ozgur, M.A. (2006). Statistical analysis of wind characteristics of Kutahya and electricity production applicability. Ph.D. Thesis. Osmangazi University, Institute of Applied Science (in Turkish).

Ozgur, M.A., and Kose, R. (2006). Assessment of the wind energy potential of Kutahya, Turkey. *Energy Exploration and Exploitation* 24:113-130.

Ozgur, M.A., Arslan, O., Kose, R., and Peker, K.O. (2009). Statistical evaluation of wind characteristics in Kutahya, Turkey. *Energy Sources Part A: Recovery, Utilization and Environmental Effects* 31:1450-1463.

Ozerdem, B., Ozer, S., Tosun, M. 2006. Feasibility study of wind farms: A case study for Izmir, Turkey. *Journal of Wind Engineering and Industrial Aerodynamics* 94:725-743.

Oztemel, E. (2003). Artificial neural networks. Istanbul: Papatya Publications (in Turkish).

Patel, M.R. (1942). Wind and solar power systems. CRC Press: Chapter 4, ISBN 0-8493-1605-7. p.35.

Ouammi, A., Sacile, R., Zejli, D., Mimet, A., and Benchrifa, R. (2010). Sustainability of a wind power plant: Application to different Moroccan sites. *Energy* 35:4226-4236.

Stevens, M.J.M., and Smulders. P.T. (1979). The estimation of parameters of the Weibull wind speed distribution for wind energy utilization purposes. *Wind Engineering* 3(2):132-145.

Sulaiman, M.Y., Akaak, A.M., Wahab, M.A., Zakaria, A., Sulaiman, Z.A., and Suradi, J. (2002). Wind characteristics of Oman. *Energy* 27:35-46.

TCMB (Central bank of the republic of Turkey) (2011). The discount rate in 2010. <http://www.tcmb.gov.tr/yeni/reeskont/rediscount.html> (access May 2011).

Thiaw, L. A. (2010). Neural network based approach for wind resource and wind generators production assessment. *Applied Energy* 87:1744-1748.

Tsoukalas, L.H,, and Uhrig, R,E. (1997). *Fuzzy and neural approaches in engineering*. New York: Wiley.

Turkish State Meteorological Service (DMI) (2011). Data and evaluation of Kutahya. < http://www.dmi.gov.tr/veridegerlendirme/il-ve-ilceler-istatistik.aspx?m=KUTAHYA> (access May 2011)

Ulgen, K., and Hepbasli, A. (2002). Determination of Weibull parameters for wind energy analysis of Izmir, Turkey. *International Journal of Energy Research* 26:494-506.

Wu, S,J. (2002). Estimating of the parameters of the Weibull with progressively censored data. 32. Japan Statistic Society p.155-163.

Zheng, W., Shi, H., Chen, S., and Zhu, M. (2009). Benefit and cost analysis of mariculture based on ecosystem services. *Ecology Economics* 68:1626-1632.

Received 11 November 2013; revised 4 September 2014

Performance analysis of a vapour compression-absorption cascaded refrigeration system with undersized evaporator and condenser

Vaibhav Jain
Department of Mechanical and Automation Engineering, MAIT, Delhi, India

Gulshan Sachdeva
Department of Mechanical Engineering, NIT, Kurukshetra, India

Surendra S Kachhwaha
School of Technology, Department of Mechanical Engineering, PDPU, Gandhinagar, India

Abstract
In a present study, the performance of a vapour compression–absorption cascaded refrigeration system (CRS) under fouled conditions was analysed. The main effect of fouling is to decrease the effectiveness of the heat exchanger. Thus, the overall conductance (UA) of the heat exchanger is decreased. Hence, another interpretation of fouling is to reduce the effective size of the heat exchanger. In the present work, the percentage decrease in the overall conductance value (UA) of evaporator and condenser due to their fouling is varied from 0 to 50% and its consequences on various aspects of CRS are generated to ascertain any possible patterns. The detailed first law analysis reveals that for a clean evaporator and condenser, the electricity consumption is 67.5% less than vapour compression system (VCS) for the same cooling capacity. CRS is able to save only 61.3% of electrical energy when evaporator and condenser conductance is reduced by 50% due to fouling. Evaporator and condenser fouling decreased the COP and rational efficiency of the system by 4.7% and 10.5% respectively. It is also important to note that irreversibility in the evaporator and condenser is increased by 42.4% and 62.1% respectively, when their individual performance is degraded by 50% due to fouling.

Keywords: fouling, vapour compression, absorption, cascaded refrigeration system, first law, second law analysis

1. Introduction

Vapour compression refrigeration systems are commonly used in a variety of commercial and industrial applications due to their high cooling capacity at low temperature, but to run these systems, high grade energy is required. High grade energy or electrical energy is one of the major inputs for the economic development of any country. It is the basic need and backbone of human activities in all sectors (industry, agriculture, transportation, etc.). Therefore, for sustainable development, high grade energy should be conserved and the utilization of renewable sources should be encouraged. Electricity consumption in vapour compression refrigeration systems can be reduced by cascading it with a vapour absorption system (VAS) as they simultaneously use both the high and low grade energy for refrigeration. Further, non-conventional sources of energy such as solar and geothermal can also be used to supply low grade energy for this system.

Cimsit and Ozturk (2012) determined that 48-51% less electrical energy is required in the cascaded refrigeration cycle as compared to the classical vapour compression refrigeration cycle. Wang *et al.* (2012) analysed the cascaded system using solar energy to supply heat in the generator and reported about 50% lower electricity consumption in the cascaded system. Fernandez-Seara *et al.* (2006) evaluated its adaptability in a cogeneration system and obtained a COP of 2.602 in the compression section. Seyfouri and Ameri (2012) showed that a cas-

caded system is more efficient and less energy consuming than a compression system to generate cooling at low temperature. Garimella *et al.* (2011) used a cascaded compression-absorption cycle for a naval ship application with a high temperature lift and observed 31% electrical energy reduction. Other researchers (Chinnappa *et al.,* 1993; Kairouani and Nehdi, 2006) have also analysed the potential of CRS to reduce electrical energy consumption compared to conventional VCS.

Published literature reveals that the CRS is analysed without considering the fouling conditions (rust formation and deposition of fluid impurities on heat transfer surfaces). These surface deposits increase thermal resistance, which reduce heat transfer, may impede fluid flow, and increase pressure drop across the heat exchanger which drops the overall performance of heat exchanger equipment. Therefore, fouling in the heat exchanger will increase the energy consumption and/or decrease cooling capacity along with the system efficiency. The main effect of fouling is to decrease the effectiveness of the heat exchanger. Thus, the overall conductance (UA) of the heat exchanger is decreased. Hence, another interpretation of fouling is to reduce the effective size of the heat exchanger. Ali and Ismail (2008) experimentally investigated the performance of a room air conditioner considering the evaporator fouling. The COP of the system was reduced by 43.6% with 330 gm of fouling materials. Pak *et al*. (2005) conducted an experimental study to investigate the effects of air-side fouling on the performance of various condenser coils used in the air conditioning system and found that the pressure drop was increased by 22 to 37%, and heat transfer performance was decreased by 4 to 5% for the double row heat exchangers. Bultman *et al.* (1993) found that the COP of VCS was

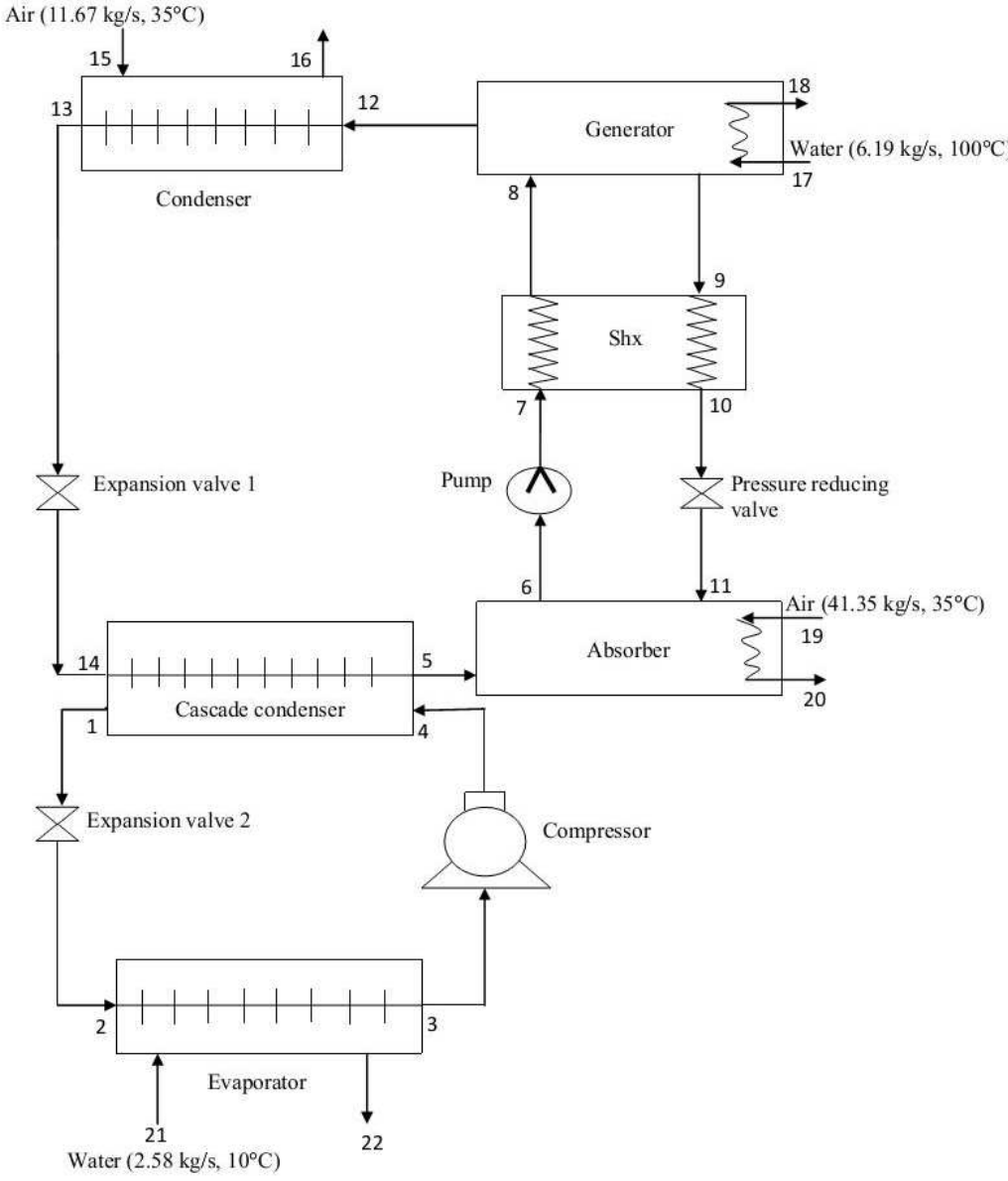

Figure 1: Schematic diagram of CRS

decreased by 7.6% when the air flow across the condenser was reduced by 40% for a constant speed fan. Bell and Groll (2011) experimentally observed 200% increment in air side pressure drop in a plate fin and micro channel coils while comparing clean and fouled conditions. Qureshi and Zubair (2011) developed a mathematical model to study the performance of a vapour compression refrigeration system under fouled conditions with alternative refrigerants.

Cascaded refrigeration systems can help to save electrical energy but relevant practical issues need to be understood (such as consequences of fouling) to ascertain these effects if such systems are to be employed in the future. Despite the importance of heat exchanger performance degradation due to fouling in a cascaded refrigeration system, a detailed analysis has not been found in the literature. Therefore, the objective of this paper is to present the effects of the consequences of condenser and evaporator outside fouling on the performance of a vapour compression-absorption cascaded refrigeration system as well as carry out an in-depth analysis of the data generated to ascertain any possible patterns. For this purpose, a property-dependent thermodynamic model that includes energy as well as exergy analysis was used. The exergy analysis is important along with the energy analysis for the process improvement of any refrigeration system (Sayyaadi and Nejatolahi, 2011). Exergy analysis accounts for the irreversibilities existing due to the finite temperature difference in the heat exchangers as well as the losses due to the non-isentropic compression and expansion in the compressors and the expansion valves, respectively.

2. Theoretical formulation of vapour compression-absorption cascaded refrigeration system

2.1 System selection

Figure 1 shows a vapour compression–absorption cascaded refrigeration system. In CRS, VCS and the single effect VAS are thermally connected in series by means of a heat exchanger called the cascade condenser. The evaporator of the compression section absorbs the refrigeration load from the water, to be cooled. The heat absorbed by the evaporator and the work input of the compressor is supplied to the evaporator of the absorption section in the cascade condenser. R22 and LiBr-Water are used as working fluid in the compression and absorption section respectively. The condenser and absorber of the proposed CRS are air cooled. The low pressure liquid refrigerant (water) of the absorption section is converted into vapour (steam) by absorbing the heat in the cascade condenser. This low pressure cold vapours i.e. steam is absorbed by the hot solution of LiBr in the absorber. The heat generated in the absorber is carried out by the circulating air. This weak solution of LiBr, being rich in refrigerant vapour, is pumped to the generator through a heat exchanger. The pump work is negligible as compared to the compressor work of the compression section as the specific volume of the liquid is extremely small compared to that of vapour. The main energy consumption in the absorption section is only in the generator in the form of low grade energy. Water (refrigerant) gets boils in the generator due to heat transfer. Since the salt does not exert any vapour pressure, the vapour leaving the generator is a pure 'refrigerant' (water vapour). Therefore, the analyser and dephlegmator do not form a part of the system. This high pressure water vapour is condensed in an air cooled condenser. The solution returning from the generator is a strong solution of LiBr in water. The pressure of this strong solution is reduced to absorber pressure through a pressure reducing valve.

2.2 Thermodynamic modelling of the vapour compression-absorption cascaded refrigeration system

The following assumptions are made in modelling the CRS (Cimsit and Ozturk, 2012):

1. The system is in a steady state.
2. All the pressure losses in different components of the system are neglected.
3. Heat loss in the suction and liquid lines are neglected in this work.
4. Refrigerant at the exit of the evaporator, cascade condenser and condenser is saturated vapour.
5. Isentropic efficiency of compressor is assumed as constant.
6. The processes occurring in the expansion valves are isenthalpic.

Thermodynamic modelling includes the following set of governing equations for a particular system component:

(i) Mass balance, $\sum \dot{m} = 0$; $\sum x\dot{m} = 0$

(ii) Energy balance, $\sum \dot{Q} + \sum \dot{W} + \sum \dot{m}\, h = 0$

(iii) Entropy generation rate, $\dot{S}_{gen} = \sum \dot{m} s_{out} - \sum \dot{m} s_{in} - \sum \frac{\dot{Q}}{T} \geq 0$

Applying these three fundamental equations to all the components of a CRS, the governing equations in the modelling of individual components are given in Table 1. The irreversible loss due to entropy generation is determined by means of the Gouy-Stodola law:

$$\dot{I} = T_o \dot{S}_{gen} \tag{1}$$

The total irreversibility of the system is given by:

$$\dot{I}_t = \dot{I}_{ev1} + \dot{I}_{evap} + \dot{I}_{cascade} + \dot{I}_{comp} + \dot{I}_a + \dot{I}_p + \dot{I}_{SHX} + \dot{I}_g + \dot{I}_{prv} + \dot{I}_{cond} + \dot{I}_{ev2} \tag{2}$$

Circulation ratio, $f = \dot{m}_6/\dot{m}_{ref,VARS}$ (3)

The COP of various systems is given by:

$$COP_{VCS} = \dot{Q}_{evap}/\dot{W} \quad (4)$$

$$COP_{VARS} = \dot{Q}_{cascade}/(\dot{Q}_g + \dot{W}_p) \quad (5)$$

$$COP_{CRS} = \dot{Q}_{evap}/(\dot{W} + \dot{Q}_g + \dot{W}_p) \quad (6)$$

Efficiency defect is defined as the ratio between the exergy flow destroyed in each component and the exergy flow required to sustain the process. Efficiency defect (δ_k) of k^{th} component of the system is expressed as (Gomri and Hakmi, 2008):

$$\delta_k = \dot{I}_k/(\dot{W} + \dot{Q}_g\theta_{Carnot} + \dot{W}_p) \quad (7)$$

where, Carnot factor $\theta_{Carnot} = 1 - T_o/T_g$

The thermodynamic perfection of the process is measured by rational efficiency which can be defined as (Nikolaidis and Probert, 1998):

$$\eta_R = 1 - \sum \delta_k \quad (8)$$

In the present paper, the effect of the evaporator's and condenser's outside fouling is taken into account. The effect of fouling is to reduce the heat transferred by the heat exchangers. As one of the fluids is undergoing a phase change, the following equation (from heat exchanger theory) is applied (Qureshi and Zubair, 2011):

$$UA = \dot{C}_{min} \ln \frac{1}{1-\epsilon} \quad (9)$$

The term UA in the heat transfer rate equation, $\dot{Q} = \dot{U}A(T_{hot} - T_{cold})$ is called the overall conductance. In Eq. (9), $\dot{C}_{min}$ is the thermal capacitance rate ($\dot{m}c_p$)of the fluid which is not undergoing a phase change. The value of UA will decrease due to fouling and can be presented as a percentage UA_{per} by the following equation:

$$UA_{per} = \left(1 - \frac{UA}{UA_{cl}}\right) 100 \quad (10)$$

In the present work, the percentage decrease in the UA value due to fouling was varied from 0 to 50% for evaporator and condenser, where zero value refers to clean conditions.

2.3 Model validation

The thermodynamic model equations given in Table 1 are highly nonlinear in nature and have been solved numerically in Engineering Equation Solver (EES). The thermophysical properties of refrigerants are taken from built-in functions. In CRS, VCS and VAS are connected in series where condenser of the compression section rejects heat to the evaporator of the absorption section. Models of VCS, VAS and CRS are individually validated.

Qureshi and Zubair (2011) have studied the effect of fouling on VCS using R134a as refrigerant. Table 2 shows the comparison of the current model results with Qureshi and Zubair (2011) for same input conditions. The percentage error in the results is within 0.03%.

The results of the thermodynamic model of VAS are compared with those by Kaynakli and Kilic (2007). The following set of data is used to generate the results for comparison purposes: T_{cond} = 35°C, T_a = 40°C, T_g = 90°C, T_{evap} = 5°C, $\dot{Q}_{evap}$ = 10 kW, η_p = 0.95 and ε = 0.7. Water-LiBr is considered as the working pair. The percentage error found in the prediction of COP is 2.60%. The large error in prediction of COP is due to usage of different correlations to determine the thermophysical properties of Water-LiBr. In this paper, the thermophysical properties of Water-LiBr are taken from built-in functions of EES.

Data from the work of Cimsit and Ozturk (2012) related to CRS was also used for the verification of the current CRS model. The following set of data was used to generate the results for comparison purposes: T_{cond} = 40°C, T_a = 40°C, T_g = 90°C, T_{evap} = 10°C, $\dot{Q}_{evap}$ = 50 kW, η_p = 0.90, η_{isen} = 0.80 and ε = 0.6. Water-LiBr is assumed as the working fluid in the absorption section and R134a is considered in the compression section. The maximum error in the prediction of calculated parameters is found to be 1.6% (Table 3).

3. Results and discussion

The thermodynamic model has been applied to evaluate the performance of a typical CRS as shown in Figure 1. The values of inputs as obtained by the literature survey are given in Table 4. Thermodynamic properties at inlet and outlet of each component of the CRS are presented in Table 5 for clean conditions. The main purpose of a CRS is to reduce the consumption of electricity in the compressor of the vapour compression section. This is done by lowering the temperature of the condenser of VCS. The following values can be predicted for VCS operating under the same conditions as mentioned in Table 4: T_{evap} = 0.4°C, T_{cond} = 46.8°C, $\dot{m}_{ref}$ = 0.5687 kg/s, η_v = 95.33%, $\dot{W}$ = 27.94 kW, $\dot{Q}_{cond}$ = 111.03 kW and COP = 2.972.

When we compare the performance of a CRS with a VCS operating under the same conditions (Table 4), it can be shown that refrigerant (R22) mass flow rate in CRS is reduced by 19.81%. The present thermodynamic model predicts the condenser and evaporator temperatures for both the VCS and the CRS. Based on the cooling capacity

Table 1: Governing equations at different components of CRS

Component	First law equations	Second law equations
Evaporator	$\dot{Q}_{evap} = (\epsilon\dot{C})_{evap}(T_{in,evap} - T_{evap}) = \dot{m}_{ref,VCS}(h_3 - h_2) = (\dot{m}_{ef}c_p)_{evap}(T_{in,evap} - T_{out,evap})$	$\dot{I}_{evap} = T_o\dot{S}_{gen,evap}$ $\dot{S}_{gen,evap} = \dot{m}_{ref,VCS}(s_3 - s_2) + (\dot{m}_{ef}c_p)_{evap}\ln\frac{T_{22}}{T_{21}}$
Compressor	$\dot{W} = \dot{m}_{ref,VCS}(h_4 - h_3)/\eta_{isen}$ $\eta_v = 1 - r\left(\frac{v_3}{v_4} - 1\right) = \frac{Vo_3}{Piston\ displacement}$	$\dot{I}_{comp} = T_o\dot{S}_{gen,comp}$ $S_{gen,comp} = m_{ref,VCS}(s_4 - s_3)$
Cascade condenser	$\dot{Q}_{cascade} = \dot{m}_{ref,VAS}(h_5 - h_{14}) = \dot{m}_{ref,VCS}(h_4 - h_1)$ $T_5 = T_1 - \Delta T_{overlap}$	$\dot{I}_{cascade} = T_o\dot{S}_{gen,cascade}$ $\dot{S}_{gen,cascade} = \dot{m}_{ref,VCS}(s_1 - s_4) + \dot{m}_{ref,VAS}(s_5 - s_{14})$
Expansion valve 2	$h_1 = h_2$	$\dot{I}_{ev2} = T_o\dot{S}_{gen,ev2}$ $\dot{S}_{gen,ev2} = \dot{m}_{ref,VCS}(s_2 - s_1)$
Absorber	$\dot{m}_5 + \dot{m}_{11} = \dot{m}_6$ $c_9\dot{m}_{11} = c_6\dot{m}_6$ $\dot{m}_{ref,VAS}h_5 + \dot{m}_{11}h_{11} = \dot{m}_6h_6 + \dot{Q}_a$ $\dot{Q}_a = \dot{m}_{ef,a}(h_{20} - h_{19})$	$\dot{I}_a = T_o\dot{S}_{gen,a}$ $\dot{S}_{gen,a} = \dot{m}_6s_6 - \dot{m}_{ref,VAS}s_5 - \dot{m}_9s_{11} + (\dot{m}_{ef}c_p)_a\ln\frac{T_{20}}{T_{19}}$
Pump	$W_p = (P_{12} - P_5)\dot{m}_6/\rho\eta_p$ $\dot{m}_7h_7 = \dot{m}_6h_6 + \dot{W}_p$	$\dot{I}_p = T_o\dot{S}_{gen,p}$ $\dot{S}_{gen,p} = \dot{m}_6(s_7 - s_6)$
Solution heat exchanger	$\dot{m}_9h_9 - \dot{m}_{10}h_{10} = \dot{m}_8h_8 - \dot{m}_7h_7$ $\varepsilon = (T_9 - T_{10})/(T_9 - T_7)$	$\dot{I}_{SHX} = T_o\dot{S}_{gen,shx}$ $\dot{S}_{gen,shx} = \dot{m}_6(s_8 - s_7) + \dot{m}_9(s_{10} - s_9)$
Generator	$\dot{m}_8 = \dot{m}_9 + \dot{m}_{ref,VAS}$ $\dot{m}_{ref,VAS}h_{12} + \dot{m}_9h_9 = \dot{m}_8h_8 + \dot{Q}_g$ $\dot{Q}_g = \dot{m}_{ef,g}(h_{17} - h_{18})$	$\dot{I}_g = T_o\dot{S}_{gen,g}$ $\dot{S}_{gen,g} = \dot{m}_9s_9 + \dot{m}_{ref,VARS}s_{12} - \dot{m}_6s_8 + (\dot{m}_{ef}c_p)_g\ln\frac{T_{18}}{T_{17}}$
Pressure reducing valve	$h_{10} = h_{11}$	$\dot{I}_{prv} = T_o\dot{S}_{gen,prv}$ $\dot{S}_{gen,prv} = \dot{m}_9(s_{11} - s_{10})$
Condenser	$\dot{Q}_{cond} = (\epsilon\dot{C})_{cond}(T_{cond} - T_{in,cond}) = \dot{m}_{ref,VAS}(h_{12} - h_{13}) = (\dot{m}_{ef}c_p)_{cond}(T_{out,cond} - T_{in,cond})$	$\dot{I}_{cond} = T_o\dot{S}_{gen,cond}$ $\dot{S}_{gen,cond} = \dot{m}_{ref,VAS}(s_{13} - s_{12}) + (\dot{m}_{ef}c_p)_{cond}\ln\frac{T_{16}}{T_{15}}$
Expansion valve 1	$h_{13} = h_{14}$	$\dot{I}_{ev1} = T_o\dot{S}_{gen,ev1}$ $\dot{S}_{gen,ev1} = \dot{m}_{ref,VARS}(s_{14} - s_{13})$

Table 2: Comparison of performance data of the current model of VCS with Qureshi and Zubair (2011)

Condition	$\dot{m}_{ref}$ (kg/s)	$\dot{m}_{ref,m}$ (kg/s)	error (%)	$\dot{W}$ (kW)	$\dot{W}_m$ (kW)	error (%)	$\dot{Q}_{evap}$ (kW)	$\dot{Q}_{evap,m}$ (kW)	error (%)	COP	COP_m	error (%)
Clean condition	0.9067	0.9068	-0.01	60.109	60.113	-0.01	100	100	0.00	1.664	1.664	0.00
Evaporator fouling	0.7992	0.7993	-0.01	55.049	55.064	-0.03	88.84	88.85	-0.01	1.614	1.614	0.00
Condenser fouling	0.9140	0.914	0.00	64.142	64.154	-0.02	91.24	91.24	0.00	1.422	1.422	0.00
Both evaporator & condenser fouling	0.8095	0.8095	0.00	58.580	58.598	-0.03	82.3	82.32	-0.02	1.405	1.405	0.00

and the effectiveness of the evaporator, the evaporator temperature for the systems is 0.4°C. The predicted condenser temperatures are 46.8°C and 45.4°C for VCS and CRS respectively. The reduction in the condenser temperature also gives a lower temperature of air at the condenser exit after cooling. Table 6 represents the values of performance parameters for the CRS.

Table 3: Comparison of performance data of the current model of CRS with Cimsit and Ozturk (2012)

Parameter	*Current CRS model*	*Cimsit and Ozturk (2012)*	*Error (%)*
$\dot{Q}_a$ (kW)	73.13	72.76	-0.51
$\dot{Q}_g$ (kW)	76.79	76.45	-0.44
$\dot{Q}_{cond}$ (kW)	61.20	61.06	-0.23
$\dot{W}$ (kW)	8.38	8.25	-1.58
COP_{VCS}	5.963	6.061	1.62
COP_{VCAS}	0.749	0.750	0.13
COP_{CRS}	0.587	0.590	0.51

The generator heat transfer rate is 130.60 kW which is highest. The heat transfer rates in the condenser and absorber are 98.04 kW and 124.70 kW respectively. The effect of the pump on the total energy inputs is found to be negligible. The prescribed temperature (T_5) for refrigerant (water vapour) and degree of overlap are 10°C and 8°C respectively in the cascade condenser. Thus, the refrigerant (R22) reached a temperature of 18°C at the exit of the cascade condenser. The power consumption is reduced by 67.5% in the compressor of CRS as compared to equivalent VCS. The volumetric efficiency of compressor is also increased by 3.4%. As subsystems of CRS, COP of vapour compression and vapour absorption subsystems are 9.173 and 0.705 respectively. Higher value of COP for the vapour compression refrigeration subsystem is due to low refrigerant temperature at the compressor exit which leads to reduction in electricity requirement of the compressor. The heat rejection in the condenser of CRS is reduced by 11.6% as compared to VCS.

Table 6 also shows the irreversibility rate of the system components. From an irreversibility rate point of view, the most sensitive component in compression and absorption sections of a CRS are compressor and generator. Their irreversibility contributes 15.5% and 19.4% respectively in total irreversibility of system (at clean condition). It is also apparent that the most efficient components of a CRS are pump and pressure reducing valve in which approximate zero entropy generation is observed. In the decreasing order of irreversible loss, these components can be arranged in the sequence as generator, absorber, compressor, cascade condenser, condenser, evaporator, solution heat exchanger, expansion valves, pump and pres-

Table 4: Value of inputs in the model of the CRS

Parameters	*Values*
Evaporator coolant inlet temperature ($T_{in,evap}$ in °C)	10
Evaporator coolant mass flow rate ($\dot{m}_{ef,avap}$ in kg/s)	2.58
Condenser coolant inlet temperature ($T_{in,cond}$ in °C)	35
Condenser coolant mass flow rate ($\dot{m}_{ef,cond}$ in kg/s)	11.67
Generator coolant inlet temperature ($T_{in,g}$ in °C)	100
Generator coolant outlet temperature ($T_{out,g}$ in °C)	95
Generator temperature (T_g in °C)	90
Absorber coolant inlet temperature ($T_{in,a}$ in °C)	35
Absorber coolant outlet temperature ($T_{out,a}$ in °C)	38
Absorber temperature (T_a in °C)	40
Rate of heat absorbed by evaporator ($\dot{Q}_{evap}$ in kW)	83.09
Effectiveness of evaporator and condenser at clean condition ( )	0.8
Capacitance rate of external fluid at evaporator ($\dot{C}_{evap}$ in kW/K)	10.81
Capacitance rate of external fluid at condenser ($\dot{C}_{cond}$ in kW/K)	11.73
Temperature at exit of cascade condenser (T_5 in °C)	10
Effectiveness of shx (ε_{shx}) 0.6	
Isentropic efficiency of compressors (η_{isen})	0.65
Electrical efficiency of pump (η_p)	0.9
Degree of overlap in cascade condenser ($T_{overlap}$) in °C)	8
Environmental temperature (T_o in °C)	25
Atmospheric pressure (P_o in kPa)	101.325

Table 5: Value of thermodynamic properties at clean condition

State point	T (°C)	P (kPa)	$\dot{m}$ (R22) (kg/s)	$\dot{m}$ (H_2O) (kg/s)	$\dot{m}$ (LiBr-H_2O) (kg/s)	$\dot{m}$ (Air) (kg/s)	h (kJ/kg)	s (kJ/kg/K)
1	18.0	860.50	0.4561				223.0	1.080
2	0.4	504.50	0.4561				223.0	1.084
3	0.4	504.50	0.4561				405.1	1.750
4	35.2	860.50	0.4561				425.0	1.773
5	10.0	1.228		0.0395			2519.0	8.899
6	40.0	1.228			0.5331		94.05	0.246
7	40.0	9.813			0.5331		94.06	0.246
8	66.4	9.813			0.5331		148.50	0.413
9	90.0	9.813			0.4936		211.10	0.512
10	60.0	9.813			0.4936		152.30	0.343
11	60.0	1.228			0.4936		152.30	0.343
12	90.0	9.813		0.0395			2668.0	8.404
13	45.4	9.813		0.0395			190.30	0.644
14	10.0	1.228		0.0395			190.30	0.674
15	35.0	101.325				11.67	308.60	5.729
16	43.3	101.325				11.67	317.0	5.756
17	100.0	101.325		6.1990			419.10	1.307
18	95.0	101.325		6.1990			398.0	1.250
19	35.0	101.325				41.35	308.60	5.729
20	38.0	101.325				41.35	311.60	5.738
21	10.0	101.325		2.580			42.09	0.151
22	2.3	101.325		2.580			9.88	0.035

Table 6: Value of performance parameters at clean condition

S. no	Performance parameters		Value of clean condition
1	Low grade energies	$\dot{Q}_{cond}$ (kW)	98.04
		$\dot{Q}_a$ (kW)	124.70
		$\dot{Q}_g$ (kW)	130.60
		$\dot{Q}_{evap}$ (kW	83.09
		$\dot{Q}_{cascade}$ (kW)	92.15
2	High grade energies	$\dot{W}$ (kW)	9.05
		$\dot{W}_p$ (kW)	0.003
3	First law parameters	COP_{CRS}	0.594
		COP_{VCS}	9.173
		COP_{VAS}	0.705
4	Second law parameters	$\dot{I}_{comp}$ (kW)	3.10
		$\dot{I}_{cascade}$ (kW)	2.84
		$\dot{I}_{ev2}$ (kW)	0.50
		$\dot{I}_{evap}$ (kW)	1.89
		$\dot{I}_a$ (kW)	3.62
		$\dot{I}_p$ (kW)	0.001
		$\dot{I}_g$ (kW)	3.87
		$\dot{I}_{shx}$ (kW)	1.68
		$\dot{I}_{prv}$ (kW)	0
		$\dot{I}_{evi}$ (kW)	0.35
		$\dot{I}_{cond}$ (kW)	2.04
		$\dot{I}_t$ (kW)	19.95
		η_R (%)	38.5
5	Other parameters		13.5
		η_v (%)	98.6

sure reducing valve. The total irreversibility rate for the entire CRS and rational efficiency are 19.95 kW and 38.5% respectively.

The total fixed cost of the CRS increases due to addition of VAS components, but the running cost will decrease due to small electricity consumption in compressor and utilization of low grade energy in the generator. The hot water obtained from the solar energy is assumed to be the source of heat for the generator of VAS in the present analysis.

3.1 Effect of evaporator fouling

The effects of evaporator fouling on the performance characteristics of CRS are shown in Figures 2 to 4. Evaporator conductance is varied from 0 to 50%, where 0 refers to clean condition. The main effect of fouling is to decrease the value of UA, which in turn, decreases the effectiveness of the heat exchanger. The effectiveness of the evaporator in a clean condition is assumed to be 0.8 and it is decreased up to 0.55, when evaporator conductance is reduced by 50%. It is observed from Figure 2 that there is 31% reduction in its effectiveness which directly lowers the cooling capacity of the system. The reduction in evaporator effectiveness caused the evaporator temperature to decrease from 0.4°C to -2.5°C, while keeping the inlet temperature of external fluid to be cooled as constant. Further, it also decreased the temperature of cas-

cade condenser (T_1) and condenser temperature (T_{13}) from 18°C to 17.3°C and 45.4°C to 44.5°C respectively. Moreover, as the evaporator temperature is decreased, the specific volume of the refrigerant at the compressor inlet is increased. Therefore, volumetric efficiency of the compressor is decreased by 0.27% with 50% reduction in evaporator conductance, as depicted in Figure 2.

Figure 3 shows the effect of evaporator fouling on low grade and high grade energies. Cooling capacity of the system is decreased from 83.09 kW to 74.93 kW and the outlet temperature of external fluid i.e. water to be cooled is increased from 2.3°C to 3.0°C with 50% reduction in evaporator conductance. Reduction in the cooling capacity of the system due to fouling also lowers the thermal load in the absorption section of the cascaded system. Figure 3 shows that the thermal load is decreased by 8.5% with the 50% reduction in evaporator conductance. Therefore, the heat load in the generator, absorber and condenser of the absorption section is also decreased. The % variation in the reduction of heat load at absorber, condenser and generator is the same as that of the cascade condenser because their variation ultimately depends on the variation in heat load a thet cascade condenser. Moreover, the mass flow rate of external fluids flowing in the absorber and generator is also decreased due to

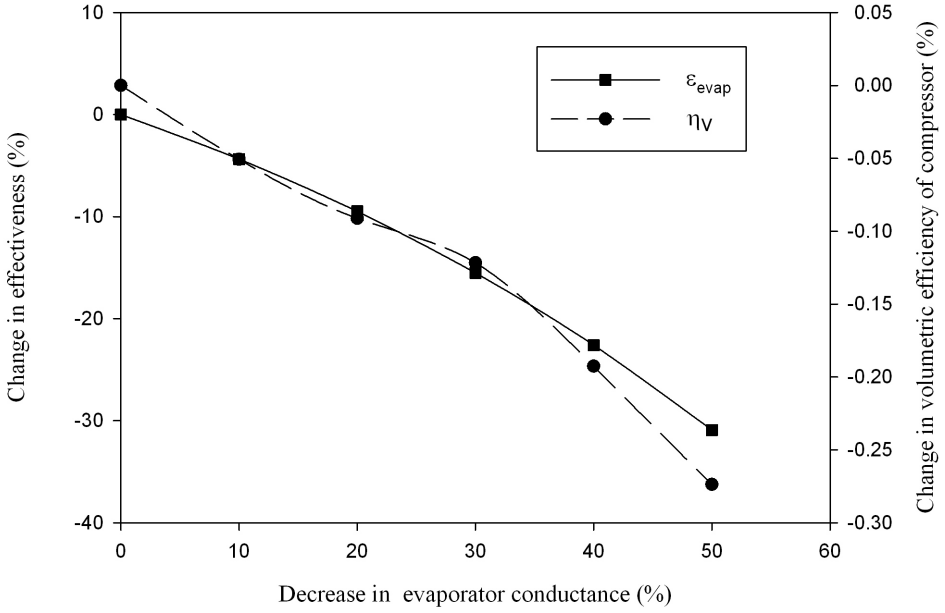

Figure 2: Effect of UA degradation of evaporator on its effectiveness and volumetric efficiency of compressor

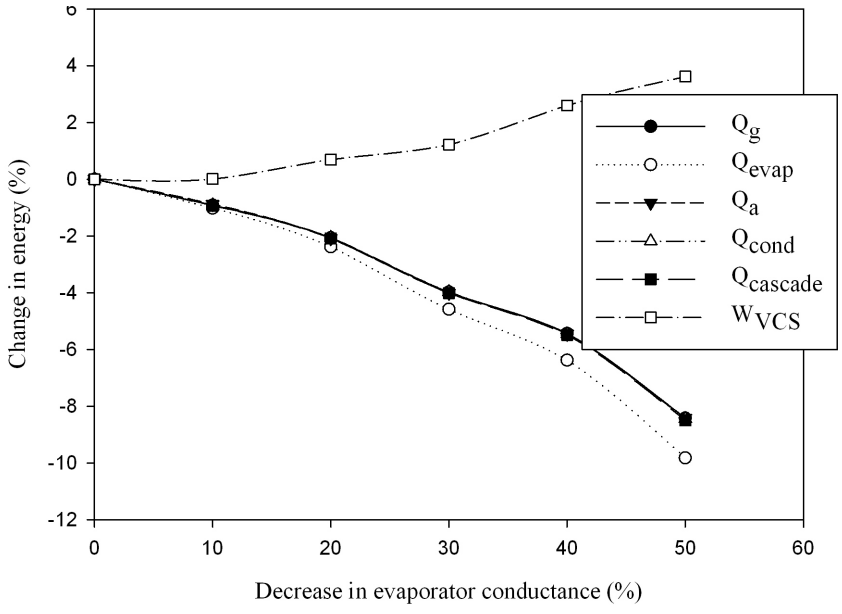

Figure 3: Figure 3: Effect of UA degradation of evaporator on high grade and low grade energies

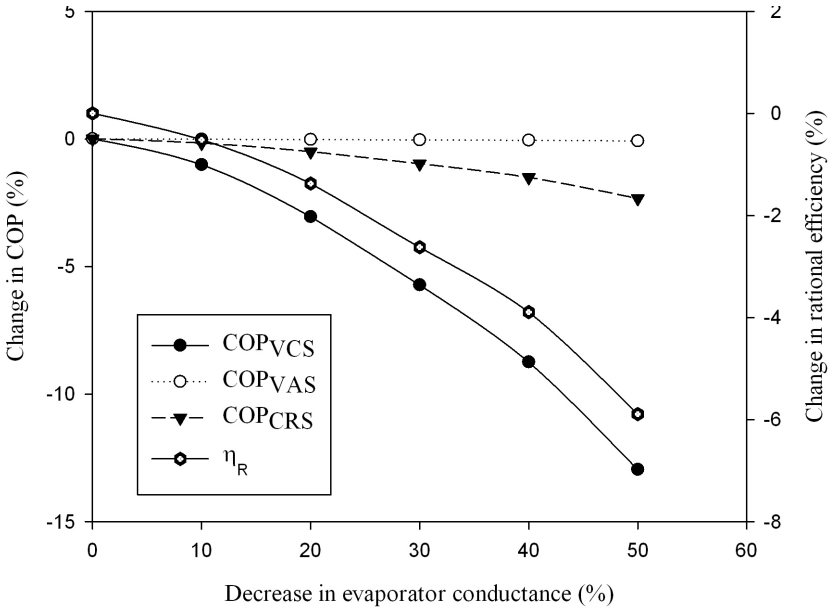

Figure 4: Figure 4: Effect of UA degradation of evaporator on COP and rational efficiency

lower heat load. Lower heat load in the condenser also caused a substantial drop of air temperature at condenser exit. Increase in specific volume of refrigerant at the compressor inlet due to evaporator fouling increased the electric power consumption (compressor work) in compressor by 3.6%. The present cascaded system saves 67.5% of compressor work in VCS at clean condition. But due to fouling, it would now be able to save 66.4% of compressor work.

Figure 4 depicts the variation of COP of system with evaporator conductance. As discussed for Figure 3, evaporator fouling decreased the cooling capacity and increased the electric power consumption in compressor; it is obvious to see that COP of the compression section is decreased due to evaporator fouling. COP of the compression section is reduced by 12.9% with 50% reduction in evaporator conductance. COP of the absorption section strongly depends on thermal load at cascade condenser and heat required in the generator. Figure 3 shows variation in the heat load of the generator and is almost the same as that in the cascade condenser. Hence, COP of the absorption section remained constant with evaporator fouling. COP of the cascaded system depends on its cooling capacity, electric power consumption in compressor of compression section and heat load on generator. The overall effect of all these parameters is to decrease the COP of cascaded system. There is a 2.3% fall in overall COP of CRS with 50% reduction in evaporator conductance.

The irreversibility in the evaporator is increased by 42.4% due to 50% reduction in evaporator conductance. Rational efficiency denotes the degree of thermodynamic perfection of the process. As shown in Figure 4, rational efficiency for CRS is decreased from 38.5% to 36.2% for 50% reduction of evaporator conductance.

3.2 Effect of condenser fouling

The effect of only condenser conductance on the performance parameters of CRS are shown in Figures 5 to 7. The evaporator is assumed to be clean in this section. The effectiveness of the condenser at a clean condition is 0.8 and it is decreased by 30.9% with 50% reduction in condenser conductance. Figure 5 shows the variation of effectiveness of condenser and volumetric efficiency of compressor with condenser conductance. The effectiveness of the condenser is decreased which increased the temperature of the condenser from 45.4°C to 50.0°C. It further caused the temperature of the cascade condenser and evaporator to increase by 19.6% and 48.8%. The pressure ratio across the compressor in clean condition is 1.70 and it increased to 1.86 with 50% reduction in condenser conductance. This 9.4% increase in the pressure ratio lowered the volumetric efficiency of compressor by 0.3%.

Increase in pressure ratio across the compressor increased the compressor work by 17.5% as shown in Figure 6, which decreased the saving in electricity consumption by 8.7% as compared to clean conditions. Moreover, the cooling capacity of the system is decreased by 2% as shown in Figure 6 and it further increased the temperature of the chilled water at the evaporator exit by 6.5%. However, reduction in the condenser conductance decreased the other low grade energies. The percentage change in the variation of generator, absorber and cascade condenser depends on % variation in the condenser heat load. Hence, their variation is almost the same.

Figure 7 presents the variation of COP of the system with decrease in condenser conductance.

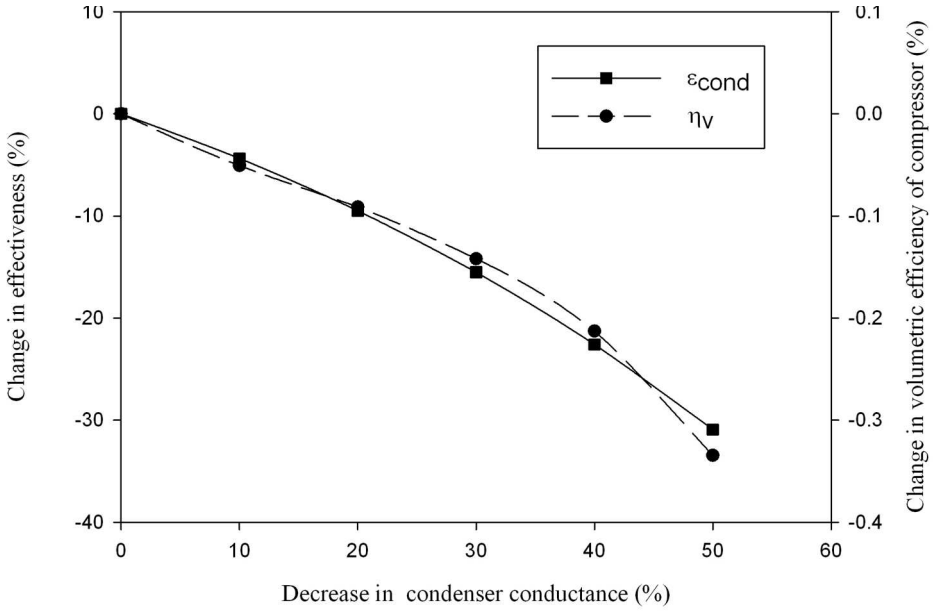

Figure 5: Effect of UA degradation of condenser on its effectiveness and volumetric efficiency of compressor

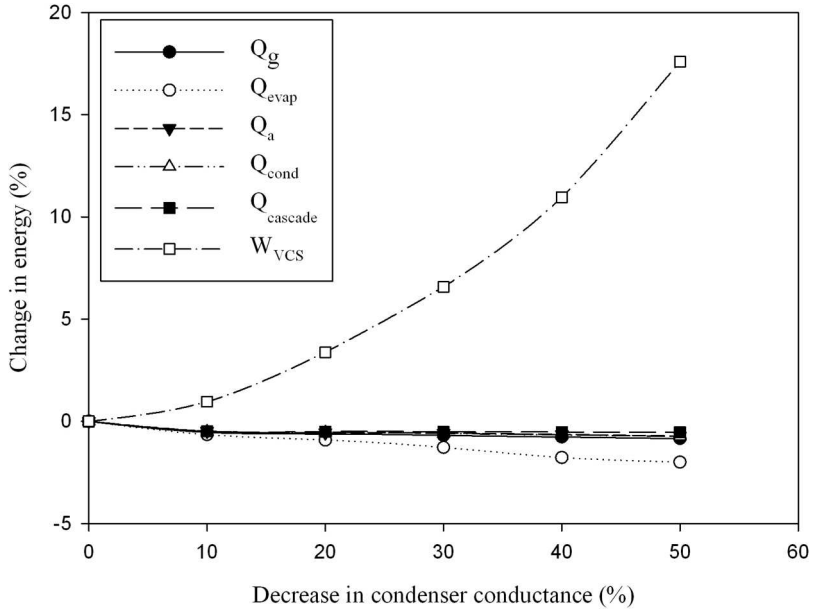

Figure 6: Effect of UA degradation of condenser on high grade and low grade energies

Condenser fouling causes the cooling capacity of evaporator to decrease and compressor work to increase. Hence, COP of the compression section decreases with condenser fouling. There is 16.6% reduction in COP of the compression section with 50% reduction in condenser conductance. COP of the vapour absorption section slightly increases with condenser fouling. COP of absorption section mainly depends on thermal load at cascade condenser and generator. Thermal load in generator and cascade condenser is decreased by 0.8% and 0.5% respectively. Hence, their overall effect is to increase the COP of absorption section. The COP of CRS is decreased by 2.6% with 50% reduction in condenser conductance. Hence, condenser fouling is more severe as compare to evaporator fouling.

The high temperature gradient inside the condenser due to its fouling caused its irreversibility to increase by 62.1%. The overall irreversibility of system is increased by 8.2% and the rational efficiency of system is decreased by 5.5%, with 50% reduction in condenser conductance.

3.3 Combined effect of evaporator and condenser fouling

The effect of both evaporator and condenser fouling are considered in this section. Figure 8 to 10 shows the variation of performance parameters of the system with equal degradation in the evaporator and condenser. The effectiveness of both the

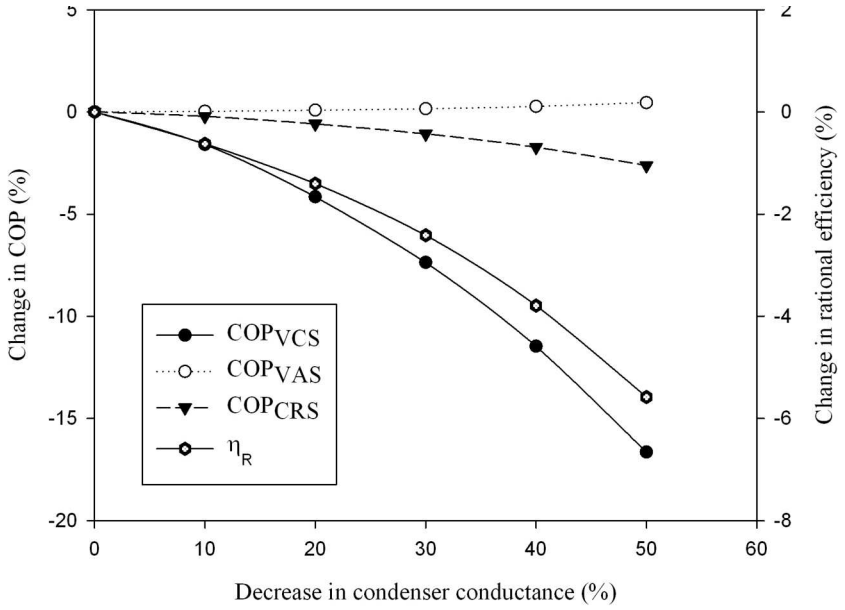

Figure 7: Effect of UA degradation of condenser on COP and rational efficiency

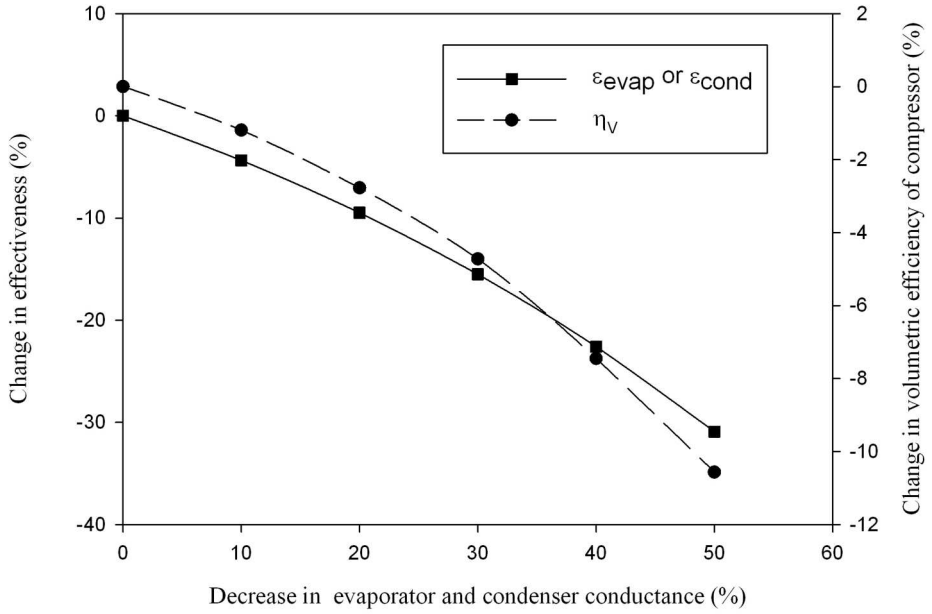

Figure 8: Effect of UA degradation of evaporator and condenser on their effectiveness and volumetric efficiency of compressor

components is decreased by 30.9% with 50% reduction in their conductance. It caused the temperature of the evaporator to decrease from 0.4°C to -2.3°C, whereas the condenser temperature is increased from 45.4°C to 48.8°C. It also increased the temperature of the cascade condenser from 18°C to 20.6°C.

Figure 8 shows that the volumetric efficiency of the compressor is decreased by 0.6% with 50% reduction in evaporator and condenser conductance. Reduction in the evaporator temperature further caused the specific volume of refrigerant to increase by 9.9%. The pressure ratio across the compressor reached to 2.10 at this point. Hence, compressor work is increased from 9.06 kW to 10.80 kW. Thus, CRS is able to save only 61.3% of electric power as compared to 67.5% in clean condition.

Figure 9 depicts that the variation in the thermal loads at the condenser, absorber, generator and cascade condenser and are almost the same. The cooling capacity of the evaporator is decreased by 10.9% and the heat rejected in the condenser is 90.03 kW under this situation whereas this magnitude was 97.32 kW under the case of condenser fouling only.

Figure 10 presents the variation of COP of the system with decrease in evaporator and condenser conductance. COP of the compression section is decreased with reduction in evaporator and condenser conductance. The trend is obvious due to

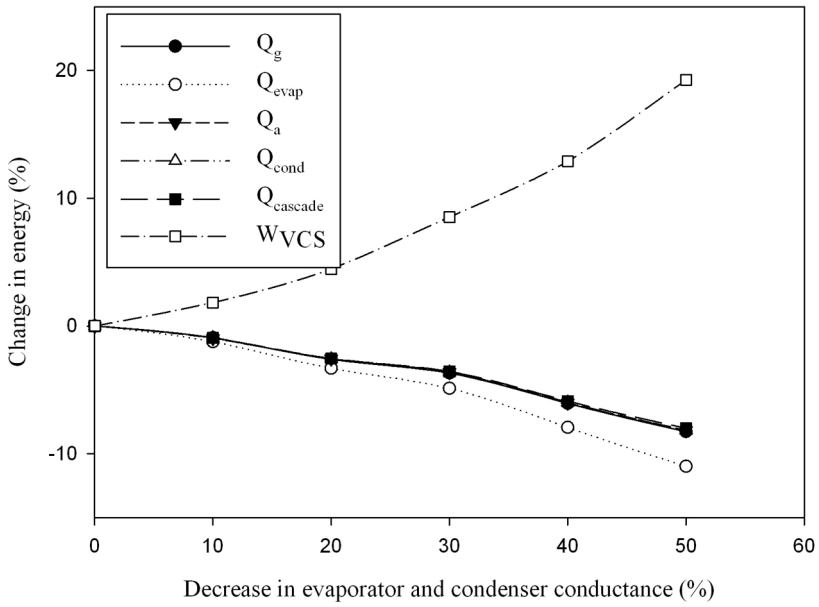

Figure 9: Effect of UA degradation of evaporator and condenser on high grade and low grade energies

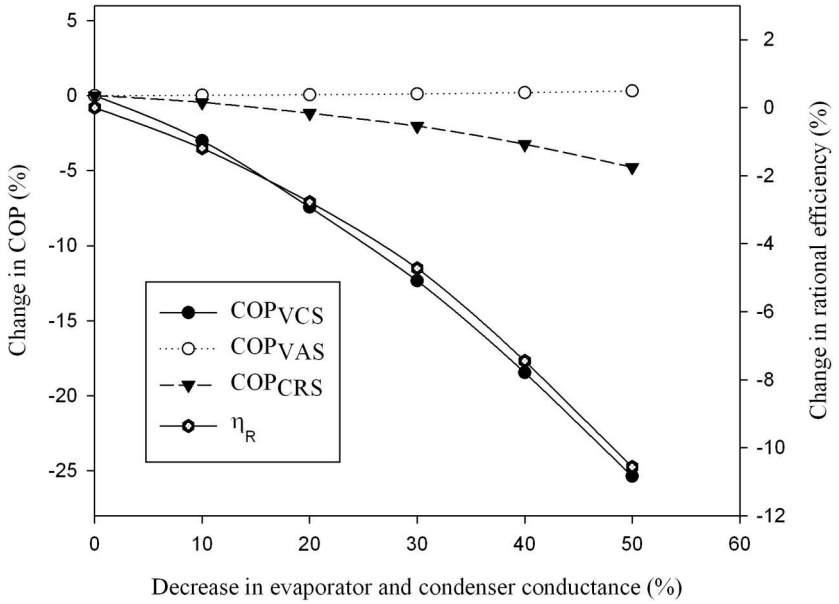

Figure 10: Effect of UA degradation of evaporator and condenser on COP and rational efficiency

reduction in cooling capacity and increment in compressor work with evaporator and condenser fouling. The COP of compression section is reduced by 25.3% with 50% reduction in evaporator and condenser conductance. COP of the absorption section is slightly increased with evaporator and condenser fouling. COP of the absorption section mainly depends on thermal loads at cascade condenser and generator. Thermal load at the generator is decreased by 8.26% whereas it is decreased by 8.1% at cascade condenser. Hence, their overall effect is to slightly increase the COP of the absorption section. The total COP of CRS is decreased by 4.7% with degradation in evaporator and condenser performance of 50% reduction in evaporator and condenser conductance.

The irreversible loss in the evaporator and condenser is increased by 38.4% and 39.1% respectively. Hence, the condenser is more sensitive as compared to the evaporator. The total irreversibility of CRS is increased by 5.9% with evaporator and condenser fouling. The rational efficiency of the system is decreased by 10.5% with 50% reduction in evaporator and condenser conductance as depicted by Figure 10.

4. Conclusions

In this paper, an extensive thermodynamic study of a vapour compression-absorption cascaded refrigeration system under fouled conditions has been presented and it is concluded that:

1. Electric power requirement in VCS is reduced by

67.5%, when it is cascaded with an absorption system in clean condition.
2. Electric power saving by CRS is decreased, when the evaporator and/or condenser foul. Degradation in their performance also decreased the cooling capacity of the system. When both the components foul, the saving in electricity consumption is reduced by 9.22%.
3. The heat load at generator, absorber, and condenser is decreased, when the evaporator and/or condenser foul.
4. COP of the compression section and total COP of CRS are decreased with degradation in the performance of evaporator and/or condenser whereas COP of the absorption section is decreased only in case of evaporator fouling. The total COP of the system decreased by 4.7%, when both these components foul.
5. Irreversibility which can be viewed as the wasted work potential is increased drastically in the evaporator and condenser when their individual fouling is taken into consideration. The irreversibility in the evaporator is increased by 42.4% due to its fouling whereas the high temperature gradient inside the condenser due to its fouling caused its irreversibility to increase by 62.1%. Further, the rational efficiency of the system is decreased by 10.5% when both the components foul.

Nomenclature

C	Heat capacitance rate of external fluid (kW/K)
c	Concentration of LiBr solution (kg LiBr/ kg water)
c_p	Specific heat at constant pressure (kJ/kg K)
COP	Coefficient of performance
f	Circulation ratio
$\dot{h}$	Specific enthalpy (kJ/kg)
$\dot{I}$	Irreversibility rate (kW)
$\dot{m}$	Mass flow rate (kg/s)
P	Pressure (kPa)
Q	Heat transfer rate (kW)
$\dot{\tau}$	Ratio of clearance volume to the displacement volume
s	Specific entropy (kJ/kg K)
S_{gen}	Entropy generation rate (kW/K)
T	Temperature (°K)
UA	Overall conductance (kW/K)
UA_{per}	Percentage overall conductance (%)
υ	Specific volume (kg/m^3)
V_o	Volumetric flow rate (m^3/s)
W	Power input (kW)

Greek symbols

ε	Effectiveness of heat exchanger
η	Efficiency
δ	Efficiency defect
θ_{carnot}	Carnot factor
ρ	Density of LiBr solution (kg/m^3)

Subscripts

a	absorber
cascade	cascade
cl	clean condition
comp	compressor
cond	condenser
ef	external fluid
ev	expansion valve
evap	evaporator
g	generator
in	inlet condition
isen	isentropic
m	results of current model
o	environmental condition
out	outlet condition
p	pump
prv	pressure reducing valve
R	rational
ref	refrigerant
shx	solution heat exchanger
t	total
v	volumetric
1,2,3….	state points

References

Ali, A.H.H. and Ismail, I.M. (2008). Evaporator air side fouling effect on performance of room air conditioners and impact on indoor air quality. *HVAC and R Research,* 14(2): 209-219.

Bell, I.H. and Groll, E.A. (2011). Air side particulate fouling of micro-channel heat exchangers: experimental comparison of air side pressure drop and heat transfer with plate fin heat exchanger. *Applied Thermal Engineering,* 31: 742-749.

Bultman, D.H., Burmeister, L.C., Bortane, V. and Tenpas, P.W. (1993). Vapour-compression refrigerator performance degradation due to condenser air flow blockage. *ASME* 93-HT-34: 1-13.

Chinnappa, J.C.V., Crees, M.R. and Murthy, S.S. (1993). Solar-assisted vapour compression/absorption hybrid air-conditioning systems. *Solar Energy,* 50(5): 453-458.

Cimsit, C. and Ozturk, I.T. (2012). Analysis of compression-absorption hybrid refrigeration cycles. *Applied Thermal Energy*, 40: 311-317.

Fernandez-Seara, J., Sieres, J. and Vazquez, M. (2006). Compression-absorption hybrid refrigeration system. *Applied Thermal Energy,* 26: 502-512.

Garimella, S., Brown, A.M. and Nagavarapu, A.K. (2011). Waste heat driven absorption/vapour-compression hybrid refrigeration system for megawatt scale, high-flux, low-temperature cooling. *International Journal of Refrigeration,* 34: 1776-1785.

Gomri, R. and Hakmi, R. (2008). Second law analysis of double effect vapour absorption cooler system. *Energy Conversion and Management,* 49: 3343-3348.

Kairouani, L. and Nehdi, E. (2006). Cooling perform-

ance and energy saving of a compression–absorption refrigeration system assisted by geothermal energy. *Applied Thermal Engineering,* 26: 288-294.

Kaynakli, O. and Kilic, M. (2007). Second law based thermodynamic analysis of water lithium bromide absorption refrigeration system. *Energy,* 32: 1505-1512.

Nikolaidis, C. and Probert, D. (1998). Exergy-method analysis of two-stage vapour compression refrigeration-plants performance. *Applied Energy,* 60: 241-256.

Pak, B.C., Groll, E.A. and Barun, J.E. (2005). Impact of fouling and cleaning on plate fin and spine fin heat exchanger performance. *ASHRAE Transactions,* 111(1): 496-504.

Qureshi, B.A. and Zuber, S.M. (2011). Performance degradation of a vapour compression refrigeration system under fouled conditions. *International Journal of Refrigeration,* 34: 1016-1027.

Sayyaadi, H. and Nejatolahi, M. (2011). Multi objective optimization of a cooling tower assisted vapour compression refrigeration system. *International Journal of Refrigeration*, 34: 243-256.

Seyfouri, Z. and Ameri, M. (2012). Analysis of integrated compression-absorption refrigeration systems powered by a microturbine. *International Journal of Refrigeration,* 35: 1639-1646.

Wang, L., Ma, A. and Tan, Y. (2012). Study on solar assisted hybrid refrigeration system. *Energy Procedia,* 16: 1503-1509.

Revised 17 May 2013; 19 September 2014

Mapping wind power density for Zimbabwe: a suitable Weibull-parameter calculation method

Tawanda Hove
Department of Mechanical Engineering, Faculty of Engineering, University of Zimbabwe, Harare, Zimbabwe

Luxmore Madiye
Department of Mechanical Engineering, Faculty of Engineering, University of Zimbabwe

Downmore Musademba
Department of Fuels and Energy, School of Engineering Sciences and Technology, Chinhoyi University of Technology, Zimbabwe

Abstract
The two-parameter Weibull probability distribution function is versatile for modelling wind speed frequency distribution and for estimating the energy delivery potential of wind energy systems if its shape and scale parameters, k and c, are correctly determined from wind records. In this study, different methods for determining Weibull k and c from wind speed measurements are reviewed and applied at four sample meteorological stations in Zimbabwe. The appropriateness of each method in modelling the wind data is appraised by its accuracy in predicting the power density using relative deviation and normalised root mean square error. From the methods considered, the graphical method proved to imitate the wind data most closely followed by the standard deviation method. The Rayleigh distribution (k=2 is also generated and compared with the wind speed data. The Weibull parameters were calculated by the graphical method for fourteen stations at which hourly wind speed data was available. These values were then used, with the assistance of appropriate boundary layer models, in the mapping of a wind power density map at 50m hub height for Zimbabwe.

Keywords: Weibull distribution parameters, graphical method, power density

1. Introduction

The energy performance analysis and economic appraisal of wind energy conversion systems require knowledge on the probabilistic distribution of wind speed, apart from just knowledge on the mean wind speed. Knowing the probability density distribution, one can assess the economic viability of installing a wind energy conversion system at a particular location (Celik *et al,* 2010; Antonio *et al.,* 2007) Various theoretical mathematical representations of probability distribution functions have been published in the literature (Ramirez and Carta, 2005; Mathew *et al.,* 2002; Seguro and Lambert, 2000; Garcia *et al*., 1998; Littella *et al.,* 1979), such as the Rayleigh, lognormal and two-parameter unimodal Weibull probability distribution functions.

Although the bimodal Weibull pdf, Jaramillo and Borja (2004) might produce a better fit on the wind speed data, especially for some locations in Zimbabwe which experience frequent null wind speeds, its use is regarded as an unnecessary addition to complexity where only the power density of the wind is required. This is because the first mode of the frequency distribution appears at null or very low wind speeds which are not important in producing useful power considering that the cut-in speed of wind turbines is typically between 7 and 10 mph (about 3 to 4.4 m/s) (Glynn, 2000). This study will therefore focus on the two-parameter unimodal Weibull probability density function for imitating wind speed frequency distribution at the sites in question. The parameters k (the shape factor) and c (the scale factor) of the two-parameter Weibull distribution will be determined by some of the various methods found in the literature.

Mathew (2006) gives a concise description of five methods that could be used to determine the values of the two-parameter Weibull distribution. The methods are; the graphical, the standard deviation, the moment, the maximum likelihood and the energy pattern factor (EPF) methods. Harrison, Cradden and Chick (2007) note that the Rayleigh distribution, which is a simplification of the Weibull distribution in which k=2, and is defined solely by mean wind speed, is often applied where specific data for k is not available. Indeed it is relied upon in many studies where time series data is not available and the Weibull parameters cannot be determined. In this paper, the Rayleigh distribution is also considered alongside the other aforementioned distributions to assess its suitability in imitating the actual wind speed data.

The criterion for assessing the suitability for each method in modelling wind speed data is its ability to estimate closely the power density at the site. The theoretical maximum power density achievable by any wind turbine – Betz Limit (van Kuik, 2007; Gorban *et al;* 2004; Hughes and George, 2002) - is used as a common yardstick for the comparison.

2. The Weibull distribution

The frequency distribution of wind speed at a given site can be modelled by the two-parameter Weibull probability density function (pdf). The Weibull pdf, p_W [s/m], can be written:

$$p_W = \left(\frac{k}{c}\right)\left(\frac{v}{c}\right)^{k-1} \exp\left[-\left(\frac{v}{c}\right)^{k}\right] \quad (1)$$

In (1), v is the wind speed (in units of speed; m/s or knots), k, the shape factor, is dimensionless, and specifies how sharp a peak the Weibull curve has. The parameter, c [m/s], the scale factor, is the weighted average speed; more useful for power calculations than the actual mean speed (Gorban *et al,* 2004). The parameters k and c vary from site to site and have to be determined for each site to fit wind speed frequency distribution for the site.

In terms of the mean wind speed, $\bar{v}$, and k, the pdf can be written (Ramirez and Carta, 2005) as:

$$p_W = \left(k\left[\left(1+\frac{1}{k}\right)\right)\left(\frac{v\left[\left(1+\frac{1}{k}\right)\right.}{\bar{v}}\right)\exp\left[-\left(\frac{v\left[\left(1+\frac{1}{k}\right)\right.}{\bar{v}}\right)^{k}\right] \quad (2)$$

The function, $\lceil x$, is the gamma function of x. Comparing (1) and (2), it can be observed that the mean speed, $\bar{v}$ is given by:

$$\bar{v} = c\left[\left(1+\frac{1}{k}\right)\right. \quad (3)$$

If k and c are known, hence the functional relationship of p_w and v known, the mean wind speed can be obtained from numerical integration of the expression:

$$\bar{v} = \int_0^{\infty} p_w\, v dv \quad (4)$$

For the measured wind data grouped in m classes of class width, w_j [m/s], (j=1 to m), and class probability density, p_j [s/m], the mean, $\bar{v}$, and standard deviation, σ, for measured data are given respectively by:

$$\bar{v} = \sum_{j=1}^{m} p_j w_j v_j \quad (5a)$$

and

$$\sigma = \sqrt{\frac{n\sum_{j=1}^{m} p_j w_j (v_j - \bar{v})^2}{n-1}} \quad (5b)$$

In (5) v_j is the class centre speed of the j[th] class. For class frequency, fj, the class frequency density for a sample population of n wind speed records is obtained as:

$$p_j = \frac{f_j}{n w_j} \quad (6)$$

The cumulative pdf can be obtained by integrating (1) from 0 to any value of v; say v_o.

$$P(v < v_o) = 1 - exp\left[\left(\frac{v}{c}\right)^{k}\right] \quad (7)$$

The power density [W/m^2] of a wind turbine is given by:

$$ED = \frac{1}{2}\rho\int_o^{\infty} C_P\; p_W v^3 dv$$

In (8), ρ is the air density [kg/m^3], and is considered constant at a given turbine height. The power coefficient, C_P, is an empirically determined function of wind speed v for a given turbine. The maximum power coefficient, independent of turbine design, is given by the Betz limit (Mathew, 2006; van Kuik, 2007; Gorban *et al.*, 2004):

$$C_{Pmax} = \frac{16}{27} \quad (9)$$

Therefore, the maximum power density is given by:

$$ED_{max} = \frac{8}{27}\rho\int_0^{\infty} p_W\, v^3 dv \quad (10a)$$

for the Weibull distribution, and

$$ED_{max} = \frac{8}{27}\rho\sum_{j=1}^{m} p_j w_j v^3 \quad (10b)$$

for grouped data.

The integral in (10a) can be solved analytically (Mathew, 2006), but can conveniently be solved numerically with the advent of various spreadsheet programs. The analytical integral for wind power density, ED, is given by:

$$ED = \frac{1}{2}\rho \int_0^\infty p_W\, v^3 dv = \frac{\rho c^3}{2}\left(\frac{3}{k}\right)\left[\frac{3}{k}\right. \qquad (11)$$

The maximum power density computed by (10a) for the Weibull functions generated from different methods, can be compared with that of (10b), for the measured wind data, in appraising a given method's accuracy in imitating the measured wind data. Another way for comparing the accuracy of the methods is by comparing the normalised root mean square error, *NRMSE*. The NRMSE is given in general by:

$$NRMSE = \frac{\left[\frac{1}{N}\sum(X_{model} - X_{observed})^2\right]^{\frac{1}{2}}}{\frac{1}{N}\sum X_{observed}} \qquad (12)$$

3. Data available for study

The finest time-step resolution of wind speed measurements available in Zimbabwe is the hour. Hourly wind speed data is available at only fourteen stations over all of Zimbabwe. Such data was obtained for two years (1991 – 1992), from the Meteorological Services Department (MSD) of Zimbabwe. The measurements are done by cup anemometers placed at a height of 10 m above ground. For each station, the data was subsequently grouped into speed–spectra frequency bins of 1 m/s range to prepare for later analysis. The grouped data for four major stations is shown in Table I for validation of the methods described in Section 4.

The models used for determining the diurnal variation of energy output for the two generating components of the hybrid system; PV array and diesel generator, are outlined in this section.

4. Methods for determining Weibull parameters from wind data

Mathew (2006) describes five different methods for determining the values of the Weibull k and c from measured wind data. These methods, namely; the graphical; the standard deviation; the moment; the maximum likelihood and the energy pattern factor methods, are reviewed in the following sections and are going to be used to determine k and c values from the data in Table I. In addition, the commonly used Weibull simplification- the Rayleigh distribution- is tested for its goodness-of-fit on the measured data.

4.1 Graphical method

The graphical method for determining *k* and *c* is based on the fact that the Weibull cumulative distribution function of (7) can be transformed into a log-linear form, and the technique of linear regression exploited. The cumulative pdf is manipulated by taking natural logarithms twice on both sides to make it a linear equation. The resulting equation is:

$$ln[-ln(1 - P\ (v \le v_o))] = klnv - klnc \qquad (13)$$

Equation (13) is linear in $ln[-ln(1 - P\ (v \le v_o))]$, the dependent variable (Y), and *lnv*, the independent variable *(X)* in $Y = a + bX$, in which $a = -klnc$ and $b = k$ are regression constants.

Hourly meteorological records of wind can now be grouped in speed –spectra frequency bins or classes, and the values of $ln[-ln(1 - P\ (v \le v_o))]$ and $\ln v_o$ calculated for each class.

The symbol v_o is the upper limit speed value of the class, and P, for each class, is the number of speed records with speed lower than v_o, divided by the total number of records in the sample (-the relative cumulative frequency). Log–linear regression fits are shown on Figures 1(a) and 1(b), for Harare and Gweru respectively.

The gradient of the regression line in Figures 1(a) and 1(b) equals the value of *k*, and the intercept equals *-klnc*, from which *c* can be inferred. The graphs show a very strong correlation of the variables with the coefficient of determination, R^2, about 0.99 in each case.

At $P = 1$, the natural logarithm of 1-*P* does not exist. In this case, 1-P is replaced by a a very small number, essentially zero, but not equal to zero, such that the logarithm of 1-*P* is computable.

4.2 The standard deviation method

The method used for the UK Wind Energy Program (WindPower and UK Wind Speed Database, 2012), called by (Mathew, 2006) the standard deviation method, relates to the ratio of the standard deviation, σ, to the mean speed, $\bar{v}$, (-the coefficient of variation), with the parameter k as follows:

$$\frac{\sigma}{\bar{v}} = \sqrt{\frac{\left[\left(1+\frac{2}{k}\right)\right.}{\left[\left[\left(1+\frac{1}{k}\right)\right]^2\right.}} \qquad (14)$$

Equation (14) is not explicit in terms of *k* and can only be solved by numerical methods. However, (Justus *et al.*, 1978) provide a simpler approximation for *k*.

$$k = \left(\frac{\sigma}{\bar{v}}\right)^{-1.090} \qquad (15)$$

The mean, $\bar{v}$, and standard deviation, σ, are obtained from the wind data using (5). Having determined k from the wind statistics, c can be evaluated by transforming (3) into:

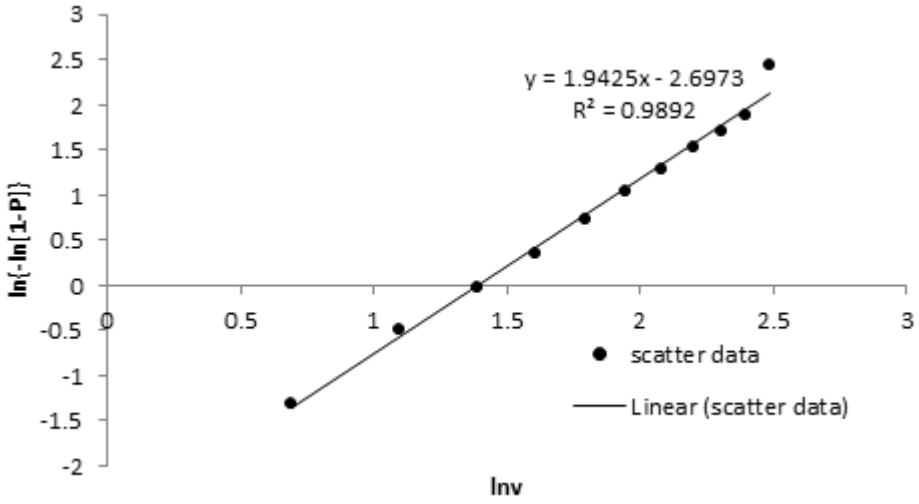

Figure 1(a): Linear regression for Harare data

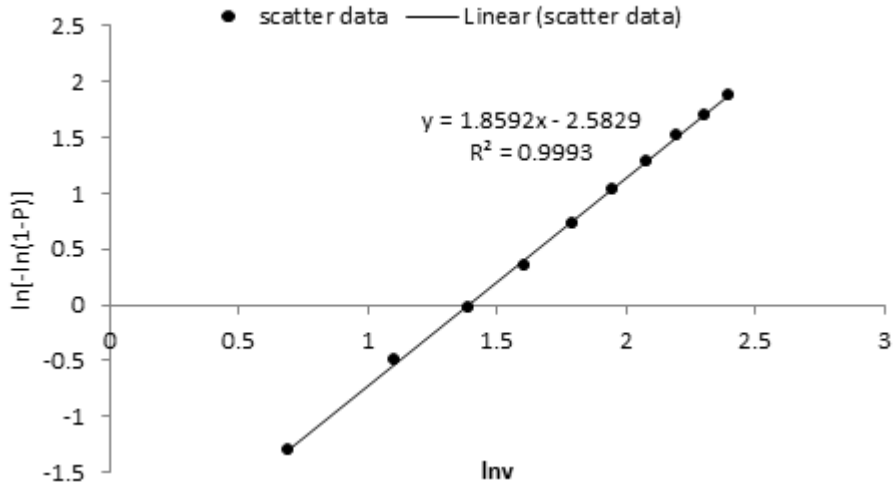

Figure 1(b): Linear regression for Gweru data

$$c = \frac{\bar{v}}{\Gamma\left(1+\frac{1}{k}\right)} \quad (16)$$

To evaluate c in (15), we have to evaluate the gamma function of $1+1/k$, which is rather complex. However, some common spread sheet programs such as Microsoft Excel include the natural logarithm of gamma in their function library. In Excel, the natural logarithm of gamma is denoted by the function name "GAMMALN". Gamma is then the exponential of GAMMALN.

Alternatively, Justus *et al.* (1978) give the following approximation expression:

$$c = \frac{\bar{v}k^{2.6674}}{0.184+0.816k^{2.73855}} \quad (17)$$

With both k and c evaluated as above, the Weibull function of (1) can be generated.

4.3 Moment method

Another method for estimating k and c is the First and Second Order Moment Method, where the nth moment M_n of the Weibull distribution is given by Mathew (2006):

$$M_1 = c^n \Gamma\left(1+\frac{n}{k}\right) \quad (18)$$

If M_1 and M_2 are the first and second moments, c can be solved as:

$$c = \frac{M_1}{M_2}\frac{\Gamma\left(1+\frac{1}{k}\right)}{\Gamma\left(1+\frac{2}{k}\right)} \quad (19)$$

Similarly, k can be solved from (18) and (19) by eliminating c, with:

$$\frac{M_2}{{M_1}^2} = \frac{\Gamma\left(1+\frac{2}{k}\right)}{\left(\Gamma\left(1+\frac{1}{k}\right)\right)^2} \quad (20)$$

M_1 and M_2 are calculated from the given wind speed data from the statistical fact that the moment is the expected value of a positive integral power of a random variable. Thus, M_1 is equal to

the mean, $\bar{v}$, and is evaluated by (5a). The second moment M_2 is computed for grouped data as:

$$M_2 = \sum_{j=1}^{m} p_j w_j v_j^2 \quad (21)$$

A numerical solution for k is required using (20), and then c is evaluated from (19).

4.4 Maximum likelihood method

In the maximum likelihood method, the Weibull parameters, k and c, are given by Cohen (1965) and Ananstasios *et al.* (2002):

$$k = \left[\frac{\sum_{i=1}^{n} v_i^k ln(v_i)}{\sum_{i=1}^{n} v_i^k}\right] - \frac{\sum_{i=1}^{n} ln(v_i)}{n} \quad (22)$$

and

$$c = \left[\frac{1}{n}\sum_{i=1}^{n} v_i^k\right]^{1/k} \quad (23)$$

The summations in (22) and (23) are replaced for grouped data as follows:

$$\sum_{i=1}^{n} V_i^k \, ln(V_i) = n \sum_{j=1}^{m} p_j w_j V_j^k ln(V_j) \quad (24a)$$

$$\sum_{i=1}^{n} V_i^k = n \sum_{j=1}^{m} p_j w_j V_j^k \quad (24b)$$

and

$$\frac{\sum_{i=1}^{n} ln(V_i)}{n} = \sum_{j=1}^{m} p_j w_j ln(V_j) \quad (24c)$$

Now, in (22), k is not expressed explicitly, and has to be solved numerically. First, a value k (any number between 0 and 2 will do), and evaluate the summations on the right hand side of (22) or their simplified versions in (24). The value of k is varied until its value is such that (22) is satisfied.
After getting a satisfactory k, the parameter c is preferably evaluated from (3) to retain consistency with the Weibull formula.

4.5 Energy pattern factor method

The Energy Pattern Factor (EPF) is the ratio of the total power available in the wind and the power corresponding to the cube of the mean wind speed (Mathew, 2006). That is:

$$EPF = \frac{\frac{1}{n}\sum_{i=1}^{n} v_i^3}{\left(\frac{1}{n}\sum_{i=1}^{n} v_i\right)^3} \quad (25)$$

In the grouped data format, the energy pattern factor can be written as:

$$EPF = \frac{\sum_{j=1}^{m} p_j w_j v^3}{\bar{v}^3}$$

Once EPF is calculated from (25), the parameter k is approximated as:

$$k = 3.957 EPF^{-0.898} \quad (26)$$

The parameter c can be calculated from Equation (3) once k is obtained.

4.6 Rayleigh distribution

In some cases where time series wind is not available but only long-term statistics like the mean wind speed are known, the aforementioned methods cannot be applied. It is common under these circumstances to assume that the Rayleigh distribution is a suitable proxy of the real distribution. The Rayleigh distribution is a simplified form of the Weibull distribution in which k=2. With this assumption, rearranging (3) and simplifying gives:

$$c = \frac{2\bar{v}}{\sqrt{\pi}}$$

Therefore, for the Rayleigh distribution, (1) becomes:

$$p_R = \frac{\pi}{2}\frac{v}{\bar{v}^2} \exp\left[-\left(\frac{\pi}{4}\left(\frac{v}{\bar{v}}\right)^2\right)\right] \quad (28)$$

and the corresponding cumulative distribution is:

$$P_R(v \le v_o) = 1 - exp\left[-\left(\frac{\pi}{4}\left(\frac{v}{\bar{v}}\right)^2\right)\right] \quad (29)$$

The validity of the Rayleigh simplification in modelling wind speed data is tested, alongside the other previously discussed methods, and the results are presented in the following section.

5. Results

The probability density functions generated by methods described in sections 4.1 to 4.6 are compared with the measured probability density function in Figures 2(a) to 2(d) for four sample stations, Harare, Gweru, Bulawayo and Masvingo, respectively. The comparisons for cumulative probability functions are shown in Figures. 3(a) and 3(b) for Bulawayo and Masvingo, respectively.

The calculated probability density functions are uni-modal, but for some sites, as is depicted for Gweru and Masvingo (a continuous curve used to give better impression), the measured distributions are bimodal. However, the first modes of these bimodal distributions occur at low wind speed (in the 0 to 1 m/s range). Using a uni-modal distribution to represent them is considered not to seriously affect power calculations.

The theoretical distributions in Figures 2(a)-2(d) and Figures 3(a) and 3(b) (cumulative distributions are shown only for Bulawayo and Masvingo) appear to imitate the measured distribution with varying capability in doing so. However, only a subjective appraisal can be made on the relative fitness

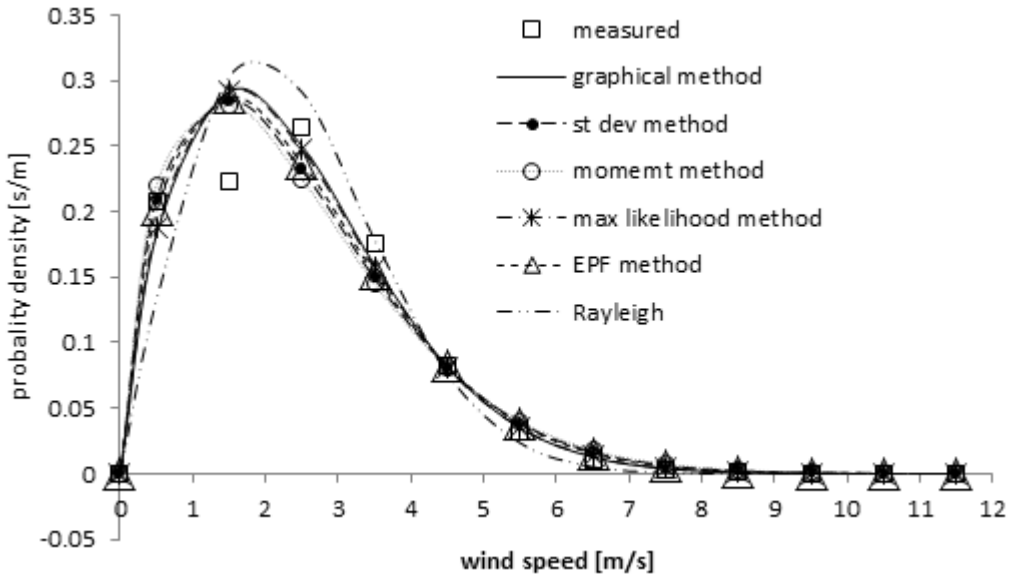

Figure 2(a): Probability distribution functions by different methods superimposed on measured distribution for Harare

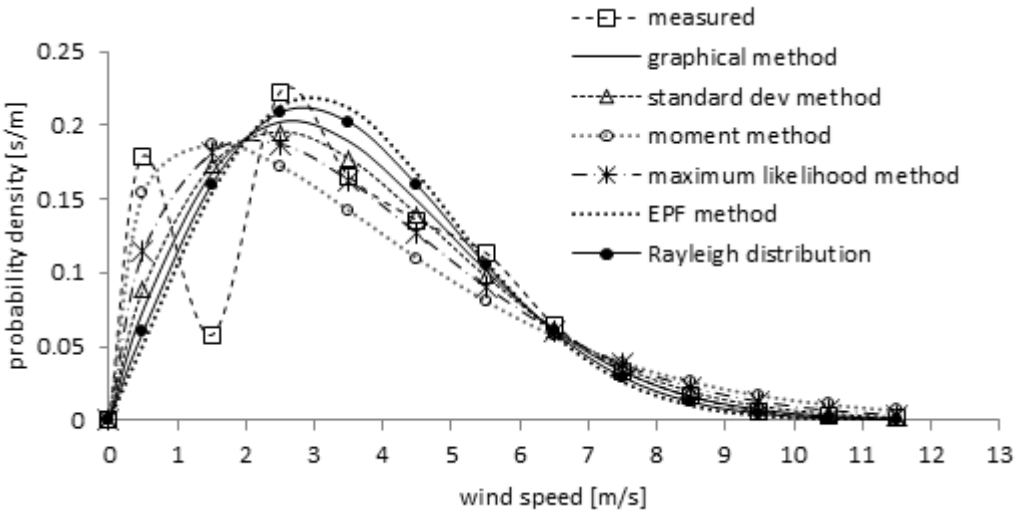

Figure 2(b): Probability density functions by different methods superimposed on measured distribution for Gweru

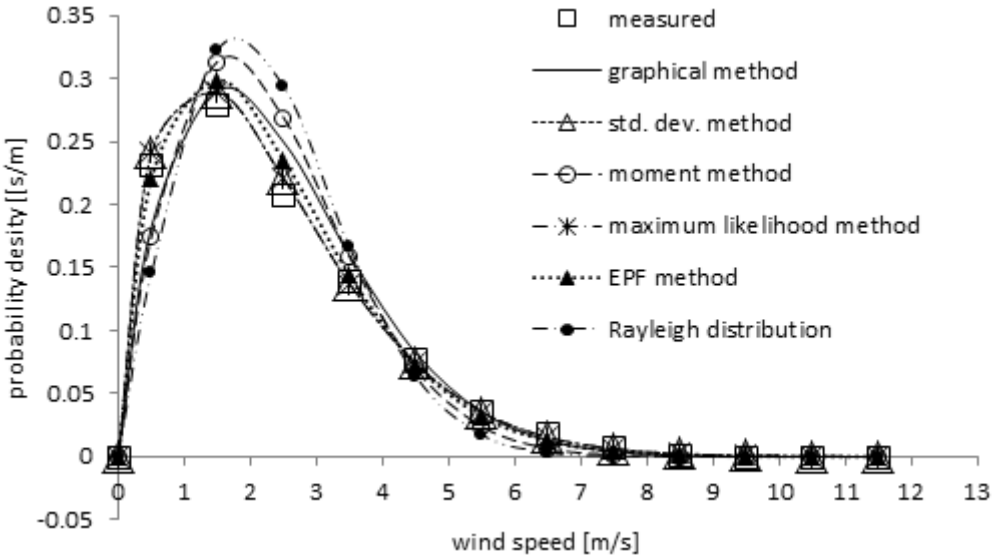

Figure 2(c): Probability density functions by different methods superimposed on measured distribution for Bulawayo

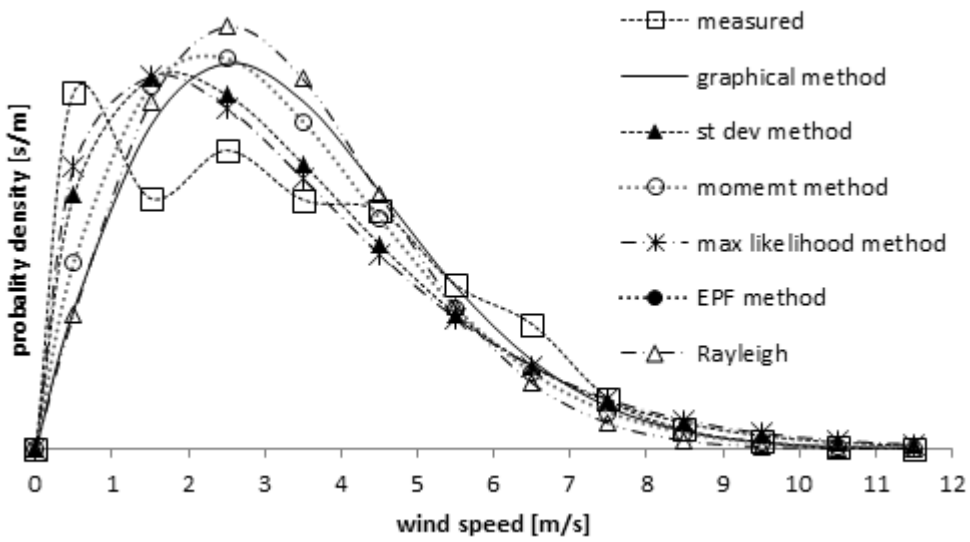

Figure 2(d): Probability density functions by different methods superimposed on measured distribution for Masvingo

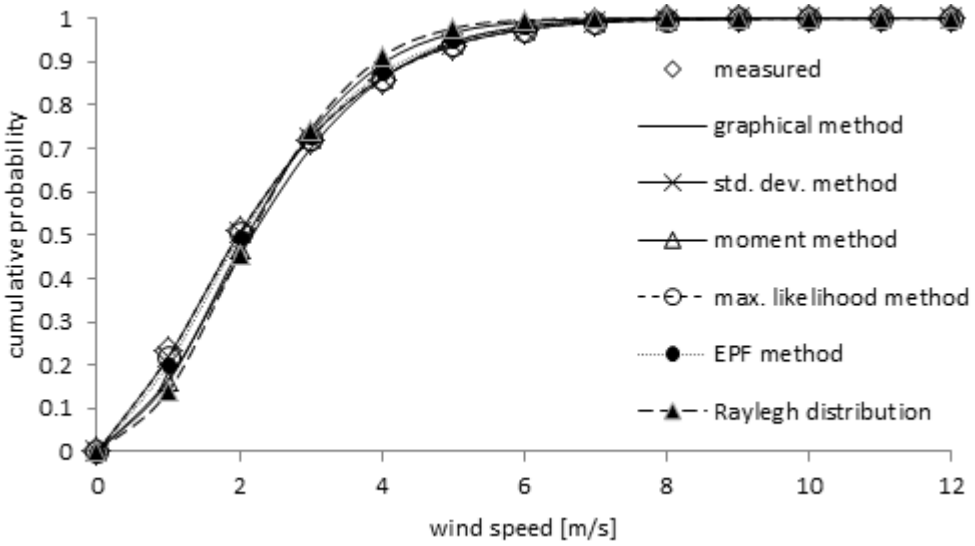

Figure 3(a): Cumulative probability distributions for Bulawayo

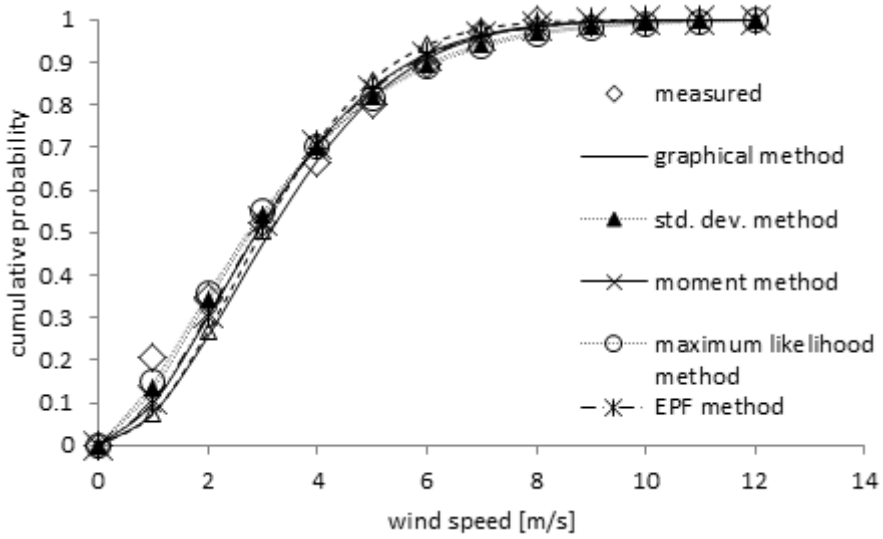

Figure 3 (b): Cumulative probability distributions for Masvingo

Table 1: Grouped wind speed data for Harare, Gweru, Bulawayo and Masvingo

Speed range [m/s]		$v_{central}$ *] [m/s*	*Harare*		*Gweru*		*Bulawayo*		*Masvingo*	
From	*To*		*Frequency*	*Cumulative frequency*	*Frequency*	*Cumulative frequency*	*Frequency*	*Cumulative frequency*	*Frequency*	*Cumulative frequency*
0	1	0.5	3584	3584	3155	3155	4071	4071	3561	3561
1	2	1.5	3855	7439	1046	4201	4896	8967	2497	6058
2	3	2.5	4584	12023	3807	8008	3639	12606	2976	9034
3	4	3.5	3044	15067	2782	10790	2456	15062	2482	11516
4	5	4.5	1419	16486	2231	13021	1353	16415	2371	13887
5	6	5.5	554	17040	1878	14899	647	17062	1632	15519
6	7	6.5	194	17234	1028	15927	329	17391	1243	16762
7	8	7.5	55	17289	524	16451	129	17520	501	17263
8	9	8.5	14	17303	234	16685	16	17536	189	17452
9	10	9.5	2	17305	84	16769	1	17537	70	17522
10	11	10.5	3	17308	38	16807	1	17538	10	17532
11	12	11.5	0	17308	19	16826	0	17538	7	17539
12	13	12.5	0	17308	0	16826	0	17538	3	17542
SUM	17308	SUM	16826	SUM	17538	SUM	17542			

Frequency unit is hours per 2 years

Table 2: Grouped wind speed data for Harare, Gweru, Bulawayo and Masvingo

Station/method		*Measured method*	*Graphical method*	*Std. Dev. method*	*Moment hood method*	*Maximum likeli- method*	*EPF distrbution*	*Rayleigh*
Harare	$\bar{v}$ [m/s]	2.37	2.39	2.39	2.39	2.39	2.40	2.39
	% dev $\bar{v}$	0	1	1	1	1	1	1
	K	-	1.71	1.58	1.53	1.69	1.62	2
	C [m/s]	-	2.68	2.66	2.65	2.67	2.67	2.69
	ED [W/m^2]	10.8	11.0	12.2	12.7	11.2	11.9	9.2
	% dev ED	0	2	13	18	3	9	-15
Gweru	$\bar{v}$ [m/s]	3.58	3.58	3.46	3.54	3.58	3.58	3.58
	% dev $\bar{v}$	0	0	-3	-1	0	0	0
	K	-	1.86	1.76	1.39	1.58	2.07	2.00
	C [m/s]	-	4.04	4.02	3.92	3.99	4.04	4.04
	ED [W/m^2]	33.6	33.5	35.0	41.4	38.4	29.6	31.1
	% dev ED	0	0	4	23	14	-12	-7
Bulawayo	$\bar{v}$ [m/s]	2.28	2.40	2.29	2.29	2.29	2.28	2.28
	% dev $\bar{v}$	0	5	0	0	0	0	0
	K	-	1.59	1.58	2.30	1.60	2.00	1.59
	C [m/s]	-	2.49	2.29	2.30	2.52	2.57	2.49
	ED [W/m^2]	11.5	11.2	11.5	8.9	11.5	10.4	8.0
	% dev ED	0	-3	0	-23	0	-9	-30
Masvingo	$\bar{v}$ [m/s]	3.2	3.2	3.3	3.2	3.2	3.3	3.2
	% dev $\bar{v}$	0	0	3	0	0	3	1
	k	-	1.90	1.54	1.77	1.46	1.73	2.00
	c [m/s]	-	3.79	3.53	3.56	3.50	3.56	3.58
	ED [W/m^2]	23.8	28.6	27.2	29.5	24.7	31.4	25.4
	% dev ED	0	-4	4	-13	10	-11	-24

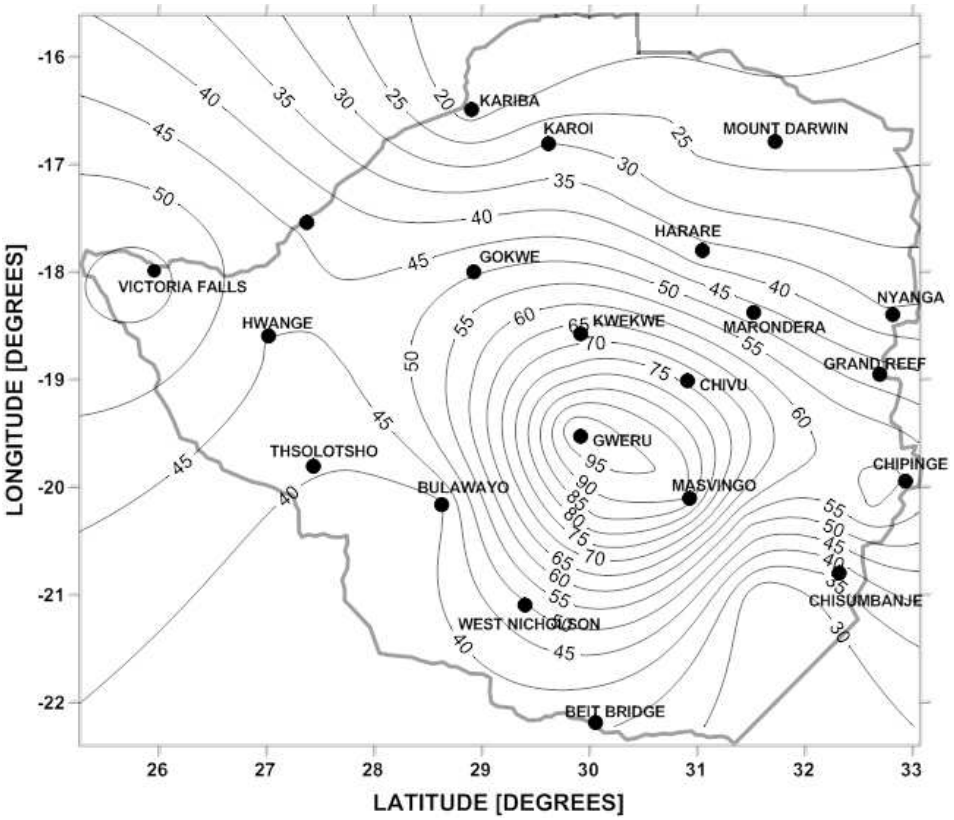

Figure 4: Zimbabwe wind power density at 50 m hub height in W/m^2 constructed using Sufer (Lawless, 2003) geostatistical software

of each method to the measured data from these pictorial presentations. A quantitative comparison is required.

To quantitatively appraise of the various methods, Table 2 is constructed. It shows the measured mean wind speed calculated according to (5a) in comparison to the mean wind speed of the theoretical distributions of methods in sections 4.1 to 4.6, computed by (4). The table shows the percent deviation of the mean speeds from the measured. Importantly, the table also makes similar presentations for the Betz-limit power density. The corresponding values of k and c are also shown on the table.

With the aid of Table 2 it can be shown that, if the power density is considered the figure of merit, the graphical method (maximum power density deviation of 4%) is the most reliable of all methods considered, followed closely by the standard deviation method (maximum deviation of 13%). All the six methods predict the actual mean speed fairly accurately (within 5%). This is expected since, except for the graphical method all the other distributions are formulated based on the mean wind speed.

The accuracy of the methods in predicting spectral power density can also be compared by calculating the normalised root mean square error (NRMSE) for each method. The power density for each wind speed spectrum calculated by the Weibull model is compared with that calculated from measured data and a NRMSE is obtained for each sample station and for all stations combined (overall). The NRMSE values for each method are listed in Table 3. The graphical method gives the least NRMSE of all the methods for all stations.

The wind power density at 50 m hub height is shown in Figure 4. To obtain the wind power density map of Figure 4, the values of k and c at the fourteen stations having hourly wind data were calculated using the graphical method. Equation (11) was then used to compute the power density at the stations, first at the measurement height of 10 m hub height, then at 50 m by applying the three-seventh-power law. The values of power density were then mapped using the ordinary kriging interpolation option of the software Surfer Version 12 (Scientific Software Group, 2013).

The wind power density for Zimbabwe is seen to be highest in the central region – the Midlands province. The power density at 50 m hub height varies between about 10 W/m^2 to 120 W/m^2. These power density levels are rather low for economical large-scale power production, lying in Class 1 of the US NREL wind power density classification (Wind Power Class, 2014). Some specially selected sites, however, may be suitable for applications such as water pumping or even power generation using special wind turbines which have low cut-in speeds.

Table 3: Comparison of Normalised Root Mean Square Error (NRMSE) between spectral power density calculated by the Weibull model and that calculated from measured data

Method	*Bulawayo*	*Gweru*	*Harare*	*Masvingo*	*Overall*
Graphical	0.3	0.28	0.12	0.28	0.22
Standard deviation	0.55	0.53	0.3	0.38	0.34
Moment	1.06	1.03	0.38	0.37	0.60
Maximum likelihood	0.56	0.36	0.14	0.44	0.43
Energy pattern factor	0.38	0.36	0.24	0.35	0.32
Rayleigh	0.9	0.87	0.27	0.52	0.45

6. Summary and conclusion

The study uses five different methods for calculating the parameters of the two-parameter Weibull distribution from measured wind speed data at fourteen locations in Zimbabwe. The Rayleigh distribution, which is a commonly used proxy to wind speed distributions, is also generated and compared with the measured data. The graphical method, for correlating the measured wind speed probability distribution with the theoretical Weibull distribution, estimated power density to within 4% of the actual in all the four illustrative cases considered. This method was then used to determine the Weibull parameters at the rest of the fourteen stations with hourly wind speed data. This enabled the mapping of wind power density over Zimbabwe. The wind power density for Zimbabwe is generally low for power generation purposes. Some considerable potential exists though in the Midlands province for applications such as water pumping that can do with low wind speed. The approach used in this study can be replicated in other countries in the region in creating their respective wind power density maps.

Acknowledgement

The authors are grateful for the financial support given by the University of Zimbabwe Research Board. The Research Grant provided enabled, among other things, the purchase of wind speed data from the Meteorological Service Department of Zimbabwe.

References

Ananstasios, B., Dimitrios, C., and Thodoris, D. K. (2002). A nomogram method for estimating the energy produced by wind turbine generators, *Solar Energy*, Vol. 72, No. 3, pp. 251-259.

Antonio, J., Carta, A., and Ramirez, P. (2007). Use of finite mixture distribution models in the analysis of wind energy in the Canarian Archipelago, *Energy Conversion and Management*, vol. 48, no. 1, pp. 281-291.

Celik A. N., Makkawi A., and Muneer T. (2010). Critical evaluation of wind speed frequency distribution functions. *Journal of Renewable and Sustainable Energy* 2:1, 013102.

Cohen, A. C. (1965). Maximum likelihood estimation in the Weibull distribution based on complete and censored data, *Technometrics*, Vol. 7, No. 4, pp. 579-588.

Garcia, A., J. Torres, J. L., Prieto, E., and de Franciscob, A. (1998). Fitting wind speed distributions: a case study, *Solar Energy*, Vol. 62 No. 2, pp.139-144.

Glynn, M. (2000). Zimbabwean wind spins at Redhill, *Home Power*, No. 76, pp. 52-54.

Gorban, A. N., Gorlov, A.M., and Silantyev, V. M. (2004). Limits of turbine efficiency for free fluid flow, Energy Resources Technology, vol. 123, no. 4, 311-317, 2001. Renewable Energy, Vol. 29, No. 10, pp. 1613-1630.

Harrison, G. P., L. C. Cradden, L. C., and Chick, J. P. (2007). Preliminary assessment of climate change impacts on the UK onshore wind resource, Invited paper for Special Issue of Energy Sources and Global Climate Change and Sustainable Energy Development.

Hughes, L., and George, A., (2002), The Weibull distribution. Available on: www.nsweep.electricalcomputerengineering.dal.ca/tools/Weibull.html, Accessed on: 20 February 24, 2013.

Jaramillo, O.A. and M. A. Borja, M.A. (2004). Wind speed analysis in La Ventosa, Mexico: a bimodal probability distribution case, *Renewable Energy*, vol. 29, no. 10, pp. 1613-1630.

Justus, C. G., Hargraves, W. R., Mikhail, A., and Graber, D. (1978). Methods of estimating wind speed frequency distribution, *J. Applied Meteorology*, Vol. 17, pp. 350-353.

Littella, R. C., Mc Clavea, J. T., and Offena, W. W. (1979). Goodness-of-fit for the two-parameter Weibull distribution, *Communications in Statistics - Simulation and Computation*, Vol. 8, No. 3, pp. 257-259.

Mathew, S. (2006). In: Wind energy fundamentals, resource analysis and economics, Berlin, Springer-Verlag, Chapter 3.

Mathew, S., Pandey, K. P. and Kumar, A. (2002). Analysis of, wind regimes for energy estimation, *Renewable Energy*, Vol. 25, No. 3, pp. 381-399.

Ramirez, P., and Carta, A. (2005). Influence of the data sampling interval in the estimation of the parameters of the Weibull probability density functions: a case study, *Energy Conversion and Management*, Vol. 46, Nos. 15-16, pp. 2419-2438.

Scientific Software Group, Surfer 12 for Windows. Available at: http://www.ssg-surfer.com. Accessed on 24 January 2013.

Seguro, J. V., and Lambert, T. W. (2000). Modern estimation of the parameters of the Weibull wind speed distribution for energy analysis, *Journal of Wind Energy and Industrial Aerodynamics*, vol. 85, no. 1, pp. 75-84.

The WindPower and UK Wind Speed Database programs (online). Available on: http://www.wind-power-program.com/wind_statistics.htm. Accessed 12 December 2012.

van Kuik, G. A. M. (2007). The Lanchester-Betz-Joukowsky limit, *Wind Energy*, Vol. 10, pp. 289-291.

Wind Power Class - Wind Energy Resource Atlas of the United States. Available at: http://rredc.nrel.gov/wind/pubs/atlas/tables/1-1T.html. Accessed 30 September, 2014.

Received 11 December 2013; revised 11 October 2014

Application of multiple regression analysis to forecasting South Africa's electricity demand

Renee Koen

Jennifer Holloway

Decision Support and Systems Analysis Research Group, Built Environment Unit, CSIR, Pretoria, South Africa

Abstract

In a developing country such as South Africa, understanding the expected future demand for electricity is very important in various planning contexts. It is specifically important to understand how expected scenarios regarding population or economic growth can be translated into corresponding future electricity usage patterns. This paper discusses a methodology for forecasting long-term electricity demand that was specifically developed for applying to such scenarios. The methodology uses a series of multiple regression models to quantify historical patterns of electricity usage per sector in relation to patterns observed in certain economic and demographic variables, and uses these relationships to derive expected future electricity usage patterns. The methodology has been used successfully to derive forecasts used for strategic planning within a private company as well as to provide forecasts to aid planning in the public sector. This paper discusses the development of the modelling methodology, provides details regarding the extensive data collection and validation processes followed during the model development, and reports on the relevant model fit statistics. The paper also shows that the forecasting methodology has to some extent been able to match the actual patterns, and therefore concludes that the methodology can be used to support planning by translating changes relating to economic and demographic growth, for a range of scenarios, into a corresponding electricity demand. The methodology therefore fills a particular gap within the South African long-term electricity forecasting domain.

Keywords: long-term forecasting, South African electricity demand

1. Introduction

In a developing country such as South Africa, understanding future patterns of electricity usage is very important in various planning contexts. The future national demand for electricity is an important consideration for electricity providers who need to plan to have sufficient and secure supply of electricity (Imtiaz *et al.*, 2006 and Soontornrangson *et al.*, 2003). Investment in electricity generation capacity, whether using fossil-based or renewable energy sources, is largely motivated through the anticipated long-term need for electricity (Ulutaş, 2005; Doriana; Franssen and Simbeck, 2006). South Africa has a growing population which creates an increasing need for housing and services, as well as a need to expand economic activity both to accommodate new entrants into the labour market and to address current high unemployment levels. Therefore, virtually all types of national and local planning, public or private, requires consideration of the implications on future electricity needs in order to establish whether there is sufficient electricity supply capacity in the country to support future plans.

This paper discusses a methodology for forecasting long-term electricity demand that was initially used for assisting with strategic planning for the South African branch of a multi-national company. The initial modelling objective expressed by the company was to be able to determine potential fluctuations in the future national demand for electricity, i.e. the amount of electricity required from the national grid, in order to assess the impact of that on their own business plans. This required a methodology that could determine the effect of possible changes in various political, demographic or economic patterns on the future national electricity consumption patterns. Therefore, forecasts using extrapolation of past trends would potentially not

suffice, and a type of scenario-based forecasting was foreseen to be more appropriate.

A methodology was developed that satisfied these needs expressed by the company and that produced scenario forecasts that could be successfully incorporated into their strategic planning processes. During the development of this methodology, various electricity forecasting studies published locally and internationally were consulted, but it was found that a scenario-based methodology using multiple regression models to forecast electricity demand in various electricity usage sectors had not been applied before. Furthermore, the extensive collection of public domain data and the interrogation process applied in order to create a usable dataset out of the various information sources had not been found in any other study. In addition, the South African electricity demand and supply patterns, and the driving forces behind them, are different from that of other countries. Therefore, this methodology could be viewed as unique, both locally and internationally.

The methodology described in this paper was applied successfully within the company it was developed for, and the same basic methodology has subsequently been used to support planning of electricity supply needs within the public sector.

This paper first discusses the objectives of the forecasting and then provides more details with regard to the data collection and validation, as well as the modelling methodologies used. This is followed by descriptions of the models used and the forecasts derived from the models. The paper concludes with a discussion of the chosen methodology as it compares to approaches used in other studies, as well as comments about the usefulness of the methodology.

2. Forecasting objectives

The main objective to be met by the forecasts, as expressed by the initial client, was to estimate the future demand for electricity from certain expected changes in the national economy and demography. This meant that a forecasting model (or set of models) had to be developed that would be able to translate aspects such as economic growth or decline into subsequent growth or decline in electricity usage. The focus was therefore placed on the development of a model(s) that could quantify historical patterns of relationships between electricity usage and the relevant economic and demographic variables, using data available in the public domain. Ultimately, the objective was to use such a model(s) to derive future electricity usage patterns from these quantified relationships once expected future values for the relevant economic or demographic variables had been estimated.

Since these objectives required the quantification of historical patterns as a basis for future forecasts, a statistical modelling and forecasting approach seemed appropriate. However, in a statistical modelling approach it would not only be important to consider the correlation between electricity usage and the variables used to predict electricity usage, but also to consider the correlation of the predictor variables with each other. Such correlation between predictor variables is called multicollinearity or near-linear dependence (Montgomery, Peck and Vining, 2006). Including variables that are highly correlated with each other as predictors in the same model can be problematic when that model has to be used for forecasting. This is especially true for scenario forecasting, since there are no guarantees that the historical relationships between variables would be maintained when creating future scenario inputs. For instance, one may want to purposefully create a scenario in which variables do not follow the same patterns as in the past. If a model exhibits high multi-collinearity, violating such relationships in the created scenario inputs could then invalidate the model's outputs. Therefore, an important consideration of the methodology development was to ensure that the models would be developed in a way that they were statistically valid, i.e. that multi-collinearity between the predictor variables used to estimate electricity demand would be managed correctly.

3. Forecasting methodology overview

In developing a statistical model(s) to use as a basis for scenario forecasting, an attempt was first made to use predictor variables to forecast future annual demand for electricity at a national level. Data on various external factors, such as Gross Domestic Product (GDP), population, electrification of households, major industrial projects (using start-up and shut-down dates) and climate variables, as well as relevant derivations and transformations of these variables, were collected and analysed. A particular problem experienced with trying to forecast the total national demand, however, was the consistent problem of multi-collinearity that was measured in any model that contained GDP and population, or transformations of these two variables. This made it difficult to develop an appropriate model that would support forecasts from scenarios that contained both of these variables.

Instead, the approach was adapted by breaking the total electricity consumption up into sectors of electricity usage, forecasting the consumption per sector and then combining these sector forecasts into a total annual forecasted demand for the country. Losses also had to be estimated and incorporated into the forecasted total. In this manner, each sector could have its own set of drivers (predictors) that were appropriate for the electricity consumption in that sector, and sectoral models could be derived that had acceptable levels of multi-

collinearity. Consultation with different experts in the field of electricity consumption forecasting also confirmed that forecasts via different electricity usage sectors give better results than directly forecasting total consumption values. The main challenge was to find reliable historical values for sector consumption to use as a basis for these forecasts, together with historical values of potential predictor variables. The problems encountered during data collection and verification are discussed in more detail in section 4, but it may be summarised by saying that reliable data on electricity consumption per sector is very difficult to find.

Multiple regression modelling was chosen as the forecasting technique for each sector as this has been noted to be the most appropriate statistical technique for long-term forecasting (Makridakis, Wheelwright, and Hyndman, 1998). There have been previous reported studies where multiple regression has been used for long-term forecasting of electricity consumption in other countries, either for total consumption (Bianco, Manca and Nardini, 2009; Mohamed and Bodger, 2005; Egelioglu, Mohamad, and Guven, 2001) or for a specific sector (Al-Ghandoora *et al*, 2008). These models used different drivers for forecasting, as appropriate within the specific country, but employed the same regression technique as discussed in this paper. Details on the regression models are provided in section 5.

4. Electricity demand and 'driver' data

A very important component of the regression modelling involved the collection of appropriate data for the relevant variables required.

Data on national electricity consumption in South Africa from 1978 to 2010 was obtained from Statistics South Africa (Stats SA), from the series of monthly publications under the Statistical Release series P4141 – Generation and consumption of electricity, available from the website (StatsSAweb). The specific time series used is defined as the 'electricity available for distribution in South Africa'. Although this data is not broken down into electricity usage sectors, it was a valuable dataset to use to reconcile other datasets containing sector data. In order to obtain an adequate data series on electricity consumption per sector, it was necessary to obtain data from various sources as no single source could give data per sector from 1972 until present. When the forecasting methodology was initially developed, and subsequently updated, the following potential sources of sector data were identified:

- Statistics South Africa (some sectors, 1964–1984) (StatsSAweb)
- Rand Afrikaans University (RAU) (now University of Johannesburg) (1972-1991) (Cooper and Kotze, 1992)
- Department of Minerals and Energy (DME), 1998 Digest (now Department of Energy) (1990-1997) (Cooper, 1998)
- Department of Minerals and Energy (DME), 2000 Digest (now Department of Energy) (1992-2000) (DIGEST2002)
- Department of Minerals and Energy (DME), 2006 Digest (now Department of Energy) (1992-2004) (DIGEST2006)
- Department of Minerals and Energy (DME) Energy Balance Spreadsheets (now Department of Energy) (1992-2009) (ENERGYBALANCES)
- National Energy Regulator of South Africa (NERSA), Electricity Supply Statistics of South Africa (1996-2006) (ESS)
- South Africa Energy Statistics (Vol. 1 and Vol. 2) (1950-1993) (SAES1, SAES2)
- Eskom Annual Reports (1997-2010) (Eskom)
- Eskom Statistical Yearbooks (1957-1996) (Eskom Year Book)

The various sources had to be checked against each other and against the Stats SA national totals. Although the total consumption figures were roughly consistent between the various sources, there were large discrepancies for many of the data points (years) at the individual sector level. This is partly due to the mismatch between the number of sectors used in each source, but also to the inconsistency between sector definitions used in the different sources for some sectors. In order to use and compare data from the different sources, the sectors had to be aligned to one common set of sectors, and for this purpose, the sectors used by NERSA, and also reported by Eskom, were used as the standard. Although the Eskom Annual Reports provide a reflection of the electricity distribution by sectors, these sectors are broken down only for Eskom's direct customers and not for the electricity that is redistributed by the municipalities. Eskom has a large sector for redistributors that is listed in their reports, but this electricity consumption cannot be broken down by Eskom into the typical economic activity sectors. However, for the purposes of our sector forecasting and in the absence of suitable data from other sources, certain sector data was estimated using Eskom's electricity consumption per sector together with the historical estimates of Eskom's percentage share in the sector, as reported by NERSA.

The data discrepancies between the different data sources were considered and potential reasons were sought for these discrepancies. Where the reasons for discrepancies could not be ascertained, representatives from the data sources were contacted in order to obtain clarity on definitions and to gain understanding as to reasons for differences between sources. Examples of data issues that arose from the discussions include:

- The NER (now NERSA) data was collected from Eskom and municipalities, but Eskom has a different financial year to that of the municipalities, with the result that the data from the two sources are not aggregated over the same periods for the year being reported.
- Municipalities did not use the NER categories on their own systems, and therefore every year they had to match their data to the categories provided by NER before submitting the data, often leading to the same municipal client being classified differently in different years. This was particularly true of the commerce and manufacturing sectors.
- The Platinum mining sector was initially not included under mining in all sources, but was classified by some as industrial based on the platinum processing plants found on mining sites.
- Data from DME (now Department of Energy) was not always consistent across years when certain users were first classified into a 'non-specified other' category and later allocated to industry, commerce and residential. If a data version was published before this re-allocation, the sector data would be incorrectly reflected in the published version.
- In one or two sources, changes were made to definitions without adjusting the data 'backwards' to match the definition change.

After an extended period of data checks and consultation, the most reliable data series to use for each sector was selected, mostly using a combination of sources. All the recommended sector data series, once confirmed, were added together, distribution and transmission losses were added, and when checked against the Statistics SA national consumption figures the recommended total was found, for the majority of the years, to be within 1% of the total national electricity consumption, with only a few years differing by an amount close to 2.5% of the total. Note that the NERSA and Eskom data had to be adjusted for those years where the financial year did not coincide with the calendar year, with the former being the time period used for reporting and the latter being the time period used for our analysis. Adjustments were also made to the NERSA data to align it better with data published in Eskom's annual reports.

The graphs in Figures 1–5 provide an illustration

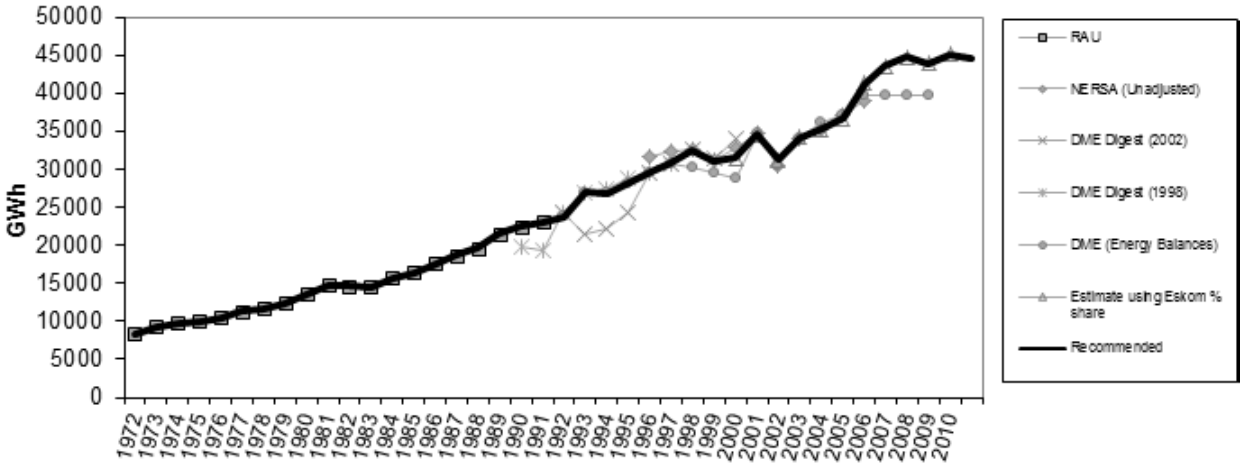

Figure 1: Comparing agricultural sector data between different sources

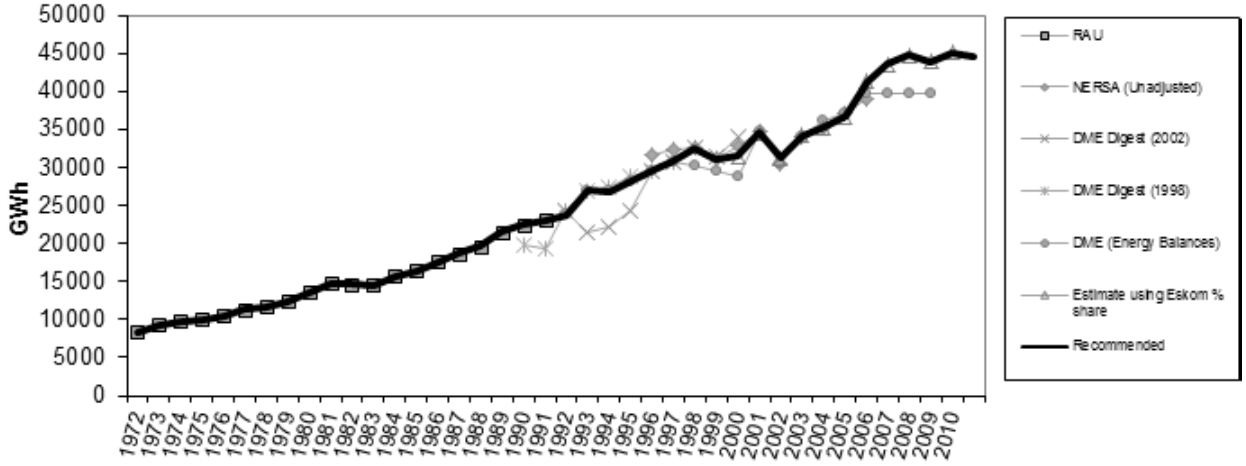

Figure 2: Comparing domestic sector data between different sources

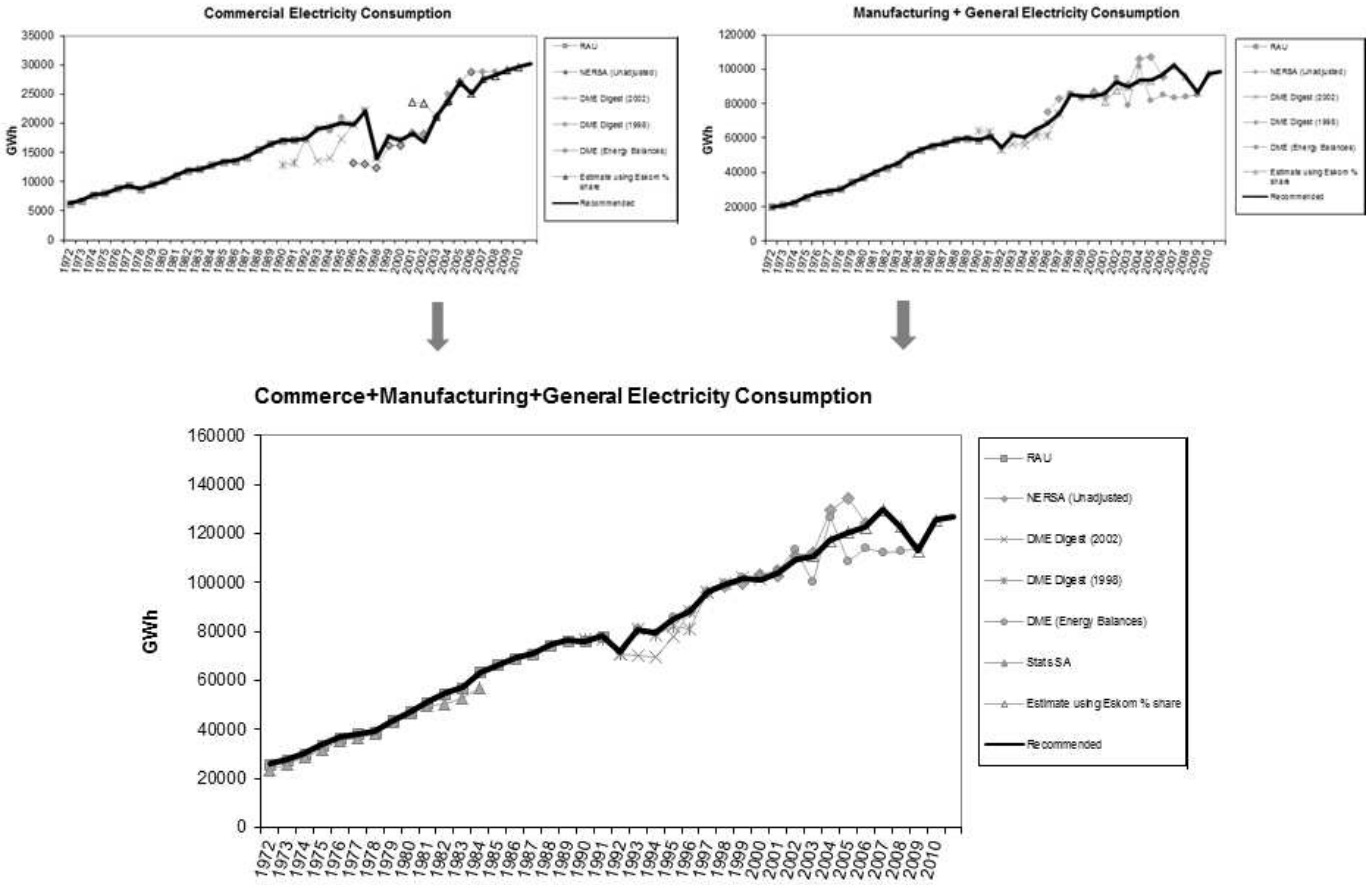

Figure 3: Combining and comparing commercial, manufacturing and general sector data between different sources

of the various data sources consulted, and the relative differences between them. The thick black line indicates the data pattern that was considered to be a reliable estimate for the sector and these patterns were therefore used as a basis for the forecasting.

Although most sources provide 'Commerce' and 'Manufacturing' (also referred to as 'Industrial') sectors, definitions differed widely between them, and even between different years of the same source. Consultation with representatives of the data sources also confirmed that differentiating between commerce and manufacturing within municipal customers was problematic and could change from year to year. Furthermore, most sources contain a 'general' category, and the definition of this category was also found to be inconsistent between sources. However, Figure 3 shows that when data on 'commerce', 'manufacturing' and 'general' sectors were combined for each of the various sources, the differences between the sources were reduced.

It can therefore be seen that the collection and selection of appropriate data for electricity consumption per sector from public domain sources was not a trivial task. However, it was considered necessary to develop a consistent and reliable set of historical data on which to apply the chosen methodology.

Data on predictor variables were also collected, but there were fewer sources for these, and sources generally had consistent patterns. Therefore, this data collection process is not discussed in as much detail as the electricity sector consumption data. Predictor data could be sourced from Statistics South Africa and the Reserve Bank of South Africa, though the electronic data download facilities on their websites (StatsSA2, SARB) and also from the Chamber of Mines (CoMines). Data on rail freight ton-kms was previously obtained from Spoornet, but has since 2003 been difficult to obtain.

5. Model development

An important step in the model development was to select a range of appropriate economic and demographic variables that could potentially affect electricity usage in the sectors, or could be proxies for the patterns observed in the sectors' electricity usage. The next step was then to collect the historical data for these variables, as discussed in the previous section. Potential variables included population figures, GDP or Gross Value Added (GVA) values per sector, mining production volumes, and so on. By investigating the strength of the statistical relationship between each of the potential predictor

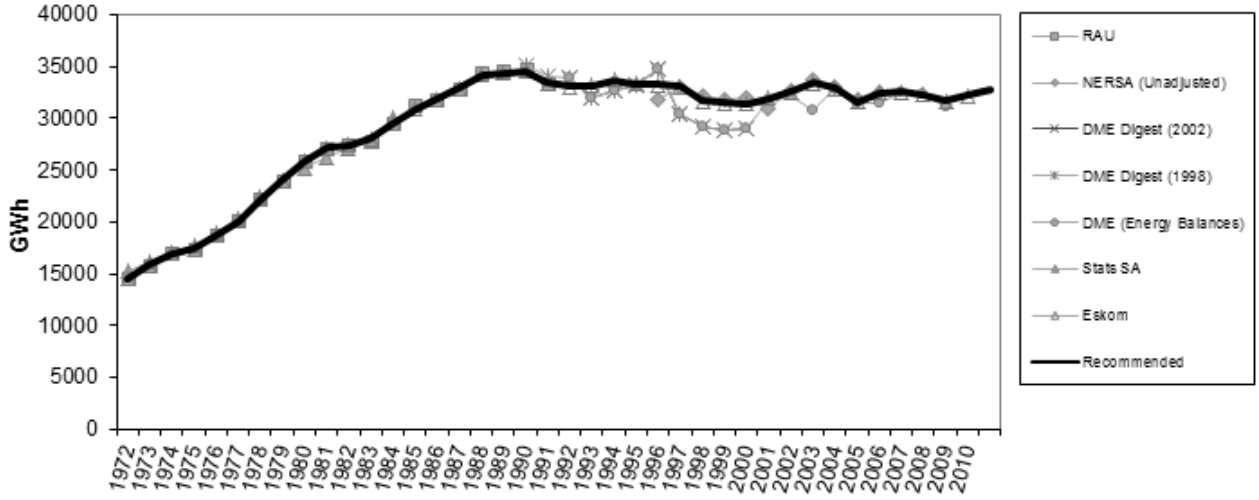

Figure 4: Comparing mining sector data between different sources

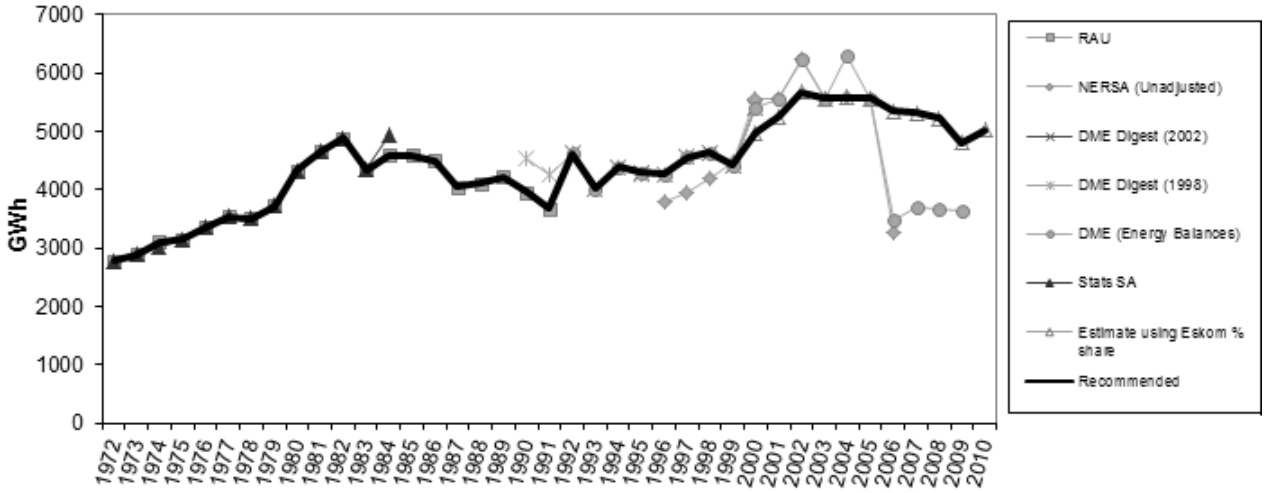

Figure 5: Comparing transport sector data between different sectors

variables and the electricity usage per sector, a smaller subset of these variables could be identified for inclusion in the final set of sector models.

The methodology followed to derive the final forecasts of total electricity consumption consequently involved an aggregation of several regression forecasts, with each sector having its own regression model. Scenarios were used to quantify the future values of various predictor variables that were identified during the regression modelling phase. Each scenario produced its own set of sector forecasts that could be added together and adjusted for estimated losses, on both distribution and transmission, to create forecasts for the total annual demand at a national level. The advantage of being able to visualise the electricity forecasts for each economic sector in a scenario, in addition to the total electricity forecast, is that one can assess the relevance and compatibility of the models and their outputs to the scenario descriptions.

In order to determine the statistical validity of the various regression models used for each electricity usage sector, the following factors were considered:

- The model had to be a statistically acceptable quantification of the relationships in the historical data, which meant that the included predictor variables had to be as few as possible but had to provide a good overall description of the electricity usage values over the period of historical data available. The goodness of fit was measured with the R^2 (correlation coefficient) and adjusted R^2 measures: the higher the R^2, the better the fit. (Note that relationships were assumed to be linear, and if non-linear relationships were found a relevant transformation, such as a logarithmic transformation, were applied to linearise the relationship).
- Residual patterns for the various model options were also considered. Residuals are defined as the difference between the values predicted from the model for a particular year and the electricity usage actually measured in that year. Very large residuals or residuals that seem to show a pattern that is not random could be an indication that the model does not fit well or that an important predictor variable was not included in the model.

- Models had to be selected in which the predictor variables showed low levels of multi-collinearity. This is measured with the condition index value – the lower the condition index, the better. A condition index of between 5 and 10 indicate low levels of multi-collinearity, while a condition index of between 30 and 100 indicate moderate levels of multi-collinearity in a model. (See the classic reference on multi-collinearity and the condition index (Belsey, Kuh and Welsch, 1980), or a discussion of the impact of multi-collinearity on regression models (Montgomery, Peck and Vining, 2006) for more information).
- The regression coefficients associated with each predictor variable had to be statistically significant. A 90% significance level was used for allowing variables to enter into any of the sectoral regression models.
- Each sectoral model should to some extent accommodate factors that are believed to be influencers of electricity consumption in that sector, i.e. be logically defensible.

Unfortunately, it is very seldom that a model will be equally good on all these criteria. Often, trade-offs had to be made. For instance, it may be that one model does not have the largest R^2 value, but has a lower condition index than another model.

For each of the individual electricity consumption sectors, a 'best' model was selected by applying an iterative procedure. A first potential model would be developed using stepwise regression, and then the model would be assessed against the above criteria. If the model was not found to be a good balance of all the criteria, changes would be made to the input variables and the process would be repeated and the resulting models would be re-assessed. Table 1 provides an indication of the predictor variables used in the initial version of the models, for the various electricity demand sectors, and typical values for the associated goodness of fit measures obtained.

Finally, although regression was chosen as the most appropriate statistical technique for this type of forecasting, it should be emphasised that the results from a regression model must be interpreted purely as a statistically proven inter-relationship. A significant relationship between the predictor variables and the variable they predict does not necessarily establish a cause and effect relationship between them. Also, note that the regression models were developed very specifically for the South African situation and were based on historical data collected from public domain sources for the South African situation.

6. Developing forecasts

After applying the sectoral regression modelling approach to the recommended sector data to obtain sector models, for example, those listed in Table 1, these models were then applied to a set of scenarios, comprising of forecasted values for the relevant predictor variables, to produce a set of electricity demand forecasts. Such a set of forecasts were initially produced using this methodology in 2003, using historical data up to 2002, for the identified client. Subsequently, updated forecasts were produced for the same client with the same methodology in two further studies, using historical data up to 2004, and then later using data up to 2006. The forecasts were incorporated by the client into various internal strategic planning processes and were based on scenarios that were matched to their strategic planning needs and questions.

The same methodology was later applied, using updated historical sector data and different scenario values as inputs, to provide a set of forecasts to compare to those prepared by Eskom for use in the Integrated Resource Plan developed in 2010 (IRP2). Since the project team that developed the forecasts using this methodology were from the CSIR, the set of forecasts developed for the IRP2 using this methodology was called the 'CSIR model' forecasts, to distinguish them from the ones produced by Eskom. Figure 6 indicates how the forecasts from this methodology, for the three scenarios used within the IRP ('High', Moderate' and 'Low'), compared to the actual values observed subsequent to the publication of the forecasts. Note that the long-term forecasts used in the IRP forecasts and the details regarding the scenarios can be obtained from the website of the Department of Energy .

Table 1: Summary of initial regression models used per sector

Electricity sector	*Predictor variables*	*Adjusted R^2*	*Condition index*
Agriculture	Final Consumption Expenditure by Households (also called Private Consumption Expenditure)	$R^2 = 0.96$	N/A if only 1 variable in model
Transport	Rail freight ton-kms and GDP	adjusted $R^2 = 0.76$	CI = 26.5
Domestic	Final Consumption Expenditure by Households (also called Private Consumption Expenditure)	$R^2 = 0.96$	N/A if only 1 variable in model
Commerce & manufacturing	Population and GDP	adjusted $R^2 = 0.98$	CI = 69.2
Mining	Platinum production volume index, Coal production volume index, Gold ore milled	adjusted $R^2 = 0.91$	CI = 44.7

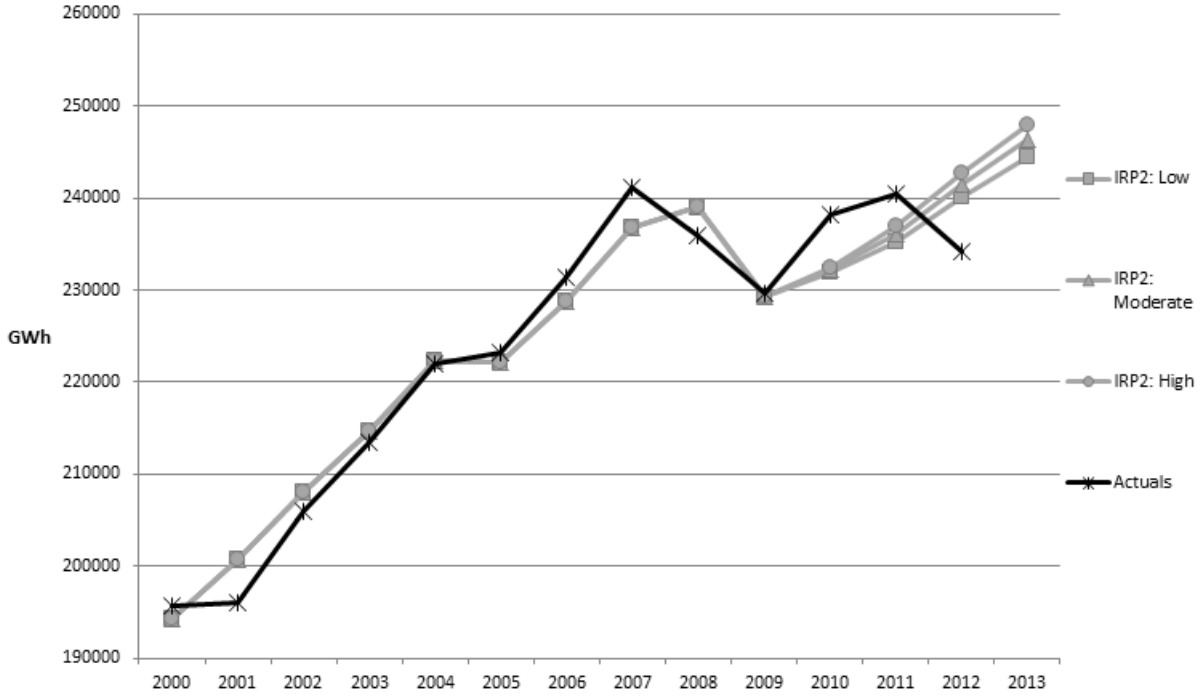

Figure 6: Forecasted values obtained for different scenarios compared to actual values observed

The forecasting methodology involved applying the quantified (statistical) relationships, identified from historical patterns, to different future scenarios relating to expected economic and demographic changes, in order to obtain the resulting forecasts for electricity usage. Since the forecasts are directly linked to scenarios for GDP and other predictor variables, the forecasted electricity values need to be interpreted within the context of these scenarios. For example, if a particular scenario was compiled using GDP growth figures that were very far from the actual grow patterns observed, then the electricity forecasts generated for this scenario may also be unrealistically high.

Therefore, although the 'true test' of any forecasts relates to how far the forecasted values were from actual recorded values, the problem with comparing the forecasts provided in Figure 6 with the actual values provided in the same figure is that the scenario values underlying the forecasts may differ from the actual recorded economic and demographic values. While scenario thinking can support planning and forecasting well, there are certain pitfalls to avoid when generating scenarios (□nkal, Sayim, and Gönül, 2013).

Therefore, to provide a better comparison of 'forecasts' to 'actuals', figure 7 needs to be considered. In Figure 7, the model that was developed in 2007 (using historical data up to 2006), as well as the model developed in 2010 for the IRP2 (from historical data updated to 2009), were both applied to the predictor variables recorded in 2007 – 2012 to develop predicted values for national electricity consumption for these years. These predicted values were then compared to the actual electricity consumption published by Stats SA (StatsSAweb).

Figure 7 shows visually that the forecasting methodology produced forecasts close to those of the actual patterns. The forecasted values from the 2007 model differed by less than 0.5% from the actual 2007 value, by 3% from the actual 2008 value, and between 4 and 7% from the actual patterns in 2009 – 2011. The IRP2 model produced forecasts that differed by less than 2% from the actual values in 2010, less than 0.5% in 2011, and was 4.4% higher in 2012 than the actual recorded value. The 2007 model therefore clearly predicted the actual values well up to 2008, but did not manage to anticipate the 'dip' over the 2008 – 2010 period which could mainly be ascribed to the effects of the global recession (Eberhard, 2011). The effect of the recession was not reflected sufficiently in the combination of drivers incorporated into the 2007 model and therefore did not successfully translate into a dip in electricity demand.

In the IRP2 model, a decision was made to use the manufacturing production volume index rather than the GDP as a predictor in the Commerce and Manufacturing sector model, and this change resulted in a much better overall fit. Note that this sector accounts for about 50% of the overall electricity usage, and so forecasting errors in this sector affects the accuracy of the overall forecast substantially. The IRP2 model therefore gave much better predictions over the 2008 – 2011 period, but overestimated demand in 2012. Subsequent studies has shown that the decrease in 2012 may have been due to improvements in energy efficiency, which in the manufacturing context equates to less electricity being used to produce the same manufacturing vol-

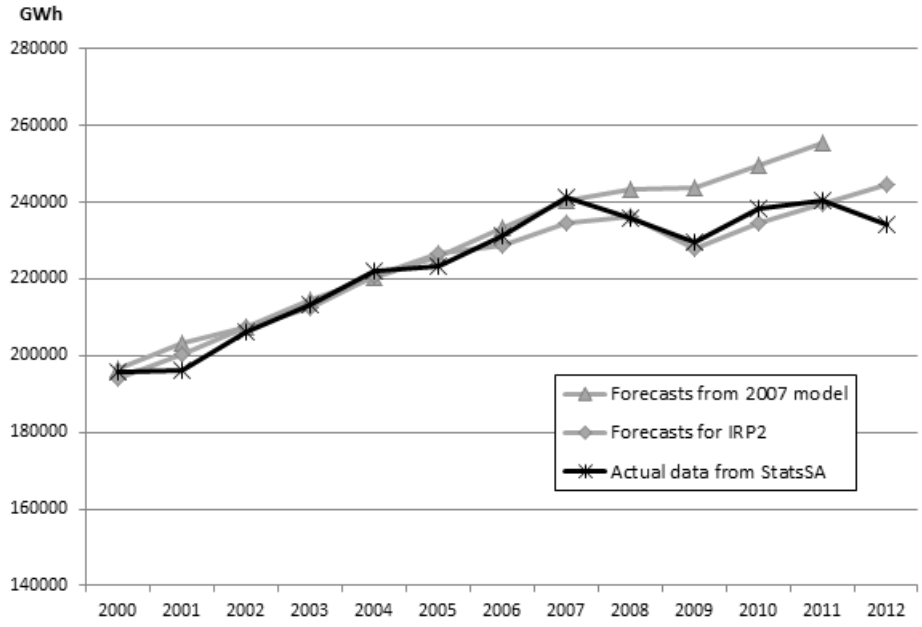

Figure 7: Comparing forecasts developed from methodology using actual predictors to actual electricity demand values measured

umes. Since these patterns have only started to appear since 2011, sufficient data is not yet available to quantify electricity efficiency improvements, but current research by the team is focusing on introducing an 'intensity factor' into some of the sectoral models.

It can therefore be said that the methodology described in this paper does provide a useful translation of economic and demographic scenarios into electricity consumption forecasts. It is, however, still necessary to continuously update these models in order to incorporate the most recent electricity usage behaviour, particularly in light of the increasing constraints on the South African energy system.

7. Concluding remarks

The methodology discussed in this paper differs from other reported studies that produced forecasts for long-term electricity demand in South Africa (Prinsloo, 2009; Van Wyk and Fourie, 2009; Inglesi, 2010). This methodology forecasts electricity within all usage sectors and then aggregates the sector forecasts to a national total, while some of the other studies (Van Wyk and Fourie, 2009; Inglesi, 2010; Inglesi and Pouris, 2010) directly forecast demand at a national level. Forecasts produced by Eskom, such as those that are provided in the IRP 2010 documentation (DOE) or done internally within the organisation (Prinsloo, 2009), are also based on data at sector level, but as the major supplier of electricity they have access to a great deal of customer-specific data, both quantitative and qualitative, from which they can provide detailed sectoral forecasts. However, such customer-specific data is confidential and not available in the public domain. The methodology described in this paper therefore fills a particular gap since it uses only publicly available data by combining data reported in the public domain by Eskom with other public domain sources, and it provides a breakdown of the forecasts per usage sector. In addition, this methodology is particularly well suited to supporting scenario-based forecasting since it forecasts the expected electricity demand based on only a few key economic and demographic indicators, thereby being able to produce a new set of forecasts for a new scenario very quickly.

This methodology is also purely data-driven, and the predictor variables are selected into the models on the basis of the strength of the statistical relationships inherent in the historical data. Although the choice of variables that are tested for inclusion in the models are based on a logical understanding of each sector, this methodology does not incorporate any theories regarding the underlying causes of patterns, which would distinguish it from econometric studies focusing on the effect of a particular pre-chosen variable(s) of interest on electricity consumption (Wolde-Rufael, 2006; Ziramba, 2008; Odhiambo, 2009; Amusa, Amusa, and Mabugu, 2009; Inglesi-Lotz, 2011). In particular, a number of these studies investigate the effect of price on electricity demand, either at the national level (Inglesi, 2010; Inglesi and Pouris, 2010; Amusa, Amusa, and Mabugu, 2009; and Inglesi-Lotz, 2011) or within electricity usage sectors (Ziramba, 2008, Inglesi-Lotz and Blignaut, 2011). The results of the studies differ, but in general seem to conclude that in the late 1990s up to the mid-2000s, real income (as defined by GDP) has had a significant effect on electricity demand, while price elasticity has not been a significant predictor.

Our chosen data-driven methodology has the disadvantage of not being able to model the effect of variables that did not play a statistically significant role in the historical data, or of causal factors which could not be quantified. The continual media interest in the Eskom price hikes in recent years may indicate the need to study the effect of the price increases on demand, and it may also be argued that constraints on the supply of electricity have since 2007 (and could in future) constrain demand and even limit economic expansion. However, in the absence of reliable, sustainable sources of publicly available information on many aspects that drive current and future demand for electricity in South Africa, the statistical models proposed in this paper, which implicitly take into account the combined effect of a number of aspects in an overall pattern, could be seen to be an appropriate way to make use of the data that is available.

A concern that has to be raised, however, is that NERSA has not released any data on electricity demand per sector since 2006, and the Department of Energy has only released limited information on electricity usage per sector within the Energy Balances documents (DOEStats). However, the information contained in the Energy Balances documents seem to be questionable, since the totals do not correspond to the national electricity consumption figures released by Statistics South Africa. Although the International Energy Agency (IEA) has published electricity usage per sector since 2006, and lists the Department of Energy, along with Eskom, as sources for the statistics they have published on South Africa, they also indicate that they used their own internal estimates to determine their published data. The total production figures published by the IEA correspond to that of Statistics South Africa, but the IEA sectoral breakdowns differ from those contained in the Energy Balances documents. If data is not available in the public domain regarding electricity usage per sector it will be difficult to use the forecasting methodology described in this paper in future and it may also affect other types of energy modelling, such as energy efficiency studies.

In conclusion, the forecasting methodology presented in this paper has a strong scientific basis, and is also suitable for providing support to future strategic planning. Although any forecasts derived from historical patterns may have certain limitations, when used within the correct context, namely as one input into a high-level strategic planning process, they can provide valuable insight to support planning for potential long-term patterns of electricity demand. If reliable data on sectoral usage of electricity is consistently available in future, this methodology could offer value to a range of such strategic planning processes.

References

Al-Ghandoora, A., Al-Hintib, I., Jaberc, J.O., and Sawalha, S.A., (2008). Electricity consumption and associated GHG emissions of the Jordanian industrial sector: Empirical analysis and future projection, *Energy Policy*, Vol. 36: p. 258-267.

Amusa, H., Amusa, K., and Mabugu, R., (2009). Aggregate demand for electricity in South Africa: An analysis using the bounds testing approach to cointegration, *Energy Policy*, Vol. 37: p.4167 – 4175.

Belsey, D.A., Kuh, E., and Welsch, R.E., (1980). Regression Diagnostics, (Chapter 3, specifically p. 104, 105, 112), John Wiley & Sons.

Bianco, V., Manca, O., and Nardini, S. (2009). Electricity consumption forecasting in Italy using linear regression models, *Energy*, Vol. 34: p. 1413–1421.

CoMines Mining production data is available from the Chamber of Mines website at http://www.bullion.org.za/content/?pid=71&pagename=Facts+and+Figures [accessed July 2013].

Cooper, C.J., (1998). Digest of South African Energy Statistics 1998, Department of Minerals and Energy (DME).

Cooper, C.J. and Kotze, D.J., (1992). *Energy Projections for South Africa*, Vol. 8, Institute for Energy Studies, Rand Afrikaans University (RAU), (Appendix A).

DIGEST2002, Digest of South African Energy Statistics 2002, Department of Minerals and Energy (DME).

DIGEST2006, Digest of South African Energy Statistics 2006, Department of Minerals and Energy (DME).

DOE, Link to document available on http://www.doe-irp.co.za/ [accessed June 2013].

DOEStats Available via the website of the Department of Energy http://www.energy.gov.za/files/energyStats_frame.html, [Accessed June 2013].

Doriana, J.P., Franssen, H.T., and Simbeck, D.R. (2006). Global challenges in energy, *Energy Policy*, Volume 34: p. 1984–1991.

Eberhard, A. (2011). The Future of South African Coal: Market, Investment and Policy Challenges, Working Paper #100, Program on Energy and Sustainable Development, Stanford University, available from http://iis-db.stanford.edu/pubs/23082/WP_100_Eberhard_Future_of_South_African_Coal.pdf [accessed September 2014].

Egelioglu, F. Mohamad, A.A., and Guven, H. (2001). Economic variables and electricity consumption in Northern Cyprus, *Energy*, Vol. 26: p. 355 – 362.

ENERGYBALANCES, Energy Balance Spreadsheets, Department of Minerals and Energy (DME).

Eskom, Eskom Annual Reports, 1990-2001, Eskom.

ESKOMYEARBOOK Eskom Statistical Yearbook, 1996, Eskom.

ESS, Electricity Supply Statistics, 1996, 1998-2001, National Electricity Regulator (NER).

Imtiaz, A.K., Mariun, N.B., Amran M. R., M., Saleem, M., Wahab, N.I.A., Mohibullah, (2006). Evaluation and Forecasting of Long Term Electricity Consumption Demand for Malaysia by Statistical Analysis, First International Power and Energy Conference, (PECon 2006) Proceedings , Art. No. 4154502, p. 257-261.

Inglesi, R., (2010). Aggregate electricity demand in South Africa: Conditional forecasts to 2030, *Applied Energy*, Volume 87, p. 197–204.

Inglesi, R. and Pouris, A., (2010). Forecasting electricity demand in South Africa: A critique of Eskom's projections, *South African Journal of Science*, Vol. 106: p. 50-53.

Inglesi-Lotz, R. (2011). The evolution of price elasticity of electricity demand in South Africa: A Kalman filter application, *Energy Policy*, Vol. 39, p.3690 – 3696.

Inglesi-Lotz, R., and Blignaut, J.N. (2011). Estimating the price elasticity of demand for electricity by sector in South Africa, *South African Journal of Economic and Management Sciences*, Vol. 14 (4): p. 449 – 465.

Makridakis, S., Wheelwright, S.C. and Hyndman, R.J. (1998). Forecasting: methods and applications (3rd Edition), John Wiley & Sons Inc., p. 521.

Montgomery, D.C., Peck, E.A. and Vining, G.G., (2006). Introduction to Linear Regression (4th Edition), John Wiley & Sons Inc., p. 109 – 111 and Chapter 11.

Odhiambo, N.M. (2009). Electricity consumption and economic growth in South Africa: A trivariate causality test, *Energy Economics*, Vol. 31: p. 635–640.

□nkal, D., Sayim, K.Zk, and Gönül, M.S. (2013). Scenarios as channels of forecast advice, *Technological Forecasting and Social Change*, Vol. 80 (4): p. 772–788.

Prinsloo, J. D. (2009). Long term electricity demand forecasting in Eskom (1987 to mid-2008), Available as part of the proceedings of the First Annual Forecasting Conference 'Forecasting in an ever changing environment', held in Midrand on 17 & 18 November 2009.

SAES1, South African Energy Statistics 1950-1989, No 1, 1990, National Energy Council (NEC), (Chapter 4).

SAES2, South African Energy Statistics 1950-1993 No 2, 1995, Department of Minerals and Energy Affairs (DMEA) and Eskom Marketing Intelligence, (Chapter 4).

SARB, The online statistical query facility of the Reserve Bank of South Africa is available at http://www.resbank.co.za/Research/Statistics/Pages/OnlineDownloadFacility.aspx [accessed July 2013].

Soontornrangson, W., Evans, D.G., Fuller, R.J., and Mohamed, Z., Bodger, P., (2005). Forecasting electricity consumption in New Zealand using economic and demographic variables, Energy, Vol. 30: p. 1833 – 1843.

StatsSAweb, Available via the automatic download facility of StatsSA, at http://www.statssa.gov.za/publications/statsdownload.asp?ppn=P4141&SCH=5562, [accessed July 2013].

StatsSA2, Interactive data download facility of Statistics SA available from http://www.statssa.gov.za/timeseriesdata/main_timeseriesdata.asp [accessed July 2013].

Stewart, D.F. (2003). Scenario planning for electricity supply, *Energy Policy*, Volume 31: p. 1647–1659.

Ulutaş¸ B. H. (2005). Determination of the appropriate energy policy for Turkey, *Energy*, Vol. 30: p. 1146–1161.

Van Wyk, L., and Fourie, E.T., (2009). Forecasting South Africa's electricity demand, available as part of the proceedings of the First Annual Forecasting Conference 'Forecasting in an ever changing environment', held in Midrand on 17 & 18 November 2009.

Wolde-Rufael, Y., (2006). Electricity consumption and economic growth: a time series experience for 17 African countries, *Energy Policy*, Vol. 34, p. 1106 – 1114.

Ziramba, E. (2008), The demand for residential electricity in South Africa, *Energy Policy*, 2008, Volume 36, p. 3460– 3466

Received 8 November 2013; revised 1 October 2014

A systems approach to urban water services in the context of integrated energy and water planning: A City of Cape Town case study

Fadiel Ahjum
Energy Research Centre, University of Cape Town, Cape Town, South Africa

Theodor J Stewart
Department of Statistical Sciences, University of Cape Town, Cape Town, South Africa

Abstract
The City of Cape Town derives the bulk of its present water supply from surface water resources and is the central water service authority for metropolitan consumers. The City is also a provider of bulk water to neighbouring municipalities. An exploration of the energy consumption for water and sanitation services for the City of Cape Town was conducted with an emphasis on water supply augmentation options for the near future (2011-2030). A systems analysis of municipal urban water services was undertaken to examine the energy requirements of supply alternatives and the efficacy of the alternatives in respect of supply availability and reliability. This was achieved using scenario based analysis incorporating a simple additive value function, to obtain a basic performance score, to rank alternatives and facilitate a quantitative comparison. Utilising the Water Evaluation and Planning hydrological modelling tool, a model for urban water services was developed for the City and used to conduct scenario analyses for a representative portfolio of previously identified options. Within the scope of the research objectives, the scenario analyses examines the direct energy consumption for the provision of water services for the City as influenced by external factors such as population growth, surface water runoff variability, available alternatives and the policies that are adopted which ultimately determine the future planning. It is contended that the modelling process presented here integrates energy and water planning for an assessment of water and energy resources required for future growth, and the optimal measures that could be pursued to reconcile the demand for water and the concomitant energy requirements.

Keywords: City of Cape Town, energy and water planning, water evaluation and planning

Introduction

South Africa is a country with a precarious energy and water resource landscape. Both sectors suffer from ageing infrastructure and the capacity to function sustainably (Coetzer, 2012; Gaunt, 2010). The energy capacity crisis of 2007/8 led to power shortages with a direct impact on economic growth (Eberhard, 2008). In the Vaal Triangle, the economic and industrial heart of the country, the water stressed industry has expressed concerned that a drought in the near future could have drastic economic consequences (Davies 2012). In the recent past in the Western Cape Province, located in the south west of South Africa, a decline in surface water storage required the imposition of water restrictions in the City of Cape Town in 2000/1 and 2004/5 (DWAF, 2007c). An investigation of future water requirements for the CCT suggested that, without any interventions, demand would exceed the available supply by 2020 for a low population and economic growth scenario and earlier if higher growth is experienced (DWAF, 2007c).

The expansion of water services infrastructure to meet growing demand in a future of increasing environmental and energy constraints requires the consideration of alternative water supplies as the capacity of the present system is reached. South Africa's White Paper on the National Climate Change Response (2011) emphasizes the investigation of other sources, beyond the traditional reliance on surface water systems, as a key element in water sector growth and security, stating the importance of 'exploring new and unused resources, particularly groundwater, re-use of effluent, and desalination'.

The scope of this study is restricted to urban municipal water services for the City of Cape Town and excludes any energy used directly by consumers in the use and disposal of water and

sewage. Figure 1 illustrates the municipal water services cycle in the context of this study. Similarly, agricultural water demands in the region are also not examined in detail except where water resources are shared such as the surface water schemes, for example.

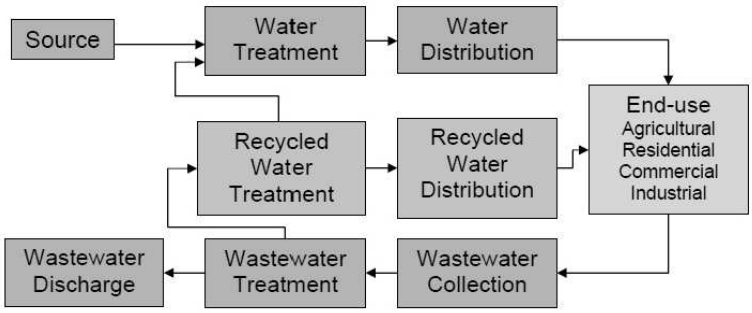

Figure 1: The municipal water services cycle
Adapted from California Sustainability Alliance 2008

It was estimated that the provision of water and sanitation services for the period 2007/08 accounted for half of the City's electricity consumption with a third attributed to waste water treatment alone (Jennings 2012). The potential for an increase in energy consumption for future water and sanitation services motivated this study which aimed to complement previous studies that have quantified the energy demands of water services (Cooley and Wilkinson, 2012; deMonsabert and Bakhshi 2009; Larabee *et al.,* 2011; Olsson, 2011).

From 'source to discharge' as water is abstracted, transformed and conveyed for the needs of the urban sector, the study aimed to evaluate the energy implications and efficacy of reconciling demand and supply of a portfolio of alternate intervention measures, which cater for future scenarios comprising: population and economic growth; reduced surface water availability (e.g. environmental constraints); and more energy intensive treatment processes. This was achieved using scenario based analysis incorporating a simple additive value function, to obtain a basic performance score, to rank alternatives and facilitate a quantitative comparison in respect of supply availability, reliability and energy intensity.

Utilising the Water Evaluation and Planning (WEAP) hydrological modelling tool (SEI, 2012b), a model for urban water services was developed for the City, as shown in Figure 2 and used to conduct scenario analyses for a representative portfolio of options previously identified by the National Department of Water Affairs (DWAF, 2007c). The modelling emphasises the direct energy consumption as studies have indicated that the operational phase is typically the most energy intensive over the life span of water and sanitation infrastructure (Buckley *et al.,* 2011; Lui, 2012; Stokes and Horvath, 2006).

The WEAP application program interface enables direct access to the WEAP model via MS-Excel in the Visual Basic Application (VBA) programming environment. This allowed water supply volumes to the City (aggregated with its bulk customers) to be to collated and categorised by type (e.g. ground water, desalination etc.) and linked with the associated energy cost path (or water transmission path). The categories utilised are indicated in Table 1.

Within the VBA environment, the transmissions paths were determined by scrutinizing the relevant WEAP data structures. Referring to Figure 2, trans-

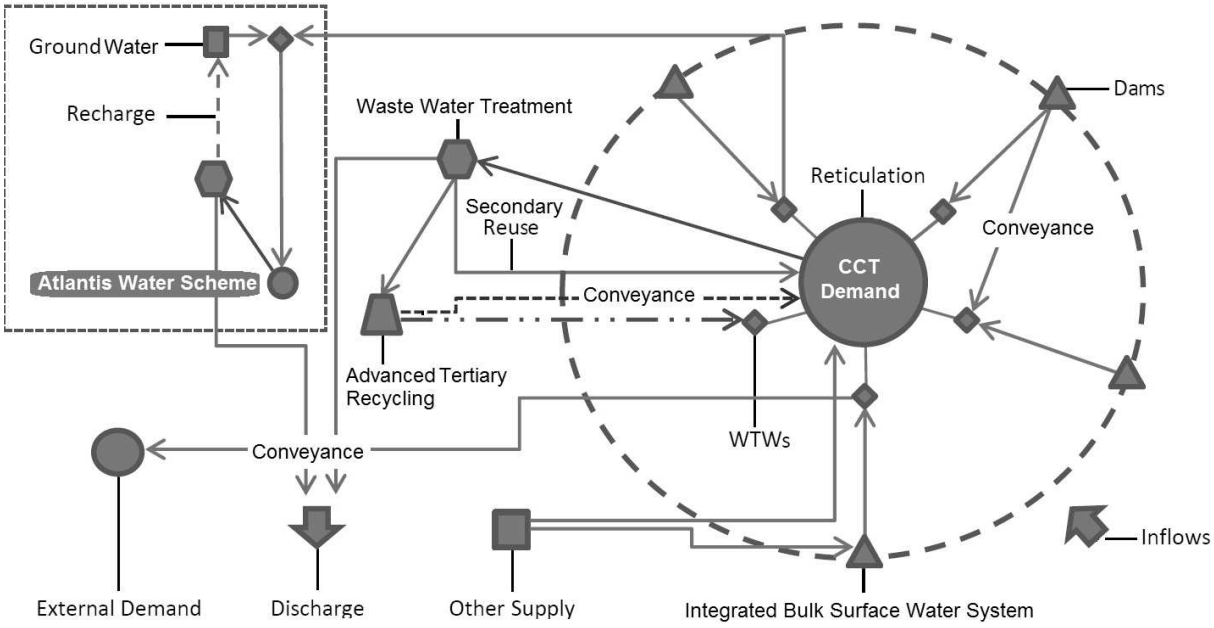

Figure 2: Conceptual municipal water services model developed for the systems analyses

Table 1: Stages or categories of the urban water cycle as implemented in WEAP

WEAP object prefix	*Description*	*Example WEAP object*
WTW	Water treatment works	'CCT WTW Faure' (Individual City WTW plant)
WWTP	Waste water treatment works	'CCT WWTP' (Lumped treatment process)
GW	Ground water	'GW TMG THK' (Specific option: Table Mountain Group)
DIST	Potable water distribution	'CCT Dist' (The City's distribution network)
SWD	Sea water desalination	'CCT SWD' (Lumped SWD option for the City)
WWR	Waste water reclamation	'CCT WWR NEWater' (Specific treatment process)
n/a	Other	Refers to conveyance of water across the system that is not accounted for (e.g. pump stations for water transfers)

mission links within WEAP connect the various stages of the water use cycle. Dams can be interconnected and linked to demand sites which are then, for example, linked to waste water treatment plants (WWTP) which process the return flows (effluent). In the model depicted, for example, these paths are located in the WEAP data branches:

- 'Supply and Resources\Transmission Links\to CCT Dist' (Supply to City's distribution network)
- 'Supply and Resources\Transmission Links\to CCT EX BULK Dist' (Supply to City's external customers)
- 'Supply and Resources\Transmission Links\to CCT Dist Atlantis_Mamre' (Supply to City's Atlantis Water Scheme)

The most recent issue of WEAP includes functionality to link directly with its companion energy modelling software tool, Long-term Energy Alternatives Planning (LEAP) system, to facilitate water-energy modelling (SEI, 2012a). At the time this research was conducted, this functionality was lacking. Therefore, energy consumption was incorporated using WEAP's financial analysis module by incorporating a user defined 'energy currency' based on the energy intensity or specific energy of a process. These 'costs' need to be assigned to the various stages of the water use cycle. This is either derived from empirical data or a first principle calculation. For example, the theoretical hydraulic energy required transporting water via a pipeline across known topography; or the energy generated at a WTW exploiting the existing hydraulic gradient (SACN, 2011) as approximated by Equation 1:

$$E(kWh)/\text{ month} = 1/e * pg\,QH/3.6MJ$$
$$E(kWh)/\text{ month} = 1/e * 0.002725\,QH \quad (1)$$

Where e = system efficiency, Q =flow rate (m^3/month), H = Head (m), p = density of water (kg/m^3), g = gravity m/s^2

The net energy cost for water and sanitation services is then the linear sum of the product of the energy intensities and the volumes of water (or effluent) that is processed at each stage. This is mathematically expressed in Equation 2. The methodology is similar to that adopted in LEAP.

$$E(kWh) = \sum_{k=1}^{n} e_k s_k \quad (2)$$

Where e = energy intensity (kWh/m^3); s=stage (m^3); k=WEAP object

In further discussion, the specific energy or energy intensity of the water sector is defined as the energy consumption per m^3 of water supplied to the distribution network or effluent conveyed and treated.

Empirical energy data for the City's Reticulation and Bulk Water Supply network were not available at the time requests were made (Allpass, 2012; Mashoko, 2012; Moll, 2012). In their absence, estimates are used as reported in the literature. Reported data was scrutinised for their applicability to Cape Town's environment as topography as well as the manner of water supply and conveyance is an important factor in the energy consumption of the water sector (Friedrich *et al.,* 2009; Kenway *et al.,* 2008). Figure 3 illustrates the modelling process.

Table 2 and Table 3 list the individual options and class of interventions comprising the options used for this case study. The interventions represent an orientation towards a particular category of supply or demand management. That is, an intervention programme which prefers sea water desalination, surface water, ground water or effluent recycling options. The interventions are also compared against a partial or continued water conservation and water demand management (WC/WDM) program.

Unrestricted and regulated usage of dam volumes for urban water consumption are also examined and compared for their relative performance. It is assumed that this simulates drought mitigation measures or water rationing that the National Department of Water Affairs and City practices to ensure a minimum reserve. In contrast, the unrestricted usage of water from the dams (aside from the allocations to agriculture) is also modelled as a comparison of the water supply and energy consumption requirements.

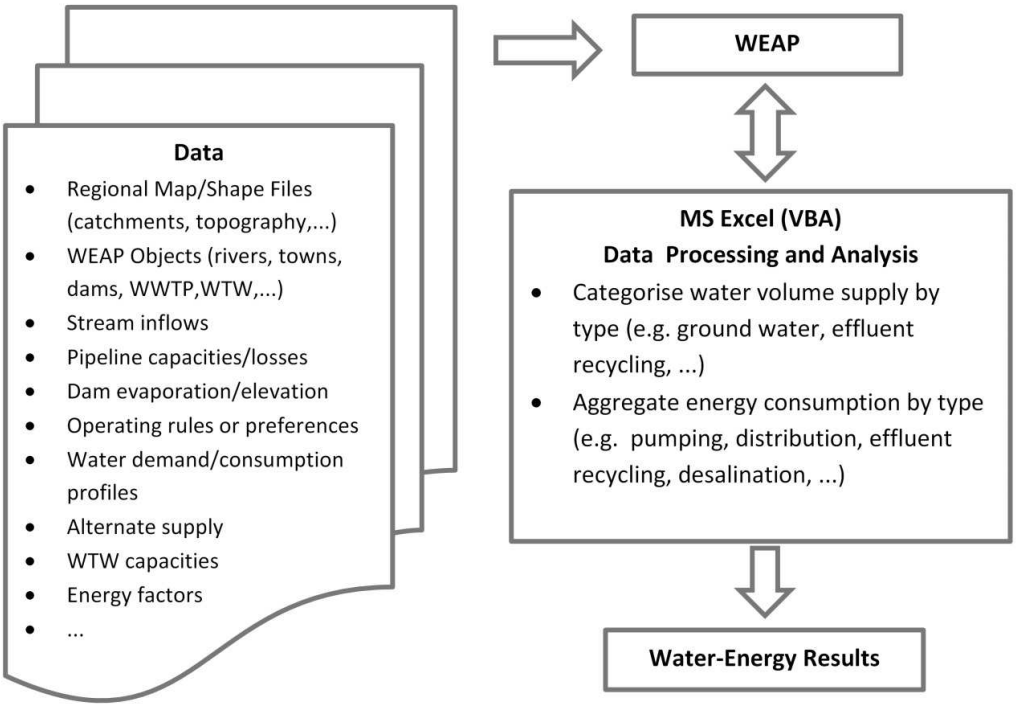

Figure 3: The integrated water-energy modelling process

Table 2: A summary of policy options for water supply and demand reconciliation in the model

(1)	Water Conservation / Water Demand Management (WC/WDM) (a): limited programme
(2)	WC/WDM (b) : extended programme
(3)	Ground Water Augmentation of Theewaterskloof dam from TMG (TMG-THK)
(4)	Additional Surface Water Options
(5)	Reuse of Secondary Treated Effluent
(6)	Advanced Recycling of Effluent (including potable augmentation)
(7)	Sea Water Desalination
(8)	Regulation of Water Releases from the Berg River and Theewaterskloof Dams

Table 3: Candidate interventions comprising the policy options modelled in WEAP

Intervention	Policy option preference
(a)	WC/WDM (1) > Ground water (3) > Reuse (5) > Desalination (7)
(b)	WC/WDM (1) > Surface (4) > Reuse (5) > Ground water (3) > Recycling-Potable (6)
(c)	WC/WDM (2) > Desalination (7) > Reuse (5)
(d)	WC/WDM (2) > Reuse (5) > Recycling-Potable (6) > Ground water (3)

The interventions are illustrative of the impact of policy decisions and do not represent an exhaustive analysis of the complete range of possibilities but rather serve to highlight the modelling process as well, which attempts to address three dimensions of water and energy planning. These are: energy consumption, water availability and assurance of supply.

The scenarios modelled are summarised in Table 4.

The water demand scenarios are based on the DWAF Future Water Requirements Study (2007), where two water demand scenarios account for a combination of high economic and population growth and conversely low economic and population growth. The 2007 DWAF forecast is depicted in Figure 4, which includes the actual demand up to the period 2009/10 along with the economic and population growth rates used. Figure 5 contrasts the DWAF forecast with the adjusted WEAP demand scenarios which utilise 2009/10 as the base year.

Water availability is quantified with a comparison of the surface water storage of the major dams at the start and end of the period. A 'System Storage Index' is created and refers to the ratio of minimum dam storage (occurring about the month of April) at the end of the period to that at the start, based on a four year average. The WEAP Reliability variable which quantifies the extent that supply is able to meet demand over the period is used to indicate the assurance of supply for a particular intervention. Within WEAP, the system reliability indicates the percentage of time that demand is met for the period (i.e. 100% = no unmet demand for the period and 50% = half the time there is unmet demand).

To facilitate a performance comparison of the interventions in relation to the three parameters mentioned, a basic performance index (α) is used. In the context of the research presented here, a favourable intervention is that which minimises

Table 4: A summary of the scenarios modelled with WEAP

Scenario	*Water demand*	*Surface inflow*	*Water quality*	*Dam waters*	*Comments*
1	High	Historic	Low degradation	Regulated	Reference Case
2	High	Historic	Low degradation	Unrestricted	
3	High	Reduced Inflow	Higher degradation	Regulated	Worst case
4	High	Reduced Inflow	Higher degradation	Unrestricted	
5	Low	Historic	Low degradation	Regulated	
6	Low	Reduced Inflow	Higher degradation	Unrestricted	

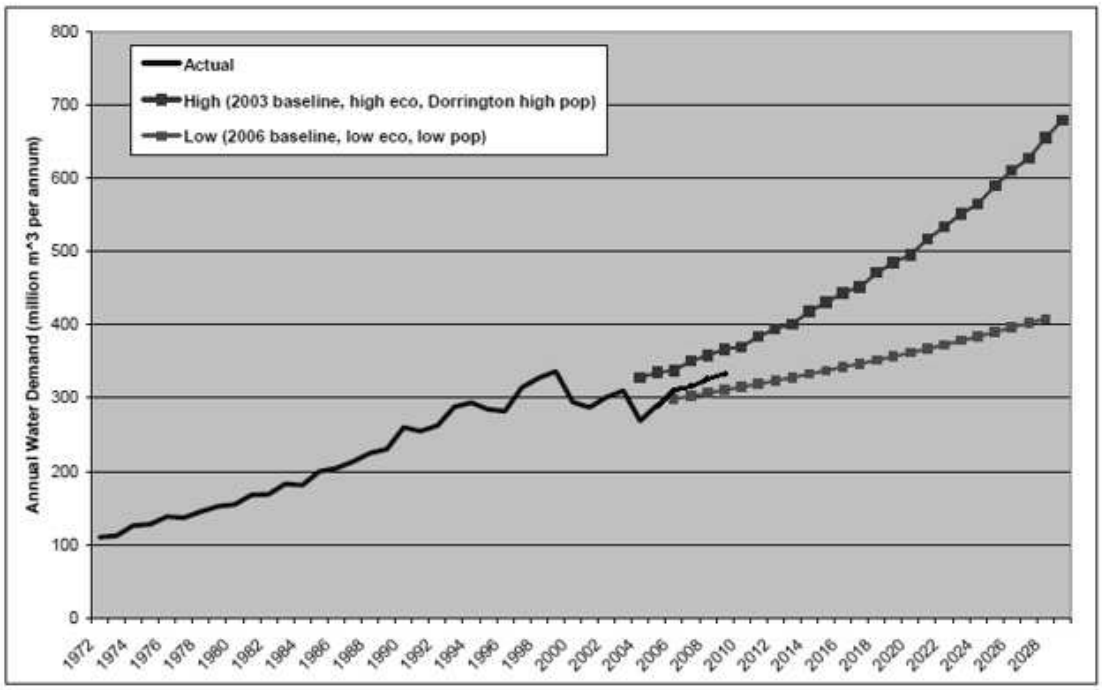

Actual and forecasted water requirement for the period 1972 to 2030 (CCT, Drakenstein and Stellenbosch)

Water requirement scenario	Average growth in water demand (%)	Population growth rate (% per annum)			Economic growth rate (% per annum)	
	2006 – 2030	2006-2011	2011-2016	2016-2030	2006-2010	2010-2030
High	3.09	1.12	1.38	1.74	4.5	6
Low	1.43	0.16	0.36	0.70	4	4

Figure 4: DWAF aggregated demand forecast for CCT (including bulk customers) with economic and population forecast growth rates

energy consumption (i.e. low energy intensity) and maximises water availability and supply. Therefore, the performance index consists of the unweighted (or neutral) product of the inverse of the system energy intensity (Ei), and the system reliability and system storage index. Expressed in Equation 3, the resultant magnitude of α suggests a more favourable intervention where α is larger.

$$\alpha = 1/Ei * Reliability * System\ Storage\ Index \quad (3)$$

Expressed in logarithmic terms, as shown in Equation 4, it can be viewed as a simple additive value function which forms the basis of decision analysis in Multi-Attribute Value Theory (MAVT) whereby selected alternatives are evaluated according to set criteria and ranked by an aggregated score as calculated by a value function (van Herwijnen, 2012). The logarithmic expression is given below in Equation 5.

$$A = \ln(\alpha) = \ln(1/Ei) + \ln(Reliability) + \ln(System\ Storage\ Index) \quad (4)$$

Although no scaling is applied to the indicators for the analyses conducted here, it should be noted that due to the logarithmic summation, a ratio preference scaling is implied for this expression. In

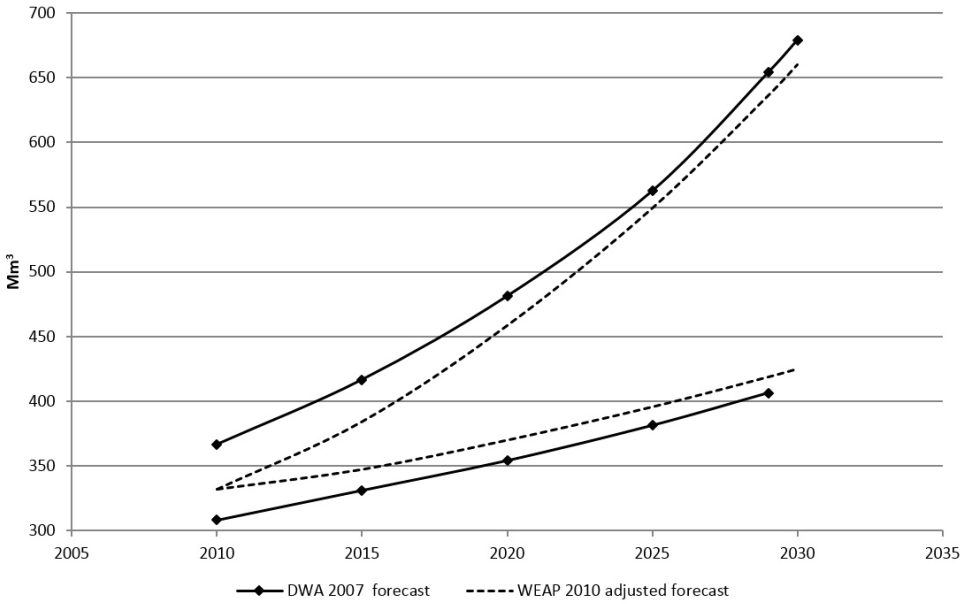

Figure 5: Aggregated demand forecast for CCT (including bulk customers) compared to the 2007 DWAF forecast

MAVT, ratio scaling provides an indication of the relative preference of one option to another by assuming that criteria are directly comparable by their weighting value (Simpson, 1994).

Results and discussion

The analyses focused on the case of high growth in water demand by the City. The options which were implemented are a representative sample of the identified set and it is likely that these are subject to future revision with improved analysis. Therefore, it is important to note that the interventions are primarily illustrative of the modelling approach itself, which provides a tool for scenario analyses where 'what if' questions can be quantitatively examined for their outcomes and compared with alternatives; and that the accuracy and precision of the results reflect the best available estimates and knowledge of the model parameters at the time.

The calculation of separate energy intensities (or specific energies) for the supply of potable water and that for sanitation becomes intractable when interventions are considered because the boundaries of the two branches become more inter-connected as in the case of effluent recycling for potable consumption or reuse. Therefore, as a comparative measure, the energy intensity of the urban cycle is used which is taken to be the ratio of the annual total energy consumed by the water sector (kWh) to the annual volume of water produced (m^3) inclusive of system losses. This would include the supply, treatment and distribution of raw, potable and waste water.

The case of prioritising the existing surface water supply system with desalination as a secondary supply option is also compared. In this case, supply from desalination is endogenously determined as a supplementary supply when other options are insufficient to reconcile demand. This is contrasted with the default implementation in which desalination operates conjunctively with the surface water system and capacities are exogenously determined.

The performance of the interventions

A reference value is used to provide a comparative figure for the performance (α) of the interventions against the aforementioned criteria for the selected scenarios. This value is obtained with the combination of the energy intensity of the reference scenario, an ideal reliability of 100% and a status quo surface water storage (i.e. storage index = 1). This gives a reference performance index of $\underline{\alpha} = 164$.

Table 5 displays the overall performance where the best performing intervention for each scenario is underlined for emphasis. The average performance of scenarios 1 and 3, which represent the extremes of scenario factors, is ca. 49 and is 20% greater than the alternate grouping of scenarios 2 and 4 for which the value is 39. However, in the context of no interventions, if assurance of supply is preferred at the expense of strategic water storage in the near future then, depending on the relative weighting, a reliable water supply system may be considered more resilient. The resultant performance can be further weighted by scenario such that, for example, the reduced inflow scenarios are given more prominence. The results for the implementation of the suggested interventions, as expected, show an improvement in reliability for all scenarios and interventions. The general pattern that emerges is that unrestricted usage increases reliability at the expense of system storage. The data in Table 5 further indicates that the intervention (d) that maximises effluent reuse-recycling in tandem with a

Table 5: The performance (α) of the candidate interventions for the case of high water demand

Scenario	*none*	*a*	*b*	*c*	*d*
1	62	80	117	96	132
2	45	96	137	104	151
3	37	49	36	71	89
4	33	46	40	59	65

continued WC/WDM programme is the best option for each of the possible scenarios considered.

A scenario comprising historical average inflows to the system dams does not reflect the historic variation in system storage and therefore a reduced inflow scenario was included to gauge the system response between the two extremes. Thus, if inflows to the system were reduced or simply less water available from the dams, then the intervention (c) comprising desalination with a continued WC/WDM programme provides the next best performance. Between the two extremes of surface water availability with (d) providing the best performance, (c) is the next preferred intervention based on the reduced inflow performance as indicated.

Referring to Table 6, the energy intensities are similar for all scenarios with no interventions as the existing infrastructure essentially remains a surface water scheme. For the case of no interventions, scenarios 2 and 4 for which dam usage is unrestricted, result in the lowest unmet demands and thus have higher reliability values. However, their storage index is lower as a result of the increased discharge of dam waters. In contrast, for the case of regulated releases, the system reliability is reduced to 60% of the latter option with ca. 50% of water demand being unmet over the period, but with enhanced water storage. This is the case for both surface water inflow scenarios (average and reduced) suggesting a more resilient intervention as existing water volumes are strategically managed or conserved.

Table 6: The performance of the candidate interventions against the individual criteria for the case of high water demand

		Indicator or category		
Intervention	*Scenario*	*Energy intensity*	*Reliability*	*System storage index*
none	1 (reference)	0.61	49	0.77
	2	0.58	85	0.31
	3	0.63	48	0.48
	4	0.59	80	0.24
a	1	1.01	84	0.97
	2	1	99	0.97
	3	1.06	84	0.61
	4	1.03	99	0.48
b	1	0.73	89	0.96
	2	0.72	100	0.99
	3	0.76	87	0.31
	4	0.73	98	0.29
c	1	0.96	92	1.00
	2	0.95	100	0.99
	3	0.98	89	0.78
	4	0.96	100	0.56
d	1	0.66	91	0.96
	2	0.65	100	0.98
	3	0.69	90	0.68
	4	0.67	100	0.44

The ground water option (3) features in all the interventions except (c). Based on the performance of (c), which includes the continued WC/WDM option, ground water appears less important as a municipal supply option for the Greater Cape in the near future. This is in contrast to the key options identified by their performance which includes desalination, effluent reuse-recycling and WC/WDM. However, since the City's WC/WDM programme includes an increase of end-user exploitation of ground water, the impact may be considered indirectly via the success of this component within the WC/WDM programme although the volumes suggested (3.6 Mm^3/a) would still represent a minor contribution should the high water demand growth trajectory be realised.

The case of low growth in water demand

The performance of the existing water supply system, as approximated in the model, is given in Table 7 for the case of low growth in water demand. Reliability and storage are similar to that of the high water demand scenarios with interventions applied. Scenario 6, for unrestricted dam usage and average surface water availability, results in no unmet demand over the period with a comparable performance in storage to scenario 5 and 7 where dam usage is restricted. This scenario has the highest overall performance and the system performance indicates that minimal additional supply augmentation would be required in the near future if water demand approaches the low growth trajectory. Allowing for the uncertainty in surface water inflows, as represented by scenario 7, a full implementation of WC/WDM would require no additional measures. A partial WC/WDM programme would potentially necessitate intervention in the period 2027/30.

The scenario interventions

Figure 6 compares dam storage and unmet demand for the scenarios with no interventions applied. Relative to the reference case, scenario 3 experiences similar unmet demand at the expense of dam

Table 7: The system performance for the low water demand scenarios without interventions

Intervention	*Scenario*	*Indicator*			*α*
		Energy intensity	*Reliability*	*System storage index*	
none	5	0.61	78	0.93	119
	6	0.59	100	0.86	146
	7	0.62	76	0.87	107

storage. Scenarios 2 and 4 display very different unmet demands over the period which is due to the unrestricted operation of the dams. In this mode of operation, the supply system is less resilient by comparison to the grouping of scenarios 1 and 3.

Municipal energy consumption

The energy intensities of the scenarios without any interventions are displayed in Figure 7.

Scenario 2 and 4, by grouping, display similar characteristics to the grouping of the reference scenario and scenario 3. Scenario 3 departs from the reference scenario due to the increased cost of water treatment, in terms of energy consumption, from the year 2015 although the average energy cost of the urban water cycle for the two predominantly surface water interventions over the period is similar. When comparing the average energy inten-

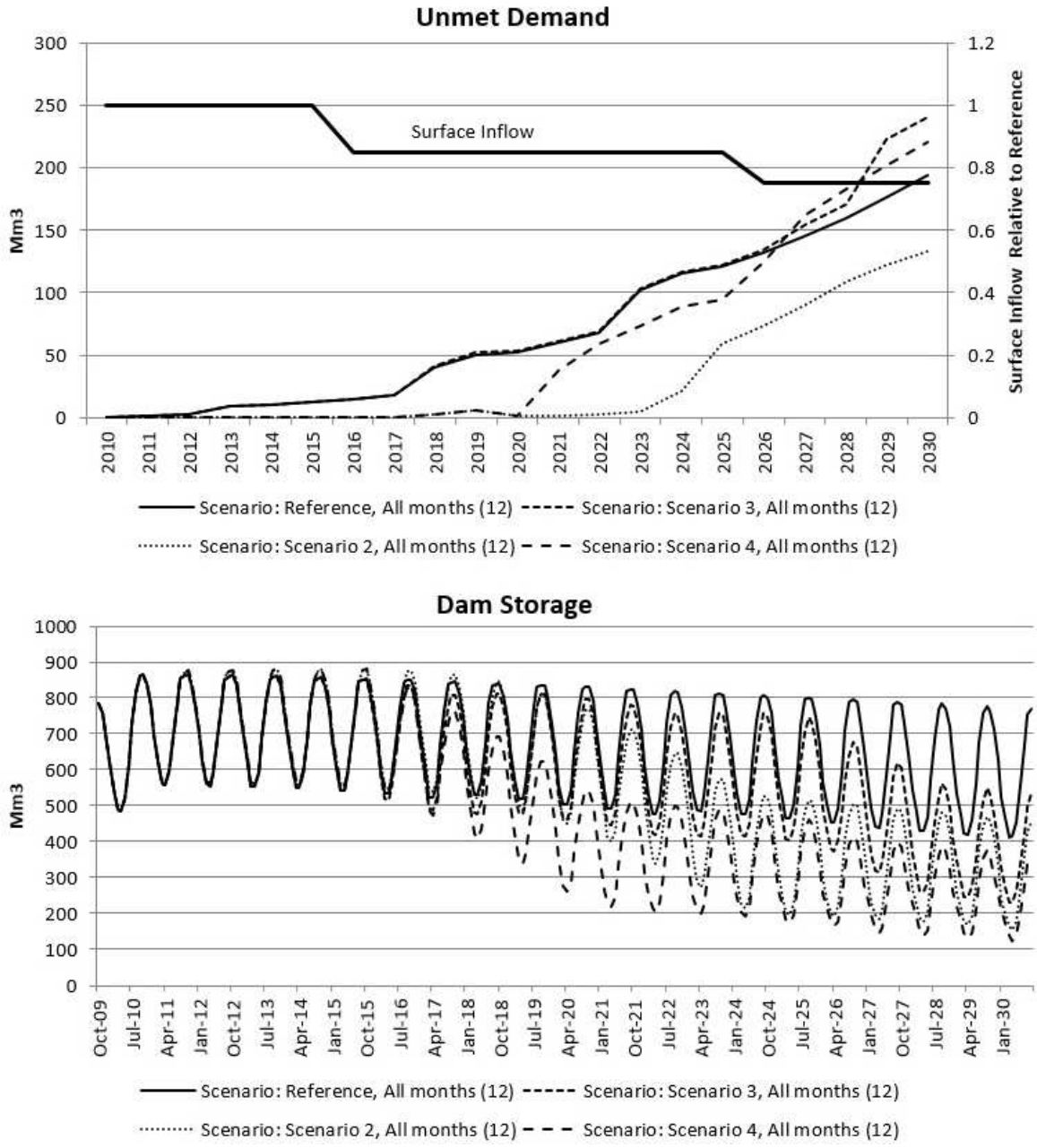

Figure 6: Dam storage and unmet demands for the scenarios without interventions

sity by five year intervals, the difference in energy consumption doubles every five years reaching 8% by 2030. The increase in energy consumption is primarily borne by the potable water treatment processes as displayed in Figure 8, which is dominated by the City's Voelvlei WTW.

In scenario 3, the Voelvlei WTW comprises 95% of water treatment energy consumption, which reduces to 75% by 2026/30. The contribution of the other WTWs is due to the influence of the continued reduction in surface inflows, which impacts the mini-hydro energy generation capacity at these plants while the WTWs at Pniel and Atlantis are modelled with no onsite generation. The peaking of energy consumption at the Voelvlei WTW correlates with the reduction in water supply from Voelvlei dam. The proportion of the total energy consumed, in scenario 3, for water treatment grows from an initial 4% (2011/15) to 11% (2026/30). This compares to the reference case, where WTWs comprise 3% to 4% of total energy consumption for the period 2011/30.

The total energy consumption of the interventions for the scenarios are given in Table 8. Figure 9 illustrates their relative impact by energy intensity – note that the energy intensities for scenarios 2 and 4 are similar for the reference case and scenario 3.

Table 8: Total energy consumption for the period 2011/30 (GWh)

Scenario	*Intervention*			
	(a)	*(b)*	*(c)*	*(d)*
1	9577	6783	8293	5499
2	9615	6740	8275	5501
3	10076	7017	8461	5794
4	9983	6794	8347	5705

An examination of the data reveals that, for a given growth demand scenario, the energy intensity of the interventions are similar between the scenarios such that the influence of surface water inflows and treatment is marginal in terms of the direct energy consumption required for the urban water cycle. This similarity is due to the equal priority of supply options in the model for the urban sector. As the bulk of the existing surface water supply options are shared with the agricultural sector, the solver within the model attempts to satisfy the urban demand with the alternative supply options firstly, in order to ensure adequate water availability for agricultural users.

Within WEAP, users with equal (demand) priority of a shared resource are granted equal privileges and unmet demands are calculated in proportion to the volume of water required. For example, with urban and agricultural users the full capacity of an alternative option such as desalination is utilised causing increased energy consumption in order to ensure minimal unmet demand for both users (assuming they have equal demand priority to the dams).

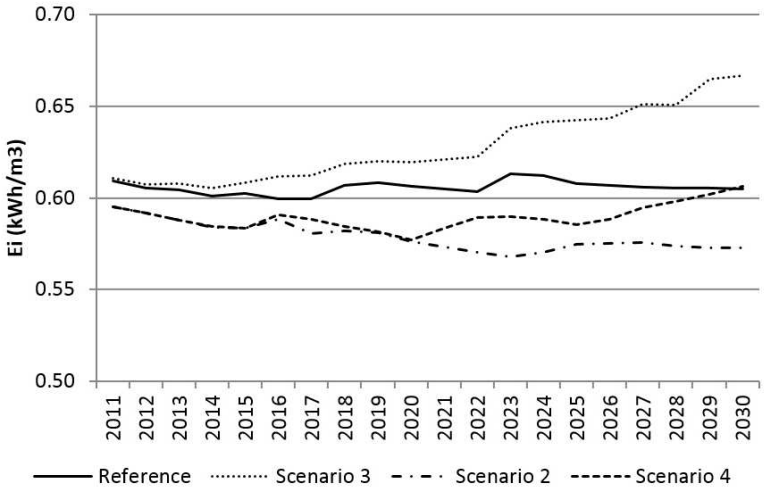

Figure 7: Energy intensities for the scenarios without interventions

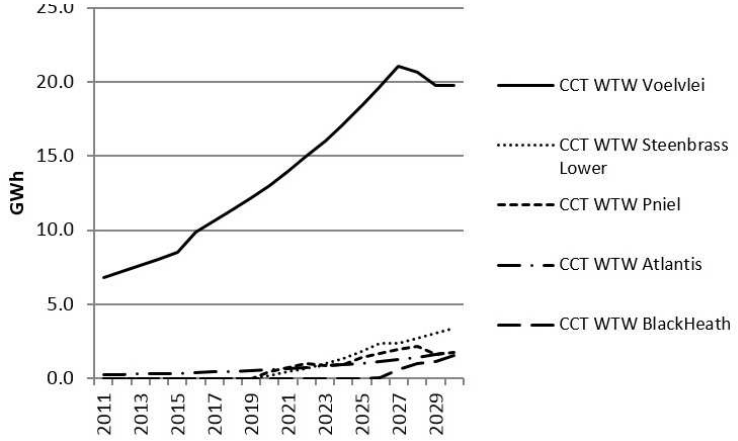

Figure 8: The estimated energy consumption for water treatment in Scenario 3 with no interventions

If the existing relatively low energy surface water interventions are prioritised over the more energy intensive desalination option, the requirement for supply augmentation by desalination varies according to whether dam water releases are regulated or not.

With desalination given secondary preference to surface water supply, the energy consumption for interventions (a) and (c) which implement desalination are listed in Table 9, while Figure 10 depicts the energy intensities. It is noted that the energy consumption for intervention (a) is now similar to the equal supply priority desalination option with a continued WC/WDM program as would occur in intervention (c). For a secondary desalination supply, intervention (c) is similar in energy consumption to the effluent oriented intervention (d).

An examination of Figure 10 highlights the grouping of the energy intensity of the scenarios by surface water usage.

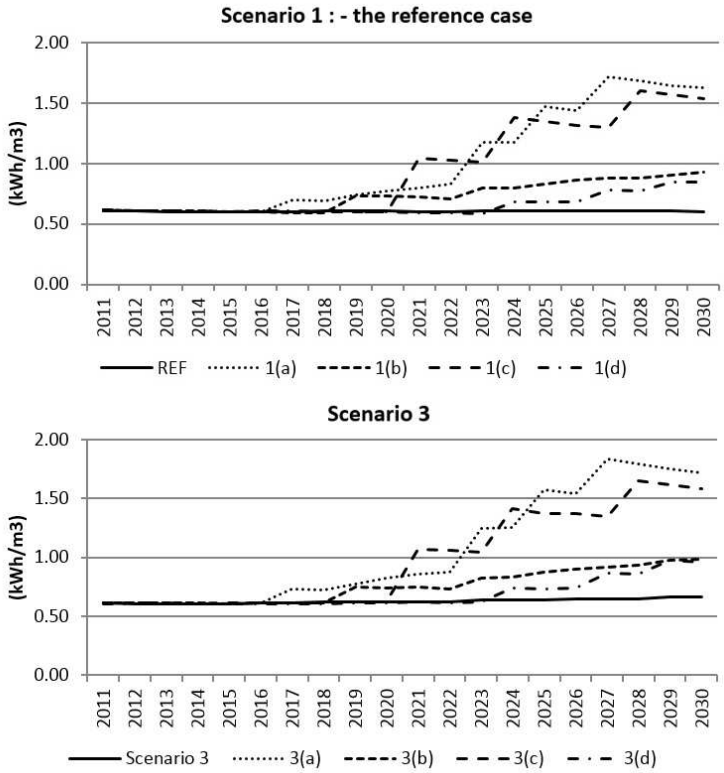

Figure 9: The relative energy intensities of the different interventions for Scenarios 1 and 3

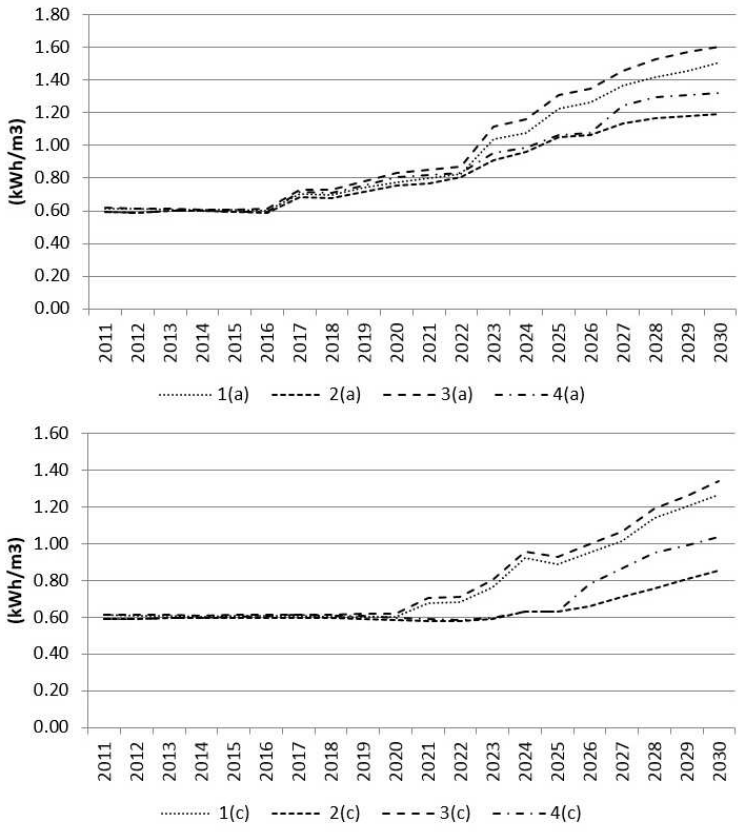

Figure 10: The energy intensity of the scenarios with surface water supplies prioritised and sea water desalination as a secondary supply

Table 9: Total energy consumption for the period 2011/30 for the urban water cycle with desalination as a secondary augmentation option

Scenario	*Intervention*	
	(a)	*(c)*
	Total (GWh)	Total (GWh)
1	8684	6537
2	7877	5421
3	9163	6749
4	8122	5738

With the surface water options prioritised, dam storage displays greater variation for the unrestricted case, while unmet demands are more susceptible to disruptions in surface inflows.

This is observed by the divergence in energy intensities for the grouping of scenarios 2 and 4 as surface water inflow is reduced. In scenario 4 an increased reliance on desalination occurs in response to a reduction in supply from the dams if desalination favoured policy were pursued in combination with unregulated usage of surface water from the dams.

Conclusions

The research presented here demonstrates the flexibility and importance of a systems approach to water resources planning. The results are indicative of a holistic appraisal of the water and sanitation sector in the context of urban municipal water services. In specific, a strategic analysis of the energy intensity of water services, comprising a suite of supply and demand options, for the City of Cape Town was conducted via a systems analysis process. The value of the research presented here, it is believed, lies primarily in the flexibility of the systems modelling approach to incorporate a multitude of water resources options (e.g. demand management or supply augmentation) in order to evaluate their performance by specific criteria for given objectives.

A systems perspective or integrated assessment further allows the examination of the interrelationship of the different stages of the urban water cycle and assists in identifying key linkages. For example, the effect of a WC/WDM programme on the extent of waste water reclamation; pumping energy for water services; or the energy intensity of water or waste water treatment for specific processes. The model parameters can be applied to specific infrastructure (e.g. Voelvlei WTW) or aggregated in the case of data paucity. The scope of analysis is also a determining factor in the necessary refinement of parameters. For example, the energy intensity of the distribution network can be aggregated when conducting a strategic appraisal. For strategic analyses the WC/WDM options were aggregated as a poten-

tial bulk yield although the model allows for a more detailed analysis with specific emphasis on particular WC/WDM measures. This may involve a *bottom-up* sectorial analysis (e.g. residential, food and beverage industry, etc.) which would be implemented to gauge the impact of specific water (or energy) efficient technologies or processes. For example, water demand elasticity functions can be included to model the response to tariffs by consumers and the resultant impact on water and energy resources.

The interventions as proposed within this analysis were examined within a context of energy and water planning for the City of Cape Town such that energy considerations or costing could be incorporated within the long term marginal costing of future water and sanitation infrastructure (Ratnayaka *et al.,* 2009). As such, the modelling process facilitated an exploration of the water–energy nexus in the context of urban municipal water services.

References

Allpass, D. (2012). City of Cape Town – Bulk Water Branch: Energy Consumption. [14 June 2012]. Cape Town.

Buckley, C., Friedrich, E. & von Blottnitz, H. (2011). Life-cycle assessments in the South African water sector: A review and future challenges. Water SA. 37(5).

California Sustainability Alliance (2008). The Role of Recycled Water in Energy Efficiency and Greenhouse Gas Reduction. California, USA: California Sustainability Alliance.

CCT (2001). Future Infrastructure Requirements. Cape Town: City of Cape Town.

CCT (2005). Water Resources and Water Resource Planning: Background Information for WSDP. Cape Town: City of Cape Town.

CCT (2010). Bulk Water Supply Infrastructure Summary Description. Cape Town: City of Cape Town.

CCT (2011). Water Services Development Plan 2011/12 to 2015/16. Cape Town: City of Cape Town.

Cooley, H. & Wilkinson, R. (2012). Implications of Future Water Supply Sources for Energy Demands. USA: WateReuse Research Foundation.

Coetzer, P. (2012). Let's be H2O wise. 42. Cape Town: Cape Media Corporation.

Davies, R. (2012). Eskom, Sasol sound warning over water supply. [Online]. Available: http://mg.co.za/article/2012-03-18-eskom-sasol-sound-warning-over-water-supply [2012, 3/18].

deMonsabert, S. & Bakhshi, A. (2009). Incorporating Energy Impacts into Water Supply and Wastewater Management. Washington: American Council for an Energy Efficient Economy.

Eberhard, A. (2008). South Africa's Power Crisis: understanding its root causes and assessing efforts to restore supply security. Cape Town: University of Cape Town.

Eindhoven University of Technology (2006). Mini-Hydro Power. Netherlands: Eindhoven University of Technology.

Friedrich, E., Pillay, S. & Buckley, C. (2009). Environmental life cycle assessments for water treatment processes – A South African case study of an urban water cycle. Water SA. 35(1).

Gaunt, T. (2010). Introduction to Electricity in South Africa. Cape Town.

Jennings, L. (2012). City of Cape Town: Municipal Energy Consumption. August 2012]. Cape Town.

Kenway, S. et al. (2008). Energy use in the provision and consumption of urban water in Australia and New Zealand. Australia: CSIRO.

Larabee, J., Ashktorab, H. & Darlow, K. (2011). From Watts to Water. USA: Santa Clara Valley Water District.

Louw, D. et al. (2012). Managing climate risk for agriculture and water resources development in South Africa: Quantifying the costs, benefits and risks associated with planning and management alternatives. Canada: International Development Research Centre.

Lui, F.et al. (2012). A primer on energy efficiency for municipal water and wastewater utilities. Washington: The World Bank.

Mashoko, P. (2012). City of Cape Town: Energy Consumption for Water and Sanitation Services. [20 June 2012]. Cape Town.

Mo, W. et al. (2011). Embodied energy comparison of surface water and groundwater supply options. Water research. 45(17):5577-5586.

Moll, A. (2012). City of Cape Town – Reticulation Branch: Energy Consumption. [5 June 2012]. Cape Town.

Nkomo, J. & Gomez, B. (2006). Estimating and Comparing Costs and Benefits of Adaptation Projects: Case Studies in South Africa and Gambia. Project No. AF 47. Washington, USA: The International START Secretariat.

Ogutu, C. (2007). Water demand management options for cape metropolitan area- South Africa. Pretoria: Tshwane University of Technology.

Olsson, G. (011). The urban water – energy nexus: energy efficiency along the water value chain. Sweden: Lund University.

Ratnayaka, D. et al. (2009). Twort's Water Supply. 6th Ed. Great Britain: Elsevier Ltd.

Simpson, L. (1994). MAVT and Outranking: A Comparison of Two Multi-Criteria Decision Analytic Methods, Report 94.3. United Kingdom: University of Leeds, Division of Operational Research and Information Systems.

Singels, A. (2012). City of Cape Town: Bulk Water Operations. 27 June]. Cape Town.

South African Department of Environmental Affairs (2011). White Paper on the National Climate Change Response. Pretoria: Government Printer.

South African Department of Water Affairs and Forestry (2004). Berg WMA: Internal Strategic Perspective. Pretoria: Government Printer.

South African Department of Water Affairs and Forestry 2006. Guidelines for Water Supply Systems

Operation and Management Plans during Normal and Drought Conditions (RSA C000/00/2305), Volume 2, Appendix A: The Western Cape Water Supply System Pilot Study. Pretoria: Government Printer.
South African Department of Water Affairs and Forestry 2007a. Western Cape Water Supply System Reconciliation Strategy Study: Scenario Planning for Reconciliation of Water Supply and Requirement. Pretoria: Government Printer.
South African Department of Water Affairs and Forestry (2007b). Western Cape Reconciliation Strategy Study: Determination of Future Water Requirements. Pretoria: Government Printer.
South African Department of Water Affairs and Forestry (2007c). Western Cape Water Supply System Reconciliation Strategy Study: Summary Report. Pretoria: Government Printer.
South African Department of Water Affairs and Forestry (2009). The Assessment of Water Availability in the Berg Catchment (WMA 19) by Means of Water Resource Related Models: Report 4. Land Use and Water Requirements Vol. 1. Data In Support Of Catchment Modelling. Pretoria: Government Printer.
South African Department of Water Affairs and Forestry (2010). The Assessment of Water Availability in the Berg Catchment (WMA 19) by Means of Water Resource Related Models: Report No. 8. System Analysis Status Report. Pretoria: Government Printer.
South African Cities Network (SACN) (2011). City of Cape Town Micro Hydro Potential Study. Cape Town: South African Cities Network.
Sparks, A. (2012). Western Cape Systems Analysis (1928-2004): before adding detailed Berg and Palmiet EWR nodes. May 2012]. Cape Town.
Stockholm Environment Institute (SEI) (2012a). Long-range Energy Alternatives Planning system. 2012. Stockholm: Stockholm Environment Institute.
Stockholm Environment Institute (SEI) (2012b). Water Evaluation and Planning System. 3.3. Stockholm: Stockholm Environment Institute.
Stokes, J. & Horvath, A. (2006). Life-cycle Energy Assessment of Alternative Water Supply Systems. The international journal of life cycle assessment. 11(5):335.
van Herwijnen, M. (2012). Multiple−attribute value theory (MAVT). Netherlands: University of Amsterdam, Institute for Environmental Studies.
Vince, F. et al. (2008). LCA tool for the environmental evaluation of potable water production. Desalination. 220(1–3):37-56.

Received 28 March 2014; revised 17 October 2014

Improving stability of utility-tied wind generators using dynamic voltage restorer

G Sivasankar

V Suresh Kumar

Electrical Engineering Department, Thiagarajar College of Engineering, Tiruparamkundaram, Madurai, TamilNadu, India

Abstract

The generation of electricity using wind power is significantly increasing and has received considerable attention in recent years. One important problem with the induction generator based wind farms is that they are vulnerable to voltage disturbances and short circuit faults. Any such disturbance may cause wind farm outages. Since wind power contribution is in considerable percentage, such outages may lead to power system stability issues and also violate the grid code requirements. Thus, improving the reliability of wind farms is essential to maintain the stability of the system. The proposed strategy is to use Dynamic Voltage Restorer (DVR), which is one of the promising devices to compensate the voltage disturbance and to improve the stability of the system. It provides the wind generator with the fault ride through capability and improves the reliability of the system. Extensive simulation results are included to illustrate the operation of DVR and fault compensation.

Keywords wind power generation, power system faults, fault detection, voltage control, and stability

1. Introduction

In recent years, wind power generation is in rapid expansion and its contribution to the power sector has been increasing day by day. This situation has forced the need for evaluation of their impact on power system dynamics. During short circuit fault or severe load variation, voltage sags are observed in the network. They are characterised by a sudden reduction in voltage and phase jump. The induction generators are not able to withstand such low voltages due to reactive power needed to restore the internal magnetic flux, once the fault is cleared (Milanovic, 2007). Figure1 shows the variation of the voltage and reactive power absorbed by the induction generator with slip. It can be seen from the figure that as the slip or the power increases, the amount of reactive power absorbed by the generator also increases. Due to the large amount of reactive power drawn from the network, the voltage across the transmission line drops. The voltage at the point of connection with the network decreases, as the slip increases. The voltage recovery after disturbance is hindered by the consumption of reactive power. This behaviour limits the fault ride through capability. Hence, wind farms are disconnected during fault for safety. In the past, the wind power penetration was low in percentage and hence, any outage might have not affected the system stability. But now these days, wind generation is in rapid expansion and its contribution to the grid is as conventional generation plants as stated by Bollen (2005). Hence, any outage of wind plant may lead to power swing and collapse the stability.

In this paper, the issues related to stability of Fixed Speed Induction Generators (FSIG) based wind farms are analysed. The wind farms are operated in two modes, one as grid integrated mode and the other as standalone mode. When a wind system is inactive, the grid supplies electricity to the consumers. When surplus electricity is produced by wind farms, it meets the local demand and the remaining power is fed to the grid. The utility employs a billing system known as net metering. Net metering is a system in which the electric bill is based on net consumption minus production. The electric billing is based on the amount of utility energy consumed minus the amount of energy provided to the grid from a renewable energy system. A safety disconnect switch is available near the point of connection, which enables service personnel to disconnect wind farms from the grid during fault condition and to be operated as a standalone system.

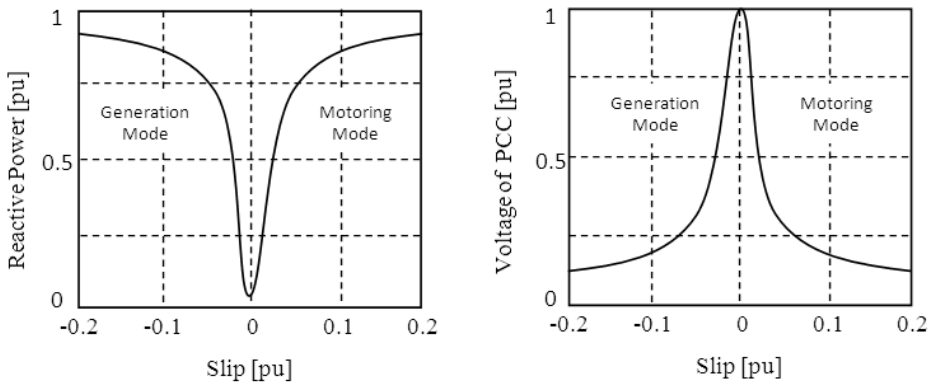

Figure 1: (a) Reactive power response for varying slip (b) Voltage response for varying slip

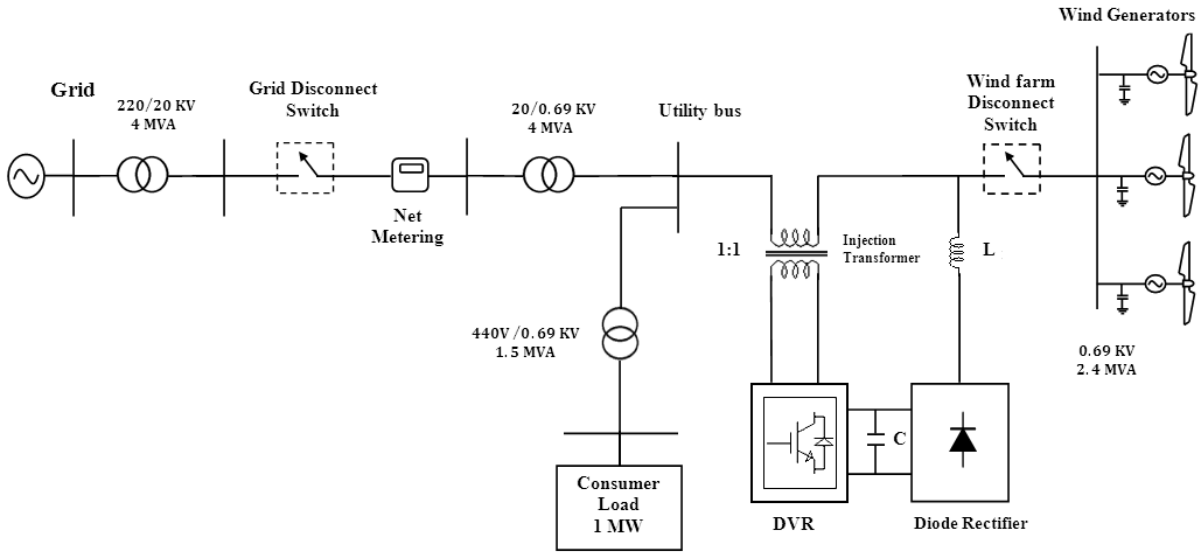

Figure 2: Grid connected FSIG with DVR protection

Hence, a wind farm serves consumers as stand-alone mode. In both modes, the wind generator suffers with stability problems by grid faults or load disturbances. Hence, the distributed generation system focuses on power quality improvement (Singh, 2011). Several schemes are under research for protection and power quality improvement (Siozinys, 2012; Vaimann, 2012). Grid tied active filters are usually designed for performance improvement (Biricik, 2013).

The proposed strategy is to use dynamic voltage restorer DVR for voltage sag compensation by series voltage injection as shown in Figure 2. DVR is a power electronic controller that can protect the wind farm from disturbances without loss of stability and guarantee the reliability of the system. The proposed DVR can also limit the fault current and protect the DG from over current due to voltage disturbance.

2. Series voltage compensation

The most commonly encountered problem in the system is voltage dip. Voltage sags are mainly caused by short duration faults in the supply line (Bollen, 1999). Hence, mitigation of sag can only be a complete solution for the aforementioned problems. The use of DVR is an appropriate solution for sag and its related issues (Al-Hadidi, 2008; Meyer and De Doncker, 2008; Nielsen, 2004). The compensation is accomplished by insertion of a voltage equal to the sag depth with appropriate phase angle in series with the line (Ryckaert, 2008; Awad, 2004). An equivalent circuit representation of a series voltage compensation scheme is illustrated in Figure 3.

The grid voltage source, the wind generator voltage source, consumer load and Series compensation source are integrated with two safety switches. The voltage dip mitigation is done by insertion of compensation voltage in series with the line. The steps involved in series compensator for mitigation as follows:

$$U_{wg}(t) = U_g(t) + U_c(t) \quad (1)$$

The imbalance at the wind generator terminal is to be cancelled by the compensating voltage to obtain balanced voltages at terminals. Therefore,

$$U_{co} = -U_{go},\ U_{c-} = -U_{g-} \quad (2)$$

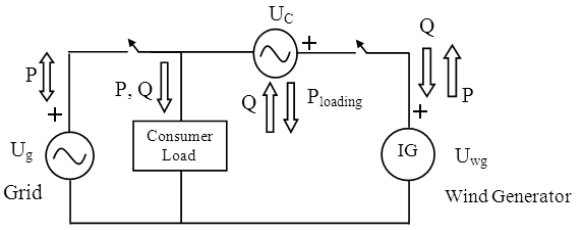

Figure 3: Equivalent circuit representation

The positive-sequence voltage magnitude of the wind generator U_{wg} should be set to the desired regulated voltage. A compensator is a positive-sequence voltage ($|U_{c+}|$) injected in series. Since the grid current flows through the series compensator the must have a phase difference of 90° with i_{g+}. This results in:

$$U_{wg+} = U_{g+} + U_{c+}(a + jb) \quad (3)$$

where (a + jb) is the unit vector. It is perpendicular to I_{g+}. Assuming $U_{wg+} = U_{wg+} \angle 0°$. Eq. 3 results in second-order equation:

$$|U_{c+}|^2 - 2a|U_{wg}||U_{c+}| + |U_{wg}|^2 - |U_{g+}|^2 = 0 \quad (4)$$

When the desired regulated voltage U_{wg} is achieved, the Eq. 4 will result in two real solutions for $|U_{c+}|$. The minimum solution is chosen for smaller rating of the DVR.

3. Control of the DVR

The control of DVR is done using a high performance vector controller (Ottersten, 2012). The vector controller scheme is illustrated as shown in Figure. 4. This control scheme of the DVR includes: reference voltage generation, control of injection voltage and protection of DVR.

3.1 Reference voltage generation

The controller has to generate an accurate reference voltage for successful compensation. The Software Phase Locked Loop (SPLL) circuit is preferred for synchronization of the system (Awad, 2005). The advantages of this thod are frequency adaptive performance, high filtering capability and relatively low computational burden. SPLL provides a successful solution for voltage distorted and frequency varying conditions. Figure 5 illustrates the structure of the SPLL, in which $U_{g(abc)}$ is the input voltage, ω_d and θ_d ($=\omega_d t + \Phi$ are the estimated frequency and angle, respectively. ω_{ff} is the nominal frequency. The input voltage is transformed to U_α and U_β coordinates which are in-phase and quadrature-phase components, respectively.

The Park (dq0) transformation is used, which is applied for a time-dependent arbitrary three-phase system. It is used to decouple variables and to refer a common reference frame. The grid voltage may contain negative and zero-sequence components due to unbalanced voltage. Hence, the system voltage is transformed into the synchronous dq0 reference frame. For an unbalanced voltage, the Park transformation results in:

$$\begin{bmatrix} U_d \\ U_q \\ U_o \end{bmatrix} = \sqrt{\frac{3}{2}} \left\{ \begin{bmatrix} U_{gp}\cos\phi_p \\ U_{gp}\sin\phi_p \\ 0 \end{bmatrix} + \begin{bmatrix} U_{gn}\cos(2\omega t + \phi_n) \\ U_{gn}\sin(2\omega t + \phi_n) \\ 0 \end{bmatrix} + \begin{bmatrix} 0 \\ 0 \\ V_{g0}\cos(2\omega t + \phi_0) \end{bmatrix} \right\}$$
$$= \begin{bmatrix} U_{dp} \\ U_{qp} \\ 0 \end{bmatrix} + \begin{bmatrix} U_{dn} \\ U_{qn} \\ 0 \end{bmatrix} + \begin{bmatrix} 0 \\ 0 \\ U_{00} \end{bmatrix} \quad (5)$$

In equation 5 U_d yields an estimation of the input voltage amplitude and gives the phase error information. The output signal U_q of the Phase Detector (PD) is passed through the Loop Filter LF to attenuate the high-frequency signals. The nomi-

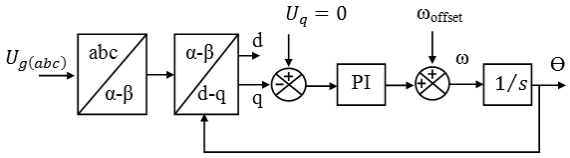

Figure 5: Software phase locked loop circuit

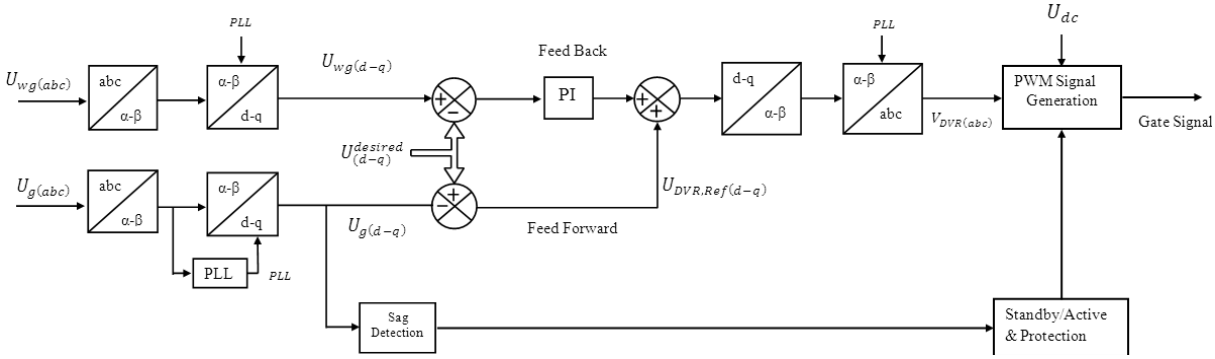

Figure 4: Vector controller scheme

nal value of the fundamental frequency ω_{ff} is then added to the output of LF to accelerate the initial lock-in process. This reduces the control effort. The resulting signal ω_d is integrated and the estimated angle is obtained. Then, the vector controller calculates the values of grid voltage U_g and wind generator voltage U_{wg} in d–q coordinates as $U_{g(d-q)}$ and $U_{wg(d-q)}$. According to Eq. 5, the dc components ($U_{gp}\cos\Phi_p$ and $U_{gp}\sin\Phi_p$) are obtained from the positive sequence component of the dq0 reference frame. Then, the U_{dp} is maintained at maximum magnitude U_M and all other components are eliminated using the compensation voltage. As a result, the reference voltage is obtained as shown as:

$$U^{ref}_{(d-q)} = \left[T_{(d-q)}(\theta_d)\right]U^{ref}_{abc} = \begin{bmatrix} U_m \\ 0 \\ 0 \end{bmatrix} \quad (6)$$

$$\text{Where} \quad U^{ref}_{abc} = \begin{bmatrix} U_g\cos(\omega t) \\ U_g\cos(\omega t + 120) \\ U_g\cos(\omega t - 120) \end{bmatrix}$$

The voltage sag detection is carried out by comparing the grid voltage with the reference voltage. The DVR reference voltage $U^{ref}_{DVR\,(d-q)}$ is generated.

$$U^{ref}_{DVR\,(d-q)} = U^{ref}_{(d-q)} - U_{g\,(d-q)} \quad (7)$$

The $U^{ref}_{DVR\,(d-q)}$ reference voltage of Eq. 7 is then inversely transformed into the abc reference frame.

3.2 Control of injection voltage

The control of injection voltage is done by the combination of grid voltage feed-forward and wind generator voltage feedback. The compensation voltage generated in the inverter and the voltage actually injected in series with the line are equalized using a PI regulator as a feedback control. The regulator output is added to DVR reference, which serves as feed forward to improve the system response speed. The dc-link voltage is used to calculate the required modulation depth to inject the difference between grid voltage and the reference voltage. Finally, a Sinusoidal Pulse Width Modulation (SPWM) is used to produce inverter switching signals.

3.3 Real and reactive power exchange

The fault ride through capability of the wind generator is not only affected by voltage disturbance but also by power dearth. The proposed DVR is capable of providing real and reactive power support. The uncontrolled shunt rectifiers are used to maintain a strong dc link which acts as a source to meet the real power demand. The reactive power compensation is done by switching the series converter in an appropriate phase angle.

3.4 DVR protection system

The series connected DVR inverter may face severe problem due to transients or fault current in the grid. Further, there is a chance of high in-rush of current reflection in to DVR, if the sag is not completely compensated. A proper protection of DVR inverter is one of the important aspects of the design, which can be done using the design scheme presented in (Newman, 2002).

3.5 Design and ratings of the proposed system

The DVR is capable of protecting wind generators from 100% voltage dips. The limitation of this compensation is that the diode rectifier and passive filter elements increase the cost of installation.

The average voltage across the DC link is calculated as follows:

$$U_{DC} = \frac{3U_m}{\pi} \quad (8)$$

where U_m is maximum of the rated voltage ($\sqrt{2}U_r$).

The energy stored in the capacitor is derived as:

$$E_{DC} = \frac{1}{2}C_{DC}U^2_{DC} \quad (9)$$

where CDC is the dc link capacitor.

The WTGs specifications are tabulated in Table I. The design parameters of DVR are presented in Table 2.

Table 1: Wind turbine generator specifications

Asynchronous SCIG		
Description	*Real value*	*pu value*
Nominal power	2.4 MVA	1
Synchronous speed	1,500 rpm	
Voltage	0.690 KV	1
Current	3.5 KA	1

Table 2: Main parameters for DVR

DVR converter	*Description*	*Real value*	*pu value*
	Power rating	2.4 MVA	1
	Voltage rating	0.690 KV	1
	Current rating	3.5 KA	1
Shunt rectifier	Voltage	690 V	1
	Current	3.5 KA	1
DC-link	Average voltage	976 V	
	DC link capacitor	6mF	
	Energy storage(488)	238 J	

4. Simulation results and discussion

4.1 Grid connected FSIG

Case 1

A Symmetrical Grid fault and its impact on FSIG are analysed. A voltage dip of 100%, due to a symmetrical fault, is created for 200ms as shown in Figure 6(a). The sequence components are shown in Figure. 6(b). It is found that during a symmetrical fault, only the positive sequence components are present whereas the negative sequences are found only at the beginning and the ending of dip. Figure.6(c) shows the current over shoot during voltage dip. This enormous current may damage the FSIG wind turbine and even transient failures may be encountered. Hence, usually the wind generators will be disconnected and isolated from the network for safety. But, this scenario leads to a stability problem. The sag mitigation is the only solution to avoid the aforementioned problem and to make the generator stay connected with the system. With the aid of DVR, a dip caused by fault is compensated and hence, normal operation is unaffected. Voltage sag magnitude is calculated and DVR reference voltage is generated for compensation. The DVR compensation voltage is depicted in Figure 7(a). The sag is compensated by an in-phase insertion of voltage in series with the line. Figures 7(b) and Fig. 7(c) show the compensated voltage and current at the wind generator using the vector controller.

Case II

The impact of asymmetrical dip, due to phase-to-phase grounded fault, is analysed in this case-II. The voltage variation at the wind generator is shown in Figure 8(a). Their sequence components are shown in Figure 8(b). The current rise due to voltage dip is shown in Figure 8(c). The impacts of unsymmetrical faults are more severe than a symmetrical fault. The negative sequence voltage and current increase the current loss and generate enormous heat, which damages the winding of the generator. The mitigation is done by generating an appropriate control signal. The reference control signal to DVR consists of two sequence parameters, one is in-phase positive sequence and the other is in phase-opposition to the negative sequence. With the combination of two sequence components, DVR inserts a voltage in series to restore the balance of the wind generator and is depicted in Figure 9(a). Hence, generator voltage and current levels are restored and are shown in Figures 9(b) and 9(c).

4.2 Stand-alone mode of operation

Case III

The Case III deals with impact of deep sag in a standalone wind generator. The deep voltage sag causes over current in the generator bus, which would cause severe problems. Hence, the generator

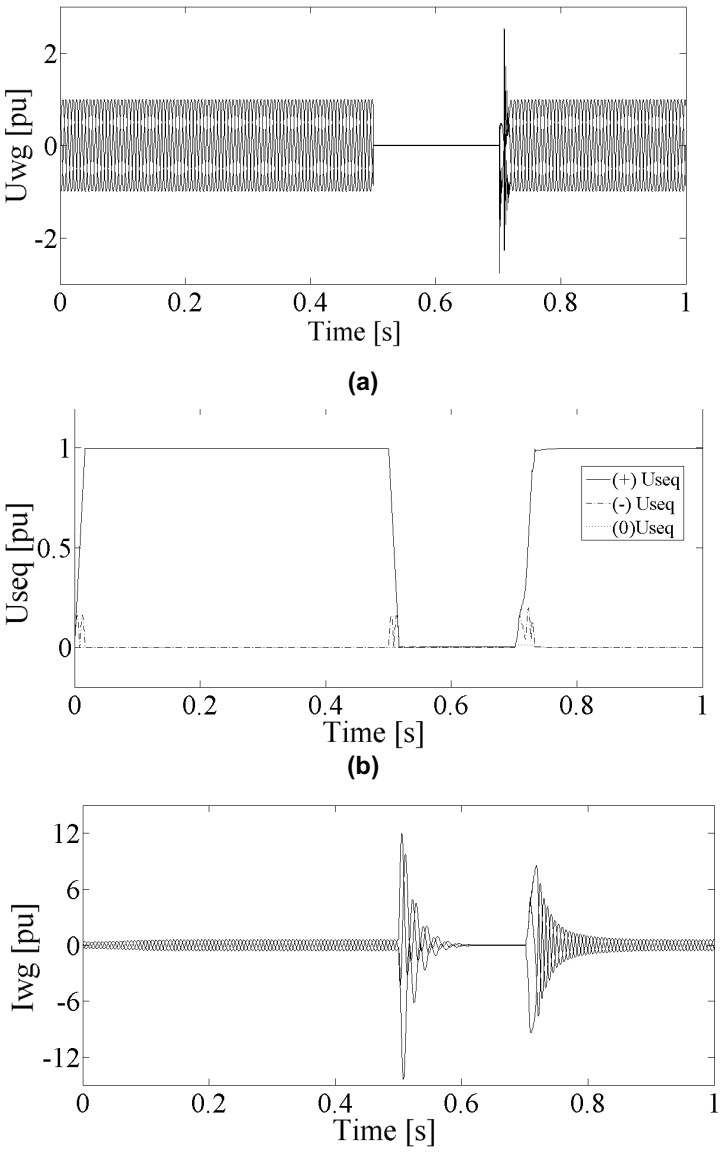

Figure 6 (a): Wind generator voltage during 100% dip before compensation (b) sequence components during dip (c) Current overshoot during dip

is usually disconnected at such an occasion. Consequently, the reliability of the system becomes poor. The DVR provides an excellent solution for the aforementioned problems. DVR can compensate deep voltage sag, as well as reduce over current and can protect the wind generator.

A severe voltage dip, which is sustained for a period of 200ms, is created. Figures 10 (a) & (b) show the wind generator voltage and current responses for the dip. In this situation, the generator is unable to continue to operate and is unstable even when the grid voltage is re-established to the nominal value after 200ms. During starting of the wind generator, nonlinearity and oscillation are found in the wave forms. This happens due to the starting characteristics of the induction machine. The proposed DVR could compensate deep sag and recover the normal operation of wind genera-

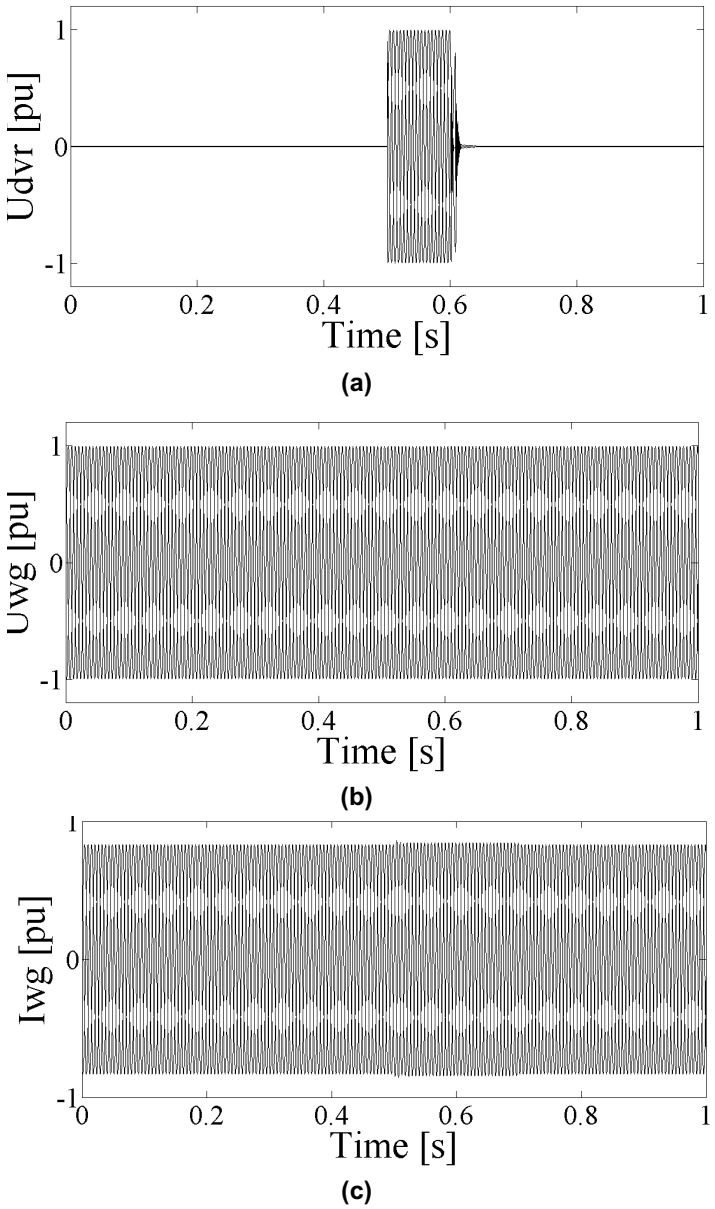

Figure 7 (a): Compensation voltage of DVR (b) Wind generator voltage after compensation (c) Wind generator current after compensation

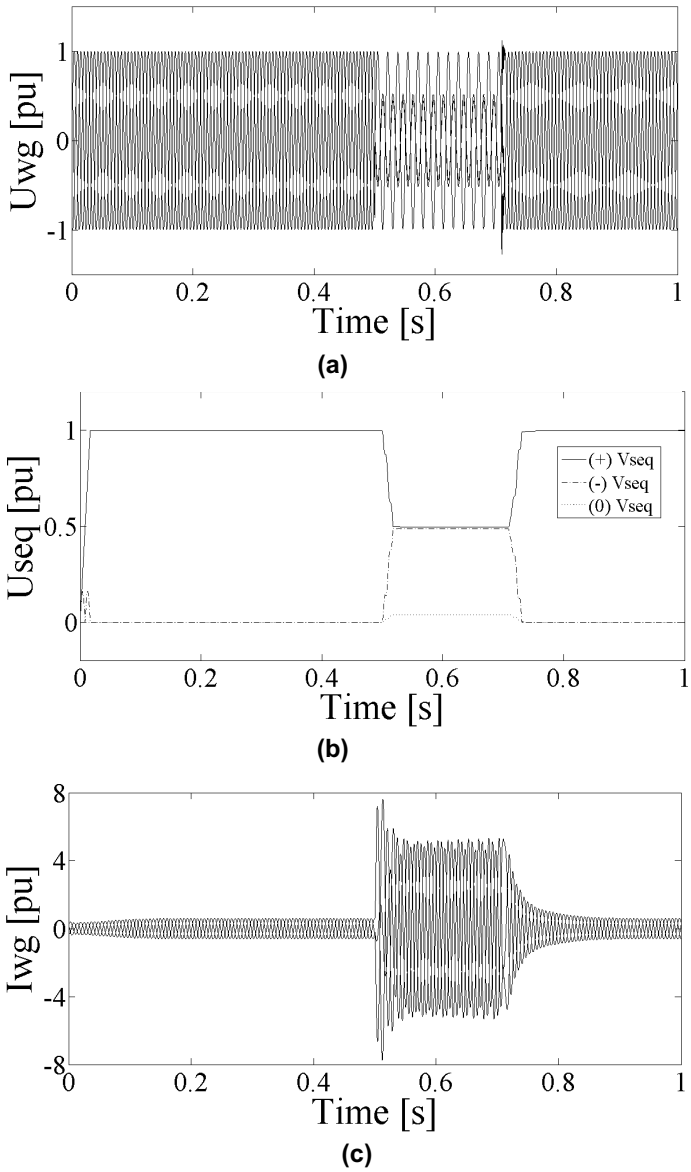

Figure 8 (a): Wind generator voltage dip during unsymmetrical fault before compensation (b) sequence components during dip (c) Current overshoot during dip

tors. The compensated wind generator voltage and current are depicted in Figures 10 (c) & (d). The starting nonlinearity and oscillation are reduced and smooth start is accomplished using DVR.

Case IV

A heavy inductive load is abruptly added at 0.5s. The inclusion of load causes an increase in real and reactive power consumption as shown in Figures 11(a) & (b). It is observed that the heavy inductive load causes the power to fluctuate. As in this case, the reactive power demanded by the additional load is taken from the generator terminals. Hence, the voltage and current in the generator bus fluctuate and it is shown in Figures 11(c) & (d). The passive component employed for reactive power compensation can only support the existing load. During the overload, the generator terminal voltage starts to reduce further as more reactive power is being absorbed by the generator. Being a reactive power consumer, the induction generator undergoes a reactive power dearth which leads to runaway. The DVR is a promising device which can provide an absolute solution for such problems. The proposed DVR can exchange the reactive power demand of induction generator and it also guarantees the stability of the system. The compensated real and reactive power is presented in Figures 12(a) & (b). The excess current consumption is reduced and the voltage is regained to its nominal value as shown in Figures 12(c) & (d).

5. Conclusions

The fault ride through capability of the induction

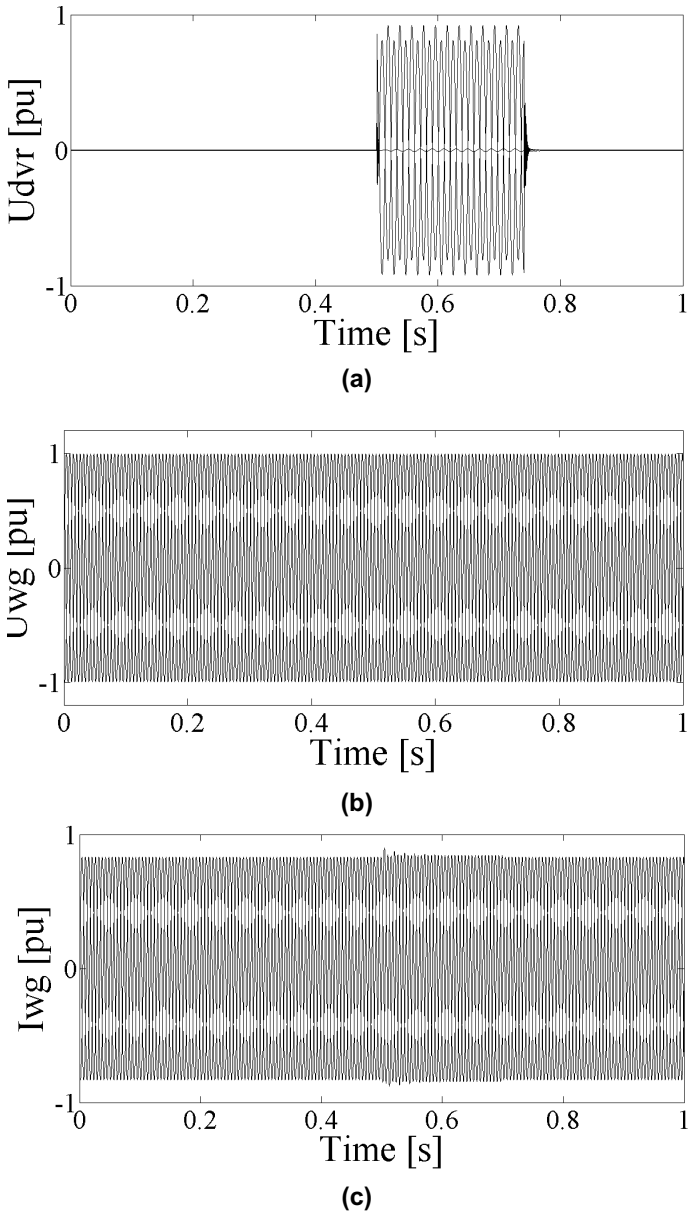

Figure 9 (a): Compensation voltage of DVR (b) Wind generator voltage after compensation (c) Wind generator current after compensation

generator based wind farm is improved with the aid of a DVR. The wind generator remains connected to the grid without loss of stability and guarantees the reliability of the system. The proposed DVR can mitigate voltage disturbance and provide reactive power support. It is also a suitable scheme for standalone operation. The developed models of Wind farm and DVR control strategies demonstrated the viability of the proposed scheme. The results show that the control technique is very effective and yield excellent compensation for voltage disturbance and associated problems.

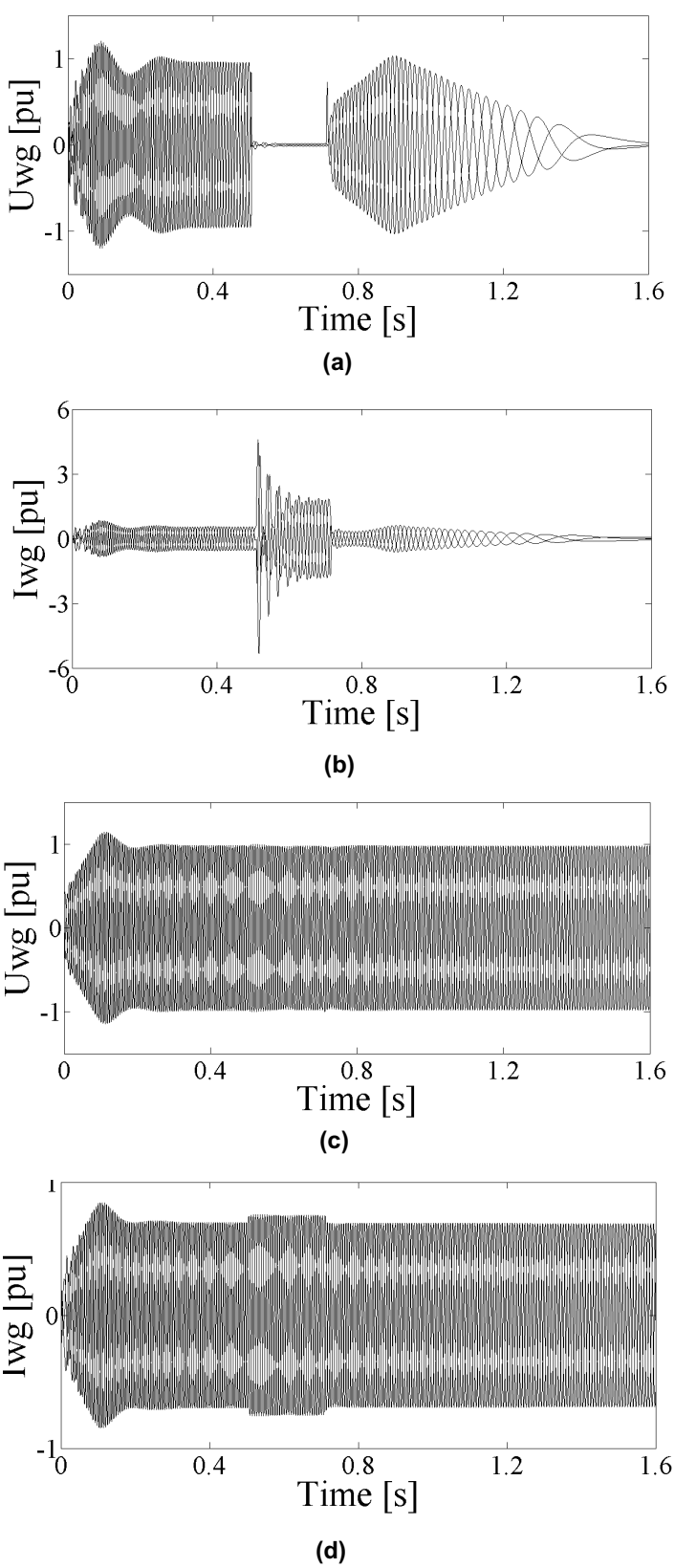

Figure 10: (a) Wind generator voltage dip during severe fault (b) Wind generator current overshoot during dip (c) Compensated voltage (d) Compensated current

References

Al-Hadidi H.K., Gole A.M., and Jacobson D.A. (2008). A novel configuration for a cascade inverter-based dynamic voltage restorer with reduced energy storage requirements," *IEEE Trans. Power Del*., Vol. 23, no. 2, pp. 881–888, April. 2008.

Awad H, Svensson J, and Bollen M.J. (2004). Mitigation of unbalanced voltage dips using static

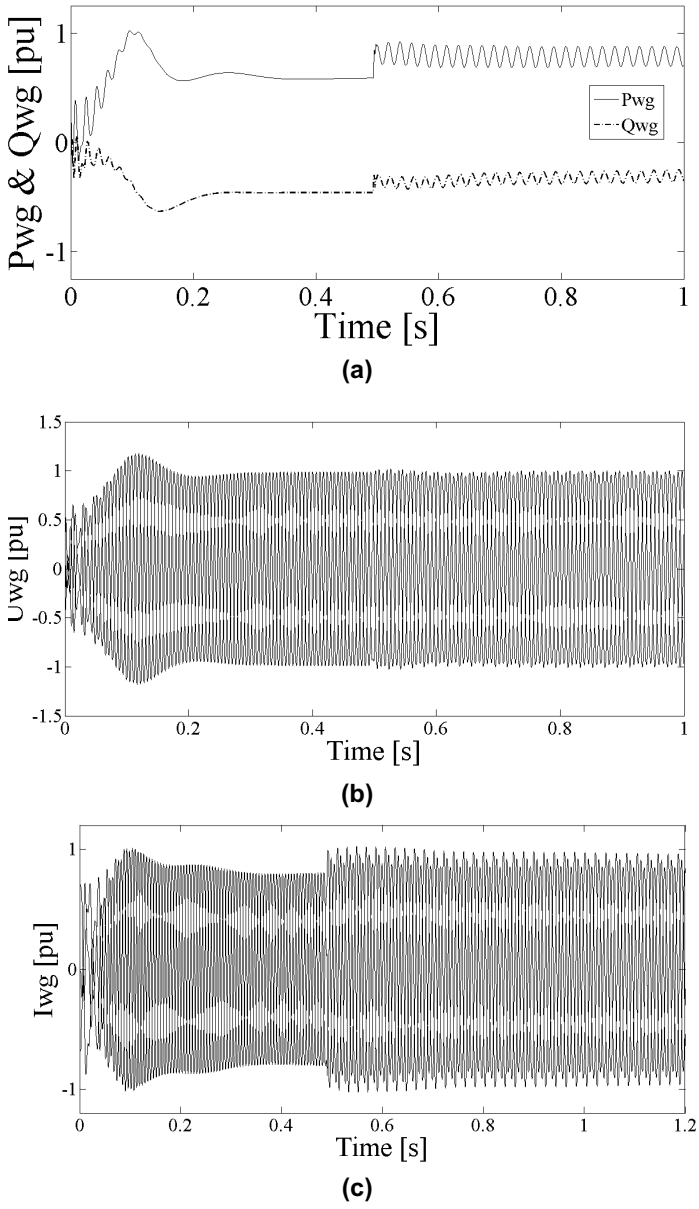

Figure 11: (a) Real and reactive power of wind generator current during sudden loading of unbalanced load (b) Wind generator current (c) Wind generator voltage

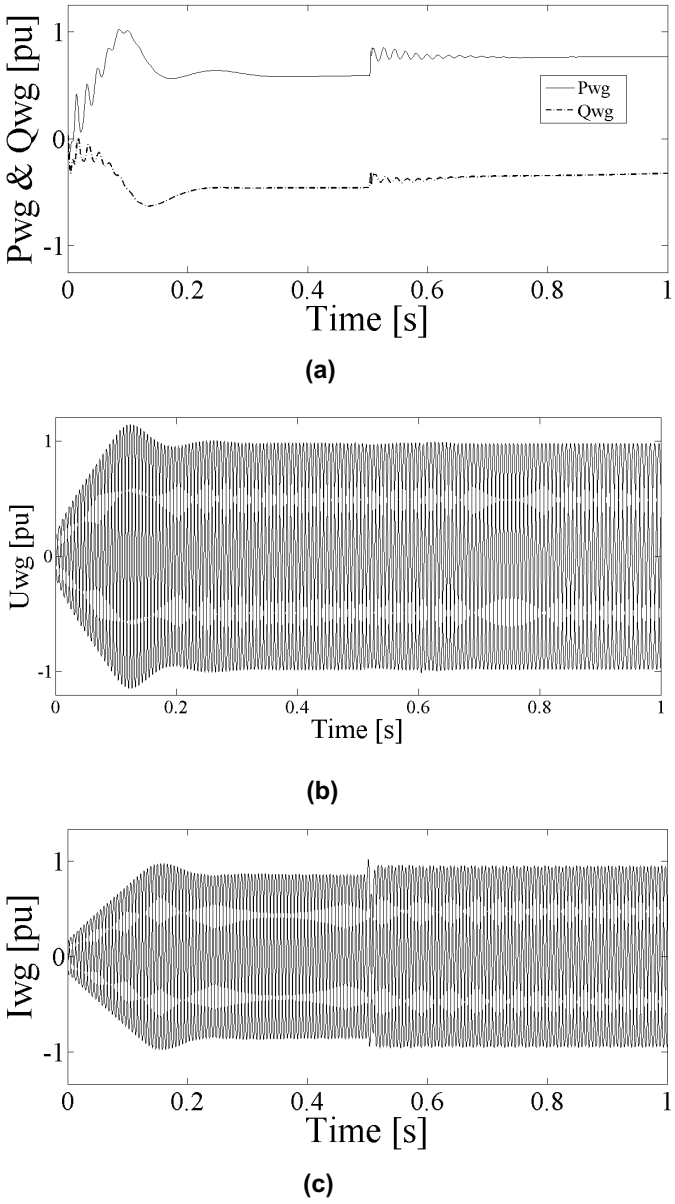

Figure 12: (a) Real and reactive power after compensation (b) Compensated wind generator current (c) Compensated wind generator voltage

series compensator, *IEEE Trans. Power Electron*., Vol. 19, no. 3, pp. 837–846, May 2004.

Awad H, Svensson J, and Bollen M.J. (2005) Tuning software phase-locked loop for series-connected converters, *IEEE Transaction on Power Delivery*, Vol. 20, no. 1 pp 300-308.

Biricik S., Ozerdem O.C., Redif S., and Kmail M.I.O. (2013). Performance Improvement of Active Power Filter under Distorted and Unbalanced Grid Voltage Conditions, *Electronics and Electrical Engineering,* Vol. 19, No 1 (2013), Biricik.

Bollen, M.H.J. (1999). Understanding Power Quality Problems: Voltage Sags and Interruptions. New York: IEEE Press.

Bollen M.H.J. and Häger, M. (2005). "Impact of increasing penetration of distributed generation of the number of voltage dips experienced by end-customers," presented at the 18th Int. Conf. Electricity Distribution, Turin, Italy, June. 6–9, 2005.

Meyer R., De Doncker W., Li Y.W and Blaabjerg, F. (2008). Optimized control strategy for a medium-voltage DVR—theoretical investigations and experimental results, *IEEE Trans. Power Electron*., Vol. 23, No. 6, pp. 2746–2754, November, 2008.

Milanovic, J.V., Ali, H. and M. T. Aung M.T. (2207). Influence of distributed wind generation and load composition on voltage sags, Inst. *Eng. Technol., Gen. Transm. Distrib*, Vol. 1, No. 1, pp. 13–22, January. 2007.

Mukhtiar S.M., Khadkikar V., Chandra A., and Varma R/K. (2011). Grid Interconnection of Renewable Energy Sources at the Distribution Level with Power-Quality Improvement Features, *IEEE Trans.Power Syst.*, Vol. 26, No. 1, pp. 307-315, January, 2011.

Newman M.J. and Holes D.G. (2002). An integrated approach for the protection of series injection invert-

ers", IEEE Transaction on Industrial Application; Vol. 38, No. 3, pp. 679-687, 2002.

Nielsen J.G, .Newman M., Nielsen H. and Blaabjerg F. (2004). Control and testing of a dynamic voltage restorer (DVR) at medium voltage level, IEEE Trans.Power Electron, Vol.19, No. 3, pp. 806-813, May 2004.

Ottersten R and Svensson J. (2002). Vector current controlled voltage source converter—Deadbeat control and saturation strategies, *IEEE Trans.Power Electron*., pp. 279–285, Mar. 2002.

Renders W. Ryckaert R., De Gussemé K, Stockman K., and Vandevelde L. (2008). Improving the voltage dip immunity of converter-connected distributed generation units, Elsevier Renew. *Energy*, Vol. 33, No. 5, pp. 1011–1018, May, 2008.

Siozinys V., and Baranauskas A. (2012). Smart Protection for Enhancement of Stability Conditions of Distributed Generators", Electronics and Electrical Engineering, Vol. 117, No 1 (2012), Siozinys.

Vaimann T., Niitsoo J., Kivipõld T., and Lehtla T. (2012), Power Quality Issues in Dispersed Generation and Smart Grids, *Electronics and Electrical Engineering*, Vol. 18, No 8 (2012), Vaimann.

Received 30 July 2013; revised 14 October 2014

Renewable energy choices and their water requirements in South Africa

Debbie Sparks

Amos Madhlopa

Samantha Keen

Mascha Moorlach

Anthony Dane

Pieter Krog

Thuli Dlamini

Energy Research Centre, University of Cape Town, Cape Town, South Africa

Abstract

South Africa is an arid country, where water supply is often obtained from a distant source. There is increasing pressure on the limited water resources due to economic and population growth, with a concomitant increase in the energy requirement for water production. This problem will be exacerbated by the onset of climate change. Recently, there have been concerns about negative impacts arising from the exploitation of energy resources. In particular, the burning of fossil fuels is significantly contributing to climate change through the emission of carbon dioxide, a major greenhouse gas. In addition, fossil fuels are being depleted, and contributing to decreased energy security. As a result of this, the international community has initiated various interventions, including the transformation of policy and regulatory instruments, to promote sustainable energy. With this in mind, South Africa is making policy and regulatory shifts in line with international developments. Renewable energy is being promoted as one way of achieving sustainable energy provision in the country. However, some issues require scrutiny in order to understand the water footprint of renewable energy production. Due to the large gap that exists between water supply and demand, trade-offs in water allocation amongst different users are critical. In this vein, the main objective of this study was to investigate and review renewable energy choices and water requirements in South Africa. Data were acquired through a combination of a desktop study and expert interviews. Water withdrawal and consumption levels at a given stage of energy production were investigated. Most of the data was collected from secondary sources. Results show that there is limited data on all aspects of water usage in the production chain of energy, accounting in part for the significant variations in the values of water intensity that are reported in the literature. It is vital to take into account all aspects of the energy life cycle to enable isolation of stages where significant amounts of water are used. It is found that conventional fuels (nuclear and fossil fuels) withdraw significant quantities of water over the life-cycle of energy production, especially for thermoelectric power plants operated with a wet-cooling system. The quality of water is also adversely affected in some stages of energy production from these fuels. On the other hand, solar photovoltaic and wind energy exhibit the lowest demand for water, and could perhaps be considered the most viable renewable options in terms of water withdrawal and consumption.

Keywords: climate change, water-energy nexus, renewable energy, water requirements, South Africa

1. Introduction

1.1 Background

Water use and energy supply are inextricably linked. The provision of energy requires water, and energy is often needed to pump, treat or transport water. The need to protect water quality and supply, and the need to ensure a stable and growing energy supply is an internationally-shared experience. These demands may create competing interests.

The mutually dependent nature of the relationship between energy and water is often referred to as the water-energy nexus. This paper focuses on water requirements for energy production (as opposed to energy for water). It will therefore consider water usage associated with various forms of energy.

The production of electricity may consume a significant quantity of water, be it in the processing of raw materials or in the generation of electricity. In light of the fact that South Africa is a water scarce country, consideration of water use by various energy technologies is important for both future planning and for policy. Climate change is expected to put added strain on water provision, since there are projected changes to seasonal and regional temperature and patterns of precipitation (Hoekstra *et al.,*. 2011; Wilson *et al.,* 2012).

South Africa has a recent history of energy shortages, electricity blackouts in 2007 and 2008, petroleum shortages in 2008 and 2011 and gas shortages in 2011 and 2012. The country is also committed to providing energy for all. However, increasing the output of energy using current production methods will increase the energy demand for water and may involve opportunity cost to the detriment of other developmental activities, or it may increase the vulnerability of communities or watersheds to future threats like changes in the rates of precipitation and evaporation associated with climate change.

South Africa has long protected the integrity of its water sources, and its National Water Act (Act 36 of 1998) is considered to be highly progressive (Seward, 2010). As part of South Africa's water management strategy, the country is divided into 19 water management areas (which have been amalgamated into 9). Each local authority is enabled to regulate the abstraction and use of water within its boundaries. Large-scale water abstraction and use, for example, by mining and some industry is regulated and licenced by the national government. Water resource management in South Africa faces various challenges, which may be compounded by its vulnerability to climate change and related stress on water resources.

To meet the foreseen electricity needs of South Africa in the context of a changing climate, the Department of Energy developed an Integrated Resource Plan (IRP) (DoE, 2010). The national strategy of the Plan is to meet growing electricity demand and at the same time to meet South Africa's international commitment to reduce greenhouse gas emissions by 34% below business as usual by 2030. The IRP strategy is to diversify our energy supply from South Africa's current primary reliance on coal-fired electricity, to an energy mix in which a third is generated by renewable sources (DoE, 2010). To meet this goal, the government is currently offering the opportunity for investment in renewable energy technologies through the Renewable Energy Independent Power Procurement Programme (REIPPP).

The South African Constitution endows each household with the right to 6 000 litres of free water and 50 kWh of electricity per month. In light of the planned changes to the energy supply technologies, and with the risk of increased water vulnerability due to climate change, it is important that the country's water and energy policies take cognisance of one another, or at the very least are not in conflict. Water supply is mostly fixed by nature (allowing for man-made transfers between water basins and for changes in water availability as a result of climate change), whereas energy supply is by design. In some instances water supply can be seen as by design at cost in environmental and economic terms. Bearing in mind what has been said, it is important to assess the demands that might be placed on the country's water resources in the context of changing energy requirements and water availability. This can inform strategic investment in future energy supply.

For sustainable development, South Africa requires secure and reliable water and energy supplies (UN 1998), however, South Africa is the thirtieth most water scarce country in the world (DTI, 2013). While water resources in South Africa are said to offer opportunities for the economy and the much needed employment creation (Odendaal, 2013), limited water supplies necessarily mean that commitment to the establishment and growth of some economic activities will be at the opportunity cost of other economic opportunities.

The imperatives of water and energy provision in the context of a growing economy are factors that should be taken into consideration in designing an energy mix. Hence the motivation for an assessment of the water use of various technologies, and especially in renewable energy (RE) technologies in support of planning for water and energy, and to inform energy and water policy with the vision of facilitating a supportive policy environment.

Previous studies on the water-energy nexus in South Africa include the work of Gulati *et al*; (2013), Carter and Gulati (2014) and Prasad *et al*. (2012). Gulati *et al*. (2013) examine the interconnectedness and interdependence between energy, water and food pricing in South Africa. They con-

sider how energy and water costs influence food prices, with the energy and water focus of their work being primarily from the perspective of energy for water (as opposed to focusing on water requirements for energy production). Their work forms part of a broader study by the World Wide Fund for Nature (WWF), considering the food-water-energy nexus, and to which the study by Carter and Gulati (2014) also contributes. Its focuses is on the food-energy-water nexus, and it briefly mentions the fact that renewable energy has lower water usage requirement. However, the primary focus of their paper is on climate change and the food-energy-water nexus in the context of food security. Prasad *et al.* (2012) describe a modelling framework project (framed within the food-energy-water nexus) being developed for South Africa, which could be used as a tool for policy planning and development. The study presented here differs from the above, since it considers only the water-energy nexus. It specifically focuses on water requirements for energy production, framed within the context of renewable energy.

1.2 Context

In order to consider renewable energy, there needs to be a brief discussion of both renewable and non-renewable (finite) energy sources and their water requirements. This allows for comparisons to be made between renewable and non-renewable sources.

1.2.1 Coal

South Africa can ascribe 92% of its electricity generation to coal (OECD, 2013). Eskom consumes roughly 2% of South Africa's national freshwater resources (334 275 megalitres (ML) (Eskom 2013a; Eskom 2013b) and most of this is associated with coal-fired power stations (Martin & Fischer, 2012). Pulverised coal is combusted to boil water and create steam, which drives electricity-generating turbines.

Water is consumed for many processes in coal mining, from the running of the equipment, dust suppression, washing and processing the coal as fuel, to rehabilitation of the area once the mine is closed. Washing coal contaminates water with sulphur compounds and dissolved iron to create sludge. The sulphur compounds and heavy metals commonly found in coal-bearing rock can contaminate ground or rain water and create a risk of acid mine drainage (AMD). The volume of water required for washing coal depends partly on the quality of the raw coal.

Coal feeds coal-fired power stations and is also used to make liquid fuels. The water impacts associated with these technologies are substantial, as is the impact associated with the mining of coal. The following sections will discuss coal power stations, carbon capture and storage (briefly) as well as coal to liquid fuels.

1.2.2 Synthetic liquid fuels from coal and gas

Liquid fuels can be produced from coal and natural gas (methane). In a typical coal-to-liquid (CTL) process, coal is first gasified to yield syngas, which is then liquefied into hydrocarbons such as gasoline and diesel in a Fischer-Tropsch (FT) process (Mantripragada & Rubin, 2013). Coal is fed into the gasfier in dry or wet form. Thus, the wet gasification process requires water to feed the coal slurry (50% water) into the gasifier (Lu *et al.,* 2012). In South Africa, Sasol and PetroSA produce liquid fuels from low-grade coal using the FT process.

In a gas-to-liquid (GTL) process, natural gas is combined with steam, carbon dioxide or oxygen to form a syngas which then goes through a Fischer-Tropsch process to produce liquid fuels (Rostrup-Nielsen, 2000). Sasol produces syngas from natural gas through three steps (Sasol, 2014):

(a) reforming natural gas with oxygen and steam to produce syngas,
(b) converting syngas to waxy hydrocarbons in a Fischer-Tropsch reactor, and
(c) selectively breaking down the waxy hydrocarbons in GTL diesel, GTL kerosene, GTL naphtha and liquefied petroleum gas (LPG).

South Africa produced an oil equivalent capacity of 150,000 bbl/day through CTL and of 45 000 bbl/day of synthetic fuel through GTL in 2011 (Telsnig *et al*., 2013).

Nevertheless, the production of syngas via a combination of natural gas and steam requires water.

1.2.3 Carbon capture and storage

The construction of a demonstration plant in South Africa is planned (Creamer, 2013) although in light of the capital investment required to retrofit the existing power stations, it remains to be seen whether this technology will be taken up. Carbon capture and storage technology (CCS) reduces emissions of carbon dioxide (CO_2), methane (CH_4) and nitrous oxide (N_2O). However, this technology reduces energy capacity and increases water consumption at coal fired electricity plants (Wilson *et* al., 2012).

1.2.4 Conventional oil

By the end of 2011, South Africa had proven reserves of 15 million barrels of oil off-shore in the Bredasdorp Basin and off the west coasts of the country (EIA, 2013). However, these reserves may not be economically viable to extract. Currently, a large proportion of the oil consumed in the country is imported from the Middle East and West Africa and is refined locally.

1.2.5 Natural gas

There are limited reserves of natural gas in South Africa, but significant potential for shale gas resources (about 137.34 billion cubic meters of technically recoverable shale gas resources mostly in the Karoo Basin) (EIA, 2013). However, exploitation of these resources requires drilling and other processes. The country imports most of its natural gas from Mozambique through a pipeline, which is transported to the Sasol Secunda plant for synthetic fuels. Only a small portion is locally produced. Natural gas is used in some of the power plants, in addition to coal.

1.2.6 Solar power

Concentrated solar power

Three concentrated solar power (CSP) production plants, all located in the Northern Cape, have been awarded contracts under the Renewable Energy Power Producer Procurement Programme (REIPPP). Of these, one is a central tower CSP near Upington with capacity of 50 MW, and two are CSP trough plants, one near Pofadder with 50 MW of production capacity, and one near Grobblersdal with 100 MW capacity (Forder, 2013).

CSP plants use mirrors to redirect sunlight on to a specific point to heat a fluid. The heat in the fluid is then used to drive generators and produce power. There are four technical designs used for CSP, the parabolic trough, power tower, linear Fresnel, and the dish Stirling.

Concentrated photovoltaic and photovoltaic panels

Photovoltaic (PV) panels convert sunlight directly into electricity by absorbing protons and releasing electrons. These free electrons are captured on an electrode and result in an electric current, which can be used as electricity (SEA, 2009).

Concentrated photovoltaic technology (CPV) uses optics such as (Fresnel) lenses or curved mirrors to focus large amounts of sunlight (radiation) onto a small area of a photovoltaic cell to generate electricity more efficiently than traditional PV (Soitec, 2013a).

In South Africa, PV is mainly used to provide electricity for telecommunications and lighting in remote areas. It is estimated that roughly 200 000 off-grid PV systems and only 10 grid-connected systems exist. There are currently three concentrated photovoltaic (CPV) farms in South Africa. A pilot project is located in Touwsrivier, with a rated capacity of 82 kWp, one in Johannesburg with a 8.2 kWp and a 480 kWp CPV plant in Hazelmere. A 44 MWp plant is under construction in Touwsrivier and is expected to come online during 2014 (Soitec, 2013b). Some businesses also made installations for their own private consumption (e.g. MTN).

1.2.7 Wind turbines

The generation of electricity by wind energy is through the use of the kinetic energy of air. The average annual energy generated on a wind farm typically varies between 0.05 and 0.25 GJ/m^2 (Blok, 2006).

In South Africa, there is currently only one large scale wind farm in operation (in Jeffrey's Bay in the Eastern Cape). There are also initial plans for other such farms (particularly in the Eastern Cape). In addition there are two small-scale wind farms in operation, viz., Klipheuwel and Darling. As part of the Renewable Energy Independent Procurement Programme (REIPPPP), the Department of Energy has awarded 20-year Power Purchase Agreements (PPA) to a number of wind projects, which will increase the wind power percentage of South Africa's electricity provision in the future. According the Integrated Resources Plan for Electricity 2010-2030 (2010), South Africa plans to install 8.4 GW of wind energy supply by 2030.

1.2.8 Hydroelectricity

Hydropower provides approximately 16% of the total world electricity supply and may be considered a reasonably clean and low-cost renewable source of energy (Hoekstra *et al.* 2011; Mekonnen & Hoekstra, 2012). In contrast, hydropower in South Africa accounts for a very small percentage of total power, at only 2%. Martin and Fischer (2012) note that just under half of this is from run-of-river plants (Gariep (260 MW), Vanderkloof (240 MW) (which are both on the Orange River) and 60% of this is from pumped storage plants (e.g. Drakensberg (100 MW) and Palmiet (400 MW)). There are also two small plants operated by Nuplanet in the Free State province of South Africa, in the vicinity of Bethlehem. A small percentage of our hydropower is imported from Mozambique (Cahora Bassa Dam), Lesotho and Zambia (Eskom, 2011).

There are a number of different methods for generating power using hydroelectricity, the most common and relevant for South Africa being conventional dams (e.g. Gariep Dam in South Africa), pumped storage (e.g. Palmiet pumped storage scheme in the Western Cape of South Africa) and run-of-river schemes (a potential option for small-scale hydro in South Africa).

1.2.9 Bioenergy

Bioenergy is globally the largest, although not always sustainable, renewable energy source, contributing to over 50% of total renewable energy. Bioenergy also contributes over 10% towards final global energy consumption. Biomass is generally derived from natural sustainable organic sources such as decomposing material from plants or animals. This may include wood, agricultural crops and manure, as well as municipal waste (not a nat-

ural sustainable source). Bioenergy is formed when biomass is converted and then directly used as fuel or converted into liquid fuel or gases (REN21, 2013). In South Africa, biofuel generation is from waste-from-crops exclusively.

1.2.10 Nuclear power

There are various nuclear technology systems available worldwide. South Africa has only one nuclear power plant in operation, viz., Koeberg Nuclear Power Station, in the Western Cape. A nuclear power plant uses uranium to produce energy, which is dependent on low enriched uranium, rather than fossil fuels, as a source of fuel to produce heat. Heat is generated during the nuclear reaction process of fission. A reactor controls the nuclear process. Energy is generated in the reactor and heats up water, which co-produces steam and drives a turbine. The turbine is connected to a generator, which ultimately produces electricity. The fission process of uranium is used as a source of heat in a nuclear power station in the same way that the burning of coal, gas or oil is used as a source of heat in a fossil fuel power plant.

1.3 Objectives

Energy requirements in the water sector need to be properly examined to establish the overall water supply chain in South Africa. Several alternatives to the energy-intensive water supply chain do exist, including the use of renewable energy sources and local waste-water re-use. However, the impact of deploying renewable energy technologies on water resources need to be considered properly. For example, to allocate water for biofuel production will require a shift in the current water allocation policy. Due to the large gap between water supply and demand, trade-offs in water allocation amongst different users and policy makers are critical. With this in mind, the primary objective of this study is to investigate renewable energy choices for South Africa and their water requirements.

2. Methodology

2.1 Justification

Water scarcity and the drive for optimized use have led to various estimations of the amount of water use (withdrawal or consumption) per MWh (or GJ) of energy output. Various approaches have been adopted in this regard. Some of the more common approaches include water footprinting (Hoekstra *et al.*, 2011), Life-Cycle Assessment (LCA) and various tools designed to help organizations to understand water use, potential impacts and associated risks. There are also a number of methods for assessing broader water use impacts relating to scarcity, stress and human health (Boulay 2013).

Water footprinting is a method for measuring the volume of water abstracted and polluted in the provision of a good or service. This tool can be used to increase awareness of water management challenges and to help consumers make informed purchase decisions (Hoekstra *et al.,* 2011; Morrison & Schulte, 2010). LCA is a systems analysis tool that was designed to measure resource use in order to assess the environmental sustainability of products and services through all components of the value chain (Morrison & Schulte, 2010). Various other tools exist for businesses, for example, to understand their water use and impact and associated water risks. These include the WBCSD Global Water Tool, which helps companies compare their water use, wastewater discharge, and facility information with validated watershed and country-level data. The tool is intended to allow investors and companies from all industry sectors to assess and quantify water-related risks across the globe (WBSCD 2013; WWF-DEG 2011).

This paper considers water use both as withdrawal and consumption, with some qualitative assessment of the water impacts where this information was available. The assessment considered upstream water use (pre-generation) and water use during the generation of energy. It was assumed that water use impacts would be similar for transmission of electricity from different sources and for different liquid fuel types. Downstream water impacts associated with various biofuels could differ, potentially, but for this study the differences have been assumed to be negligible.

The approach therefore in part adopts elements of the footprint methodology (by assessing stages of pre-generation and post generation), however a full assessment of different forms of energy generation was not within the scope of this study. Most of the data has been gathered from secondary sources (literature) and therefore the assessment boundaries are not fully comparable.

An attempt has been made to identify the significant water uses and impacts during pre-generation and generation from the literature and based on interviews with experts. For example, the impact associated with the mining of Rare Earth Elements, as an input into the construction of wind turbines, is included but the impacts associated with the production of the concrete used to build the turbines was not regarded as significant according to the literature and experts. In the same way water use associated with cement used to construct nuclear power stations is not included, as this does not represent a significant water use impact. This approach is intended to identify the most significant water use impacts associated with each energy technology. Assumptions around what can be considered as 'significant' water use impacts will be tested during future workshops as part of the larger study.

This study focuses on the water use impacts associated with the pre-generation and generation

of renewable energy. However, in order to make comparisons and to contribute to a decision-support tool for policy-makers to use when planning energy investments that consider water impacts, the study includes an assessment of the pre-generation and generation water use impacts associated with non-renewable energy.

2.2 Data collection

The assessment included a review of the available literature. This focused on trying to identify South African specific data on water use impacts associated with the various energy types. A review of international literature was undertaken (not presented here) to provide comparative data or to be used as proxy data where gaps existed in the South African context. An attempt was made to fill these gaps through engaging with local experts. The engagement with experts involved semi-structured interviews focused on accessing quantitative data to fill gaps. In many cases, the investment in renewable energy generation is still in a very early stage of development and thus data were not available. Expert judgement was sought on the likely (qualitative) impacts expected in the South African context relative to international contexts. Future engagements (through project workshops) during later phases of this project will hopefully yield more qualitative data, as some of these projects should be in further stages of development.

2.3 Data processing

Each fuel undergoes several stages during energy production. In a given stage (i^{th} stage) of energy production, water is withdrawn (W_i), consumed (C_i) discharged (D_i) and recycled (R_i) (Fthenakis & Kim, 2010). However, most of the available data in the literature is on water withdrawals and consumption. Consequently, the total water withdrawal (W) and consumption (C) factors over the lifecycle can be computed by using:

$$C = \sum_{i=1}^{i=n} C_i \qquad \textit{Equation 2.1}$$

$$W = \sum_{i=1}^{i=n} W_i \qquad \textit{Equation 2.2}$$

where i = 1, 2, …n, is the number of stages, and S is the summation sign.

Some energy production stages involve several processing options. For example, coal transportation can be through batch (by train) or continuous (such as slurry by pipeline) means. In such cases, the lowest and highest values were identified using Excel. The total withdrawal (W_L) and consumption (C_L) lower-limit factors were calculated from:

$$C_L = \sum_{i=1}^{i=n} C_{i,L} \qquad \textit{Equation 2.3}$$

$$W_L = \sum_{i=1}^{i=n} W_{i,L} \qquad \textit{Equation 2.4}$$

Similarly, upper-limit consumption factors were added to find the upper limit of water usage over the lifecycle of each fuel considered in this study. Bar graphs of these lower and upper values (based on data reported by previous researchers) were plotted for ease of fuel inter-comparison, depending on data availability (see section 4 in this paper).

3. Findings

3.1 Water use in energy production in South Africa

It is reported that the Energy Sector in South Africa uses 2% of the total national water allocation (Wassung, 2010). In addition, coal is currently the main source of electricity in the country. However, disaggregated data on water withdrawal and consumption at specific stages of energy generation is scarce across fuels. Consequently, the coal-water nexus has been investigated more extensively than other fuels.

Conventional energy sources

Some of the reported data for conventional energy is presented in Table 1. It is observed that coal uses more water in plant cooling (1 380-1420 litres/MWh). Using pre-generation values from this table, 263-1646 litres/MWh of water is used between the pre-generation and generation stages. The lower limit is the sum of the minimum values of pre-generation (mining and washing, 183 litres/MWh) and generation (1 380 litres/MWh). For lifecycle usage, Wassung (2010) reported water intensities of 1 534-3 326 litres/MWh), which is comparable to the international consumptive usage (3 460 litres) of water reported by Wilson *et al.* (2012).

South Africa has one nuclear power plant (Koeberg) currently in operation, with an installed capacity of 1 800MW and a capacity factor of 83.1%. Koeberg uses seawater flowing at 80 000 litres/second to cool the condensers (Eskom, 2013a). Using these values, the intensity of water use during generation has been estimated as 192 539 litres/MWh. This value is consistent with findings from other studies. Fthenakis and Kim (2010) reported a water withdrawal value of 120 000 litres/MWh for a nuclear power plant using once-through cooling method. Diesel is also used in backup generators. Water use by dry-cooled generators is relatively low.

Renewable energy sources

There is sporadic data on water usage in renewable energy in South Africa. Gerbens-Leenes *et al.* (2009) report water use for various fuel crops (most of them being food crops). The exploitation of food crops to generate energy creates competition between food and fuel for the same resources. In view of this, the Biofuels Industrial Strategy of the

Table 1: Water usage in energy production by using thermal electric cycles

Fuel	*Energy production stage*	*Water use[a] (litres/MWh)*	*Reference*
Coal	Pre-generation, mining& washing	183-226	Martin & Fischer (2012)
	Generation, cooling	1420	Eskom (2013b)
	Generation, dry cooling	100	Eskom (2013c)
	Generation, indirect dry cooling	80	Martin & Fischer (2012)
	Generation, cooling	1380	Martin & Fischer (2012)
Nuclear	Generation, cooling	192 539[b]	Eskom (2013a)
Diesel	Generation, dry cooling, water for purging	0.54	Eskom (2009)

[a] Sources of this data report it as water use, without specifying whether withdrawal or consumption.
[b] This is seawater used at Koeberg nuclear power plant, and so it has negligible impact on the fresh water resources.

Republic of South Africa initially excludes maize from usage as a feedstock in the production bioethanol (DME, 2007). Consequently, agricultural residues from food crops (such as maize husks, stalks and leaves) are predominantly used as a source of thermal energy (DME, 2003). Stone *et al.* (2010) found that production of bioethanol from grain and grain sorghum consumes the highest quantity of water compared to other feedstock.

Data on usage of water in the production of energy from CSP and PV is scarce. Olivier (pers comm., 2013) reported water consumption of 767 000 litres during the construction phase of a 4.5 MW hydro power plant. For wind, Hagemann (pers. comm., 2013) reported water usage of 817 000 litres in the construction phase of a 120MW power plant. The plant would use 3650 litres during operation phase. Assuming a capacity factor of 30%, this yields a water intensity of 0.79 litres/MWh during operation. Over the lifecycle, Wilson *et al.* (2012) reported a water-consumption value of less than 1 litres/MWh.

The analysis to follow has been categorised by fuel type (i.e. coal, oil/natural gas, solar, wind turbines, hydroelectricity, bioenergy and nuclear). As mentioned in the methodology, conventional fuels have been considered in addition to renewable fuels, as this is essential for comparative purposes and in decision-making between renewable and conventional fuel choices. This discussion covers water and water impact for each fuel.

4. Discussion

4.1 Coal power plants

Results from other countries show that wet-cooled thermal power plants withdraw and consume the highest amounts of water on a lifecycle basis. Most of this water is required during the generation stage, for the process of wet-cooling. This shows that more attention needs to be paid to this stage of energy production. However, disaggregated water usage data (stage-by-stage withdrawal and consumption levels) for South Africa is scarce. In view of this, water usage pattern from other countries can be used as an indicator of the situation in this country. More attention is required to curtail the volume of water withdrawal and consumption in the generation stage.

Coal-fired power has a substantial water impact. New technologies may reduce water consumption and impact. In this respect, Eskom has invested in research to use dry processing to purify coal by removing stone – a major source of the ash, sulphur and abrasive components found in coal. This research focuses on removing these components using dry (waterless) techniques to reduce the volume of coal to be transported, improve coal combustion rates and lower emissions (Eskom 2013b; de Korte, 2010).

Eskom has implemented a dry-cooling system in power plants wherever feasible. This is despite the fact that dry-cooled plants are comparatively less energy- efficient than wet-cooled, leading to higher carbon emissions. Moreover, there are higher capital and operating costs associated with dry cooling. Nevertheless, efforts to invest in dry cooling could also have significant water benefits. According to Eskom (2013b), approximately 85% of the total quantity of water supplied to a power station evaporates through these open cooling towers. In contrast, dry-cooling technology does not rely on open evaporative cooling for the functioning of the main systems. Overall power station water use associated with dry cooling is approximately 15 times lower than a conventional wet-cooled power station. This water conservation effort results in an estimated combined saving of over 200 Ml/day, or in excess of 70 000 million litres/annum (Eskom, 2013b).

Matimba Power Station near Lephalale in the Limpopo Province is the largest direct-dry-cooled power plant in the world, with an installed capacity greater than 4 000 MW. It makes use of a closed-circuit cooling system similar to the radiator and fan system used in motor vehicles (Eskom 2013a).

Consequently, water withdrawal and consumption at this plant station is significantly associated with upstream operational stages such as coal mining, processing and transportation.

An additional technology option is indirect dry cooling. This entails the cooling of the water through indirect contact with air in a cooling tower, a process during which virtually no water is lost in the transfer of the waste heat. Eskom is undertaking various other water management projects to reduce water requirements in energy production (Eskom, 2013a). These local efforts are consistent with the observation (from international data) that most of the water is withdrawn and consumed in the generation stage.

4.2 Coal liquefaction

Sasol uses about 4% of the water resources available from the Vaal River System. The water use in operations at Sasol's Synfuels in South Africa is 12 000 litres per tonne of product (Sasol, 2013). Specific withdrawals are not disclosed by Synfuels operations in South Africa (only withdrawals associated with global operations are disclosed).

During 2011 Sasol's main operating facilities at Sasolburg and Secunda set voluntary internal water efficiency targets, which took into consideration site-specific constraints and opportunities. With usage in 2010 as a baseline, Sasol Synfuels at Secunda has a target to improve its water use intensity (volume of water used per tonne of product) by 5% by 2015, while at Sasolburg, Sasol Infrachem is targeting a 15% improvement (Sasol, 2013).

According to Sasol's Water Disclosure Report Submission (Sasol, 2012), "A study has been conducted to determine the relationship between energy usage (and related carbon emissions) and water usage for alternative cooling technologies for the design of new coal to liquid (CTL) and gas to liquid (GTL) facilities." These results will be used to determine the most appropriate cooling technology selection for new facilities, depending on the availability of water at the specific location.

4.3 Carbon capture and storage

The construction of a demonstration plant in South Africa is planned (Creamer, 2013) although in light of the capital investment required to retrofit the existing power stations it remains to be seen whether this technology will be taken up. Carbon capture and storage technology (CCS) reduces emissions of carbon dioxide (CO_2), methane (CH_4) and nitrous oxide (N_2O). However, the technology reduces the energy capacity and increases water consumption (Wilson *et al.,* 2012). CCS technology requires more fuel to produce the same amount of energy as non-CCS technology. Water withdrawal and consumption for CCS power plants is estimated to be between seven and fifty times greater than the water required for non-CCS technology (Wilson *et al.,* 2012). The water impact of CCS is very high.

4.4 Nuclear power

Koeberg Nuclear Power Station has three different water systems, known as the primary, secondary and tertiary circuits. The three water systems are used to cool down the heat produced by the fission energy process. The primary water system is a closed system and is radioactive. No water consumption is involved in this system. The secondary and tertiary systems use seawater to produce steam to turn the turbines (Eskom, 2013a). Water use for a nuclear power station such as Koeberg is extensive (mostly seawater), but uses a negligible volume of fresh water. It is presented here for completeness.

Water is required at a power plant to cool the system and also to condense the low-pressure steam and finally to recycle it. When the steam in the internal system condenses back to water, the excess heat, which is removed from the system, needs to be recycled and transferred to either the air or to a body of heat. At most coal-fired power stations, the indirect method is used to remove the excess heat. The system uses water and by releasing steam into the air using large cooling towers, the excess heat is removed from the system.

The Koeberg Nuclear Power Station is built adjacent to an abundant water source (the ocean) and hence uses the direct cooling method to cool down its system. This method uses water only once to cool down the internal water system and circulates the water back into the ocean at an increased temperature level. Water consumption is marginal, with a small proportion the withdrawn water being consumed. The small amount of water consumed and/or lost refers to the evaporation that occurs when the water circulated back into the ocean and being a few degrees warmer than the ocean temperature (World Nuclear Association Cooling power plants: accessed 15 October 2013). The use of seawater reduces the competition for fresh water. Nevertheless, the elevated temperature of the discharged water may affect the ecosystem at the discharge point.

4.5 Oil and natural gas

Extraction of oil by hydraulic fracturing involves pumping a mixture of water, sand and other additives into the ground, thereby creating cracks. The oil is then forced out through these cracks. In addition, water is used in oil or gas-fired thermal electric generators that are wet-cooled. Most of the water used in the production chain of oil/gas-fired thermoelectric power is during generation.

Hydraulic fracturing contributes to contamination of ground water (Kharak *et al,*. 2013). Some of the contaminants include methane, benzene and gasoline and diesel range organics. In some cases,

well-fed tap water has become flammable due to the presence of these contaminants (Wilson *et al.,* 2012). The high demand of water for wet cooling puts stress on water resources.

For natural gas, there have been environmental concerns regarding water usage and hydraulic fracturing in the Karoo area. It has been estimated that about 10-15 million litres of water may be required to drill one well (Sovacool, 2014). However, in light of the fact that the Karoo area is an arid environment, water will have to be sourced from a distance. In addition, water is used in gas-fired thermal electric generators that are wet-cooled. Most of the water used in the production chain of oil/gas-fired thermoelectric power is during generation (up to 5 850 MWh/litre), (Wilson *et al.,* 2012).

4.6 Concentrated solar power and photovoltaics

Concentrated solar power (CSP) plants use water in the resource extraction and the manufacturing of the components in the collector. Most of the water used during manufacturing is linked to the heating, ventilation and air-conditioning (HVAC) system of the manufacturing plant. The parabolic trough, power tower and linear Fresnel technologies can use wet, dry or hybrid cooling systems. The dish Stirling does not require a cooling system (the heated fluid is hydrogen).

CSP plants using steam cycles require cooling to condense the steam exiting the turbines. In this study, it has been found that these plants withdraw 500-5 000 litres/MWh and consume 300-5 000 litres/MWh, which is in agreement with finding from other studies (2 000-3 000 litres/MWh reported by IEA-ETSAP & IRENA (2013).

Dry (air) cooling is an option for areas where water is a constraint, but dry (air) cooling is less efficient than wet cooling and this reduces the capacity (or output) of the plant. Compared with wet cooled CSP plants, electricity production is typically reduced by 7% and the capital cost increased by 10% in dry cooled plants (IEA-ETSAP & IRENA 2013). The water impact of CSP plants is very low.

Water is used in the production of PV-cells. The water use can be divided into two groups of users. Firstly the manufacturing plant and its infrastructure, for example water use for HVAC, sanitary use, and landscaping. The second group is the manufacturing process itself where standard and highly purified de-ionized water is used to manufacture PV cells (Williams, 2011). The water use is associated with removing chemical residues from equipment and rinsing of substrate wafers and panels.

A study done by Sinha *et al.* (2013) states that half of the life cycle water withdrawal is associated with the manufacturing of the module and the water consumption during the manufacturing of a CdTe PV-cell is a quarter of the water withdrawal. The water consumption is linked to cooling tower evaporation and site irrigation.

Water is also used during the project construction, but with no documented figures easily accessible. The water use during generation is linked to the cleaning/washing of the PV-panels. International literature suggests figures of 15 litres/MWh for CPV and PV (NREL, 2002; Fthenakis & Kim, 2010). How often cleaning occurs in SA is not yet quantified. It is likely to be dependent in part on the (climate) area where the system is installed.

4.7 Wind power

Wind power does not use water in the acquisition or supply of energy *per se*. It does, however, use water in the refinement of the rare earth minerals required for the production of the turbines. Rare earth metals are a group of 17 metals that used to be considered a by-product of mining but are now seen as an important component of many "green technologies" such as electric cars, solar panels, and wind turbines. They are not so much rare as mixed up with other rare earth minerals, making them at times uneconomical to mine. The magnets used in wind turbines have an important rare earth component known as neomycin. Presently, neomycin is imported almost entirely from China, although there are rare earth element sources available in the USA, South Africa, and elsewhere. A large wind turbine (approximately 3.5 MW) generally contains 600 kg of rare earth metals.

Wind energy does not require water for its generation (assuming the land used is still offered for other uses such as agriculture) (Gleick, 1994; Martin & Fischer, 2012), Water use for the turbine construction phase has been deemed negligible (Gleick, 1994). There is also likely negligible water use in the washing or the turbine blades from time to time. The water use in the production of rare earth elements such as neomycin does not impact on water use in South Africa, but they do impact on the water footprint globally.

4.8 Hydroelectricity

No additional water is used in acquiring or supplying of hydropower. However, a substantial quantity of water is needed to ensure a constant fuel supply source (Pegram *et al.* 2011). Some suggest that no water is used in the process of hydropower generation, since the water used in generation is returned to the water resource and it hence qualifies as in-stream water user. Others argue that evaporation losses associated with the hydropower plant are significant and that hydroelectricity is a significant consumer of water (Hoekstra *et al.,* 2011; Mekonnen & Hoekstra 2012).

One of the seminal papers that have considered water and energy, making reference to hydropower water consumption is that of Gleick (1994).

Important omissions in this paper are previous environmental evaporation and negligibilty of seepage (Pegram *et al*., 2011). Gleick (1994) estimates a range of hydropower evaporation values, varying from a minimum of 0.04 m^3/MWh, to a maximum of 210 m^3/MWh, with an average of 17 m^3/MWh.

In South Africa, evaporation rates vary spatially across the country (see Schulze (2008) to some degree mirroring the annual rainfall rates spatially too. The highest rates are in the North West (NW) and central regions of the country, decreasing eastwards towards the east coast. Such spatial evaporative losses are important to consider in terms of future planning for hydropower dam placements. Nonetheless, when considering evaporation losses, the size of the reservoir (a deep reservoir with a lower surface area will have less evaporative loss) is more important than the climate itself.

Mekonnen and Hoekstra (2012) consider the blue water footprint of hydroelectricity, linking this to the evaporation loss associated with the artificial reservoirs created behind hydroelectric dams. In their study, they calculated the blue water loss through a series of equations and assumptions, and came up with a figure of 90Gm^3yr^{-1}. In perspective, this equates to 10% of the blue water footprint of global crop production in 2000, which they find to be relatively large when compared to other renewable sources of electricity (Mekonnen & Hoekstra, 2012).

Pegram *et al.* (2011) point out that Mekonnen and Hoekstra (2012) do not consider evapotranspiration of natural vegetation, in their interpretation of water consumption. When considering evaporation losses in terms of hydropower, Pegram *et al.* (2011) argue that it is net evaporation loss that needs to be considered, as opposed to total evaporation loss. Net evaporation loss refers to the difference the evaporation deviates from a natural reference condition (e.g. natural vegetation) (Pegram *et al.,* 2011). This, they believe will reflect a more accurate picture. Other studies in different environments e.g. in New Zealand (Herath *et al.,* 2011) highlight the need for taking the local environment into consideration, since their values are notably lower than the global averages presented by Gleick (1994).

In addition to considering evaporation losses, it is important to remember that hydropower is generally responsible for changing the flow regime (Pegram *et al.* 2011). This in turn may impact on the environment as well as water availability to users downstream. Conceptually it is also worth noting that a nominal amount of water is used in constructing a hydropower plant, albeit negligible (Pegram *et al.* 2011).

4.9 Bioenergy

Water use in the production and application of bioenergy varies. Dominguez-Faus *et al.* (2009) estimated that ethanol production from corn requires from 2 270 000 to 8 670 000 litres/MWh, whilst soybean based biodiesel pre-generation and generation utilizes between 13 900 000 and 27 900 000 litres/MWh compared to the 10-40 litres/MWh required for petroleum extraction.

Closer to home, de Fraiture *et al.* (2008) indicated that South Africa uses approximately 416 million litres of water to produce sugarcane for bioethanol production per annum, which is equivalent to 9.8% of total irrigation that is directed at biofuels production. This is a significant amount for a water-stressed country.

The global production of bioethanol from grain and grain sorghum consumes the highest quantity of water compared to other feedstock. In contrast, sugar cane appears to have the lowest water footprint in ethanol production. Stone *et al.* (2010) explain this wide disparity by arguing that only the grain in the corn is used to produce ethanol, whilst the rest of the crop, that is, the lignocellulosic materials (i.e. leaves, stalk and stem) are not utilised in the process. Furthermore, the authors indicate that sugar cane and corn have different photosynthetic processes, which could, in part, explain their dissimilar water requirements aside from the obvious fact that they are two different crops (Stone *et al,.* 2010). Soybean is also water inefficient in that it requires very high quantities of water for irrigation and even more for the actual production of biodiesel. To further attest to this, some commentators contend that over 180 000 litres of water would be required to generate sufficient amounts of biodiesel from soybean to power a household for a month (Jones, 2008).

More disaggregated and updated (recent) data is required for water usage in biofuels production in both the global sphere and South African context. For instance, no data could be identified for the processing phase of ethanol production using sugar cane *viz.* cane washing, condenser multi-jet in evaporation and vacuum, fermentation cooling and alcohol condenser cooling, barring an indication that in 1997 all this was estimated to consume 21m^3/ton and that this has reduced over time to 1.83 m^3/ton in 2004 (Goldemberg *et al.* 2008).

While all the authors concur that in some regions, rainfall meets the irrigation requirements of the production of biofuel feedstock, they readily admit that the production of biofuels is and will continue to compete for limited water stocks in many countries, including the USA. Needless to say, this will put additional pressure on limited natural resources for agricultural production (Dominguez-Faus *et al.,* 2009; de Fraiture *et al,.* 2008; Stone *et al,.* 2010). In the case of the USA, this is exacerbated by the Government requirement to produce 57 billion litres of ethanol from corn by 2015 (de

Fraiture *et al.,* 2008). On the other hand, the strategy on biofuels in South Africa initially excludes the use of maize to produce bioethanol (DME, 2007), thereby reducing the energy-food competition for natural resources.

All this points to the fact that while a low carbon economy is important, it comes with a significant price tag for water resources – "green energy for blue resources" as de Fraiture *et al.* (2008) point out in the title of their paper.

5. Conclusion

Water usage in the production of energy from conventional and renewable fuels has been explored. Data have been acquired through a combination of a desktop study and expert interviews. Water withdrawal and consumption levels at a given stage of energy production have been investigated. Results show that, for South Africa, there is limited data on all aspects of water usage in the production of energy, accounting in part for the significant variations in the values of water intensity reported in the literature (with some approximations). It is vital to take into account all aspects of the energy life cycle to enable isolation of stages where significant amounts of water are used.

Conventional fuels (nuclear and fossil fuels) withdraw significant quantities of water (this is seawater in the case of nuclear) over the life-cycle of energy production, especially for thermoelectric power plants operated with a wet-cooling system. The quality of water is also adversely affected in some stages of energy production from these fuels. Hydro is by nature the most water-intensive source of energy (among all the energy sources covered in this work). However, it is limited in terms of its water consumption. Similarly, biomass is water intensive, but this water would have been used in the production of crops regardless. Thus, these two renewable energy sources have a perceived high impact on water resources. It should be noted, however, that in South Africa biofuel generation is by means of waste-from-crops only. Solar photovoltaic (PV) and wind energy exhibit the lowest demand for water, and could perhaps be considered the most viable *renewable* options in terms of water withdrawal and consumption. Moreover, the observed water usage in these renewable energy technologies is predominantly upstream.

It would be beneficial to consider relevant renewable energy case studies for water consumption and withdrawal in South Africa. This would allow for water consumption and withdrawal comparisons between fuels to be made. The two fuels that would perhaps be most worthwhile in terms of case studies, are wind and solar. The Darling Wind Farm (and proposed extensions), or one of the new wind farms proposed for the Eastern Cape or West Coast of South Africa, would be interesting to study. In terms of CSP the two plants being constructed *viz.* Kaxu Solar 1 and Khi Solar 1 would be beneficial to follow up on. The Aquilla CPV plant in Touws River would also be worthwhile considering

.

Acknowledgements

This paper is based on a report titled: *Renewable energy choices and water requirements in South Africa* (project number K5/2239/1), submitted to the Water Research Commission by the Energy Research Centre (2013). We gratefully acknowledge the funding provided by the Water Research Commission to support the relevant research.

References

Blok, K. (2006). *Introduction to energy analysis*, Amsterdam, the Netherlands: Techne Press.

Boulay, A.M. (2013). *Quantitative method comparison*, Available at: http://www.wulca-waterlca.org/pdf/Quantitative_method_comparisoAM Boulay_SETAC2013.pdf.

Carter, S. and Gulati, M. (2014). *Climate change, the good energy water nexus and food security in South Africa,* WWF Report.

Creamer, T., (2013). SA pushing ahead with carbon-capture plans despite global headwinds. *Mining Weekly*. Available at: http://www.miningweekly.com/article/sa-pushing-ahead-with-carbon-capture-plans-despite-global-headwinds-2013-10-03 [Accessed October 17, 2013].

De Fraiture, C., Giordano, M. & Liao, Y.(2008). Biofuels and implications for agricultural water use: Blue impacts of green energy. *Water Policy*, 10 (Supplement 1), pp.67–81.

DoE (Department of Energy) (2010). *Integrated resource plan for electricity 2010–2030*, Pretoria, South Africa: Accessible at http://www.doe-irp.co.za/content/IRP2010_promulgated.pdf.

DME (Department of Minerals and Energy) (2003). White Paper on Renewable Energy. Department of Minerals and Energy, Pretoria.

DME (Department of Minerals and Energy), 2007. DME, *Biofuels Industrial Strategy of the Republic of South Africa*. Department of Minerals and Energy, Pretoria.

Dominguez-Faus, R. , Powers, S.E., Burken, J.G., Alvarez, P.J. (2009). The water footprint of biofuels: A drink or drive issue? *Environment Science & Technology*, 43, pp.3005–3010.

DTI (2013). Water is critical for socio-economic development, says Deputy Minister Thabethe. Available at: http://www.info.gov.za/speech/DynamicAction?pageid=461&tid=105439 (Accessed October 25, 2013).

EIA (2013). Independent statistics and analysis: Country report, South Africa. Available at: http://www.eia.gov/countries (Accessed September 16, 2013).

Eskom (2011). *Annual report*, Available at: http://finan-

cialresults.co.za/2011/eskom_ar2011/.

Eskom (2013a). *Integrated report. http://overendstudio.co.za/online_reports/eskom_ar2013/pdf/full.pdf*,

Eskom (2013b). *Water Management. Available: http://www.eskom.co.za/c/article/240/water-management*,

Forder, S. (2013). Utililty scale projects. Available at: http://energy.org.za/knowledge-resources/renewable-energy-projects-south-africa/utility-search (Accessed October 17, 2013).

Fthenakis, V. & Kim, H.C. (2010). Life-cycle uses of water in US electricity generation. *Renewable Sustainable Energy Review*, 14, pp.2039–2048.

Gerbens-Leenes, W., Hoekstra, A.Y. & van der Meer, T.H. (2009). The water footprint of bioenergy. *Proceedings of the National Academy of Sciences of the United States of America*, 106(25), pp.10219–23. Available at: http://www.pubmedcentral.nih.gov/articlerender.fcgi?artid=2736406&tool=pmcentrez&rendertype=abstract.

Gleick, P.H.,(1994). Water and energy. *Annual Review of Energy and the environment*, 19, pp.267–299.

Goldemberg, J., Coelho, S.T. & Guardabassi, P. (2008). The sustainability of ethanol production from sugarcane. *Energy Policy*, 36(6), pp.2086–2097. Available at: http://linkinghub.elsevier.com/retrieve/pii/S0301421508001080 (Accessed October 17, 2013).

Gulati, M., Jacobs, I., Jooste, A., Naidoo, D. & Fakir, S. (2013). The water-energy-food security nexus: Challenges and opportunities for food security in South Africa. *Aquatic Procedia* 1(2013), 150-164.

Herath, I., Deurer, M., Horne, D., Singh, R., & Clothier, B. (2011). The water footprint of hydroelectricity: A methodological comparison from a case study in New Zealand. *Journal of Cleaner Production*.

Hoekstra, A.Y. , Chapagain, A.K., Aldaya, M.M. & Mekonnen, M.M. (2011). *The water footprint assessment manual*, London: Earthscan.

Hurst, C., (2010). China's rare earth elements industry: What can the West learn? Accessible at http://www.iags.org.

IEA-ETSAP & IRENA (2013). *Concentrating solar power: Technology brief E10*,

Jones, W.D. (2008). How much water does it take to make electricity? Natural gas requires the least water to produce energy, biofuels the most, according to a new study. Available at: http://spectrum.ieee.org/energy/environment/how-much-water-does-it-take-to-make- (Accessed August 27, 2013).

Kharak, Y.K., Thordsen, J.J., Conaway, C.H. & Thomas, R.B. (2013). The energy-water Nexus: Potential groundwater-quality degradation associated with production of shale gas. *Procedia Earth and Planetary Science*, 7, pp.417–422. Available at: http://linkinghub.elsevier.com/retrieve/pii/S1878522013002130 [Accessed October 18, 2013].

De Korte, G.J. (2010). Coal preparation research in South Africa. *The Journal of The Southern African Institute of Mining and Metallurgy*, 110(July), pp.361–364.

Lu, X., Norbeck, J.M., & Park C.S. (2012). Production of Fischer-Tropsch fuels and electricity from bituminous coal based on steam hydrogasification. *Energy* 48, pp.525-531.

Mantripragada, H.C. & Rubin, E.S. (2013). CO_2 implications of coal-to-liquids (CTL) plants. *International Journal of Greenhouse Gas Control*, 16, pp.50–60.

Martin, B. & Fischer, R. (2012). *The energy-water nexus: energy demands on water resources. EMG Water and Climate Change Research Series*, Cape Town.

Mekonnen, M.M. & Hoekstra, A.Y. (2012). The blue water footprint of electricity from hydropower. *Hydrology and Earth System Sciences*, 16(179-187), pp.Hydrol. Earth Syst. Sci., 16, pp.179–187, doi:10.5194.

Morrison, J. & Schulte, P. (2010). *Corporate Water Accounting. An analysis of tools and methods for assessing water use and its impacts*, Available at: http://ceowatermandate.org/files/corporate_water_accounting_analysis.

NREL (2002). *Fuel from the sky: Solar power's potential for Western Energy Supply, NREL/SR-550-32160*,

Odendaal, N. (2013). Water security critical to SA's economy. *Engineering News*. Available at: http://www.engineeringnews.co.za/article/water-security-critical-to-sas-economy- 2013-03-22 (Accessed October 25, 2013).

OECD. (2013). OECD Economic Surveys: South Africa 2013.

Pegram, G., Eaglin, F. & Laing, K. (2011). *Conceptual framework for assessing water use in energy generation, with a focus on hydropower. Final draft*, Cape Town.

Prasad, G., Stone, A., Hughes, A. & Stewart, T. (2012). *Towards the development of an energy-water-food security nexus based modelling framework as policy and planning tool for South Africa*. Paper presented "Towards Carnegie III", University of Cape Town.

REN21 (2013). *Renewables 2013: Global status report*, Paris. Available at: http://www.ren21.net/REN21Activities/GlobalStatusReport.aspx.

Rostrup-Nielsen, G.R. (2000). New aspects of syngas production and use. Catalysis Today 63, pp.159-164.

Sasol (2014). Technology. http://www.sasol.co.za/innovation/gas-liquids/technology,

accessed on 28 October 2014.

Sasol (2013). *Annual financial statements, Johannesburg.*

Sasol (2012). *Water disclosure report submission,*

Schulze, R.E. (Ed.) (2008). *South African atlas of climatology and agrohydrology*.

SEA (2009). *How to implement renewable energy and energy efficiency options: Support for South African local government*, Cape Town.

Seward, P. (2010). Challenges facing environmentally sustainable ground water use in South Africa. *Ground Water*, 48(2), pp.239–245.

Sinha, P. *et al.* (2013). Life Cycle Water Usage in CdTe Photovoltaics. *IEEE Journal of Photovoltaics*, 3(1), pp.429–432. Available at:

http://ieeexplore.ieee.org/lpdocs/epic03/wrapper.htm?arnumber=6313879.

Soitec (2013a). Soitec CPV power plants with Concentrix™ technology..

Soitec (2013b). Concentrix™ technology in action around the world. Available at: http://www.soitec.com/en/products-and-services/solar-cpv/our-references/ [Accessed October 25, 2013].

Sovacool, B.K. (2014.). Cornucopia orcurse? Reviewing the costs and benefits of shale gas hydraulic fracturing (fracking). *Renewable and Sustainable Energy Reviews 37*, pp.249-264.

Stone, K.C.C., Hunt, P.G., Cantrell, K.B. and Ro, K.S. (2010). The potential impacts of biomass feedstock production on water resource availability. *Bioresource Technology*, 101(101), pp.2014–2025. Available at: http://dx.doi.org/10.1016/j.biortech.2009.10.037.

Telsnig, T., Tomaschek, J., Özdemir, D.E., Bruchof, D., Fahl, U., Eltrop, L. (2013). Assessment of selected CCS technologies in electricity and synthetic fuel production for CO_2 mitigation in South Africa. *Energy Policy* 63, pp.168-180.

UN (1998). Economic aspects of sustainable debvelopment in South Africa. Available at: http://www.un.org/esa/agenda21/natlinfo/countr/safrica/eco.htm (Accessed October 25, 2013).

Wassung, N. (2010). Water Scarcity and Electricity Generation in South Africa Part 1: Water Use in the Coal-to-Electricity Process. Master of Philosophy Thesis, School of Public Management and Planning, University of Stellenbosch. University of Stellenbosch, Western Cape.

WBSCD (2013). The Global Water Tool (GWT). Available at: http://www.wbcsd.org/work-program/sector-projects/water/global-water-tool.aspx [Accessed October 17, 2013..

Williams, R. (2011). Solar cell makers, consider another (potentially) renewable resource: Water. Available at: http://www.renewableenergyworld.com/rea/news/article/2011/06/solar-cell-makers-consider-another-potentially-renewable-resource-water (Accessed October 17, 2013).

Wilson, B.W., Leipzig, T. & Griffiths-sattenspiel B. (2012). *Burning our rivers: The water footprint of electricity*, Portland, Oregan.

World Nuclear Association, Cooling power plants. Available at: http://world-nuclear.org/Search/?term=cooling power plants (Accessed October 15, 2013a)..

WWF-DEG (2011). Assessing Water Risk. Available at: http://awsassets.panda.org/downloads/deg_wwf_water_risk_final.pdf .

Received 3 April 2014; revised 28 October 2014

Energy consumption and economic growth nexus: Panel co-integration and causality tests for Sub-Saharan Africa

Basiru Oyeniran Fatai
Trade Policy Research and Training Programme, Department of Economics, University of Ibadan, Nigeria

Abstract
This study reassesses the causal relationships between energy consumption and economic growth in 18 Sub-Saharan Africa countries over the period 1980-2011. The Panel Unit Root Test results show that variables (both exogenous and endogenous) are stationary at their first difference with individual effects and individual linear trends, while the results of panel co-integration tests show that energy consumption and economic growth do have a stable long-run equilibrium relationship. There is unidirectional causality from energy consumption to economic growth in East and the Southern Africa Sub-region, which supports the growth hypothesis. As a result, the related authorities in the regions should take a special interest in different sources of energy and invest more in this sector, make suitable policies in this regard and find new alternative and cheap sources of energy. But, there is no causality between energy consumption and economic growth in Central and the West Africa Sub-region, which is in line with the neutrality hypothesis. In other words, both energy consumption and economic growth are neutral with respect to each other. Our results confirm the inconclusive nature of a causality relationship between energy consumption and economic growth.

Keywords: energy consumption, economic growth, panel co-integration, causal relationship

JEL classification c*odes: O13; Q43; C33*

1. Introduction

Energy plays an essential role in an economy on both demand and supply. On the demand side, energy is one of the products a consumer decides to buy to maximise his or her utility. On the supply side, energy is a key factor of production in addition to capital, labour and materials and is seen to play a vital role in the economic and social development of countries, being a key factor in increasing economic growth and living standards. This implies that there should be a causal relationship running from energy consumption to national income or GDP and vice versa (Chontanawat *et al.,* 2006).

Economic growth is among the most important factors to be considered in projecting changes in world energy consumption. In this regard, the analysis of the relationship between energy consumption and economic growth has received a great deal of attention during recent years. Indeed, whether the economic growth promotes energy consumption or energy itself is a stimulus for economic growth has motivated interest among economists and policymakers. Over the two last decades, there has been a large body of published research investigating the causal links between energy consumption and economic growth. This is because the direction of causality has significant policy implications. For instance, if energy consumption is a vital component in economic growth, energy conservation policies which reduce energy consumption may adversely affect real GDP. However, a unidirectional causality running from economic growth to energy consumption signifies a less energy dependent economy such that energy conservation policies may be implemented with little or no adverse effect on economic growth (Eggoh *et al*., 2011).

Although energy is not included in the standard growth models as an input of economic growth, the importance of energy in a modern economy is unquestionable. For instance, Hall and Klitgaard

(2012) emphasized the role that energy has played in economic growth and the limit to continued growth given our reliance on fossil fuels. Stern (2010) opined that when energy is scarce it imposes a strong constraint on the growth of the economy but when energy is abundant its effect on economic growth is much reduced. This explains the industrial revolution as a releasing of the constraints on economic growth due to the development of methods of using coal and the discovery of new fossil fuel resources. Also it was found that the elasticity of substitution between a capital-labour aggregate and energy is less than unity, which implies that when energy services are scarce they strongly constrain output growth resulting in a low income steady-state. When energy services are abundant the economy exhibits the behaviour of the 'modern growth regime' with the Solow model as a limiting case (Stern, and Kander, 2012).

The inconclusive nature of the relationship between energy consumption and economic growth led to four major views in the literature: The first view is *the growth hypothesis*, which suggests that energy consumption plays an important role in economic growth. It implies that economic growth is dependent on energy consumption just as a decrease in energy consumption may restrain economic growth. The second is *the conservative hypothesis*, which argues for unidirectional causality from economic growth to energy consumption. It suggests that energy conservation policies may have little or no impact on economic growth. The conservative hypothesis is supported if an increase in real GDP causes an increase in energy consumption. The third view is *neutrality hypothesis*, which argues that there is no causality between energy consumption and economic growth. In other words, both energy consumption and economic growth are neutral with respect to each other. While the last view is *feedback hypothesis,* which suggests that there is a bi-directional causal relationship between energy consumption and economic growth reflecting the interdependence and possible complementarities associated with energy policies and economic growth.

The contributions of this paper are the following: First, we employ recent data and methodology, for instance, in order to determine the variables' order of integration, the Levin, Lin and Chu Test, which assumes that there is homogeneity across the cross sections; likewise, the Im, Pesaran and Shin Test, ADF Fisher Chi Square Test and PP Fisher Chi Square tests which give room for heterogeneity across the cross-sections that were used. We also adopted a residual-based panel cointegration test (that is the Kao test), the Johansen-type panel cointegration test, and the error-correction–based panel cointegration tests developed by Westerlund (2007), which is general enough to allow for a large degree of heterogeneity, both in the long-run cointegrating relationship and in the short-run dynamics, and dependence within as well as across the cross-sectional units. Second, we consider specific analyses for prominent sub-regions in SSA namely, Central Africa, East Africa, Southern Africa and West Africa; to the best of our knowledge no study has broken SSA into these sub-regions.

The next section deals with the literature review, followed by the methodology employed in this study. Empirical results are presented in section four, while section five presents the Conclusion and Policy Implications.

2. Literature review

The relationship between energy consumption and economic growth has been examined thoroughly since the pioneer work of Kraft and Kraft (1978). However, the direction of causality between energy consumption and economic growth remained controversial.

Oh and Lee (2004) examined the causal relationship between energy and GDP in Korea over the period 1970–1999. The authors also included variables measuring capital and labour in their causality tests. There was a unidirectional causality from energy consumption to GDP in the short-run and bi-directional causality in the long-run. Odhiambo (2009) also found that there is a unidirectional causal relationship running from energy consumption to economic growth for Tanzania. But Cheng and Lai (1997) established a unidirectional causality from energy consumption to employment and also unidirectional causality from economic growth to energy consumption for Taiwan.

However, Jumbe (2004) found bi-directional causality between electricity consumption and economic growth but a unidirectional causality running from non-agricultural GDP to electricity consumption in Malawi; Lee and Chang (2005) established that, in the long-run energy acts as an engine of economic growth, and that energy conservation may harm economic growth in Taiwan; also a study by Belloumi (2009) assessed the causal relationship between per capita energy consumption and per capita gross domestic product for Tunisia. The results show a long-run bi-directional causal relationship between the two series and a short-run unidirectional causality from energy to gross domestic product; while, Ouedraogo (2010) found that there is evidence of a positive feedback causal relationship between electricity use and real GDP for Burkina Faso.

Wolde-Rufael (2006) found a unidirectional causality from economic growth to electricity consumption in 5 African countries, whereas bi-directional causality was found for 2 countries and no evidence for causal relationship in 7 African countries. While Akinlo (2008) employed the bounds

cointegration test to examine the long-run relationship between energy consumption and economic growth in 11 SSA countries: Cameroon, Cote d'Ivoire, Congo, Gambia, Ghana, Kenya, Nigeria, Senegal, Sudan, Togo, and Zimbabwe. The author employed a multivariate framework which included energy consumption, GDP, government expenditure, and the consumer price index. The co-integration tests supported cointegration in 7 countries (Cameroon, Cote d' Ivoire, Gambia, Ghana, Senegal, Sudan and Zimbabwe. The Granger causality tests showed that economic growth causes energy in 2 countries (Sudan and Zimbabwe). Bi-directional causality was found for 3 countries (Gambia, Ghana and Senegal). For 5 countries (Cameroon, Cote d' Ivoire, Nigeria, Kenya and Togo) no causality was found.

In similar vein, Odhiambo (2010) reassessed the causal relationship between energy consumption and economic growth in three SSA countries. He added the prices as an additional variable because of its effects on both energy consumption and economic growth. He discovered that the causality between energy consumption and economic growth varies significantly across the three countries. The results indicated that for South Africa and Kenya there is a unidirectional causal relationship from energy consumption to economic growth, while for Congo (DRC) it is economic growth that drives energy consumption.

Wolde-Rufael (2005) investigated the causal relationship between energy and GDP using data for 19 African countries over the period 1971–2001. The author used the bounds test for co-integration and then employed the Toda and Yamamoto causality test. The bounds co-integration test showed the existence of a stable long-run relationship between energy and growth in 8 countries, while there was no cointegration in 11 countries. The results of causality tests showed that causality runs from economic growth to energy consumption in 5 countries (Algeria, Democratic Republic of Congo, Egypt, Ghana, and Cote d'Ivoire) while energy causes economic growth in 3 countries (Cameroon, Morocco and Nigeria). There was bi-directional causality in 2 countries (Gabon and Zambia) while no causality was found in 9 countries (Benin, Congo Republic, Kenya, Senegal, South Africa, Sudan, Togo, Tunisia and Zimbabwe).

Esso (2010) examined the long-run and the causality relationship between energy consumption and economic growth for seven SSA countries during the period 1970-2007. Using Gregory and Hansen (1996, 1997) testing approach to threshold cointegration, he found that energy consumption is cointegrated with economic growth in Cameroon, Ivory Coast, Ghana, Nigeria and South Africa. Furthermore, causality tests suggest bi-directional causality between energy consumption and real GDP in Ivory Coast and unidirectional causality running from real GDP to energy use in Congo and Ghana.

Masih and Masih (1996) examined the causal relationship between energy consumption and GDP in Asian countries, using data over the period 1955–1990 for India, Pakistan, Malaysia, Singapore, Indonesia, and the Philippines. The co-integration tests showed that energy consumption and GNP are co-integrated in India, Pakistan and Indonesia. There was no evidence of co-integration in Malaysia, Singapore and the Philippines. The results of causality tests showed that there is no causality between energy consumption and GDP in Malaysia, Singapore and the Philippines. The results showed unidirectional causality from GDP to energy consumption in Indonesia, unidirectional causality from energy consumption to GDP in India, and bi-directional causality in Pakistan. The authors attributed the divergent results to the fact the countries are implementing different energy-growth policies. But Apergis and Payne (2010) used panel causality and cointegration tests of nine South American countries over 1980-2005.They found both short-run and long-run causality from energy consumption to economic growth.

Chontanawat *et al.* (2006) examined causality between energy consumption and GDP using data for 108 countries. The sample consisted of 78 non-OECD and 30 OECD countries. For the non-OECD countries, the authors employed data over the period 1971 – 2000 while for the OECD countries, data was used over the period 1960 – 2000. Taking all countries together, the results of causality tests showed that there is unidirectional causality from GDP to energy consumption in 20 countries while unidirectional causality runs the other way in 23 countries. There was bi-directional causality in 34 countries while there was no causality in 31 countries. A breakdown of the results showed that there was a higher prevalence of causality in OECD than non-OECD countries. The authors' explanation for this finding was that less developed countries are predominantly agrarian based and thus less energy dependent.

The review of Literature shows the direction of causality between energy consumption and economic growth remained controversial, therefore making this paper a worthwhile exercise, especially with the use of recent data and methodology.

3. Methodology

3.1 Estimation procedure

The analyses in this paper are carried out in three phases. First, we conduct Panel unit root tests using prominent tests namely Levin, Lin and Chu Test, Im, Pesaran and Shin Test, ADF Fisher Chi Square Test and PP Fisher Chi Square Test. Second, we perform Panel cointegration tests using the

Residual-Based DF and ADF Tests (Kao Tests), Johansen Fisher Panel Cointegration Test and the error-correction–based panel cointegration tests developed by Westerlund (2007). Third, we estimate Toda and Yamamoto Causality Analysis. We used many statistical tests so as to account for important similarities and differences of the sampled countries.

3.2 Data

Annual data over the period 1980 to 2011 for 18 SSA countries has been used in this study. As earlier mentioned, these countries are further divided into sub-regions for region-specific analyses.[1] All data is from the World Development Indicators (WDI) Database. Energy consumption is energy use in kilotons of oil equivalent and real GDP is gross domestic product converted to international dollars using purchasing power parity rates. All variables are in natural logarithms.

3.3 The model

A number of panel data unit root tests have been proposed such as: Maddala and Wu (1999), Choi (2001), Levin, Lin and Chu (2002), and Im, Pesaran and Shin (2003). These tests are generally based on the AR(1) process:

$$\gamma_{it} = \mu_i + \tau_{it} + \rho_i \gamma_{it-1} + \varepsilon_{it} \quad (1)$$

Where t = 1,…, T is the number of periods and i =1, …, N is the number of countries. τ_i is an individual trend, μ_i is the country specific fixed effect, ρ_i is an autoregressive coefficient, and ε_{it} is the error term. There is a unit root in γ_{it} if $/\rho_i/ = 1$. Panel unit root tests are broadly classified into two based on their assumptions concerning whether ρ_i is constant or varying.

In this study, the long-run relationship between energy consumption, and Real GDP will be estimated by the following equation:

$$\log EC_{i,t} = {}_i + \beta_i \log RGDP_{i,t} + \varepsilon_{i,t} \quad (2)$$

Where *i, t,* α_i and $\varepsilon_{i,t}$ denote the country, the time, the fixed country effect and the white noise stochastic disturbance term respectively. β_i is the energy consumption elasticity of Real GDP (the variables are in natural logs, denoted Log).

We also use the panel cointegration tests proposed by Westerlund (2007) to examine the relationship between real GDP, energy consumption and auxiliary variables in SSA countries. The Westerlund (2007) tests avoid the problem of common factor restriction and are designed to test the null hypothesis of no cointegration by inferring whether the error-correction term in a conditional error-correction model is equal to zero. Therefore, a rejection of the null hypothesis of no error-correction can be viewed as a rejection of the null hypothesis of no cointegration. The error-correction tests assume the following data-generating process:

$$\Delta Y_{it} = \delta_i' d_t + \alpha_i (Y_{it-1} - \beta_i' X_{it-1}) + \sum_{j=1}^{p_i} \alpha_{ij} \Delta Y_{it-j} + \sum_{j=0}^{p_i} \gamma_{ij} \Delta X_{it-j} + \varepsilon_{it} \quad (3)$$

Where d_t contains the deterministic components, Y_{it} denotes the natural logarithms of the real GDP and X_{it} denotes a set of exogenous variables, including energy consumption. Equation (3) can be rewritten as:

$$\Delta Y_{it} = \delta_i' d_t + \alpha_i Y_{it-1} + \lambda_i' X_{it-1} + \sum_{j=1}^{p_i} \alpha_{ij} \Delta Y_{it-j} + \sum_{j=0}^{p_i} \gamma_{ij} \Delta X_{it-j} + \varepsilon_{it} \quad (4)$$

Where $\lambda_i = -\alpha_i \beta_i'$. The parameter α_i determines the speed at which the system $Y_{it-1} - \beta_i' X_{it-1}$ corrects back to the equilibrium after a sudden shock. If $\alpha_i < 0$, then the model is error correcting, implying that Y_{it} and X_{it} are cointegrated. If $\alpha_i = 0$, then there is no error correction and, thus no cointegration. The null hypothesis for all countries of the panel is:

$H_0 : \alpha_i = 0$ for all i =1,..., N
versus $H_1 : \alpha_i \neq 0$ $H_1 : \alpha_i \neq 0$ for i =1,..., N
and $\alpha_i = 0$ for $i = N_1 + 1, \ldots, N$.

The alternative hypothesis allows α_i differing across the cross-sectional units.

Westerlund (2007) proposed four different statistics to test panel cointegration, based on least squares estimates of α_i and its t-ratio. While two of the four tests are panel tests with the alternative hypothesis that the whole panel is cointegrated ($H_1 : \alpha_i = \alpha_i = \alpha < 0$ for all i), the other two tests are group-mean tests which test against the alternative hypothesis that for at least one cross-section unit there is evidence of cointegration ($H_1 : \alpha_i < 0$ for at least one i). The panel statistics denoted P_τ and P_α test the null hypothesis of no cointegration against the simultaneous alternative that the panel is cointegrated, whereas the group mean statistics G_τ and G_α test the null hypothesis of no cointegration against the alternative that at least one element in the panel is cointegrated. The test proposed by Westerlund (2007) does not only allow for various forms of heterogeneity, but also provides p-values which are robust against cross-sectional dependencies via bootstrapping.

Following Toda and Yamamoto (1995), we estimate VAR(p) systems that are asymptotically χ^2 distributed to employ Wald tests for k linear restrictions. The lag length p is the sum of k, the lag length indicated by Schwarz' information criteria (SBC) and dmax, i.e., the maximum order of integration, so p = k+d max. We include

Table 1: Panel unit root test (at level)

SSA zones		*At level*			
		LLC	*IPS*	*ADF*	*PP*
Central Africa	Log(EC)	4.22 *(1.00)*	3.15 *(1.00)*	0.56 *(1.00)*	0.26 *(1.00)*
	Log(RGDP)	2.06* *(0.00)*	0.66 *(0.25)*	24.58 *(0.54)*	39.50 *(0.04)*
astern Africa	Log(EC)	1.46 *(0.07)*	0.98 *(0.84)*	2.34 *(0.89)*	1.74 *(0.94)*
	Log(RGDP)	3.68 *(0.99)*	4.17 *(1.00)*	1.26 *(0.99)*	1.12 *(1.00)*
Southern Africa	Log(EC)	1.91 *(0.97)*	2.17 *(0.98)*	5.51 *(0.70)*	2.02 *(0.98)*
	Log(RGDP)	0.79 *(0.21)*	1.29 *(0.10)*	16.18* *(0.04)*	7.80 *(0.45)*
Western Africa	Log(EC)	0.05 *(0.52)*	2.85 *(0.99)*	2.15 *(1.00)*	2.34 *(1.00)*
	Log(RGDP)	9.25 *(1.00)*	4.68 *(1.00)*	0.01 *(1.00)*	1.45 *(1.00)*

Note: LCC, IPS, ADF and PP implies Levin, Lin and Chu Test; Im, Pesaran and Shin Test; ADF Fisher Chi Square and PP Fisher Chi Square Tests respectively. The number in parenthesis represents the probability value, while *, **, and *** represent 1%, 5% and 10% level of significance respectively.

Table 2: Panel unit root test (at first difference)

Countries		*At first difference*				*Order of integration*
		LLC	*IPS*	*ADF*	*PP*	
Central Africa	Log(EC)	5.29* *(0.00)*	3.78* *(0.00)*	44.05* *(0.00)*	46.09* *(0.00)*	I (1)
	Log(RGDP)	4.67* *(0.00)*	3.70* *(0.00)*	37.96* *(0.00)*	59.68* *(0.00)*	I (1)
East Africa	Log(EC)	2.65* *(0.00)*	1.73* *(0.04)*	13.47* *(0.03)*	18.96* *(0.00)*	I (1)
	Log(RGDP)	4.11* *(0.00)*	3.88* *(0.00)*	26.46* *(0.00)*	37.79* *(0.00)*	I (1)
Southern Africa	Log(EC)	2.66* *(0.00)*	7.28* *(0.00)*	13.54** *(0.09)*	32.52* *(0.00)*	I (1)
	Log(RGDP)	3.00* *(0.00)*	4.29* *(0.00)*	33.36* *(0.00)*	73.72* *(0.00)*	I (1)
West Africa	Log(EC)	5.89* *(0.00)*	5.34* *(0.00)*	52.20* *(0.00)*	94.29* *(0.00)*	I (1)
	Log(RGDP)	4.91 *(0.00)*	8.48* *(0.00)*	86.15* *(0.00)*	87.32* *(0.00)*	I (1)

Note: LCC, IPS, ADF and PP implies Levin, Lin and Chu Test; Im, Pesaran and Shin Test; ADF Fisher Chi Square and PP Fisher Chi Square Tests respectively. The number in parenthesis represents the probability value, while *, **, and *** represent 1%, 5% and 10% level of significance respectively.

individual, state-specific effects (μ_i) and common time effects (v_t), our VAR(p)s have the following form:

$$X = C_0 + \sum_{j=1}^{k+d} X_{t-j} + \sum_{j=1}^{k+d} Y_{t-j} + \mu_i + v_t + \varepsilon_{xt} \quad (5)$$

$$Y = C_0 + \sum_{j=1}^{k+d} Y_{t-j} + \sum_{j=1}^{k+d} X + \mu_i + v_t + \varepsilon_{yt} \quad (6)$$

Where X represents logEC, and Y represents log RGDP; ε_{xt} and ε_{yt}denote the residuals.

4. Empirical results

4.1 Panel unit root test

Tables 1 and 2 present the results of the unit root tests conducted for all the variables both at their levels and first differences respectively. The tests are conducted for all the selected SSA countries subregions (namely, Central Africa, East Africa, Southern Africa, and West Africa). Descriptive statistics like the line plot reveal that the variables used have individual effects and individual linear trends. Hence, the unit root tests carried out take cognizance of these characteristics of the data used. The results show that all the variables (both exogenous and endogenous) are stationary at their first difference with individual effects and individual linear trend. Having established the order of integration of the variables, we further conduct the panel cointegration test.

4.2 Panel cointegration test

Having established that all my variables are integrated at the same order, we adopt a residual-based panel cointegration test (that is the Kao test), the Johansen-type panel cointegration test, and the error-correction–based panel cointegration tests developed by Westerlund (2007) to examine if there is a long run relationship among the variables used. As presented in Table 3a and 3b, the null hypothesis of no cointegrating relationship among the variables can be rejected and we accept that there is at least one cointegrating vector for the subregions at 5 percent level of statistical significance.

In order to check the robustness of the previous results, we considered four additional cointegration tests proposed by Westerlund (2007) that allow for cross-sectional dependence. Table 3b summarizes the outcome of Westerlund's cointegration tests.

Table 3a: Panel cointegration test

Kao Residual Cointegration Test				
	Test statistics	*P value*		
Central Africa	2.542*	0.01		
East Africa	3.323*	0.00		
Southern Africa	1.736*	0.04		
West Africa	3.253*	0.00		
Johansen Fisher Cointegration Test				
			Maximum Eigenvalue	
	Trace test	*P value*	*Test*	*P value*
Central Africa	21.73	0.017	19.05	0.04
East Africa	16.55	0.011	13.9	0.03
Southern Africa	24.43	0.002	21.47	0.09
West Africa	47.5	0.000	18.79	0.01

Table 3b: Panel cointegration test

Westerlund (2007) Cointegration Test				
	Test statistics	*Value*	*Z-value*	*P-value*
	Gt	-3.946	-8.399	0.00
Central Africa	Ga	-29.075	-10.956	0.00
	Pt	-10.948	-2.311	0.01
	Pa	-23.005	-9.98	0.00
East Africa	Gt	-3.987	-8.616	0.00
	Ga	-27.066	-9.675	0.00
	Pt	-11.051	-2.431	0.01
	Pa	-23.957	-10.656	0.00
Southern Africa	Gt	-4.067	-9.036	0.00
	Ga	-28.267	-10.441	0.00
	Pt	-11.884	-3.401	0.00
	Pa	-5.449	2.489	0.994
West Africa	Gt	-3.785	-7.547	0.00
	Ga	-36.864	-15.924	0.00
	Pt	-11.142	-2.537	0.01
	Pa	-24.219	-10.842	0.00

Table 4: Toda and Yamamoto causality analysis

Direction of causality analysis			
		Wald test statistics (prob. value)	
	Variables	*Log(EC)*	*Log(RGDP)*
Central Africa	Log(EC)	–	1.1658(0.56)
	Log(RGDP)	0.8943(0.64)	–
East Africa	Log(EC)	–	1.9787(0.37)
	Log(RGDP)	5.1950(0.07)	–
Southern Africa	Log(EC)	–	0.0976(0.95)
	Log(RGDP)	4.8123(0.09)	–
West Africa	Log(EC)	–	1.9000(0.397)
	Log(RGDP)	0.4104(0.81)	–

The null hypothesis of no cointegration is rejected at the 1% significance level. The results with the bootstrapped p-values (that take cross-country dependence into account) provide stronger evidence of cointegration relationship between energy consumption, and Economic Growth.

4.3 Toda and Yamamoto causality analysis

The existence of long run relationship between the variables leads us to examine the direction of causality between Energy consumption and Real GDP using the Toda and Yamamoto (1995) test with maximum lag order 2 reported in Table 4. The results from the significance of the p-values of the Wald (WALD) statistics show causality from energy consumption to economic growth in the selected SSA countries, likewise, in East and Southern Africa Sub-region. But, there is no causality between energy consumption and Economic growth in Central and Western Africa Sub-region.

5. Discussion of results

Our findings that Energy Consumption in the East and Southern Africa Sub-region Granger, cause economic growth, and suggest that energy consumption plays an important role in economic growth. It implies that economic growth is dependent on energy consumption, and a decrease in energy consumption may restrain economic growth. This in some respects corroborates some earlier studies on energy consumption and Economic growth; see for example, Odhiambo (2009) for Tanzania; Adeniran (2009) for Nigeria; likewise, Odhiambo (2010) for South Africa, Kenya and Congo Democratic Republic; Apergis and Payne (2009), Khan and Qayyum (2007) for Pakistan, Bangladesh, India and Sri Lanka; and Soytas and Sari (2003) for France, Germany and Japan.

However, it was found that there is no causality between energy consumption and economic growth in the Central and Western Africa Sub-region. In other words, both energy consumption and economic growth are neutral with respect to each other in the two sub-regions. Other studies that are in line with this neutrality hypothesis are; Sarkar *et. al.,* (2010) for Bangladesh; Yu and Choi (1985) and Cheng (1995) for the United States as well as Menegaki (2010) for 27 European countries; and Acaravci and Ozturk (2010) for 15 Transition economies. Our results confirm the inconclusive nature of causality relationship between Energy consumption and Economic Growth.

6. Conclusion and policy implications

This paper reassessed the causality between energy consumption and Economic growth using data for 18 Sub-Saharan Africa countries for the period 1980 – 2011. We made use of panel unit root and co-integration tests to address order of integration and long run relationship respectively, likewise, Toda and Yamamoto causality analyses were conducted so as to give more efficient results, towards achieving the objectives of the paper.

We found a stable long-run relationship between energy consumption and Economic growth. The results of Toda and Yamamoto causality analyses supported growth hypothesis for the East and Southern Africa Sub-region, as we found causality from energy consumption to Economic growth. This indicates that energy is a force for economic growth in the long-run. We can say high Energy Consumption tends to come with high economic growth. In the light of this discussion, it is reflected that energy serves as an engine of economic growth and economic activity will be affected in the result of changes in Energy Consumption. This means that continuous energy use does produce a continuous increase in output. So the related authorities in the East and Southern Africa Sub-regions' economies should take a special interest in different sources of energy and invest more in this sector, and invite foreign investors to invest in this sector, and make suitable policies in this regard and find new alternate and cheap sources of energy. Enhancement in or establishment of Research and Development departments and increase their efficiency is also needed in time, so that it creates a multiplier effect on GDP and as a result prosperity will come into these economies.

On the other hand, it was found that there is no causality between energy consumption and economic growth in Central and Western Africa Sub-region. This is in line with the neutrality hypothesis. In other words, both energy consumption and economic growth are neutral with respect to each other. The conservation policies in favour of the energy sector have no effect on economic growth.

Note

1. SSA countries used in the analysis:

Central Africa	*E Africa*	*Sthn Africa*	*W Africa*
Cameroon	Ethiopia	Angola	Benin
Congo DR	Kenya	Botswana	Cote d'Ivoire
Congo, Rep	Tanzania	Mozambique	Ghana
Gabon		South Africa	Nigeria
Zambia			Senegal
			Togo

References

Acaravci, A. and Ozturk, I. (2010). Electricity consumption and real GDP causality nexus: Evidence from ARDL bounds testing approach for 11 MENA countries. *Applied Energy*, 88, 2885-2892.

Adeniran, O. (2009). Does Energy Consumption Cause Economic Growth? An Empirical Evidence from Nigeria. @http://www.yasni.com/ext.php and Statistics 69(6), 709-748.

Akinlo, A.E. (2008). Energy Consumption and Economic Growth: Evidence from 11 Sub-Sahara African Countries, *Energy Economics*, 30, pp. 2391-2400.

Apergis, N., and Payne, J.E. (2009). Energy consumption and economic growth in Central America: evidence from a panel cointegration and error correction model. *Energy Economics* 31, 211-216.

Apergis, N., and Payne, J.E. (2010). Energy consumption and economic growth in South America: evidence from a panel error correction model. *Energy Economics* 32, 1421-1426.

Belloumi, M. (2009). Energy consumption and GDP in Tunisia: cointegration and causality analysis. 37 (7), 2745-2753.Cheng, B. S. (1995). An Investigation of Cointegration and Causality between Energy Consumption and Economic Growth. *Journal of Energy and Development*, 21, Pp.73-84.

Charles A. S. H. and Klitgaard, K. A. (2012) 'Energy and the Wealth of Nations: Understanding the Biophysical Economy'. Springer Publisher, New York, NY.

Cheng, B. S. and Lai, T. W. (1997). An Investigation of Co-integration and Causality between Energy Consumption and Economic Activity in Taiwan, *Energy Economics*, 19, pp. 435-444.

Choi, I. (2001). Unit Root Tests for Panel Data, *Journal of International Money and Finance*, 20, pp. 249-272.

Chontanawat, J., Hunt, L. C. and Pierse, R. (2006). Causality between Energy Consumption and GDP: Evidence from 30 OECD and 78 Non-OECD Countries, Discussion Paper no. 113, Surrey Energy Economics Centre, Department of Economics, University of Surrey.

Esso, L.J., (2010). Threshold cointegration and causality relationship between energy use and growth in seven African countries. *Energy Economics* 32, 1383-1391.

Im, K. S., Pesaran, M. H. and Shin, Y. (2003). Testing Unit Roots in Heterogeneous Panels, *Journal of Econometrics,* 115, pp. 53-74.

Jude C. Eggoh, J. C., Bangaké, C., and Rault C. (2011) 'Energy Consumption and Economic Growth Revisited in African Countries' CESIFO Working Paper No. 3590.

Jumbe, C.B.L. (2004). Cointegration and causality between electricity consumption and GDP: empirical evidence from Malawi. *Energy Economics* 26, 61-68.

Khan, M.A., and Qayyum, A. (2007). Dynamic Modelling of Energy and Growth in South Asia, *The Pakistan Development Review*, Vol. 46(4), pp. 481–498.

Lee, C.C., and Chang, C.P. (2005). Structural breaks, energy consumption, and economic growth revisited: evidence from Taiwan. *Energy Economics*, 27, 415-427.

Levin, A., Lin, C. F. and Chu, C. S. J. (2002). Unit Root Tests in Panel Data: Asymptotic and Finite-Sample Properties, *Journal of Econometrics*, 108, pp. 1-24.

Maddala, G. S. and Wu, S. (1999). A Comparative Study of Unit Root Tests with Panel Data and a New Simple Test, *Oxford Bulletin of Economics and Statistics*, 61, pp. 621-652.

Masih, A. M. M. and Masih, R. (1996). Energy Consumption, Real Income and Temporal Causality: Results from a Multi-country Study Based on Co-integration and Error-correction Modelling Techniques, *Energy Economics,* 18, pp. 165-183.

Menegaki, A. (2010). Growth and renewable energy in Europe: A random effect model with evidence for neutrality hypothesis. *Energy Economics*. doi:10.1016/j.eneco.2010.10.004, pp.1-7.

Odhiambo, N.M. (2009). Energy consumption and economic growth nexus in Tanzania: An ARDL bounds testing approach. *Energy Policy*, 37, pp.617–622.

Odhiambo, N.M. (2010). Energy consumption, prices and economic growth in three SSA countries: A comparative study. *Energy Policy* 38(5), 2463-2469.

Oh, W., and Lee, K. (2004). Causal relationship between energy consumption and GDP revisited: the case of Korea 1970-1999. *Energy Economics* 26, 51-59.

Ouedraogo, I.M. (2010). Electricity consumption and economic growth in Burkina Faso: a cointegration analysis. *Energy Economics* 32(3), 524-531.

Sarkar, M., Rashid, A., and Alam, K. (2010). Nexus between electricity generation and economic growth in Bangladesh. *Asian Social Science*, Vol. 6 (12). pp. 16-22.

Soytas, U., and Sari, R. (2003). Energy Consumption and GDP: Causality Relationship in G-7 Countries and Emerging Markets, *Energy Economics,* 25, pp.33– 37.

Stern, D. I. (2010) 'The Role of Energy in Economic Growth' CCEP working paper 3.10, Crawford School, The Australian National University.

Stern, D. I. and Kander, A. (2012) 'The Role of Energy in the Industrial Revolution and Modern Economic Growth' *The Energy Journal*, Vol. 33, No. 3.

Toda, H.Y. and Yamamoto, T. (1995). Statistical inferences in vector autoregressions with possibly integrated processes. *Journal of Econometrics*, 66, pp.225-250.

Westerlund, J. (2007). Testing for error correction in panel data. *Oxford Bulletin of Economics* Volume 69, Issue 6, pages 709–748.

Wolde-Rufael, Y. (2005). Energy Demand and Economic Growth: The African Experience, *Journal of Policy Modelling,* 27, pp. 891-903.

Wolde-Rufael, Y. (2006). Electricity consumption and economic growth: a time series experience for 17 African countries. *Energy Policy* 34, 1106-1114.

Yu, E. S. H., and Choi, J. Y. (1985). The Causal Relationship between Energy and GNP: an International Comparison. *Journal of Energy and Development*, 10, pp.249-72.

Received 13 January 2014; revised 25 October 2014

Energy models: Methods and characteristics

Najmeh Neshat

Mohammad Reza Amin-Naseri

Farzaneh Danesh

Department of Industrial Engineering, Tarbiat Modares University, Tehran, Iran

Abstract

Given the importance of models in complicated problem solving, an inappropriate energy model can lead to inaccurate decisions and poor policy prescriptions. This paper aims at developing a decision support tool with which the selection of appropriate model characteristics can be facilitated for developing countries. Hence, it provides a comparative overview of different ways of energy models characterization and extracts the underlying relationships amongst them. Moreover, evolution of dynamic characteristics of energy models for developing countries is identified according to the previous studies on the developed and developing countries. To do this, it reviews the related literature and follows a systematic comparative approach to achieve its purposes. These findings are helpful in cases where model developers themselves are looking for appropriate characteristics in terms of certain purpose or situation.

Keywords: energy models; energy models characterization; developing countries

1. Introduction

Over the past three decades, energy planning and management (EPM) has played an essential role in long-term social, environmental, and economic policy making of countries. Energy systems as an integral part of socio-economic systems of societies have several cross-disciplinary interactions with economy, society, and environment. To name a few, (1) the energy-economy interactions consist of changes over time in price elasticity of demand and also impacts of macroeconomic activity on energy demand; (2) the energy-society interactions are the impacts of energy cost on labour productivity, capital formation, energy consumption and therefore, economic growth and enhancing welfare and equality in the long term; (3) the energy-environment interactions include the impacts of energy policy on environmental phenomena such as climate change, resources stocks, ecosystem and human health. Therefore, the major difficulty of the EPM not only lies in its multi scales aspects (temporal and geographical), but also in the necessity to take into account the economic, technical, environmental and social criteria. Modelling of complex problems can lead to better decisions by providing decision makers with more information about the possible consequences of their choices. Hence, energy models as valuable tools for dealing with complicated problems can help decision makers to overcome this difficulty. Energy models are useful mathematical tools based on the system approach and the best model should be determined based on the problem that decision makers endeavour to solve.

Recently, the total number of developed energy models has grown tremendously and they vary considerably in characteristics and features. Hence, the key question is that 'which model(s) and characteristics are most suited for a certain purpose and situation?' Also 'what are the underlying relationships amongst these characteristics?' Given the diversity of the possible characterization approaches, this study aims at developing a comparative picture of them which can provide insight not only in the differences and similarities between them but also in the underlying relationships amongst them. Moreover, the evolution of dynamic characteristics of energy models for developing countries is identified according to the previous studies on the developed and developing countries. To do this, it reviews the related literature and follows a systematic comparative approach to achieve its purposes.

In this paper, we will first give an introduction to the different energy model categorization approaches as section 2 and then indicate their relationships via a schematic diagram. Trends in dynamic char-

acteristics of energy model for developing countries are also extracted from the related literature in section 3.

2. Approaches of characterizing energy models

The energy models existing in the literature can be categorized via different ways; however, these categorizations are related to each other. In the following, we will discuss each of these ways in more details.

Model type

Descriptive or prognostic models depict or describe how things actually work or might work, and answer the question, 'What is this?' In comparison, normative models are prescriptive and suggest what should be done (how things ought to work) according to an assumption or standard. The first approach belongs to the concept of planning as reaction and the second approach involves goal attainment and assumes autonomous planning or planning as an action. Descriptive models comprise different methods of econometrics or simulation, while normative models lie within the scope of optimization.

Purpose

Energy models are usually designed to address specific questions and hence, are only suitable for the purpose they were developed. For our categorization, we will make a distinction between three purposes i.e., Prediction/Forecasting, Exploring, and Back-casting purpose as follows (Beek, 1999):

1. Prediction/forecasting

Basically, forecasting focuses on extrapolation of trends found in historical data. A prior condition for this method is that the critical underlying parameters remain constant. Therefore, this method can be applied for analysing relatively medium to long term impacts of actions. In fact, forecasting is about what things will look like in the future and the method used for forecasting depends on the situation. Prediction uses past observations to extrapolate future short-term observations. Long-term forecasting is usually made by econometrics methods and short-term prediction uses extrapolation methods (Armstrong, 2001).

2. Exploring:

Scenario analysis is utilized for exploring the future. In this method, a limited number of developed scenarios are compared with a Business As Usual (BAU) reference scenario. In developing scenarios, some assumptions like economic growth and technological progress, which are not relied on the parameters extracted from the past behaviour, are made.

3. Back casting:

This approach is used to determine the conditions of a desired future and to define steps to attain a desired vision of the future. This is an alternative to traditional forecast which relies on what is known today and the future is viewed as a continuum of past or present. Back-casting is a planning methodology under uncertain circumstances that is particularly helpful when problems are complex, and there is a need for major change and in cases in which it is risky to view the future just in the mirror of the past (Holmberg, 2000).

Modelling paradigm

The difference between top-down and bottom-up models is related to the technological and sectoral aggregation. A broader economy is investigated by use of top-down models in order to examine effects between different sectors and they do not consider details of energy production technologies. Smooth production functions are used to represent energy sectors in an integrated way. In such models, substitution is determined by elasticity. On the other hand, technologies are represented in detail in bottom-up models, but they miss to take into account economy-wide interactions such as price distortions (Bohringer, 1998).

Grubb *et al.* (1993) stated that the top-down approach addresses the 'descriptive' economic paradigm, while the bottom-up approach is associated with– but not exclusively restricted to– the 'normative' engineering paradigm. In the economic paradigm, technology is considered as a set of processes by which inputs such as capital, labour, and energy can be transferred into useful outputs and the 'best' or most optimal techniques are defined by efficient markets. However, in the engineering paradigm, the developed model is independent of observed market behaviour. In other words, the economic paradigm is based on market behaviour and aggregated data, while the engineering paradigm tends to ignore existing market constraints and uses disaggregated data. For example, in the top-down approach the key question is 'By how much does a given energy price movement change energy demand or energy-related carbon emission?' In contrast, in bottom-up the question is 'How can a given emission reduction task be accomplished at minimum costs?'(e.g., see Frei *et al.* 2003).

While the traditional top-down approach follows an aggregated view and believes in the influence of price and markets, the bottom-up models focus on the technical characteristics of the energy sector. Hybrid models try to bridge the gap between top-down and bottom-up by including elements of both approaches. They attempt to combine the benefits of both top-down and bottom-up modelling schemes using each modelling vision where appropriate and a modular structure to integrate the dis-

parate systems. The hybrid models undertake to consider economic effects on model outcomes through taking into consideration the market behaviour. Market behaviour is a result of interactions among the economy sector, supply side and demand side entities.

The underlying methodology

In the following part, an overview of commonly used methodologies in developing energy models will be presented.

1. Econometrics: Econometric methodology focuses on statistical methods to extrapolate past market behaviour into the future. They use aggregated data measured in the past to predict the short- or medium-term future in terms of labour, capital, or other inputs. They are frequently used to analyse energy-economy interactions. The experience of the expert using this method is a key element for achieving reliable results. Another shortcoming of this model is that it needs a large amount of data from the past and aggregated data is required to reduce the fluctuations over time. Furthermore, the stability of economic behaviour is a prerequisite for using this method.
2. Macro-economics: The macro-economic methodologies are methodologies that consider the entire economy of a society and the interaction between sectors. The economy-energy interaction is analysed by input-output tables. These tables describe transactions between different sectors of the economy that is viewed as a whole in this method. Therefore, energy is just a small sector between all sectors considered in the macroeconomic model and cannot concentrate on energy technologies, specifically in details. This approach is common in energy demand analysis when taken from a neo-Keynesian perspective (i.e., output is demand determined).
3. Economic equilibrium: In economic equilibrium methodology, the energy sector is considered as part of the overall economy and it focuses on interrelations between the energy sector and the rest of the economy sectors. Economic equilibrium models are sometimes also referred to as resource allocation models. Very long term growth paths are simulated by this method, but the underlying path towards the new equilibrium is not clear enough. The treatment of equilibrium in a single market is considered as partial equilibrium in which the price plays a key role in equilibrating demand and supply. General equilibrium indicates conditions allowing simultaneous equilibrium in all markets in the economy. In this extension a coherent theory of the price system and the coordination of economic activity have to be considered.
4. Optimization: An optimization problem consists in finding a good choice out of a set of alternatives by minimizing or maximizing one or some real functions. Input values are selected from an allowed set and must satisfy some constraints. Energy optimization models are used to optimize energy investment decisions endogenously and the outcome represents the best solution for input variables while meeting the given constraints. This method is a branch of applied mathematics and requires a relatively high level mathematical knowledge and that the included processes must be analytically defined. Optimization models often use Linear Programming (LP), Non-linear Programming (NLP), and Mixed Integer Linear Programming (MILP) techniques.
5. Simulation: According to the World Energy Conference (1999), simulation energy models are descriptive models based on a logical representation of an energy system, and they are used to present a simplified operation of this system. Simulation models are usually used as an alternative, when it is impossible, hard or really costly to do experiments with the real system (Rosseti *et al.,* 2009).
6. Back-casting: The back-casting methodology is used to construct visions of desired futures based on experts' ideas in the fields and subsequently by looking at which changes are required or needed to be carried out to accomplish such futures.
7. Multi-criteria: The multi-criteria methodology can be used for including various criteria such as economic efficiency and cost reduction. It can include quantitative as well as qualitative data in the analysis. This approach is not yet widely applied in energy models.
8. Hybrid: The hybrid methodology consists of two or more aforementioned methodology.

Resolution technique

At the level of concrete models, a further distinction can be made considering the resolution tools utilized in the models. Linear Programming (LP), is widely used for modelling energy supply (e.g., capacity expansion planning) because of its simplicity in solution.

Mixed Integer Linear Programming (MILP) models the problems in which some variables are discrete. This technique has been widely used in MES (Multi-Energy Systems) planning problems, where various energy carriers with different units in terms of size and type are considered.

When there are nonlinear relations in either constraints or objective functions, the problem is modelled as a Non-Linear Problem (NLP). Often, endogenizing the model variables such as technological learning leads to convert a linear model into a nonlinear one. The multi-criteria models are used when

there is more than one criterion, usually conflicting ones, as the objective functions to be optimized.

Dynamic Programming (DP) divides the problem into sub problems to be able to solve them more easily. In addition, in most recent studies fuzzy programming (FP) or stochastic and/or interval programming (SP) methods have been applied to deal with uncertainties. Energy demand, price market, and learning rate of technologies are common parameters assumed uncertain in the energy system modelling (Salas, 2013).

Techniques such as Artificial Neural Networks (ANN), Autoregressive, Adaptive Neural Fuzzy Inference Systems (ANFIS), and Markov chain techniques are extensively used for forecasting/prediction purposes (Ettoumi *et al.*, 2003).

Geographical coverage

Energy models may analyse different levels of geographical and spatial areas. This level will effectively influence the structure of the model. The world economy is investigated in global energy models as a whole at a large scale. These models are designed to replicate how the world energy markets function. They are practical tools that generate region by region projections for different scenarios. In the regional models international areas like Latin America, South-East Asia and Europe are taken into consideration. National models study all major sectors inside one country endogenously, while the world energy parameters are considered exogenously in the model. The local level is related to the models encompassing regions inside a country.

According to the available literature, the comprehensiveness of models relying on the global or national level often (not always) requires aggregated data and uses economic (top-down) approach. In this regard, the models focusing on regional or local level often (not always) disregard macro-economic effects on energy system applying an engineering (bottom-up) approach.

Sectoral coverage

The economy can be divided into certain sectors. Based on this division, models can be classified, into sub-sectoral, sectoral, and economy wide models. Sub-sectoral models provide only information in just one particular sector and do not take into account the macro-economic linkages of that sector with the rest of the economy. The other sectors of the economy are simplified in these models. Sub-sectoral models addressing specific short-term concerns e.g., dispatch scheduling of a set of power generating units in a utility, fall into the first category. On the other hand, sectoral models investigate more than one sector of the economy and the interaction between the studied sectors. Sub-sectoral or sectoral models having one year to few years of planning horizon can be classified as medium-term and long-term models with implications at national or global level.

The time horizon

The time frame defined in energy models are usually categorized as short term (day, month, till 5 years), medium term (from 5 to 15 years), and long term (beyond 15 years) (Grubb et al., 1993). The structure of the models differs in different time horizons. Technological changes, paradigm shifts, long-range scenario analysis and multi-stage modelling are an innate part of the long term energy models. While in daily or monthly analysis of one energy sector, these issues are of less importance.

Data type

Aggregated and disaggregated data are two extremes for required data of energy models. Top-down models use aggregated data for short term predicting purposes, while bottom-up models use disaggregated data for exploring purposes. Most of models usually need quantitative data. But in some circumstances that little quantitative data is available or the available quantitative data is unreliable, the models should be able to deal with qualitative data. Furthermore, it may happen that considering stochastic or fuzzy data, instead of deterministic data, will lead the model to better and more robust results.

Endogenization degree

A model with high endogenization degree is one that its parameters are incorporated within the model equation so as to minimize the number of exogenous parameters. The analytical approach is in a close relationship with the level of endogenization. A high level of endogenization is considered in top-down models while in bottom-up engineering energy models, many parameters are reflected exogenously. It is very common that population growth, economic growth or even energy demand is carried out exogenously in bottom-up energy models.

Addressed side

Energy models are usually designed to deal with demand side issues such as demand forecasting, or supply side (e.g., capacity expansion plans) or both of them so called energy system models. Forecasting energy demand can be performed in just one sector like electricity, natural gas, heat, or in all different types of energy as a whole. In these models, both forms of final or useful demand may be predicted and is usually regarded as a function of income, population, price, etc. In the supply side, the demand is usually put into the model exogenously so as to investigate conditions needed to reach equilibrium between demand and supply. Technological aspects are concerned in more detail

and financial aspects of each technology are used for evaluation of different scenarios.

Figure 1 relates the different ways of energy model characterization to each other while they vary along a spectrum. However, a few exceptions can be founded in the literature. This figure provides guidelines to facilitate efficient selection of the model characteristics based on the available models in the literature.

As it can be seen in Figure 1, almost all of the models addressing demand side are descriptive with a top-down modelling paradigm. The purpose of these models is often (not always) a prediction with aggregate data while underlying methodologies for data processing are econometrics or macro-economics. Given the widely applications of AR and ANN techniques in these models, the endogenization degree of these models are high. In contrast with these models, the models addressing supply side are often normative with a bottom-up modelling paradigm. The general purpose of these models is often (not always) exploring and they rely on disaggregated data rather than aggregated data. Long-term considered time horizon and hence, low a endogenization degree are the main characteristics of these models.

For instance; Dilavar and Hunt (2011) applied a structural time series analysis to forecast industrial electricity demand of Turkey in 2020, by focusing on the relationship between electricity consumption of industries, value added of industries, and the price of electricity. The annual data over the period 1960 to 2008 is used to develop the industrial electricity demand function. This descriptive demand side model uses aggregated data of annual industrial electricity consumption from the International Energy Agency, IEA, and industrial value added from the World Bank in the econometric estimation model. No technological details are considered in this national sectoral model. Also, a long term model for natural gas and electricity expansion planning developed by Unsihuay-Vila *et al.* (2010), named Gas Electricity Planning Model (GEP). They used a mixed integer linear programming model for this energy supply planning model. The objective of the model is to minimize investment and operational cost of new facilities by selecting the optimum ones for power generation. Different technologies, with their related costs and constraints are taken into account. Disaggregated data with specific details for different supply technologies is required to be able to deal with this bottom-up model. This is a normative model, since an optimization is performed for the optimum selection of NG and electricity expansion facilities in order to meet the future growth of energy demand.

3. Trends in energy models characteristics

A first step in developing an appropriate model is to make decision about its characteristics (which were previously introduced) according to the defined problem. Some of these characteristics are static, i.e. they do not change over time, such as 'Model type' or 'Purpose' and the rest are dynamic and will change over time such as 'Analytical approach'. Therefore, to select dynamic characteristics of a model, it is necessary to consider their evolutions in the future. Understanding the evolution of a dynamic characteristic help identifying the requirements set of characteristics and features of a model in order to be in accordance with its future needs. This section undertakes to extract the evolution of dynamic characteristics, i.e. analytical approach, problem formulation, problem environment, sus-

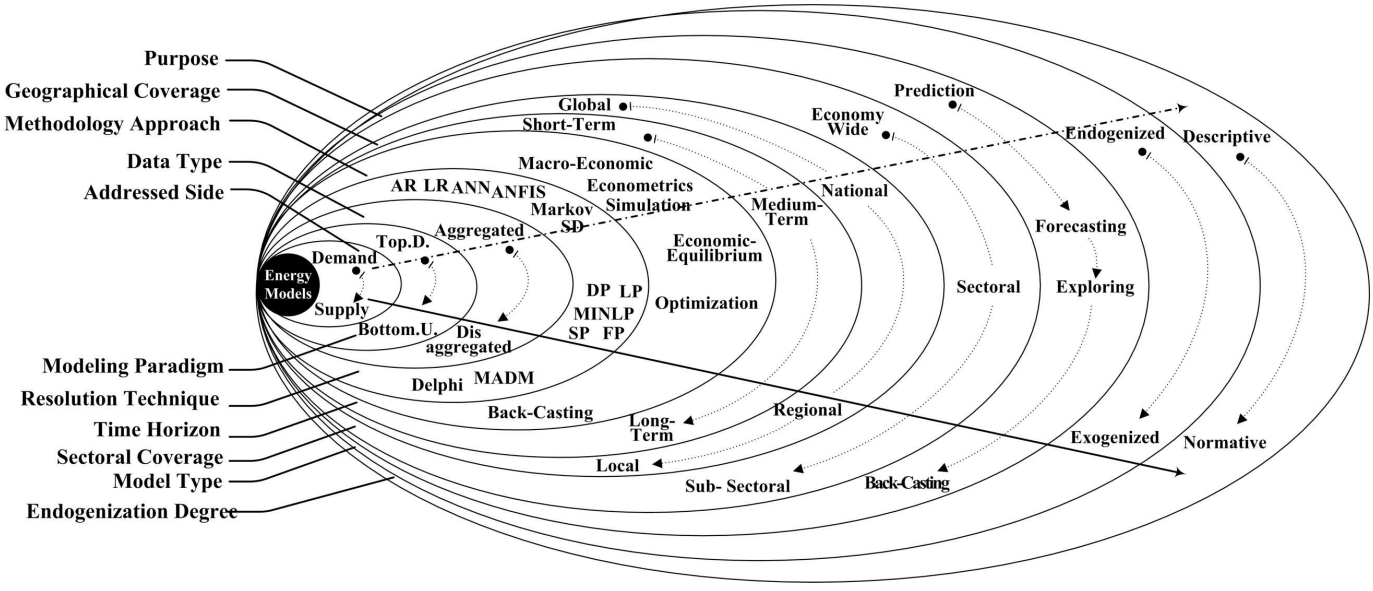

Figure 1: Schematic diagram of relations between different ways of energy model characterization

tainable criteria, and solution techniques for developing countries according to the previous studies on the developed and developing countries. To do this, it introduces different states for each key characteristic, and addresses them by mentioning the first related paper as well as an example (as a representative of other studies). It should be noted that this section aims at determining the evolution of dynamic characteristics of energy models for developing countries, rather than reviewing all relevant studies of the energy model literature.

Analytical approach

Top-down and bottom up approaches are two extreme modelling paradigms. Several authors linked bottom-up energy models to top-down ones in order to simulate the macro-level economy and micro-level technology details of the energy systems. The available integrated models can be generally categorized as: (1) the models which try to endogenize the market price using game theory and real option concepts in the bottom-up models (Botterud and Korpås, 2007; Pereira and Saraiva, 2011); (2) the models which employ System Dynamics or Computable General Equilibrium (CGE) techniques to incorporate price dynamics of demand and supply into the bottom-up models (Frei *et al.,* 2003; Andreas Schafer *et al.*, 2006; Wei *et al.*, 2006; Pereira and Saraiva, 2011); and (3) the integrated multi-agent based models that consider not only inter-temporal price dynamics of supply and demand but also demand side interactions in the model (Hodge *et al.*, 2008; Jiang Chang and Shu-Yun Jia, 2009; Logenthiran *et al.*, 2011; Ma and Nakamori, 2009).

Generally, there are two main solution approaches used in these studies. In the first approach, a combination of LP and an econometric demand equation is used to determine equilibrium price and quantities of fuels. This approach demonstrates perfect foresight and is proved to be non-realistic and unsuitable for the resulting year by year analysis. The second approach namely; a modular approach is developed in order to compute equilibrium price and quantities by iterative interactions between various modules

Problem formulation

Energy systems as an integral part of socio-economic systems of societies have several cross-disciplinary interactions with the economy, society, and environment. Moreover, a set of interdependencies between its parameters and variables exists that all cause an uncertain problem environment for energy systems. Endogenizing uncertain parameters is an effective way to reduce the uncertainty of the problem environment. A parameter is endogenized into the model through developing it internally within the model equation. To name a few, endogenizing: the future demand (Cerisola *et al.,* 2009; Choi and Thomas, 2012; 'EIA – The National Energy Modeling System: An Overview 2003-Overview of NEMS,' 2011; Hodge *et al.*, 2008; Ko *et al.*, 2010; Murphy and Smeers, 2005); the energy market price (Pereira and Saraiva, 2011), the technological change (Duncan, 2012; Hedenus *et al.,* 2005; Ma and Nakamori, 2009; Messner, 1997; Tödtling, 2012); the discounted rate (Neuhoff, 2008); and the marginal cost (Olsina *et al.*, 2006; Pereira and Saraiva, 2011) are addressed in this manner.

Problem environment

According to the literature, both certain and uncertain environments have been assumed for EPM problems. The uncertain information in energy systems is usually classified into three types (i.e., possibility distributions, probability distributions, or single/dual discrete intervals). In order to address these uncertainties, three corresponding inexact programming techniques i.e., fuzzy programming (e.g., Li and Cheng (2007)), stochastic programming (e.g., Lin and Huang (2009)) and single/dual interval-parameter programming (e.g., Zhu et al. (2012)) have been widely applied for energy systems modelling.

These approaches mostly focused on particular type of uncertainty or certain hybrid uncertainties within energy systems. However, in many real-world problems, multiple uncertainties may coexist in energy planning and management systems, of which the systems complexities may not be adequately reflected through the current approaches. Moreover, system dynamics associated with multi-stage decision makings are frequently confronting decision makers, which also need to be integrated and addressed in the same modelling framework. Thus, it brings about the requirement that can directly incorporate system uncertainties expressed as fuzzy membership functions, probability density functions, discrete intervals and dual intervals within a multi-stage modelling framework. Fuzzy dual-interval multi-stage stochastic (FDMS) approach is an efficient one that could not only tackle uncertainties with single/dual interval values and possibility distributions existed in energy, economy and environment systems, but also conduct in-depth analysis of long-term stochastic planning problems within multi-layer scenario trees (e.g., Li et al, 2014).

Sustainable criteria

The most common definition of sustainable development is a development which meets the needs of the present without compromising the ability of future generations to meet their own needs. This definition first appeared in the World Commission on Environment and Development's report, Our

Common Future (World Commission on Environment and Development, 1987).

Nowadays, the assessment criteria (economic, environmental, and social) of sustainable development are becoming important because of the rapid increase in awareness of the importance of sustainability. The energy system (supply, transport and usage) is of the highest importance in the context of sustainable development. According to the literature, the energy systems are required to meet several important goals, including conformance with the environmental goals (e.g., Akisawa et al., 1999; Bala and Khan, 2003; Dong et al., 2013; 'LEAP: Long range Energy Alternatives Planning system – Stockholm Environment Institute,' 2011; Reich-Weiser et al., 2008); economical goals (e.g., Grubb et al., 1993; Gustafsson, 1993; Heinzelman *et al.*, 2000; Kanniappan and Ramachandran, 1998; Liu, 2007; Sadeghi and Mirshojaeian Hosseini, 2006; Sirikum and Techanitisawad, 2005); social (e.g., Correljé and van der Linde, 2006; Pereira and Saraiva, 2011; Sirikum and Techanitisawad, 2005); or integrated goals (e.g., Bazmi and Zahedi, 2011; Cai, 2010; Ren et al., 2010b; Thery and Zarate, 2009; van Vliet et al., 2012) of sustainable development.

Underlying solution techniques

Exact solution algorithms which are suitable for linear (e.g., MILP, LP) and nonlinear (NLP) problems encourage shortages rather than inexact algorithms when problems are complex, non-smooth or non-convex. Despite its name, optimization does not necessarily mean finding the optimum solution to a complex problem with non-smooth function, since it may be unfeasible due to the characteristics of the problem, which in many cases are included in the category of NP-hard problems. Optimization problems with no polynomial time algorithm need exponential computation time in the worst case to obtain the optimum, which leads to computation times that are too high for practical purposes.

In recent years, due to issues such as hybridizing energy models, considering uncertainty in modelling, necessity of modelling with large geographical coverage and examining global changes such as global warming, the size and complexity of energy problems have increased and accurate algorithm have failed to solve this class of problem, given too huge convergence time and required computer memory. Consequently, in recent decades, many authors have proposed approximate methods, including heuristic approaches to solve NP-hard problems instead of using traditional solution methods, such as Mixed Integer programming (MIP) technique (Mirzaesmaeeli, 2007; Ren *et al.,* 2010a); Nonlinear Complementary programming (NCP) algorithms ('EIA – The National Energy Modeling System: An Overview 2003-Overview of NEMS,' 2011; Messner, 1997); quadratic programming (QP) techniques (Cai, 2010); and fuzzy-parameter linear programming techniques (Agrawal R.K. and Singh1 S.P., 2001; Li *et al.*, 2010; Sadeghi and Mirshojaeian Hosseini, 2006).

Heuristic methods as simple procedures provide satisfactory, but not necessarily optimal solutions to large instances of complex problems rapidly. Meta-heuristics are generalizations of heuristics in the sense that they can be applied to a wide set of problems, needing few modifications to be addressed to a specific case. Based on our knowledge, heuristic methods have not been yet used for energy system planning, however, several studies have been adopted (meta)heuristic algorithms to generation expansion planning problem (Chung *et al.,* 2004; Pereira and Saraiva, 2011; Safari *et al.,* 2013; Sirikum and Techanitisawad, 2005; Subramanian *et al.,* 2006).

The detailed survey is summarized in terms of developing and developed countries as Table 1.

3.1. Synthesis results of literature

According to Table 1, we grasped the literature analytically and made a digest of the related literature chronologically and addressed the key issues. The important findings extracted from Table 1 are listed here:

- The developing countries often experience the lagging research concerns of developed countries. For instance, in the 2000s, the focus was based on merging two analytical modelling paradigms in developed countries, while this is postponed to the next decade for developing countries. In fact, promoting some changes in energy strategies of developed countries can be a strategy for future energy of developing countries.
- In the late 2000s, the efforts have been directed to merge top-down and bottom-up modelling paradigms so as to consider economic, social, and environmental impacts simultaneously. The uncertainty and risks of such extensions are large and the validity of behavioural assumptions, technological specifications and resource allocations becomes complex in developing economies. This has led to incorporation of uncertainty analysis into the system analysis on one hand, and new model development initiatives on the other hand in these countries.
- Recently, the researchers have approached the endogenized models in order to capture the economic and technological effects and especially, to take care of structural changes and competition in the emerging markets and the uncertain patterns of business environment in developing countries.
- Given the used solution techniques, the energy planning problems experience a rapid growth in

Table1: Trends in energy models characteristics in terms of developing and developed countries

Key issues \ Timespan			1990-2000	2000-2005	2005-2013
Analytical approach	*Top-down*		■ e.g., Neubauer et al., 1997 ▲ e.g., Shresth, 1999	■ e.g., Sun, 2001 ▲ e.g., Volkan, 2003	▲ e.g., Shafiei et al., 2009 ■ e.g., Duran, 2007
	Hybrid			■ As pioneer, Messner and Schratten, 2000	▲As pioneer, Chen, 2005 ■ e.g., Andreas Schafer et al., 2006
	Bottom-up		▲ e.g., Luhanga et al., 1993	▲ e.g., Kumar, 2003 ■e.g.,Rosakis et al., 2001	▲ e.g., Ghaderi et al., 2006 ■ e.g., Liu, 2006
Problem formulation	*Exogenous* ↕ *Endogenous*		■ e.g., Halliwell & Sherif 1990; Pereira & Pinto, 1991 ■ e.g., Luhanga et al., 1993 ▲ As pioneer, Wu and Chen, 1990	▲ e.g., Frei et al., 2003 ■ e.g, Messner & Schrattenholzer, 2000; Rozakis et al., 2001	▲ e.g, Shafiei et al., 2009 ■ e.g, Andreas Schafer et al., 2006; Liu, 2006; Pereira & Saraiva, 2011
Problem environment	*Certain*		■ e.g, Ellis et al., 1995	–	–
	Uncertain	*Stochastic*	■ e.g, Scott et al., 1999 ■ e.g, Messner et al., 1996	▲ e.g, Jain &Lungu, 2002	▲ e.g, Xie et al., 2010 ■ e.g, Liu, 2009 No Def. Li and Cheng, 2007
		Fuzzy	–	▲As Pioneer, Agrawal R.K. & Singh1 S.P., 2001	▲ e.g, Sadeghi et al., 2008 ▲ e.g, Lin, 2008; ▲Kaya and Kahraman, 2011; ▲Jebari and lniyan, 2007; ▲ e.g, Xie et al. 2010; ▲ e.g, Saboohi et al., 2006
		Vague		–	■ e.g, Pereira & Saraiva, 2011
Sustainable criteria	*Economic*		■ e.g, Henning, 1997; ▲e.g, Kanniappan & Ramach, 1998		▲ e.g, Sadeghi and Mirshojaei & Hosseini, 2006
	Environmental		■ e.g, Akisawa et al., 1999; Ang & Zhang, 2000	■ e.g, Kumar A. et al., 2003	▲e.g, Liu, 2006; e.g, Mirzaesmaeeli, 2007; Cai, 2010 ▲ e.g, Lin, 2008 ▲ e.g, Ghaderi et al., 2006
	Social		-		
	Integrated		■ e.g, Akisawa et al., 1999	▲ e.g, Bala and Khan, 2003	–
Underlying solution techniques	*Traditional*		■ e.g, Ang, 1995; ■ e.g, Ramanathan & Ganesh, 1995 ■ e.g, Malik et al., 1994	▲ e.g, Beccali et al. 2003 ■ e.g, Sirikum & Techanitisawad, 2005	■ e.g, Andreas Schafer et al., 2006; Pereira & Saraiva, 2011 ▲ e.g, Ghaderi et al., 2006; Sadeghi & MirshojaeianHosseini, 2008 ■ e.g, Pham et al., 2011
	Heuristic				■ e.g, Subramanian et al., 2006; Pereira & Saraiva, 2011

Legend ■ Developed countries; ▲ Developing countries

magnitude and also computational difficulties associated with non-convex and non-smooth objective functions.
- In recent years, multi dimension integrated criteria has attracted much interest rather than single dimension criteria such as cost or profit.

Although there is a huge variation amongst developing countries in terms of socio-economic structure, a few features are found in common in the energy sector of many developing countries. These characteristics include: (1) reliance on traditional energies, (2) the existence of large informal sectors which are sometimes as large as the formal sector, (3) prevalence of inequity and poverty, (4) structural changes of the economy and accompanying transition from traditional to modern lifestyles, (5) inefficient energy sector characterized by supply shortages and poor performance of energy utilities, and (6) existence of multiple social and economic barriers to capital flow and slow technology diffusion make developing countries' energy systems significantly different from that of developed countries.

Top-down models use a price-driver which play a limited role in developing countries and cannot capture informal sector or traditional energies adequately. These models also have difficulties in capturing the technological diversity, besides, they require high skill levels. Bottom-up models have a good description of technological features of the energy sector with high-level skill needs. Moreover, the problems of subsidies and shortages are also not adequately captured as the demand in these models. Hence, hybrid models appear to be more appropriate for developing country contexts because of their flexibility and limited skill requirement.

It can be concluded that most of the standard (computer based) models are perhaps not suitable for developing countries applications considering their underlying assumptions. As most of the standard models are designed and developed in the developed world, they fail to capture the specific needs of the developing countries because they are incapable of reflecting the specific features of energy models of developing countries.

4. Conclusions

Up to now, many characterizations have been made for energy models, whereas the relationship among them is under question. In this study, we gave an introduction to the different ways of energy model categorization approaches (e.g., modelling paradigm, endogenization degree, model type, and addressed side) and the relationships behind these approaches were indicated schematically. The designed diagram as a decision support tool facilitates efficient selection of the model characteristics based on the examined models in the literature. But some characteristics are dynamic and will change over time such as analytical approach. Therefore, in order to select the dynamic properties for a model, it is necessary to consider their evolution in the future. The evolution of dynamic energy model characteristics for the developing countries were extracted from the related literature digests.

The findings of this paper confirms the fact that it is required to incorporate the specific features of developing countries in energy system modelling and to consider the informal sector and traditional energy use in the analysis of these systems.

This study suggests identifying the evolution of dynamic energy model characteristics for developing countries in terms of geographic coverage (global, national, regional, local) as future research.

References

Adams, F. G., and Shachmurove, Y. (2008). Modelling and forecasting energy consumption in China: Implications for Chinese energy demand and imports in 2020. *Energy economics*, 30, 3, 1263-1278.

Agrawal R.K., and Singh S.P. (2001). Energy allocations for cooking in UP households (India) – A fuzzy multi-objective analysis. *Energy Convers. Manag.* 42, 2139–2154.

Akisawa, A., Kang, Y.T., Shimazaki, Y., and Kashiwagi, T. (1999). Environmentally friendly energy system models using material circulation and energy cascade—the optimization work. *Energy* 24, 561–578.

Bala, B., and Khan, M. (2003). Computer Modeling of Energy and Enviroment: The Case of Bangladesh. Prime Publishing House, Utter Pradesh, India.

Bazmi, A.A., and Zahedi, G. (2011). Sustainable energy systems: Role of optimization modeling techniques in power generation and supply—A review. Renew. Sustain. *Energy Rev.*15, 3480–3500.

Beek, V.N. (1999). Classification of Energy Models (Working Paper No. FEW 777). Tilburg University.

Bhattacharyya, S.C. and Timilsina, G.R. (2010). Modelling energy demand for developing countries: are specific features adequately captured. Energy Policy, 38, 4, 1979-90.

Cai, Y. (2010). Integrated energy-environmental modeling and climate change adaptation planning under uncertainty. The University of Regina (Canada), Canada.

Cerisola, S., Baíllo, Á., Fernández-López, J.M., Ramos, A., and Gollmer, R. (2009). Stochastic Power Generation Unit Commitment in Electricity Markets: A Novel Formulation and a Comparison of Solution Methods. *Oper Res* 57, 32–46.

Choi, D.G., and Thomas, V.M. (2012). An electricity generation planning model incorporating demand response. *Energy Policy* 42, 429–441.

Chung, T.S., Li, Y.Z., and Wang, Z.Y. (2004). Optimal generation expansion planning via improved genetic algorithm approach. I*nt. J. Electr. Power Energy Syst.* 26, 655–659.

Correljé, A., and van der Linde, C. (2006). Energy supply security and geopolitics: A European perspective. *Energy Policy* 34, 532–543.

Dilaver, Z., and Hunt, L. C., (2011). Industrial electricity demand for Turkey: a structural time series analysis. *Energy Economics*, 33(3), 426-436.

Dong, C., Huang, G.H., Cai, Y.P., and Liu, Y. (2013). Robust planning of energy management systems with environmental and constraint-conservative considerations under multiple uncertainties. *Energy Convers. Manag.* 65, 471–486.

Duncan, R.C., (2012). Technological change in the arid zone of New South Wales. *Aust. J. Agric. Resour. Econ.* 16, 22–33.

EIA – The National Energy Modeling System: An Overview 2003-Overview of NEMS [WWW Document], 2011. URL http://www.eia.gov/oiaf/aeo/overview/overview.html (accessed 9.3.11).

Ettoumi, F.Y., Sauvageot, H., and Adane, A.E..H. (2003). Statistical bivariate modelling of wind using first-order Markov chain and Weibull distribution. *Renew. Energy* 28, 1787–1802.

Frei, C.W., Haldi, P.A., and Sarlos, G. (2003). Dynamic formulation of a top-down and bottom-up merging energy policy model. *Energy Policy* 31, 1017–1031.

Grubb, M., Edmonds, J., Brink, P.T., and Morrison, M. (1993). The Costs of Limiting Fossil-Fuel CO2 Emissions: A Survey and Analysis. *Annu. Rev. Energy Environ.* 18, 397–478.

Gustafsson, S.I. (1993). Mathematical modelling of district-heating and electricity loads. *Appl. Energy* 46, 149–159.

Hedenus, F., Azar, C., and Lindgren, K., (2005). Induced Technological Change in a Limited Foresight Optimization Model. Ssrn Elibrary.

Heinzelman, W.R., Chandrakasan, A., and Balakrishnan, H. (2000). Energy-efficient communication protocol for wireless microsensor networks. Presented at the System Sciences, 2000. Proceedings of the 33rd Annual Hawaii International Conference on, p. 10 pp. Vol. 2.

Hodge, B.M., Aydogan-Cremaschi, S., Blau, G., Pekny, J., and Reklaitis, G. (2008). A prototype agent-based modeling approach for energy system analysis, in: 18th European Symposium on Computer Aided Process Engineering. Elsevier, pp. 1071–1076.

Jebaraj, S., and Iniyan, S., (2007). An optimal energy allocation model using fuzzy linear programming for energy planning in India for the year 2020. I*nt. J. Energy Technol. Policy* 5, 509 – 531.

Jiang Chang, and Shu-Yun Jia, (2009). Modeling and application of wind-solar energy hybrid power generation system based on multi-agent technology 3, 1754–1758.

Kanagawa, M., and Nakata, T. (2007). Analysis of the energy access improvement and its socio-economic impacts in rural areas of developing countries. *Ecological Economics*, 62, 319-29.

Kanniappan, P., and Ramachandran, T. (1998). Optimization model for energy generation from agricultural residue. *Int. J. Energy Res.* 22, 1121–1132.

Kaya, T., and Kahraman, C. (2011). Multicriteria decision making in energy planning using a modified fuzzy TOPSIS methodology. *Expert Syst Appl* 38, 6577–6585.

Ko, F.-K., Huang, C.-B., Tseng, P.-Y., Lin, C.-H., Zheng, B.-Y., Chiu, H.-M., (2010). Long-term CO_2 emissions reduction target and scenarios of power sector in Taiwan. *Energy Policy* 38, 288–300.

LEAP: Long range Energy Alternatives Planning system – Stockholm Environment Institute [WWW Document], 2011. URL http://sei-international.org/leap-the-long-range-energy-alternatives-planning-system (accessed 9.3.11).

Li, S.-T., Cheng, Y.-C. (2007). Deterministic fuzzy time series model for forecasting enrollments. *Comput. Math.* Appl. 53, 1904–1920.

Li, Y.F., Li, Y.P., Huang, G.H., Chen, X. (2010). Energy and environmental systems planning under uncertainty-An inexact fuzzy-stochastic programming approach. *Appl. Energy* 87, 3189–3211.

Lin, Q.G., and Huang, G.H. (2010). Interval-fuzzy stochastic optimization for regional energy systems planning and greenhouse-gas emission management under uncertainty—a case study for the Province of Ontario, Canada. *Clim. Change* 104, 353–378.

Liu, P. (2007). Energy systems planning for the Province of Saskatchewan. The University of Regina (Canada), Canada.

Liu, Y., (2006). A dynamic two-stage energy systems planning model for Saskatchewan, The University of Regina, Canada.

Logenthiran, T., Srinivasan, D., and Khambadkone, A.M. (2011). Multi-agent system for energy resource scheduling of integrated microgrids in a distributed system. *Electr. Power Syst. Res*. 81, 138–148.

Ma, T., and Nakamori, Y. (2009). Modeling technological change in energy systems – From optimization to agent-based modeling. *Energy* 34, 873–879.

Messner, S. (1997). Endogenized technological learning in an energy systems model. *J. Evol. Econ.* 7, 291–313.

Mirzaesmaeeli, H., (2007). A multi-period optimization model for energy planning with carbon dioxide emission consideration. University of Waterloo, Canada.

Murphy, F.H., Smeers, Y., (2005). Generation Capacity Expansion in Imperfectly Competitive Restructured Electricity Markets. *Oper. Res*. 53, 646–661.

Neuhoff, K. (2008). Learning by Doing with Constrained Growth Rates:An Application to Energy Technology Policy. *Energy J.* Volume 29.

Olsina, F., Garcés, F., and Haubrich, H.J. (2006). Modeling long-term dynamics of electricity markets. *Energy Policy* 34, 1411–1433.

Pandey, R. (2002). Energy policy modelling: agenda for developing countries. *Energy Policy*, 30, 97-106.

Pereira, A.J.C., and Saraiva, J.T. (2011). Generation expansion planning (GEP) – A long-term approach using system dynamics and genetic algorithms (GAs). *Energy* 36, 5180–5199.

Reich-Weiser, C., Fletcher, T., Dornfeld, D.A., Horne, S. (2008). Development of the Supply Chain Optimization and Planning for the Environment (SCOPE) tool – applied to solar energy. Presented at

the Electronics and the Environment, 2008. ISEE 2008. IEEE International Symposium on, pp. 1–6.

Ren, H., Zhou, W., Gao, W., and Wu, Q. (2010a). A Mixed-Integer Linear Optimization Model for Local Energy System Planning Based on Simplex and Branch-and-Bound Algorithms. *Life Syst. Model. Intell. Comput*. 63, 361–371.

Ren, H., Zhou, W., Nakagami, K., Gao, W., and Wu, Q. (2010b). Multi-objective optimization for the operation of distributed energy systems considering economic and environmental aspects. *Appl. Energy* 87, 3642–3651.

Sadeghi, M., and Mirshojaeian Hosseini, H. (2006). Energy supply planning in Iran by using fuzzy linear programming approach (regarding uncertainties of investment costs). *Energy Policy* 34, 993–1003.

Safari, S., Ardehali, M.M., and Sirizi, M.J. (2013). Particle swarm optimization based fuzzy logic controller for autonomous green power energy system with hydrogen storage. *Energy Convers. Manag.* 65, 41–49.

Sirikum, J., Techanitisawad, A. (2005). Power generation expansion planning with emission control: a nonlinear model and a GA□based heuristic approach. I*nt. J. Energy Res*. 30, 81–99.

Salas, P. (2013). Literature Review of Energy-Economics Models, Regarding Technological Change and Uncertainty. 4CMR Working Paper Series 003, University of Cambridge, Department of Land Economy, Cambridge Centre for Climate Change Mitigation Research.

Schafer, A. and Jacoby, H. D. (2006). Experiments with a Hybrid CGE-MARKAL

Subramanian, K., Slochanal, S.M.R., Subramanian, B., and Padhy, N.P. (2006). Application and Comparison of Metaheuristic Techniques to Generation Expansion Planning Incorporating Both Bilateral and Multilateral Transactions. *Int. J. Emerg. Electr. Power Syst.* 6, 1–12.

Thery, R., and Zarate, P. (2009). Energy planning: A multi-level and multicriteria decision making structure proposal. *Cent. Eur. J. Oper. Res.* 17, 265–274.

Tödtling, F. (2012). Technological change at the regional level: the role of location, firm structure, and strategy. *Environ. Plan*. 24, 1565–1584.

Urban, F., Benders, R.M.J., and Moll, H.C. (2007). Modelling energy systems for developing countries. Energy Policy, 35, 6, 3473-□□82.□

Van Vliet, O., Krey, V., McCollum, D., Pachauri, S., Nagai, Y., Rao, S., and Riahi, K. (2012). Synergies in the Asian energy system: Climate change, energy security, energy access and air pollution. *Energy Econ*. 34, Supplement 3, S470–S480.

Wei, Y.-M., Wu, G., Fan, Y., Liu, L-C. (2006). Progress in energy complex system modelling and analysis. *Int. J. Glob. Energy Issues* 25, 109–128.

Zhu, Y., Huang, G.H., He, L., and Zhang, L.Z. (2012). An interval full-infinite programming approach for energy systems planning under multiple uncertainties. I*nt. J. Electr. Power Energy Syst.* 43, 375–383.

Received 13 October 2013; revised 27 September 2014

Hybrid electromechanical-electromagnetic simulation to SVC controller based on ADPSS platform

Lin Xu
Sichuan Electric Power Research Institute; Sichuan Electric Power Company; State Grid Cooperation of China, Chengdu, China

Yong-Hong Tang

Wei Pu

Yang Han
Department of Power Electronics, School of Mechanical, Electronic and Industrial Engineering, University of Electronic Science and Technology of China, Chengdu, China

Abstract
To test the dynamic performance and damping features of a static var compensator (SVC) controller accurately in large-scale interconnected AC/DC hybrid power systems, it is of vital significance to build the detailed electromagnetic transient model. However, it is unrealistic and time-consuming to build the detailed models of all the devices in the actual large-scale power grid. Utilizing the hybrid simulation function in the advanced digital power system simulator (ADPSS) and by dividing the large-scale power grid into the electromagnetic transient sub-grids and electromechanical sub-grids, the computation speed of real-time simulation is remarkably enhanced by the parallel computational capabilities of digital simulator. The SVC controller and the nearby substation are modelled in the electromagnetic transient sub-grid, and the residue subnetworks are modelled in the electromechanical sub-grid. This paper focuses on the mechanism of the hybrid electromechanical and electromagnetic simulation, the detailed modelling and the ADPSS-based digital closed-loop test methodologies of the SVC controller. Eventually, the validity and effectiveness of the modelling and control methods are confirmed by the experimental results.

Keywords: advanced digital power system simulator, Hhybrid eectromechanical-Eelectromagnetic simulation, static var compensator, Phillips-Heffron model.

1. Background

The electric power grid in China has entered an era of large area interconnected ultra-high voltage (UHV) AC and DC networks. The transmission capacity of UHV AC and DC transmission systems is more than 200GW. The network connects the Northwest, North China, Central China and East China Power Grid, and a large power base and load centre of UHV power grid is formed (Qian *et al.*, 2011).

Figure.1 shows the three major electric power transmission corridors which connect the energy bases of the western regions with the industry bases of the eastern regions. The upper transmission corridor utilizes the ultra-high voltage AC transmission (UHVAC) lines to transmit the electric power from Shanxi and Meng-Dong coal bases to the Yangtze Delta region in Shanghai. The middle corridor is characterized by the high voltage DC transmission (HVDC) lines to connect the Three Gorges Hydroplant with the south eastern provinces. The lower corridor adopts the ultra-high voltage DC transmission (UHVDC) lines to transmit the electric power generated by the Southwest hydro base to Guangdong, Hong Kong, and Macao (Long *et al.*, 2007).

On the other hand, the static var compensator (SVC) is a shunt device, of the Flexible AC Transmission Systems (FACTS) family, using power electronics to control power flow and improve transient stability on power grids (Rstamkolai *et al.*, 1990). The SVC regulates voltage at its terminals by controlling the amount of reactive power injected into or absorbed from the power system. When the

system voltage is low, the SVC generates reactive power (SVC capacitive). When system voltage is high, it absorbs reactive power (SVC inductive). These power electronic devices improve the stability of the paralleled-connected AC line, increase the transmission capacity and improve the reliability and flexibility of the interconnected system. However, the response time of the various electric components in the power system dynamics due to the voltage and frequency variations ranges from a few microseconds, milliseconds to a few minutes, or even hours (Dickmander *et al.*, 1992). Facing such a large range of time-domain dynamic process simulation, system analysis using small time constants would result in high computational complexity and inefficiency (Schauder et al., 1995).

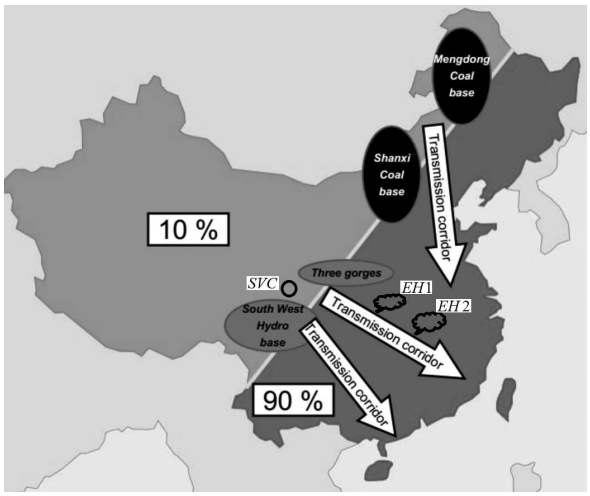

Figure 1: The power transmission corridors in China

At present, the power system simulation methods can be categorized into three types, namely, the electro- magnetic transient simulation, the electromechanical transient simulation, and medium-and long-term dynamic process simulation. Electromagnetic transient simulation adopts complex and precise mathematical models. The differential equation solving process is complicated, so the simulation scale is limited, and the simulation step-size is selected as 20~200us. The commonly used simulation programs are: EMTP, PSCAD-EMTDC, NETOMAC, PSIM, SABER, SPICE, PSPICE, etc. Electromechanical transient simulation is used for transient stability analysis under large disturbance and static stability analysis under small perturbation. The fundamental frequency phasor theory is applied for analysis and calculation, and the calculation step-size is about 10ms (Hingorani and Gyugyi, 2000). The popular programs for electromechanical simulation are: PSASP, BPA, PSS/E, SIMPOW, etc. The dynamic process of the medium-and long-term analysis focuses on the large-scale system disturbances, arising from the active and reactive power generation and consumption imbalance (Erickson and Maksimovic, 1997).

With the progress of the National Ultra High-Voltage grid construction as well as the formation of the national interconnected grid, the existing physical models, the dynamic models and the mixed analogue-digital simulation are unable to meet the need of the actual power grid due to the limitations of laboratory equipment. Currently, the China Electric Power Research Institute (EPRI) has developed an integrated power system simulation platform – Power System Analysis Software Package (PSASP). On the one hand, the PSASP electromechanical transient simulation can provide the large-scale grid simulation and ten thousand nodes scale grid simulation can be realized. By using PSASP electromagnetic transient simulation, the voltage and current transient process of the power system components can be achieved.

Meanwhile, by using the inverse-matrix method of sub-network parallel algorithms, the difficulty of real-time digital simulation of large-scale electric grid is resolved. The fully digital real-time simulation of power system simulator (advanced digital power system simulator, ADPSS) was developed by China EPRI. Several innovative techniques were adopted in the ADPSS platform to achieve real-time simulation of large-scale power systems, such as the electromechanical transient sub-network parallel computing method, the split AC-DC parallel real-time simulation, the mechanical and electrical hybrid parallel simulation method.

Inter-process synchronization and real-time control are used to achieve electromechanical and electromagnetic mixed transient simulation of large-scale power systems, and system scale and simulation accuracy can also be ensured. The external physical control equipment is connected to the physical interface of the ADPSS, and the operating characteristics of the actual grid are simulated without network equivalent simplification. Hence, the behaviour of the test device in a large grid scale and its effect on the grid dynamic characteristics can be fully investigated (Chang *et al.*, 2013).

This paper is organized as follows. Section 2 presents a brief review of the static var compensator (SVC). Section 3 presents the power system modelling with the SVC controller. Section 4 presents the principles of the power swing damping controller (PSDC). Section 5 presents the network interfacing methodology between the electromagnetic and electromechanical transient programs. Section 6 presents the implementation issues of the SVC controller on the ADPSS platform. Section 7 concludes this paper.

2. A brief review of the static var compensators (SVCs)

Figure 2 shows the single-line diagram of a static

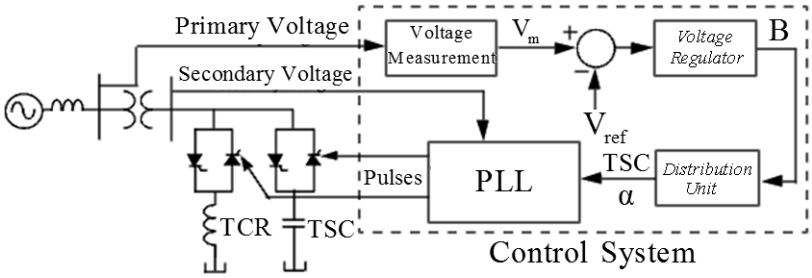

Figure 2: The single-line diagram of the SVC and its control system

var compensator and its control system. The variation of the reactive power is performed by switching three-phase capacitor banks and inductor banks connected on the secondary side of a coupling transformer. Each capacitor bank is switched on and off by three thyristor switches (Thyristor switched capacitor, TSC). Reactors are either switched on and off (Thyristor switched reactor, TSR) or phase-controlled (Thyristor controlled reactor) (Hingorani and Gyugyi, 2000).

The control system consists of the following aspects:

1. A measurement system to detect the positive-sequence voltages and currents;
2. A Fourier-based measurement system using a one-cycle running average method;
3. A voltage regulator that uses the voltage error (difference between the measured voltage Vm and the reference voltage Vref) to determine the SVC susceptance B needed to keep the system voltage constant;
4. A distribution unit that determines the TSCs (and eventually TSRs) that are switched on and off, and computes the firing angle of TCRs;
5. A synchronizing system using a phase-locked loop (PLL) synchronized on the secondary voltages and a pulse-generator that sends appropriate pulses to the thyristors.

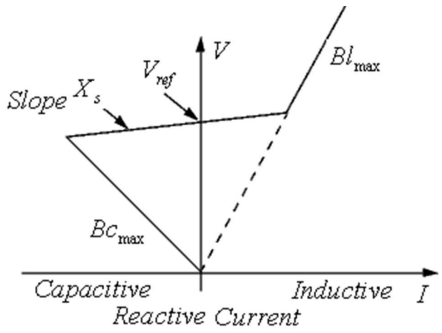

Figure 3: The V-I characteristics of the SVC

The SVC can be operated in two different modes: In voltage regulation mode (the voltage is regulated within limits as will be explained). In var control mode the SVC susceptance is kept constant. When the SVC is operated in voltage regulation mode, it implements the following V-I characteristic (Figure 3) (Hingorani and Gyugyi, 2000).

As long as the SVC susceptance (*B*) stays within the maximum and minimum susceptance values imposed by the total reactive power of capacitor banks (Bc_{max}) and reactor banks (Bl_{max}), the voltage is regulated at the reference voltage V_{ref}. However, a voltage drop is normally used (usually between 1% and 4% at maximum reactive power output), and the *V-I* characteristic has the slope indicated in Figure 3 The *V-I* characteristic is described by the following three equations:

$$V = V_{ref} + X_s \cdot I \ , \ (-Bc_{max} < B < Bl_{max}) \qquad (1)$$

$$V = -\frac{I}{Bc_{\max}} \ , \text{ capacitive mode } (B = Bc_{max}) \qquad (2)$$

$$V = \frac{I}{Bl_{\max}} \ , \text{ inductive mode } (B = Bl_{max}) \qquad (3)$$

where V denotes the positive sequence voltage (p.u.); I denotes the reactive current (p.u./P_{base}) ($I>0$ indicates an inductive current); X_s denotes the slope or droop reactance (p.u./P_{base}); Bc_{max} denotes the maximum capacitive susceptance (p.u./P_{base}) with all TSCs in service, no TSR or TCR; Bl_{ma} denotes the maximum inductive susceptance (p.u./P_{base}) with all TSRs in service, or TCRs at full conduction, without TSC.

When the SVC is operating in voltage regulation mode, its response speed to a change of system voltage depends on the voltage regulator gains (proportional gain K_p and integral gain K_i), the droop reactance X_s, and the system strength (short-circuit level). For an integral-type voltage regulator (K_p=0), if the voltage measurement time constant T_m and the average time delay T_d due to valve firing are neglected, the closed-loop system consisting of the SVC and the power system can be approximated by a first-order system having the following time constant:

$$T_c = \frac{1}{K_i \cdot (X_s + X_n)} \qquad (4)$$

where T_c represents the closed-loop time constant, K_i represents the proportional gain of the voltage

regulator, X_s represents the slope reactance, and X_n represents the equivalent power system reactance.

3. Power system modelling with static var compensator (SVC)

Figure 4 shows the single-machine power system with the SVC connected to an infinite bus. The nonlinear differential equations from which the Phillips-Heffron linear model without an SVC is derived as (Hingorani and Gyugyi, 2000):

$$\left.\begin{aligned}
&\dot{\delta} = \omega_0 \Delta\omega \\
&\Delta\dot{\omega} = (P_m - P_e - D\Delta\omega)/2H \\
&\dot{E}_q^{'} = (-E_q + E_{qe})/T_{d0}^{'} \\
&\dot{E}_{qe} = K_A(V_{t0} - V_t)/(1+sT_A) \\
&P_e = E_q^{'}V_b \sin\delta / X_{d\Sigma}^{'} - V_b^2(X_q - X_d^{'})\sin 2\delta / 2X_{d\Sigma}^{'}X_{q\Sigma} \\
&E_q = X_{d\Sigma}E_q^{'} / X_{d\Sigma}^{'} - (X_d - X_d^{'})V_b \cos\delta / X_{d\Sigma}^{'}
\end{aligned}\right\} \quad (5)$$

where $X_{d\Sigma} = X_d + X_l$, $X_{q\Sigma} = X_q + X_l$.

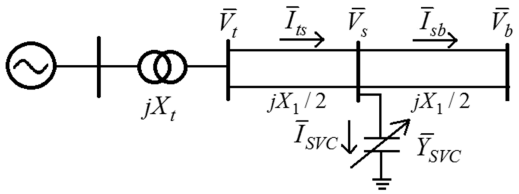

Figure 4: Single-machine power system with SVC

The equivalent admittance of a thyristor-controlled reactor and fixed-capacitor type SVC with voltage control is:

$$\bar{Y}_{SVC} = [2 - 2\alpha + \sin 2\alpha]/jX_L - 1/jX_C \quad (6)$$

From the circuit diagram, we get:

$$\left.\begin{aligned}
&\bar{I}_{sb} = \bar{I}_{ts} - \bar{Y}_{SVC}\bar{V}_{SVC} \\
&\bar{V}_{SVC} = jX_l\bar{I}_{sb}/2 + V_b
\end{aligned}\right\} \quad (7)$$

Hence, $\bar{V}_t = jX\bar{I}_{ts} + V_b/C$, where

$$C = 1 + jX_lY_{SVC}/2 \text{ and } X = X_l(1+1/C)/2.$$

Similarly, on the d-q axis we obtain:

$$\left.\begin{aligned}
&I_{td} = (E_q^{'} - V_b\cos\delta/C)/X_{d\Sigma}^{'} \\
&I_{tq} = V_b\sin\delta/CX_{q\Sigma} \\
&V_{td} = X_qV_b\sin\delta/CX_{q\Sigma} \\
&V_{tq} = XE_q^{'}/X_{d\Sigma}^{'} + V_bX_d^{'}\cos\delta/CX_{d\Sigma}^{'} \\
&V_{svcd} = (V_b\sin\delta - I_{tq}X_l/2)/C \\
&V_{svcq} = (V_b\cos\delta + I_{td}X_l/2))/C
\end{aligned}\right\} \quad (8)$$

By linearizing these equations around the steady-state operating point of the power system, the extended Philips-Heffron model of the power system with SVC can be obtained as:

$$\left.\begin{aligned}
&\dot{\delta} = \omega_0\Delta\omega \\
&\Delta\dot{\omega} = (-K_1\Delta\delta - K_2\Delta E_q^{'} - K_p\Delta\alpha - D\Delta\omega)/2H \\
&\Delta\dot{E}_q^{'} = (-K_4\Delta\delta - K_3\Delta E_q^{'} - K_q\Delta\alpha + \Delta E_{qe})/T_{d0}^{'} \\
&\Delta\dot{E}_{qe} = [-\Delta E_{qe} - K_A(K_5\Delta\delta + K_6\Delta E_q^{'} + K_V\Delta\alpha)]/T_A
\end{aligned}\right\} \quad (9)$$

where:

$$\left.\begin{aligned}
&K_1 = \partial P_e/\partial\delta, K_2 = \partial P_e/\partial E_q^{'}, K_p = \partial P_e/\partial\alpha \\
&K_4 = \partial E_q/\partial\delta, K_5 = \partial E_q/\partial E_q^{'}, K_q = \partial E_q/\partial\alpha \\
&K_5 = \partial V_t/\partial\delta, K_6 = \partial V_t/\partial E_q^{'}, K_V = \partial V_t/\partial\alpha
\end{aligned}\right\} \quad (10)$$

4. Power swing damping control (PSDC) – principles and solutions

Oscillations in power systems are caused by various disturbances. If the system is not series-compensated, the typical range of oscillation frequencies extends from several tenths of 1 Hz to nearly 2 Hz. Several modes of oscillation may exist in a complex, interconnected power system. The behaviour of the generator oscillations is determined by two torque components: the *synchronizing torque* and the *damping torque*.

The synchronizing torque ensures that the rotor angles of different generators do not drift away following a large disturbance. (In other words, the synchronizing torque binds the different generators into synchronism, assuring transient stability.) In addition, the magnitude of the synchronizing torque determines the oscillation frequency. Meanwhile, the damping torque influences the decay time of oscillations. Even if a power system is stable, the oscillations may be sustained for a long period without adequate damping torque (Hingorani and Gyugyi, 2000).

Referring to the system in Figure 4, the SVC regulates the middle point voltage V_s. Let:

$$\left.\begin{aligned}
&v_t = V_t\sin(\omega t + \delta) \\
&v_s = V_s\sin(\omega t + \delta/2) \\
&v_b = V_b\sin(\omega t)
\end{aligned}\right\} \quad (11)$$

For the sake of simplicity, it is assumed that V_t=V_b=V. The electrical power P_e transmitted across the line can be derived as follows for a sending-end voltage magnitude:

$$P_e = \frac{VV_s}{X_l/2}\sin\frac{\delta}{2} \quad (12)$$

The incremental change in the electrical power can be derived by linearizing Eq.(12) as:

$$\Delta P_e = \frac{\partial P_e}{\partial V}\Delta V + \frac{\partial P_e}{\partial V_s}\Delta V_s + \frac{\partial P_e}{\partial \delta}\Delta\delta \quad (13)$$

It is further assumed that the sending-end voltage is constant, thus $\Delta V = 0$. Besides, swing equation of the system can be written as:

$$M\frac{d^2\delta}{dt^2} = P_M - P_e \quad (14)$$

where P_M denotes mechanical power, M denotes the mechanical torque. For small-signal analysis, the Eq. (14) is linearized as:

$$M\frac{d^2\Delta\delta}{dt^2} = \Delta P_M - \Delta P_e \quad (15)$$

The mechanical power is assumed to be constant during the time of analysis, hence we get:

$$M\frac{d^2\Delta\delta}{dt^2} = -\Delta P_e \quad (16)$$

Therefore, we get:

$$M\frac{d^2\Delta\delta}{dt^2} + \frac{\partial P_e}{\partial V_s}\Delta V_s + \frac{\partial P_e}{\partial \delta}\Delta\delta = 0 \quad (17)$$

Equation (17) describes the small-signal dynamic behaviour of the system, in which the effect of the SVC is represented by the middle term $\partial P_e \Delta V_s / \partial V_s$. If the SVC is operated to maintain the midpoint voltage V_s strictly constant, as is done for voltage control, ΔV_s becomes zero, in which case Eq.(17) reduces to:

$$M\frac{d^2\Delta\delta}{dt^2} + \frac{\partial P_e}{\partial \delta}\Delta\delta = 0 \quad (18)$$

The roots of the characteristic equation result in un- damped oscillations in the rotor angle with a frequency of:

$$\omega_n = \sqrt{\frac{1}{M}\frac{\partial P_e}{\partial \delta}\bigg|_0} \quad (19)$$

where $\partial P_e / \partial \delta$ denotes the synchronizing power coefficient. Obviously, an SVC operating on a pure- voltage control mode is unable to provide any system damping. However, the SVC can contribute to system damping if it is allowed to modulate the middle voltage instead of maintaining it strictly constant. Specifically, the midpoint voltage can be modulated as a function of $d(\Delta\delta)/dt$, that is,

$$\Delta V_s = K\frac{d(\Delta\delta)}{dt} \quad (20)$$

where K is a constant. Substituting Eq. (20) in Eq. (17) results in a modified incremental-swing equation:

$$M\frac{d^2\Delta\delta}{dt^2} + \frac{\partial P_e}{\partial V_s}\bigg|_0 K\frac{d(\Delta\delta)}{dt} + \frac{\partial P_e}{\partial \delta}\bigg|_0 \Delta\delta = 0 \quad (21)$$

Therefore, the damping ratio can be derived as:

$$\xi = \frac{K}{2M}\frac{\partial P_e}{\partial V_s} \quad (22)$$

With the introduction of voltage-modulating control, the SVC transforms the power system into a positively damped system. Hence, any oscillations in the rotor angle will decay with time. Such an additional control feature is termed *supplementary control*, or *power-swing damping control* (PSDC) [Mahdad *et al.,* 2009].

5. Interface methodology for the electromechanical-electromagnetic transient simulation

a. Equivalent networks for the electromagnetic and electromechanical subsystems

Figure 5 shows the equivalent representations of the electromagnetic and electromechanical transient networks. According to the multi-port Thevenin principle, the electromagnetic and electromechanical transient networks are solved separately. The electromechanical transient network is denoted by the Thevenin equivalent network when computing the electromagnetic transient parameters. Similarly, the electromagnetic transient network is represented by the Norton equivalent network when computing the electromechanical parameters.

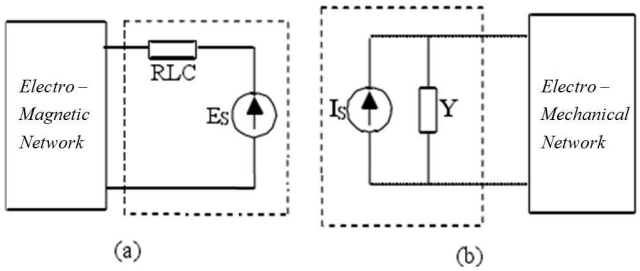

Figure 5: The equivalent representation of the electromagnetic and the electromechanical networks

Figures 6 and 7 show the data exchange model and interface model respectively, between the

electromechanical and electromagnetic sub-networks. In the initialization process, the positive sequence, negative sequence and zero-sequence equivalent impedance matrix Z of the electromechanical network are sent to the electromagnetic transient simulation program. At each interface point, the positive, negative sequence and zero sequence current Iemt, and voltage Vemt at boundary points of the electromagnetic transient program are sent to the electromechanical transient program. Meanwhile, the positive, negative and zero sequence equivalent potential (E) at the boundary points of the electromechanical transient program is sent to the electromagnetic transient program. The simulation step-sizes of the electromagnetic network and the electromechanical network are 100μs and 20ms.

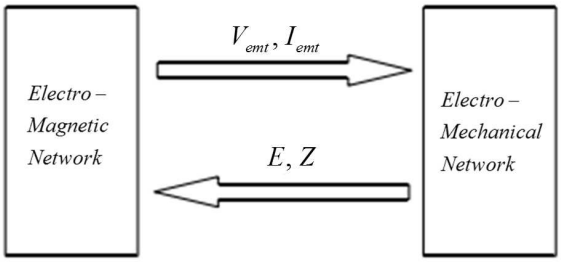

Figure 6: The illustration of data exchange between the electromagnetic and electromechanical networks

b. The simulation step-size of the two sub-networks

Figure 8 shows the timing-sequence of the electromagnetic and electromechanical simulation programs in the normal operation conditions. The step-size of the electromagnetic transient program is selected as 0.01s, and the step-size of the electromechanical transient program is selected as 50 microsecond. The simulation procedure is as follows:

1. Initialization process, the equivalent impedance Z and potential E at the boundary points of the electro- mechanical program are sent to the electromagnetic program;
2. The electromagnetic transient program start calculation during T_0 to T_1;
3. The fundamental frequency voltages, currents at boundary points of the electromagnetic transient program are sent to the electromechanical transient program, and the new Z and E parameters are acquired from the electromechanical transient program;
4. The electromechanical program starts calculation during T_0 to T_1 period and the electromagnetic transient program starts calculation during T_1 to T_2 period after the Z and E parameters are acquired;
5. The fundamental frequency voltages, currents at boundary points of the electromagnetic transient program are sent to the electromechanical transient program at T_2, and the new Z and E parameters sent to the electromagnetic transient program;
6. $T=T+\Delta t$ Δt denotes simulation step-size
7. Repeating procedures 4–6, unless the system topology evolves or simulation terminates.

c. Electric network partitioning scheme

Figure 9 shows the single-line diagram of the practical SVC in the 500kV substation. In order to study the characteristics of SVC controller, a closed-loop control system based on actual controller and ADPSS platform is established. The electric network is simulated in the ADPSS platform, by using parallel computing and hybrid simulation approach, the real-time simulation of the whole system is achieved. Based on the ADPSS platform, the power flow and grid network diagram are set up, the sys-

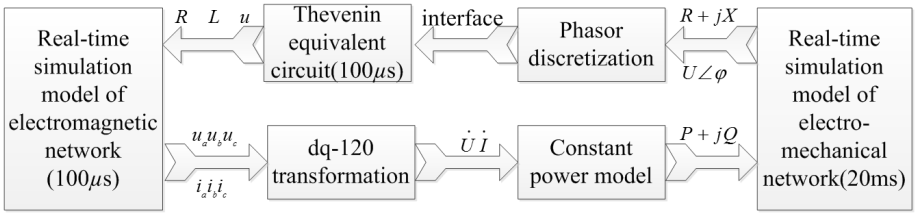

Figure 7: Interface model based on ADPSS

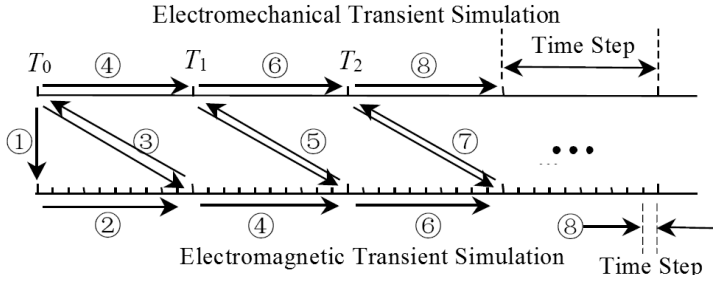

Figure 8: Electromagnetic and electro-mechanical simulation time sequence

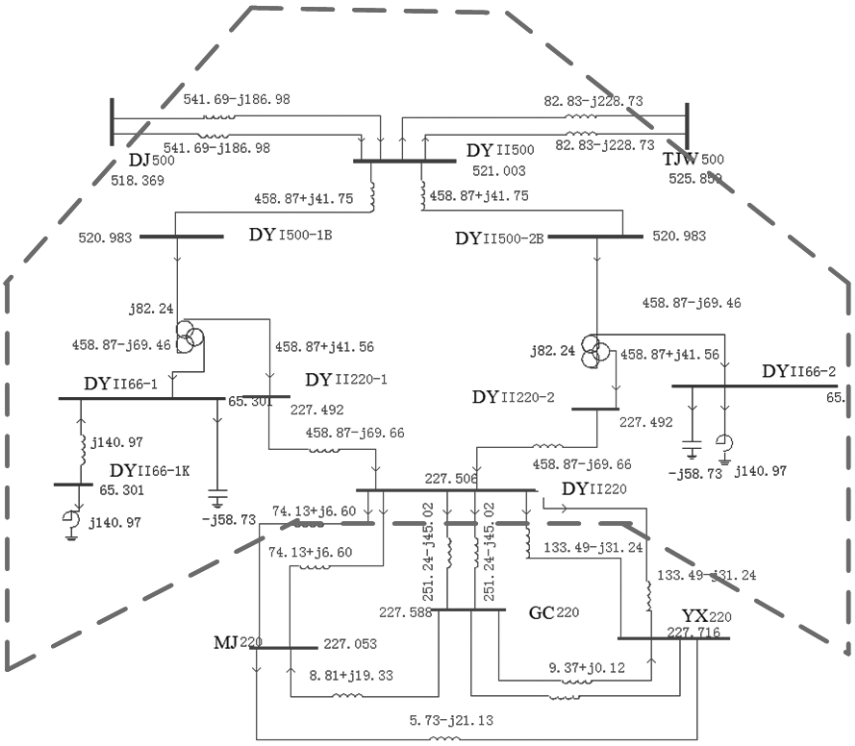

Figure 9: Single-line diagram of a practical SVC in 500kV substation

tem is divided into twelve electromechanical networks and one electromagnetic network by using the automatic sub-network partitioning functions inherent in ADPSS platform. The individual subnetworks are distinguished and kept in contact through the tie-lines between the sub-networks.

As shown in Figure 9, the electromagnetic subnetwork is encircled by the dotted line, i.e., the region where the SVCs are installed in the 500kV substation. In this region, the detailed electromagnetic simulation through ADPSS hardware device is required. By connecting the PSASP hardware interface with the actual external SVC controller, the closed-loop control of the SVC controller is achieved. Meanwhile, the electromechanical transient simulation is responsible for the area outside the dotted line in Figure 9. The data communication between the sub-networks is achieved by the bus or line information exchange between electromechanical and electromagnetic processes.

Figure 10 shows the physical interface system (including power amplifier) of two sets of SVC controller with the ADPSS simulation system. Figure11 shows a photo of the experimental facilities with SVC controller and ADPSS in the lab. The ADPSS simulation device provides the desired voltage and current signals to the two sets of SVC controllers and TCR branches through the physical interface

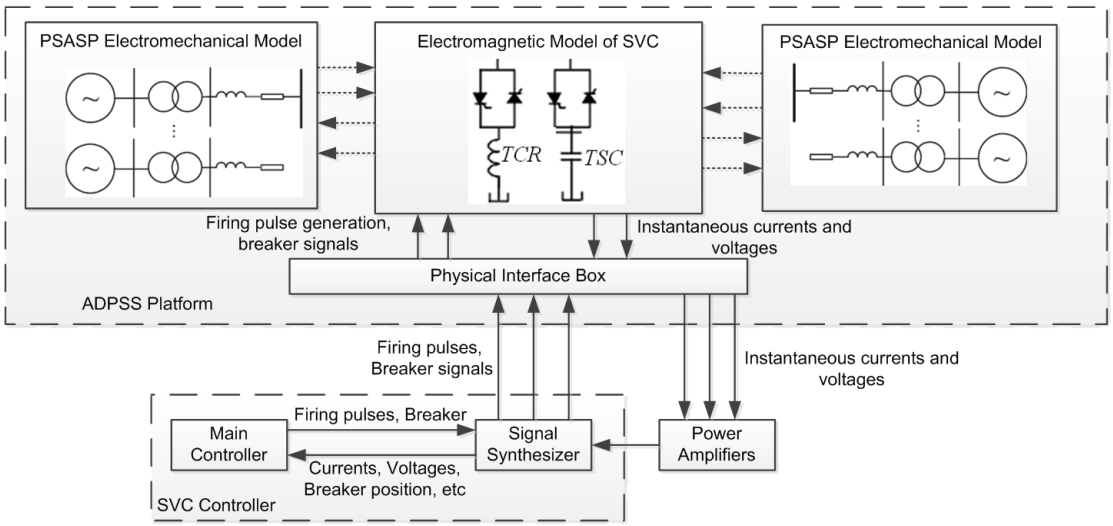

Figure 10: The system block diagram of the SVC controller and the ADPSS platform

(including power amplifier), and also provides the SVC controllers with the switching positions of the filter branches, the parallel capacitors, and the reactors.

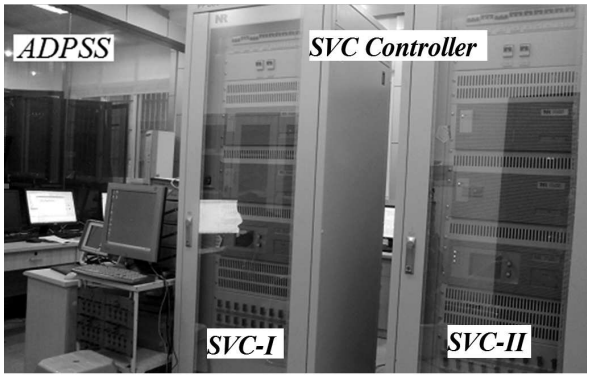

Figure 11: Experimental facilities with SVC and ADPSS

As shown in Figure 10, the thyristor trigger signals as well as the opening/closing of each branch switching signals generated by the two sets of the SVC controller are sent back to the ADPSS platform. Furthermore, the SVC controllers acquire the voltage, current and switching position signals of each branch from the physical interface box (including the power amplifier). After the execution of complicated control algorithm, and output trigger pulse signals and the sub-closing signals of the SVC controllers are sent back to the ADPSS platform. Following the last procedure, the closed-loop controller test of the static var compensator (SVC) is realized in the advanced digital power system simulation platform.

6. Implementation of the SVC controller on ADPSS platform

Figure 12 shows the control block diagram of the SVC controller in the ADPSS platform, which consists of three blocks, namely, transient compensation, transient voltage control and power swing damping control. The transient compensation is activated under a severe grid fault, when the voltages of the 500kV substation reduce to 70% of the nominal values. The transient voltage control is activated when the grid voltages of the 500kV substation reduces to 90% of the nominal values and last for 10ms. And the transient voltage control is suspended after the voltages recovers to 94.5% of the nominal values and last for 3s. After the transient control process, the steady-state voltage control is enabled.

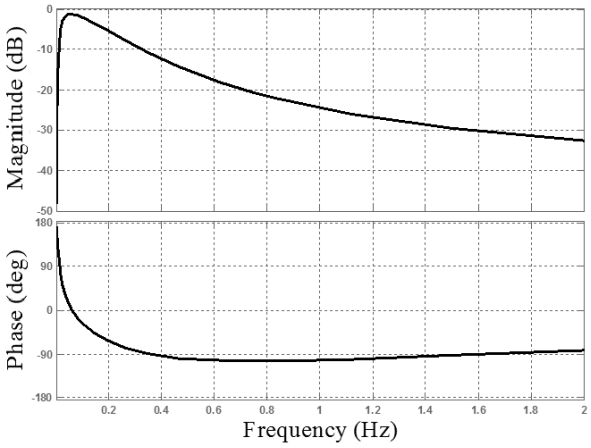

Figure 13: The bode-diagram of the power swing damping controller

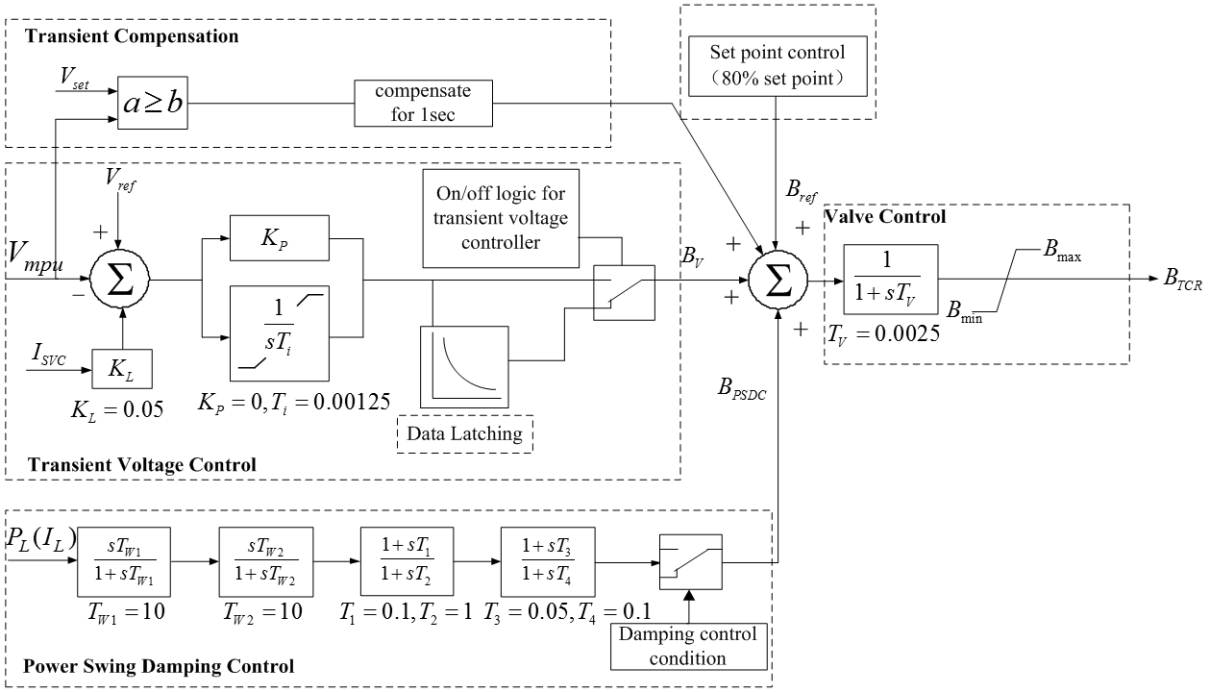

Figure 12: Control diagram of the SVC in the ADPSS platform

The root-mean-square (RMS) values of the DY-DJ (Figure.9) line currents are utilized as input signals of the power swing damping controller, which is formed by two dc rejection filters and first-order low-pass filters. The bode-diagram of the PSDC is shown in Figure 13. It can be observed that the oscillation frequency is around 0.34Hz, and the phase lagging between the input and output signal is about 90 degree. The PSDC has a phase lag of 90°~105° during the low frequency range of 0.3~2Hz, which achieves effective low frequency oscillation damping.

Dynamic behaviour of the SVC controller

In order to investigate the transient voltage stability and the characteristics of the damping controller, the remote electromechanical sub-network is subjected to the three-phase to ground fault at t = 4.0s, with a zero grounding impedance and a duration of five fundamental cycles. The fault is cleared at t = 4.1s, and the SVC bus voltages and the injected reactive power, line active power and the RMS value of line current are observed.

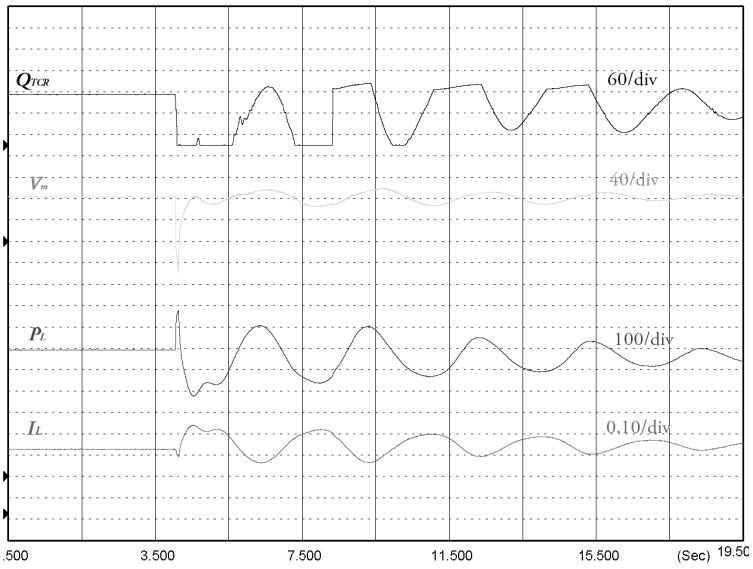

Figure 14: Experimental results of V_m, Q_{TCR} and P_L, I_L of the line DY-DJ500kV after the remote N-1 fault

As shown in Figure 14, when the remote *N*-1 fault occurs, the RMS voltage of the DJ-500kV bus V_m reduces to 0.27 p.u. The TCR brunch of the SVC adjust the equivalent conductance and 144MVar reactive power is released to remarkably enhance the transient stability of the system. Based on the experimental results, Table 1 summarizes the maximum and minimum value of the RMS voltage V_m, the total active power PL of the DY and DJ buses.

Enhancement of system transient stability

According to the experiment results of several faults, it can be concluded that, when the TX-DS line N-2 grid fault occurs, the ultra-high voltage (UHV) EH1 and EH2 suffer the most serious decline. The islanding conditions of EH1 and EH2 are that: (1) the voltage of EH1 is less than 0.64pu and has 0.15s duration. (2) The voltage of EH2 is less than 0.49pu and has 0.15s duration. Figure 15 shows the voltage waveforms of EH1 and EH2 with or without SVC, where the red line represents with SVC condition, the black line represents without SVC condition. It can be seen that when the SVC controller is not in operation, EH2 has reach the islanding condition, when SVC is enable, the lowest voltage of EH1 and EH2 increase 0.075pu and 0.13418p.u, and EH2 will not break down. Therefore, SVCs can substantially enhance the transient stability of the system, and enhance the support ability of UHV voltage under serious faults.

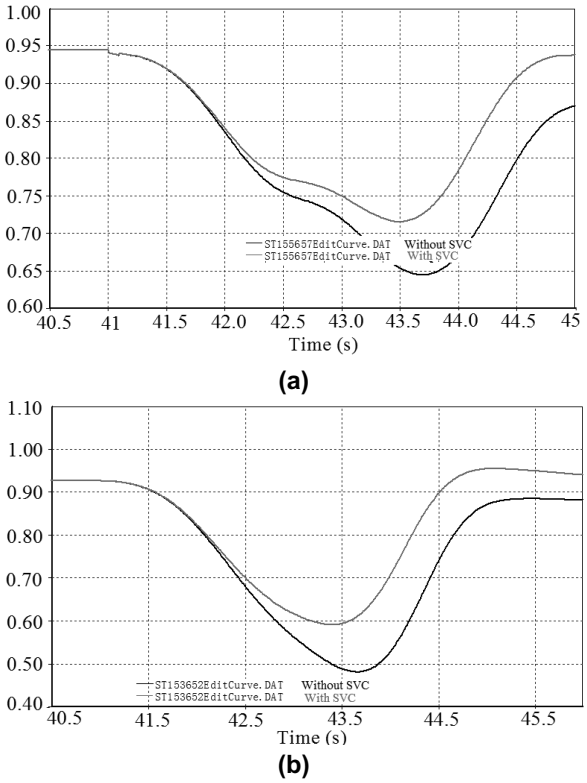

Figure 15: The transient voltage waveforms of EH1 and EH2 under TX-DS line N-2 grid fault

Table 1: The maximum and minimum value of V_m, PL, Q_{TCR} under remote N-1 fault

Fault type	*D-II500kV voltage (kV)*			*DII-DJ active power (MW)*		
	max	*min*	*max-min*	*max*	*min*	*max-min*
N-1 fault	540	506	34	1329	795	534

Note: This table is obtained by the second swing parameters.

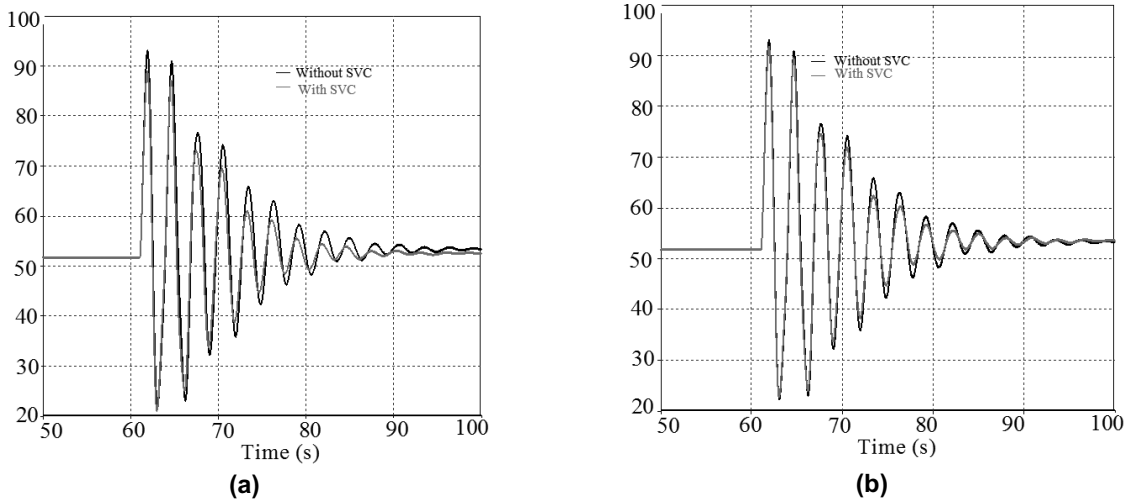

Figure 16: the power angle curves between ERTAN and Three Gorges hydro-plant under faults at DJ-SZ line: (a) N-1 fault; (b) N-2 fault

Enhancement of system damping

Figure 16 shows the real-time simulation results of the power angle curve between ERTAN and the Three Georges hydro-plant under N-1 fault and N-2 fault at DJ-SZ line, respectively. Table 2 summarizes the first swing amplitude and damping ratio comparison results of power angle under different faults with SVC or without SVC. From the test results, it can be observed that the oscillation frequency is about 0.34Hz, the rotor angle increases following a fault, and goes through an over swing. The damping ratio of the power swing angle is substantially increased with SVC controller. It can be concluded that the SVC controller is effective to damp power swing and provides low frequency oscillation damping thus increase system damping ratio.

The experimental results demonstrate that the presented modelling and control strategies, based on the hardware -in-the-loop (HIL) approach is quite effective to study the SVC controller, and the similar analysis can be extended to other FACTS controllers for voltage regulation, oscillation damping and stability enhancement for the large interconnected electrical power systems.

5. Conclusions

The dynamic modelling and power swing damping control of the static var compensator is presented in this paper, using the hardware-in-the-loop approach based on the advanced digital power system simulator platform. Firstly, a brief review of the SVC and Phillips-Heffron model of the power system with the SVC controller are presented.

Table 2: The first swing amplitude and damping ratio comparison of power angle between ERTAN and Three Gorges hydro-plant under different faults with SVC or without SVC

Fault position	*Fault form*	*The first swing amplitude(o)*		*Damping ratio(%)*	
		without SVC	*with SVC*	*without SVC*	*with SVC*
DJ-SZ	N-1	92.93	88.85	3.89	4.62
DJ-SZ	N-2	92.97	91.63	3.89	4.42
TJW-NC	N-1	86.43	85.08	4.41	5.04
HG-BQ	N-1	96.65	96.27	3.08	4.07
TX-LW	N-1	95.13	93.88	4.19	4.47
TX-LW	N-2	97.26	96.03	3.72	4.32
SM-YA	N-1	64.79	63.89	5.10	6.08
SM-YA	N-2	66.04	65.05	5.06	6.54
DJ Tran	N-1	83.62	82.39	4.46	5.26
JS Tran	N-1	97.61	96.41	4.39	5.09
TX Tran	N-1	96.85	96.22	4.05	5.11
SZ Tran	N-1	89.86	88.32	5.78	6.97
SZ-JS	N-1	89.12	87.75	4.07	4.52
YA-SZ	N-2	74.42	73.19	5.41	5.68
YA-JS	N-2	71.48	70.52	5.37	6.44

To enhance power system damping and mitigate low frequency oscillation, the power swing damping control is designed. The interfacing methodology between the electromagnetic and the electro-mechanical transient programs is proposed. The closed-loop control strategy of the SVC controller on the ADPSS platform is presented to analyse the dynamic control behaviour of the SVC. Finally, the validity and effectiveness of the devised modelling and control methodologies are confirmed by the experimental results.

Acknowledgement

This work is financially supported by the research project 'Research on the key technologies and practical application of the 110kV hybrid SVC controllers' from the State Grid Corporation of China (SGCC) under grant No. 521997140003.

References

Boynuegri, A.R., Vural, B., Tascikaraoglu, A., Uzunoglu, M., and Yumurtaci, R. (2012). Voltage regulation capability of a prototype static var compensator for wind applications, *Applied Energy,* 93,422-431.

Chang, Y.C. (2013). Fitness sharing particle swarm optimization approach to FACTS installation for transmission system loadability enhancement, *Journal of Electrical Engineering and Technology*, *Korea,* Vol. 8, No.1, pp.31-39, 2013.

Chang, Y.C. and Chang, R.F. (2013). Maximization of transmission system loadability with optimal FACTS installation strategy, *Journal of Electrical Engineering and Technology*, *Korea,* 8, .991-1001.

Dickmander, D. L., Thorvaldsson, B. H., Stromberg, G. A., Osborn, D. L., Poitras, A. E., and Fisher, D. A. (1992). Control system design and performance verification for the chester, maine static VAr compensator, *IEEE Transactions on Power Delivery,* 7, 1492–1503.

Erickson, R. W., and Maksimovic, D., (1997). *Fundamentals of Power Electronics*. Norwell, MA: Kluwer.

Hingorani N. G., Gyugyi, L., (2000). Understanding FACTS-Concepts and Technology of Flexible AC Transmission Systems. Piscataway, NJ: IEEE Press.

Long, W., and Nilsson, S. (2007). HVDC transmission: Yesterday and today, *IEEE Power and Energy Magazine,* 5, 22–31.

Mahdad, B., and Srairi, K. (2013). A study on multi-objective optimal power flow under contingency using differential evolution, *Journal of Electrical Engineering and Technology (IJEET)*, *Korea,* 8, 53-63.

Mahdad, B., Bouktir, T., Srairi, K., and Benbouzid M.E.L. (2009). Optimal Power Flow with Discontinuous Fuel Cost Functions Using Decomposed GA Coordinated with Shunt FACTS, *International Journal of Electrical Engineering & Technology*, Korea, 4, 315-322.

Qian, M., Hongtao, L., He H., and Chuang F. (2011). Application of static var compensator in China southern power grid, *Southern Power System Technology,* 5, 17-21.

Rostamkolai, N., Piwko, R. J., Larsen, E. V., Fisher, D. A., Mobarak, M. A., and Poitras, A. E. (1990). Sub synchronous interaction with static VAr compensators – Concepts and practical implications, *IEEE Transactions on Power Systems,* 5, 1324–1332.

Schauder C., Gernhardt M., Stacey E., Lemak T., Gyugyi L., Cease TW., and Edris A. (1995). Development of a ±100 MVAr static condenser for voltage control of transmission systems, *IEEE Transactions on Power Delivery,* 10, 1486-1496.

Received 23 February 2014; revised 10 October 2014

Investigations on the absorption spectrum of TiO_2 nanofluid

A L Subramaniyan
Department of Physics, Thiagarajar College of Engineering, Madurai, India

Sukumaran Lakshmi Priya
Department of Physics, Thiagarajar College of Engineering, India

M Kottaisamy
Department of Chemistry, Thiagarajar College of Engineering, Madurai, India

R Ilangovan
Department of Nanoscience and Technology, Alagappa University, Karaikudi, India

Abstract
Nanofluids are tailored nano- colloidal suspensions of nanoparticles in a suitable base fluid. This present work investigates the absorption spectrum in TiO_2-water nanofluids to identify the potential application of nanofluids in Direct Absorption Solar Collectors (DASC). Nanoparticles of Titanium dioxide (TiO_2) are prepared by sol gel and characterized by X Ray Diffraction (XRD) and Scanning Electron Microscopy (SEM). TiO_2-water nanofluids with weight fraction of 0.1% are prepared by a two-step process with sonication. The prepared nanofluids are investigated for their stability by a gravity sedimentation method and for their optical property by UV-Vis spectroscopy. Stability of nanofluid is essential for the applications of nanofluid in DASC. TiO_2 nanoparticles with a crystallite size of 43nm are obtained .The SEM image reveals the agglomerated state of TiO_2 nanoparticles and the stability of TiO_2 nanofluid is reported as 9-10days. UV results indicate the decrease in absorption from 440-500nm, complete absorption from 500-700nm and increase in absorption from 700-900nm.TiO_2 nanofluids are recommended as potential candidates for DASC in UV and IR regions.

Keywords: nanofluid, TiO_2, sedimentation, absorption, DASC

1. Introduction

Increased consumption and growing demands of electrical appliances across the globe have posed a threat on the non- renewable energy resources and has made us exploit the maximum of renewable energy resources among which solar energy is the ultimate choice. Solar energy has been investigated for photovoltaic and thermal applications (Duffie, 1980). A major thrust in materials development is to identify new materials in order to increase the efficiency of Solar Thermal Collectors .The development of nanotechnology contributed to nano suspensions, which can increase the efficiency of DASC. Conventional solar collectors transfer the heat from the flat plate to the working fluid but have the drawback of high heat loss .The concept of Direct absorption solar collectors in which working fluid acts as absorber and carrier of heat started replacing the conventional solar collectors (Otanicar, 2009). Since thermal conductivity of pure liquids are much lesser in comparison to solids, suspension of solid particles in liquid could enhance the thermal conductivity and required optical properties. Micro colloidal suspensions suffered from drawbacks like abrasion and sedimentation for which nanofluids were substituted by Robert Taylor (2009). The term nanofluid was coined by Stephen Choi in 1995. Nanofluids are suspensions of nano-sized solid particles (1-100nm) in suitable base fluids. From 1995 till 2008, nanofluids have been explored as a heat transfer fluid and the best results have been reported by Eastman and Choi (2001).

In the past five years, nanofluids have also been explored for their electrical (Ganguly, 2009) and magnetic properties (Philip, 2009).

Nanofluids can be prepared in two ways, a single step method (Zhu, 2004) or a two-step method (Eastman, 1997). One step method is based on simultaneous synthesis of nanoparticle and nanofluid and two step methods involve synthesis of nanoparticles in the first step followed by dispersion in a suitable base fluid. The success of nanofluid for DASC depends on suitable choice of base fluid and nanoparticles. The best nanofluids for energy harvesting demands high stability and high absorption of solar radiation. In this present work, an attempt has been made to identify stability and absorption property of 0.1wt% TiO_2-water nanofluid.

2. Experimental

2.1 Preparation of TiO_2 nanoparticle and TiO_2 nanofluid

TiO_2 nanoparticles were prepared via a sol–gel method using titanium tetraisopropoxide (TTIP), distilled water, and ethyl alcohol as the starting materials. All the reagents used were of Analytical grade. 10 ml of Titanium tetraisopropoxide was dissolved in absolute ethanol (20 ml) and distilled water was added (30 ml). The obtained solutions were kept under slow-speed constant stirring on a magnetic stirrer for 40 min at room temperature to obtain a thick solution. The thick solution was dried at 50°C for 1.5 hours to evaporate water and carbon to the maximum extent. After hand milling the dried powders obtained were calcined at 400°C for 2 hours to obtain desired TiO_2 nanoparticles, as reported by (Thangavelu, 2013). A flow chart for synthesis of TiO_2 is represented in Figure 1 and the nnaoparticles of TiO_2 before milling is shown in Figure 2.

0.1g of prepared TiO_2 nanoparticles are dispersed in 1 litre of water and sonicated as shown in Figure 3 to obtain TiO_2 nanofluid .Sonication is done at a frequency of 42 KHz for 15 minutes to obtain a uniform dispersion of TiO_2 in water. The prepared TiO_2 nanofluid is shown in Figure 4.

2.2 Sedimentation test

Ideal nanofluids have high stability and poor suspensions can alter the thermal and solar absorption properties of nanofluid drastically. The importance of stability of nanofluids and different methods of sedimentation analysis and mechanisms is discussed by (Mukherjee, 2013).In the present work, sedimentation is evaluated by gravitational sedimentation column method for TiO_2 nanofluid as shown in Figure 5. As time progresses, the nanoparticles tend to settle at the bottom .The thickness of the sediment is observed as a function of time to plot the sedimentation profile of TiO_2 nanofluid.

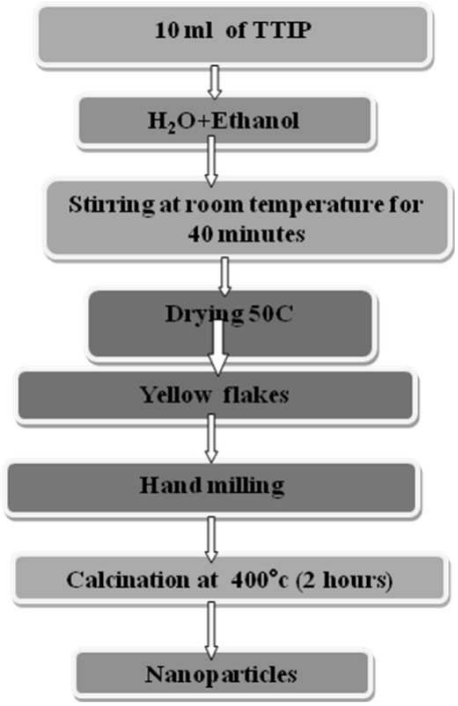

Figure 1: Flow chart for synthesis of TiO_2 nanoparticles

Figure 2: TiO_2 flakes before milling

3. Results and discussion

3.1 Results of preparation TiO_2 nanoparticle and nanofluid

Constant stirring on a magnetic stirrer after 30 minutes indicates a milky white solution which confirms the formation TiO_2 nanoparticles from TTIP. .After drying at 50°C, yellow colour TiO_2 flakes are obtained as shown in Figure 2.

3.2 Structural characterization

Figure 6 shows the X-Ray Diffraction pattern of final calcined TiO_2 nanoparticles. The X-ray diffraction peaks of prepared nanoparticle is in confirmation

Figure 3: Sonication of nanofluid samples

Figure 4: TiO_2 nanofluid

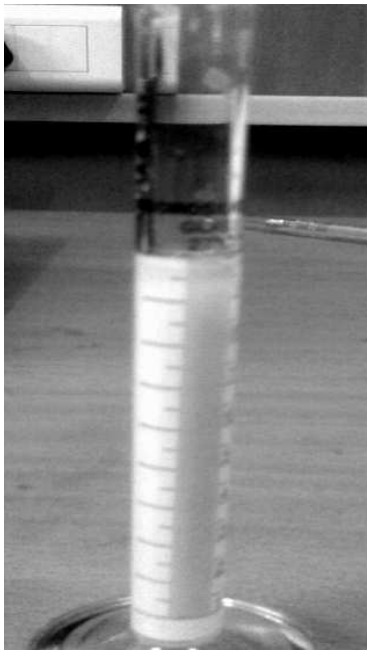

Figure 5: Sedimentation of TiO_2 nanofluid

with JCPDS-89.4203. (Joint Committee for Powder Diffraction Society). This shows the broad peaks at 25.36, 37.91, 48.04 and 55.05 (anatase phase of TiO_2). The broad peaks are obtained due to randomly oriented crystals in a nano crystalline material as indicated by (Akbari, 2011). Average crystalline size of samples TiO_2 are determined by the Debye-Scherer formula, $D = 0.91\lambda$ ($\beta\cos\theta$) and were found to be 42.77nm.The SEM image (Figure 7) of nanoparticles reveals the high agglomeration. This may be due to lack of usage of surfactants during preparation of TiO_2. Surfactants were not used purposely because they would alter the optical

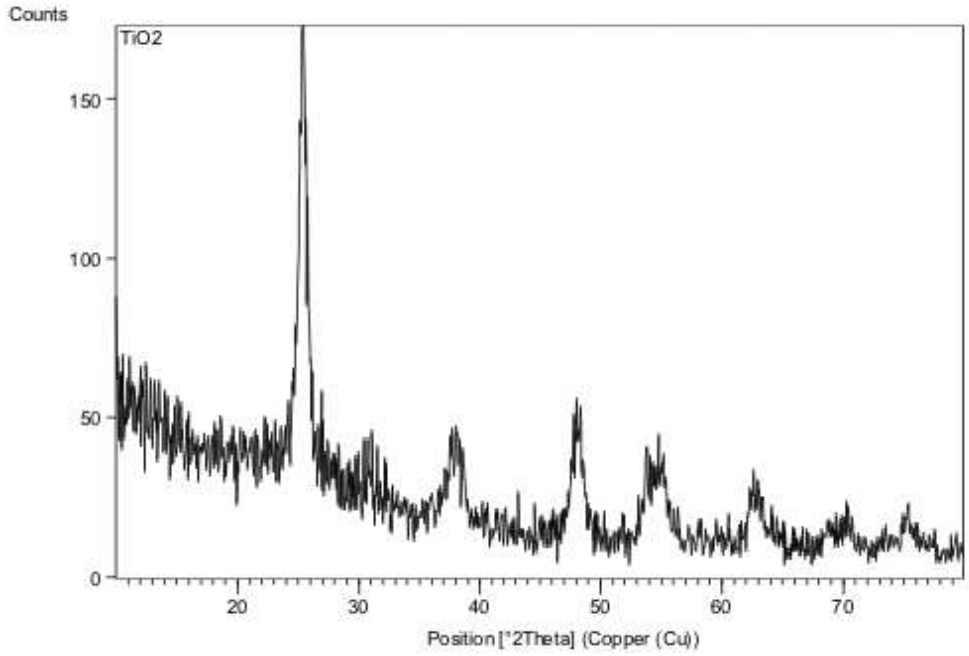

Figure 6: XRD OF TiO_2 nano particles

absorption of nanofluids. The average diameter of SEM can also correspond to 50-100nm thus supporting the results from XRD.

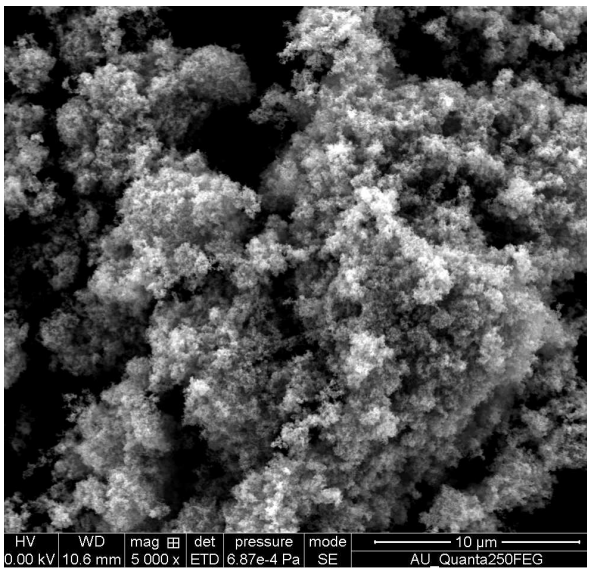

Figure 7: SEM of TiO_2

3.3 Sedimentation characterization of TiO_2

A plot of thickness of the sediment and the time (Figure 8) reveals the sedimentation profile of TiO_2 .The time taken for the 25% formation of pure base fluid or the sediment to decrease to 75% of the original nanofluid column is 9.79 days.

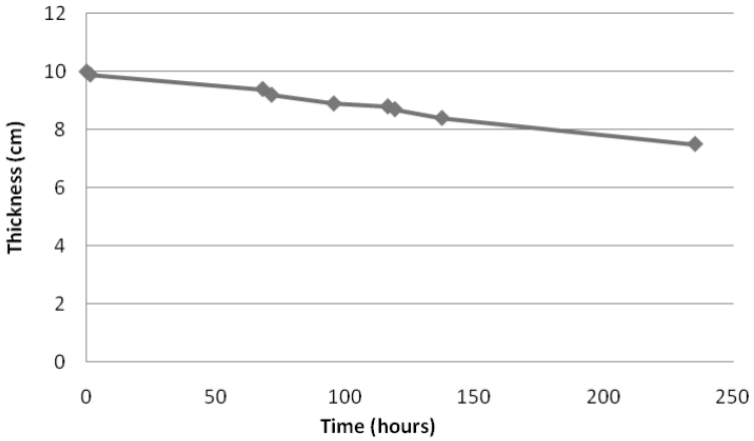

Figure 8: Sedimentation profile of TiO_2 nanofluid

3 .4 Optical characterization

The prepared TiO_2 nanoparticles were investigated for their optical properties by UV Visible absorption spectrophotometer at room temperature. The spectrum is recorded from 400 nm to 900 nm as shown in Figure 9. The absorption of TiO_2 nanofluids decreases from 440-500 nm and increases from 700-900 nm, which proves the absorption and attenuation of TiO_2 nanofluids in the visible range and IR regions. The results in IR region are in slight contradiction to the latest results of TiO_2, 0.1vol% - water nanofluid reported by (Said, 2014). The variation in results are attributed to the nanoparticle size (43 nm), lack of surfactant and vol%. (Said, 2014) has investigated optical properties of TiO_2 nanofluid with 21nm, surfactant and 0.1 and 0.3vol%.The prepared nanoparticles have a range of particle size as revealed by SEM which are also responsible for variation in previously reported results. Thus, TiO_2 water nanofluids are good for direct absorption in UV and IR pectrum in the absence of surfactants .

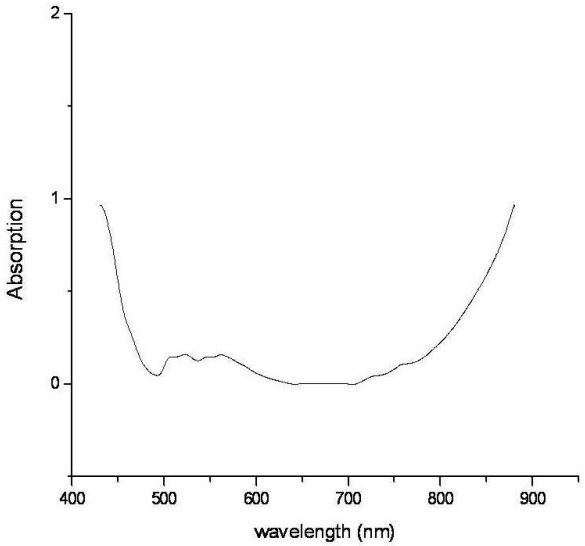

Figure 9: UV-Vis absorption spectrum of TiO_2 Nanofluids

4. Conclusions

Our conclusions are as follows:

1. TiO_2 nanoparticles were prepared by the sol-gel method. XRD results show that TiO_2 particles have an anatase phase and is crystalline in nature with crystallite size of 42.77 nm.
2. From SEM images, it is evident that TiO_2 has an inhomogeneous size with high agglomeration and the average particle diameter is in the range of 50 -100 nm.
3. From sedimentation profile, the sedimentation time of TiO_2 is 9-10 days. Lesser weight fraction of TiO_2 nanofluids are recommended for higher stability.
4. TiO_2 nanofluids without surfactants are better absorbers of ultraviolet and infrared wavelengths in comparison to TiO_2 nanofluids with surfactants Nanofluids without surfactants may be less stable but better absorbers of solar radiation and may aid in efficient DASC.
5. Higher absorption can be obtained with increasing weight fraction of naoparticles in base fluid but a low weight fraction of naoparticle can give a more stable nanofluid.

Acknowledgements

The authors would like to thank Dir. V. Abhai Kumar, Principle, TCE, Madurai, for the constant support and encouragement and the facilities provided by Dr R. Vasuki, TCE, Madurai. Special thanks are conveyed to the Department of Industrial Chemistry, Alagappa University Karaikudi for providing SEM facilities. The authors are thankful to the reviewers and editor for their constructive comments which has added quality.

References

Akbari, B. Tavandashti, M.P. and Zandrahim, M. (2011). *Iranian Journal of Materials Science & Engineering*, 8(2), 48-56.

Choi, S.U.S (1995). FED-Vol.231/MD-Vol-66, 99-105.

Duffie, J.A., and Beckman, W.A. (1980). Solar Engineering of Thermal Processes, New York, John Wiley & Sons.

Eastman, J.A., Choi, S.U.S, Thompson, L.J., and Lee S. (1997). Materials Research Societ, Symposium-Proceedings, 457, 3-11.

Eastman, J.A., Choi, S.U.S., Li, S. Yu, W. and Thompson, J. (2001). , *Applied Physics Letters,* 78(6), 718-720.

Ganguly, S., Sikdar, S. and Basu, S. (2009). *Powder Technology*, 196, 326-330.

Mukherjee, S. and Paria S. (2013). *IOSR JMCE,* 9(2), 63-69.

Otanicar, T.P., and Golden J.S., (2009). Comparative Environmental and Economic analysis of conventional and nanofluid solar hot water technologies, *Environ Sci Technol*, 43, 6082-6087.

Said, Z., Saidur, R., and Rahim, N.A, (2014). *International Communications in Heat and Mass Transfer*, 59, 46-54.

Shima, P.D. Philip, J. and Baldev R. (2009). , *Applied Physics Letters*, 95,133112.

Taylor, R.A., Phelan, P.E., Otanicar, T.P., Arvind, R., and Prasher, R. (2011). *Nanoscale Research Letters* 6:255.

Thangavelu, K., Annamalai, R., and Arulnandhi, D. (2013). *IJETAE*, Vol. 3, 636-639.

Zhu, H., Lin, Y. and Yin Y (2004). Journal of Colloidal & Interfacial Science, 227, 100-103

Received 17 May 2014; revised 6 November 2014

Dynamic performance improvement of wind farms equipped with three SCIG generators using STATCOM

Othman Hasnaoui

Mehdi Allagui
University of Tunis El Manar, LSE-ENIT, Tunis Tunisia
University of Tunis, ENSIT-DGE, Tunis, Tunisia

Abstract
The main causes of wind farms disconnection from the grid is the three-phase grid faults at the point common coupling (PCC) e.g. the voltage dip. The use of a Static Synchronous Compensator (STATCOM) which is from the family of Flexible AC Transmission System (FACTS) devices can be used effectively in a wind park based on FSIG to provide transient voltage and to improve wind system stability. Due to the asynchronous operation nature, system instability of wind farms based on FSIG (Fixed Speed Induction Generator) is largely caused by the reactive power absorption by FSIG because due to the large rotor slip during grid fault. STATCOM contributes to control the grid voltage at PCC and maintain wind farm connection to the grid during some severe conditions of grid faults and used for power flow control and for damping power system oscillations. The evaluation of this control strategy using (STATCOM) is investigated in terms of regulation reactive power and transient stability of the wind farm during grid disturbances.

Keywords: wind farm, grid code, STATCOM, voltage dips

1. Introduction

During the present energy crisis, renewable energy sources have emerged as the most preferable alternatives for generating electric power. Presently, wind energy is the most developed of the renewable technologies due to the massive number of wind turbines that are installed around the world, as well as many projects currently in progress. In the past, power production through wind turbines did not have any severe effects on the wind power system, but now it actively involved in the grid because the wind power penetration level is increasing quickly with the different used technologies.

One of the important fields of investigation of wind energy systems is their stability issue when they are connected to the grid. In the past, wind turbines were disconnected during faults on the grids, but this led to dynamic instability and blackouts (Mukund, 2006) to maintain wind turbines connected to the grid, ride through the problems, without disconnection from the grid. Two of the strategies objectives are reactive power control in normal operation case and Low fault ride-through capability during grid fault case (Allagui *et al.,* 2014).

The primary role of normal operating requirements is to maintain the voltage between the two is qualified for security and energy quality limits. Given reactive power can be transmitted long distance, it must be provided locally (Jayam, 2009). So in grid specifications connection farms turbines are generally required to contribute to reactive power (and sometimes voltage) control (Kadam *et al.,* 2014). The opportunities for large-scale integration of wind appear, and the need of a contribution to the stability of the system was recognized in low voltage demands and most requirements for grid connection to the present-day (Review of Grid Codes, 2011). The majority of existing wind parks using the induction machine with fixed speed. These generators consume significant quantities of reactive power from the grid to magnetize their stator.

For the reason that this specified generator cannot supply adaptable reactive power (Tsili *et al.,* 2009) it needs the support of external loops 'FACTS' as that Static Synchronous Compensator 'STATCOM' to ameliorate the stability of the power system operation so as to stay connected during grid faults.

The connection of a largest wind farm will usually be a connection agreement between the proprietors of the wind park and the grid. The connection agreement sets specific technical requirements to be met by the wind park e.g. Fault ride through capability (Sedighizadeh *et al.,* 2010).

2. Wind turbine and electronic models

The mathematical relationship for the extracting of mechanical power from wind may be given by:

$$P_t = \frac{1}{2} \cdot \rho \cdot \pi \cdot R^2 \cdot V^3 \cdot C_p(\lambda, \beta) \quad (1)$$

Where P_t is the established power from the wind, ρ is the air density [kg/m3], R is the blade radius [m] and Cp is the power coefficient, which depends on both the tip transmission ratio λ and the blades angle of inclination, β [deg]. A general equation used to model C_p (λ, β), based on the modelling turbine characteristics is given by:

$$\left(\chi_2\left(\frac{1}{\lambda+0.08\beta}-\frac{0.0035}{\beta^3+1}\right)-\chi_3\beta-\chi_4\right)\varepsilon^{-\chi_5\left(\frac{1}{\lambda+0.08\beta}-\frac{0.0035}{\beta^3+1}\right)}+\chi_6\lambda \quad (2)$$

Where the coefficient C_1 to C_6 are constants:

$$\chi_1 = 0.5176 \quad \chi_2 = 116 \quad \chi_3 = 0.4$$
$$\chi_4 = 5 \quad \chi_5 = 21 \quad \chi_6 = 0.0068$$

And

$$\frac{1}{\lambda_i} = \frac{1}{\lambda+0.08\beta} - \frac{0.035}{1+\beta^3} \quad (3)$$

In this level, the pitch control is disabling and the pitch angle Beta (β) is set to 0°. When the wind speed exceeds its rated value, the rotor speed cannot be controlled within the limits by growing the generator or the converter. In this case, the pitch strategy is operated to raise the pitch angle to decrease the mechanical power output (Appala Narayana *et al.,* 2013).

The Cp-λ curves are shown in Figure 1 for different values of Beta.

In order to generate power, the induction speed must be slightly greater than the synchronous speed, but the speed variation is typically so low that WTIG is considered to be an affixed speed wind generator (Elsady *et al.,* 2010).

3. The stability of induction generators

The normal operation point is achieved when cutting the mechanical torque of the electric torque curve. Assuming condition of the generator, the generator will speed up during fault in the power

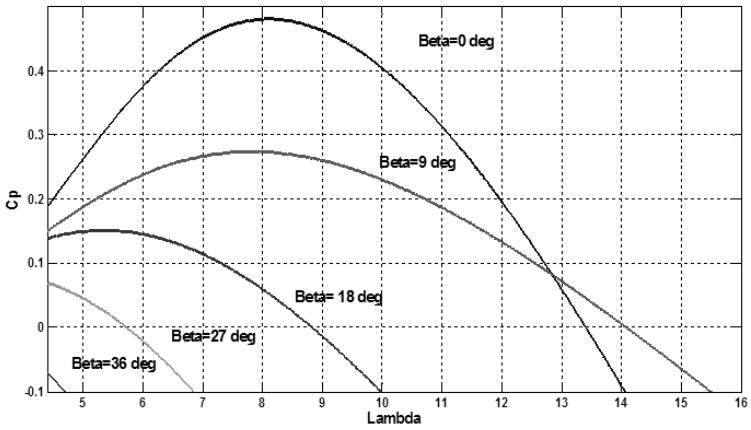

Figure 1: CP-λ curves for different pitch angles

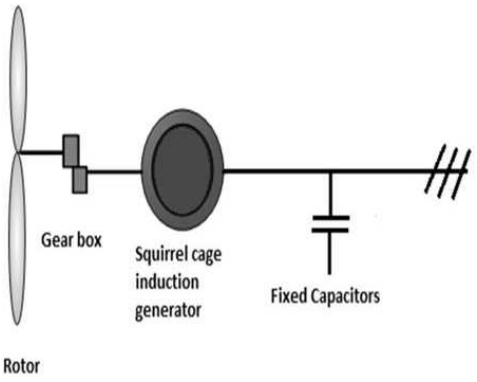

Figure 2: Wind turbine and induction generator

system in accordance with the next equation of movement:

$$\frac{d}{dt}\omega_m = \frac{1}{2H} \cdot (T_m - T_e) \quad (4)$$

A typical torque-speed static characteristic of an induction machine is presented in Figure 3.

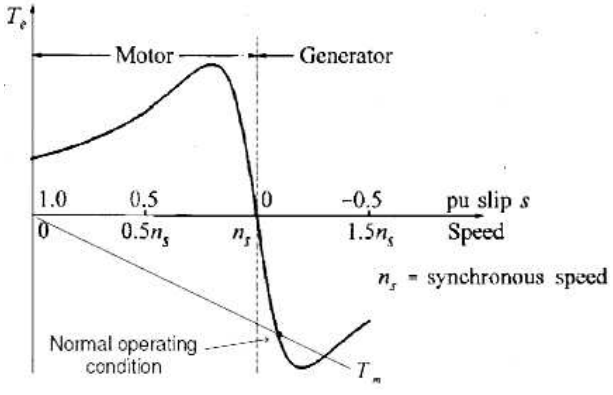

Figure 3: Typical torque-speed characteristic of an induction machine
(Paulo Fischer et al., 2005)

During the grid faults in the power system, T_m is the mechanical torque almost unchanged; in con-

trast, the electrical torque will drop because the electrical torque is proportional to the square of the voltage. This means that the speed allowed in depends on the inertia constant H of the generator, the fault duration and severity of the fault (Paulo Fischer *et al.,* 2005; Jahangir Hossain *et al*., 2010).

To improve the transient voltage stability and therefore help the wind during grid faults, an alternative is to utilize dynamic reactive power compensation such as a STATCOM as considered in this study.

4. STATCOM

4.1 STATCOM operation

The STATCOM is a FACTS controller that can be treated as a solid-state synchronous condenser connected in shunt with the AC system. The output current of this controller is adjusted to control either the nodal voltage magnitude or reactive power injected at the bus. STATCOM is a new breed of reactive power compensators based on VSC as shown in Figure 4. It has a characteristic similar to a synchronous condenser, but because it is an electrical device it has inertia and it is superior to the synchronous condenser in several ways (Wei, 2007). Lower investment cost, lower operating and maintenance costs and better dynamics are big advantages of this technology (Zhang *et al.*., 2006).

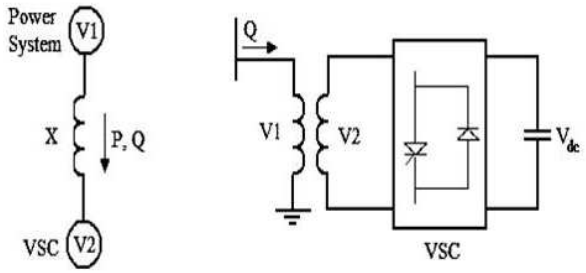

Figure 4: Schematic representation of working principle of STATCOM
(Jernej, 2012)

With the VSC voltage and the bus voltage, the output of the VSC can be expressed as follows:

$$\begin{cases} P = \dfrac{V_1 V_2}{X}\sin\delta \\ Q = \dfrac{V_1 V_2}{X}\cos\delta - \dfrac{V_1^2}{X} \end{cases} \quad (5)$$

where P and Q are respectively the active and reactive power of the VSC. V1 and V2 are the bus voltage and VSC voltage respectively. X is the reactance of the coupling transformer and δ is the phase difference between the voltage V1 and V2 (Noureldeen, 2009). The assumption that no active power shall be traded between STATCOM and the gate (operation without loss) for the voltage the controller is consistent with the voltage. If the amplitude of the compensation voltage is lower than the voltage at the connection node, the current flows from the gate of STATCOM (Ilyas *et al.,* 2014). In such cases, reactive power is consumed. If reverse is true for the reactive power, it is delivered to the gate.

4.2 STATCOM model

The following equations describe the STATCOM modelling, shown in Figure 5:

$$\bar{V}_{sh}^{(d,q)} = V_{shd} + jV_{shq} = v\cos\theta + jv\sin\theta \quad (6)$$

$$v = m * U_{dc} \quad (7)$$

With m: modulation index.

The model of STATCOM through a conversation on the axes d and q equations in the following voltages and currents are found:

$$V_d - mU_{dc}\cos\theta = R_{sh}I_{shd} + L_{sh}\frac{dI_{shd}}{dt} - L_{sh}.\omega.I_{shq} \quad (8)$$

$$V_q - mU_{dc}\sin\theta = R_{sh}I_{shq} + L_{sh}\frac{dI_{shq}}{dt} - L_{sh}.\omega.I_{shd} \quad (9)$$

In this case, when the harmonics and switching losses are neglected, Psh is given by the following equations:

$$P_{sh} = \frac{3}{2}(V_{shd}I_{shd} + V_{shq}I_{shq}) \quad (10)$$

$$U_{dc}I_{dc} = \frac{3}{2}(V_{shd}I_{shd} + V_{shq}I_{shq}) \quad (11)$$

The dynamic model of SATCOM is shaped in following matrices:

$$\frac{d}{dt}\begin{bmatrix} I_{shd} \\ I_{shq} \\ U_{dc} \end{bmatrix} = \begin{bmatrix} \dfrac{-R}{L_{sh}} & \omega & \dfrac{-m}{L_{sh}}\cos\theta \\ -\omega & \dfrac{-R}{L_{sh}} & \dfrac{m}{L_{sh}}\sin\theta \\ \dfrac{3}{2}\dfrac{m}{C}\cos\theta & -\dfrac{3}{2}\dfrac{m}{C}\sin\theta & -\dfrac{1}{R_c C} \end{bmatrix}\begin{bmatrix} I_{shd} \\ I_{shq} \\ U_{dc} \end{bmatrix} + \begin{bmatrix} \dfrac{1}{L_{sh}} & 0 \\ 0 & \dfrac{1}{L_{sh}} \\ 0 & 0 \end{bmatrix}\begin{bmatrix} V_d \\ V_q \end{bmatrix} \quad (12)$$

When the resistor Rc represents the losses of the converter, which may be significant, according to the number of switches and the switching frequency (Campos, 2004).

For this study we will neglect the phase angle θ.

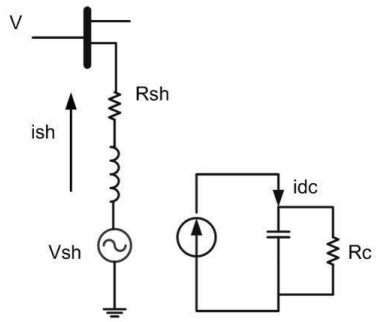

Figure 5: STATCOM model

4.3 Control scheme of the STATCOM

The reactive power exchange of STATCOM with the ac system is controlled by regulating the output voltage amplitude of VSC. The AC terminals of VSC are connected to the point of common coupling (PCC) through the leakage inductance of the coupling transformer (Allagui *et al.,* 2013).

Reference currents are obtained from the powers desired in Figure 6.

$$\begin{bmatrix} I^*_{shd} \\ I^*_{shq} \end{bmatrix} = \frac{2}{3}\frac{1}{V_d^2+V_q^2}\begin{bmatrix} V_d & -V_q \\ V_q & V_d \end{bmatrix}\cdot\begin{bmatrix} P^*_{sh} \\ Q^*_{sh} \end{bmatrix} \qquad (13)$$

The current reference on the axis d and q are obtained from a linear controller type Proportional integral (PI). The control of power is carried out by controllers that are set so to ensure proper servo line currents hand report their values. Indeed, the use of two PI controllers is required (Allagui *et al.,* 2014). Then the controllers inject a voltage (Vshd, Ishq) (Paulo Fischer *et al.,* 2005). The cross-coupling terms between the d and q axes whether (+ω Ishq, –ω Ishd) are detected. Those cross-coupling terms are as see in Figure 7 are subjoined to the PI controllers as feed-forward expression. To regulate the DC voltage of the outer control loop to its constant value a PI controller is used.

This method is investigated from equations (14) (15) (16).

$$\frac{d}{dt}\begin{bmatrix} I_{shd} \\ I_{shq} \end{bmatrix} = \begin{bmatrix} \frac{-R_{sh}}{L_{sh}} & \omega \\ -\omega & \frac{-R_{sh}}{L_{sh}} \end{bmatrix}\cdot\begin{bmatrix} I_{shd} \\ I_{shq} \end{bmatrix} + \frac{1}{L_{sh}}\begin{bmatrix} V_d - V_{shd} \\ V_q - V_{shq} \end{bmatrix} \qquad (14)$$

$$\frac{1}{L_{sh}}\begin{bmatrix} V_d - V_{shd} \\ V_q - V_{shq} \end{bmatrix} = \begin{bmatrix} X_1 \\ X_2 \end{bmatrix} \qquad (15)$$

$$\begin{cases} X_1 = (K_p + \frac{K_i}{s})(I_{shd}{}^* - I_{shd}) - \omega I_{shq} \\ X_2 = (K_p + \frac{K_i}{s})(I_{shq}{}^* - I_{shq}) + \omega I_{shd} \end{cases} \qquad (16)$$

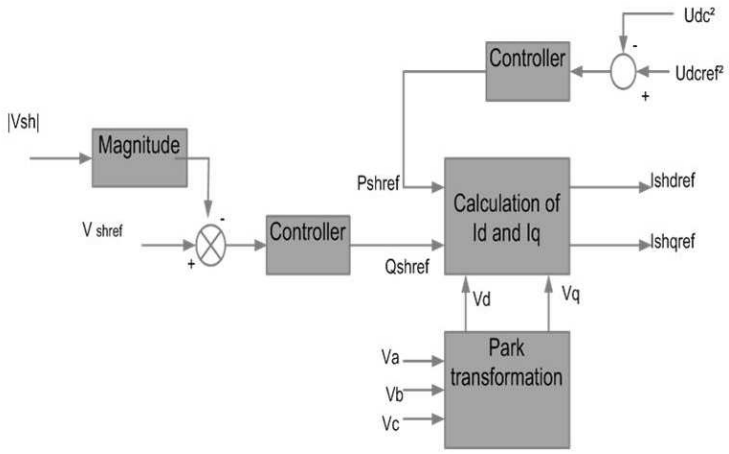

Figure 6: Block diagram of currents references controller

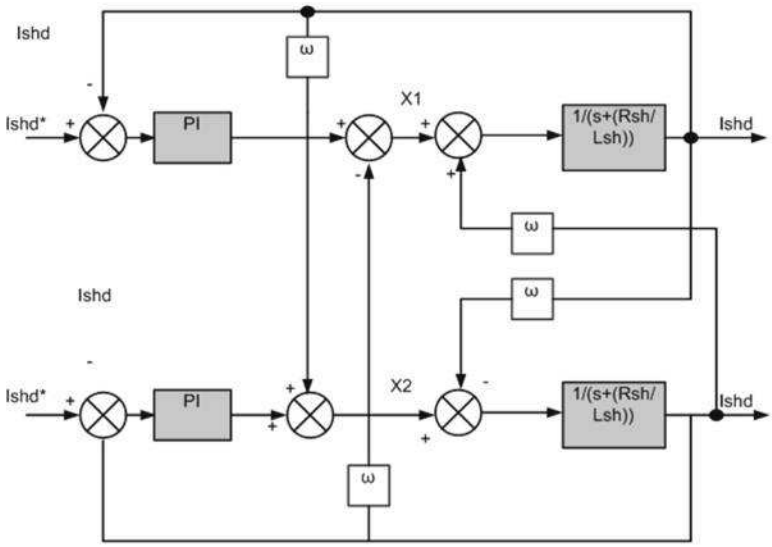

Figure 7: the Watt- Var decoupled contro

The STATCOM control strategy used in this paper is shown in Figure 8.

For synchronizing the output of the full scale converter of wind turbine, a Phase Locked Loop

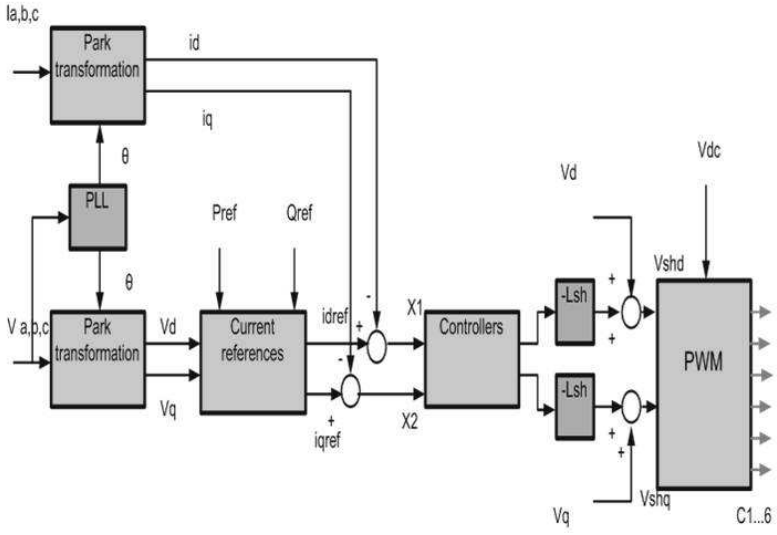

Figure 8: General control scheme of STATCOM

(PLL) algorithm is used. For Park transformation, the information about the angle of grid voltage is required. It is determined by a Phase Locked Loop (PLL) algorithm. This algorithm is very important because it makes synchronization with the grid possible. A change of the angle of grid voltage through time gives us the information about grid frequency f (Teodorescu *et al.,* 2006; Jernej, 2012).

5. Studied system and results

The wind farm is organized into a grid consisting of three units for the wind turbine as describe in Figure 9. Each of these wind turbine units is equipped with a rotor, gearbox, squirrel-cage induction generator, a 400 KVAR fixed capacitor banks; applied for the reactive power compensation; connected at each unit a low voltage bus (25-Kv) which presented the main bus of the investigated wind park. The wind farm is connected to the 120-kV transmission through a 25 km 25-kV grid voltage. The studied power system is simulated using Simulink Matlab software package.

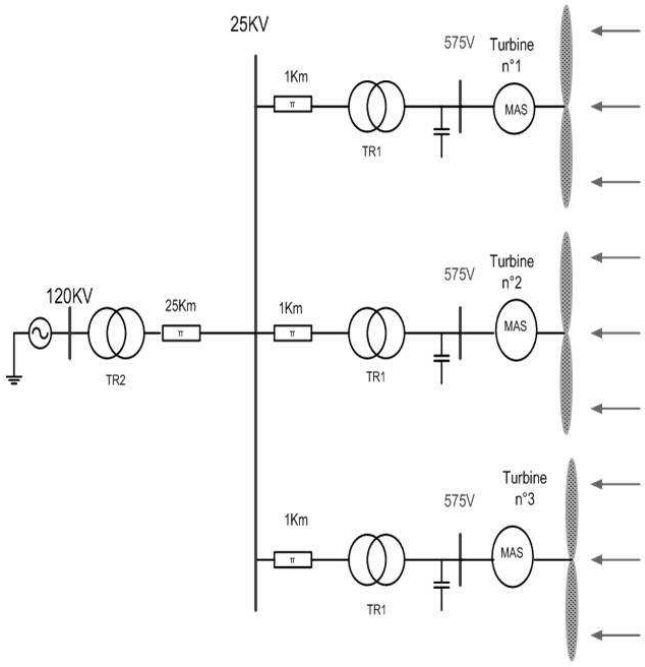

Figure 9: Test system

In this paper, the simulated disturbance is shown in Figure 10 starts at the seventh second, for 150 ms duration. According to the studied required grid code E.ON Netz, which clarifies the minimum voltage dip level and the profile of maximum duration of the occurrence, for which the production is obliged to remain 'online' are specified as described in Figure 11 (Margaris *et al.,* 2007; Noureldeen, 2011; Hasnaoui *et al.,* 2008).

To study the effect of STATCOM, the operation of the wind farm is monitored twice. The one is without STATCOM and the other with STATCOM connection at the main bus 25 of the wind farm.

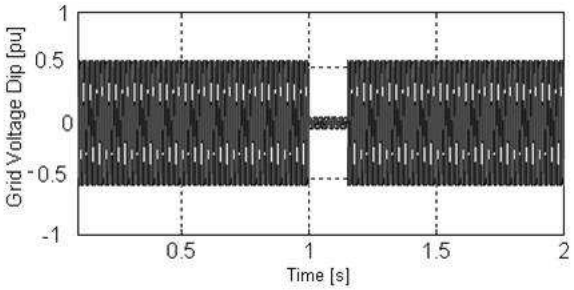

Figure 10: Behaviours of grid voltage dip

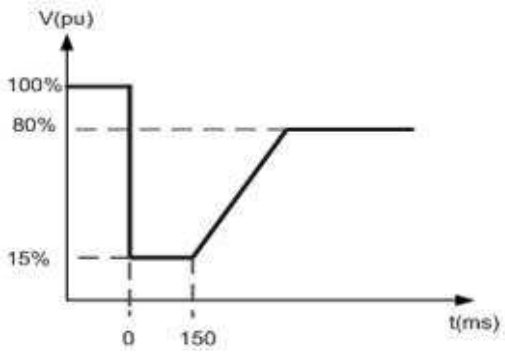

Figure 11: Voltage profile according to the requirements of LVRT capability of wind turbine according to E.ON Netz, 2006

5.1 Steady state results

When the generator is accelerated to the synchronous speed, 1200 rpm (1pu), the circuit breaker is closed and the generator is directly connected to the grid. The simulated waveforms for the generator are illustrated in Figure 12, where the system is simulated at the rated wind speed for the turbine which is 9 m/s. During the transitional system, a high inrush currents empties into the generator and a DC offset current appears in every of the stator currents isa, isb and isc, but the sum of these currents is zero compensated due to a balanced three-phase system. Such as a rotating magnetic range is designed and the core is magnetized by the generator stator current, an electromagnetic torque Te is produced.

It can be noticed that after the direct connection to the grid, the active power will exceed its nominal value and reach its maximum value .The wind turbine generates active power at a steady state -2.915 MW, reactive power of 1.47 MVAR. It reached the steady state after 2.15 s from the time of direct connection to the grid.

5.2 Disturbance state results without STATCOM connection

In this case, the protection system uses the circuit breaker if this grid faults lasts longer than 150 ms.

It is obvious that the wind turbine (MW 3) is activated when it senses a failure of wind reactive power support. Due to the lack of reactive power and the electrical torque in a wind turbine starts to speed up induction as illustrated in Figure 14.

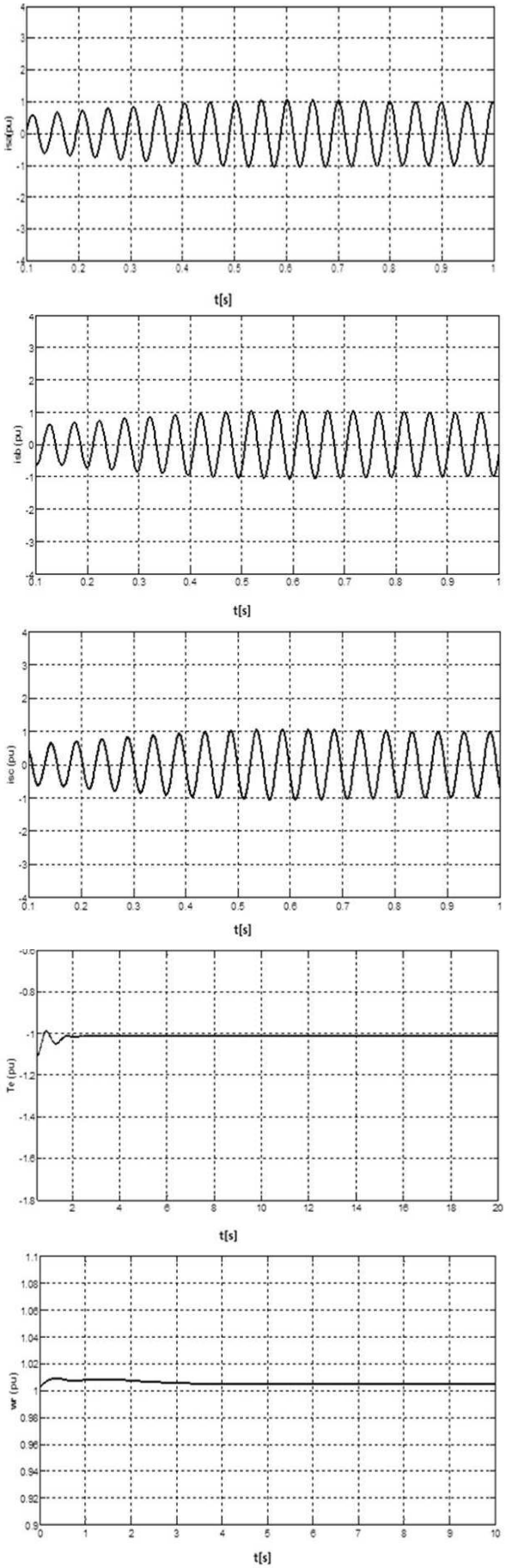

Figure 12: Dynamic behaviours of SCIG with direct grid connection

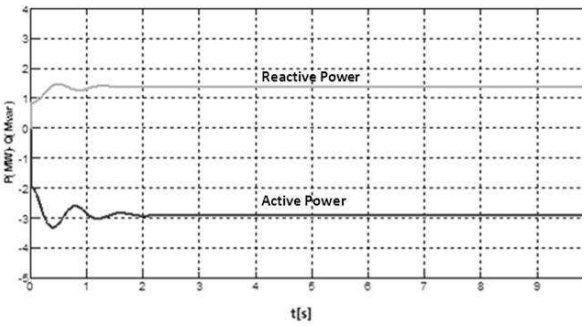

Figure 13: Response of active and reactive powers

Without STATCOM, the total produced active power during a grid fault decreased and drops to zero where the protection system trips the wind farm.

5.3 Results with STATCOM connection during grid fault

STATCOM delivers to the wind farm a reactive power and supports the grid voltage and providing the required power to the grid fault.

When connection of 30 MVAR STATCOM, the wind park remains in normal operation and the wind system restores back to initial state after duration of post-disturbance period. On the other side, in case of 3 MVAR STATCOM the delivered reactive power to the grid is still decreased to zero and the wind system is disconnected from the grid using the protection systems.

6. Conclusion

Flexible AC Transmission System (FACTS) is one aspect of the power electronics revolution that happened in all areas of electric energy.

This paper investigates the using of the STATCOM which is one of the FACTS's family to support the fixed speed wind power plant in order to fulfil the required voltage-dip ride-through capability. An 85% Low Voltage Ride through LVRT for 150 ms on the grid side is studied based on E.ON grid code. It is applied to a 9 MW fixed speed wind farm connected grid. Simulation studies show that the studied SCIG wind farm cannot stay connected under the studied voltage dip without STATCOM connection to its terminal and, with low rating STATCOM, while through 30 MVAR STATCOM connection at the main bus of the studied wind farm, it can stay connected.

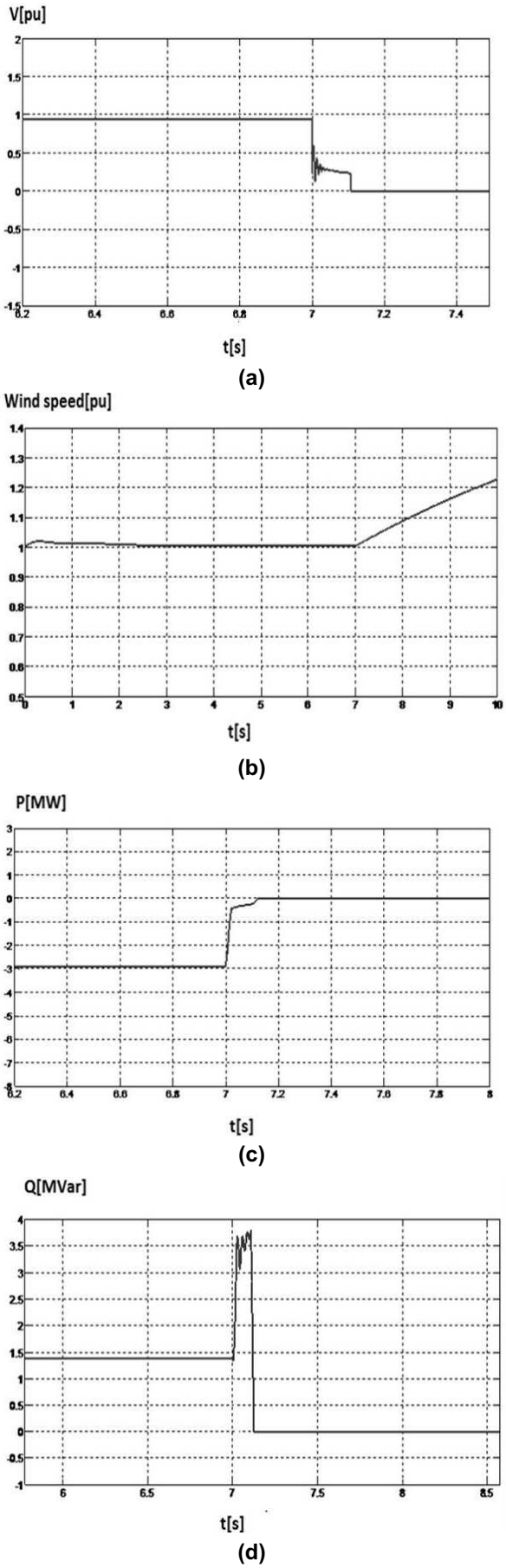

Figure 14: (a) Voltage at bus 25, (b) rotor speed, (c) Active power, (d) Reactive power

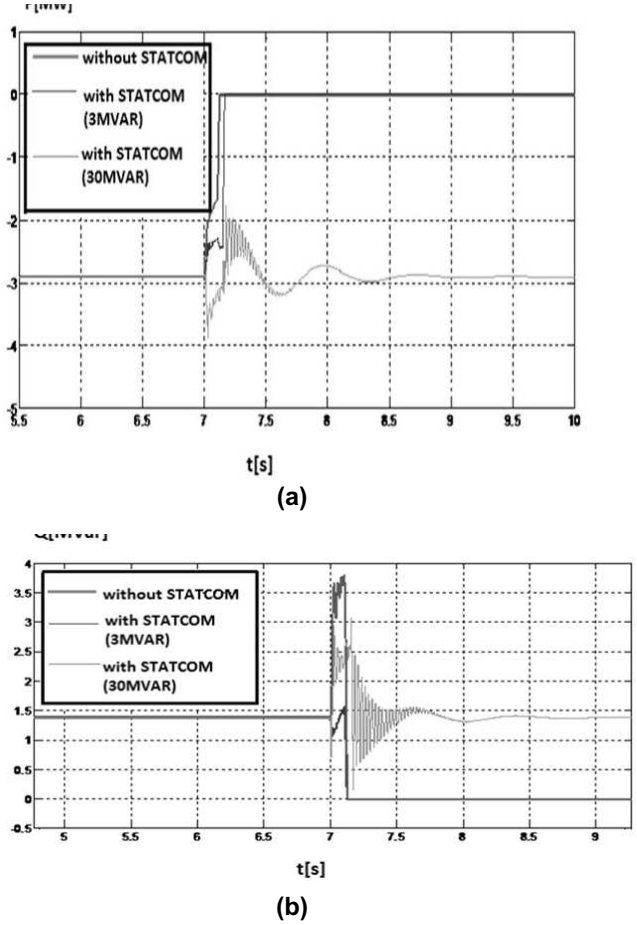

Figure 15: (a) Active power at B25 (b) reactive power at B25

Acknowledgment

This work was supported by the Tunisian Ministry of High Education, Research and Technology.

References

Allagui, M., Hasnaoui, O.B.K., and Belhadj, J. (2013). Exploitation of pitch control to improve the integration of a direct drive wind turbine to the grid, Journal of Electrical Systems, 9(2), 179-190.

Allagui, M., Hasnaoui, O.B.K., and Belhadj, J. (2014). A 2 MW Direct Drive Wind Turbine; Vector Control and Direct Torque Control Techniques Comparison, Journal of Energy of Southern Africa, 25(2), 117-126.

Appala Narayana, C.H., Ananth, D.V.N., Syam, K.D., Prasad, CH., Saibabu, SaiKiran, S., and PapiNaidu, T. (2013). Application of STATCOM for Transient Stability Improvement and Performance Enhancement for a Wind Turbine Based Induction Generator, International Journal of Soft Computing and Engineering (IJSCE) ISSN: 2231-2307, Volume-2, Issue-6.

Campos, F.G.R., and Penteado, A.A.Jr. (2004). Wind Energy generation Simulation with asynchronous generator connected to ENERSUL distribution System, IEEE/PES Transmission and Distribution conference and Exposition, Latin America, pp. 149-

154.
Elsady, G., Mobarak, Y. A., and Youssef, A-R, (2010). STATCOM for Improved Dynamic Performance of Wind Farms in Power Grid, Proceedings of the 14th International Middle East Power Systems Conference (MEPCON'10), Cairo University, Egypt, Paper ID 207.
E.ON Netz GmbH (2006). Netzanschlussregeln für Hoch- und Höchstspannung, Bayreuth.
Hasnaoui, O. BK., Belhadj, J., and Elleuch, M. (2008). Direct Drive Permanent Magnet Synchronous Generator Wind Turbine investigation: Low Voltage Ride Through capability,-Dynamic behaviour in presence of grid disturbance, Journal of Electrical Systems, 4(3).
Ilyas, M., and Ubaid Soherwardi, M., (2014). STATCOM_for_Improved_Dynamic_Performance_of_Wind_Farms in Power Grid, published in International Journal of Modern Engineering Research, IJMER.
Jahangir Hossain, M., Hemanshu, R. P., Valeri, A., Rodrigo, A. (2010). .Simultaneous STATCOM and Pitch Angle Control for Improved LVRT Capability of Fixed-Speed Wind Turbines, IEEE TRANSACTIONS ON SUSTAINABLE ENERGY, Vol. 1, No. 3.
Jayam, A.P. (2009). Improving the dynamic performance of wind farms with STATCOM, Bechtel Oil, Gas & Chem. Inc., Houston, TX Chowdhury, B.H. Published in, Power Systems Conference and Exposition.
Jernej, C. (2012). Laboratory prototype of a Static VAr compensator, XIV International PhD Workshop OWD.
Kadam, D.P., Kushare, B.E. (2014). LVRT Issue in Wind Farm System, International Research Journal of Sustainable Science & Engineering, IRJSSE / Volume: 2 / Issue: 1.
Margaris, I., Tsouchnikas, A., and Hatziargyriou, N. (2007). Simulation of Doubly Fed Induction Generator Wind Turbines, School of Electrical and Computer Engineering, National Technical University of Athens, Athens, Zografou 15780, Greece.
Mukund, R., (2006). Wind and Solar Power Systems Design, Analysis, and Operation, 2ND, New York: CRC Press Taylor &Francis Group.
Noureldeen, O. (2009). Characteristics of Fixed Speed Wind Turbines Interconnected Grid during Wind Speed Variations, 13th Middle East power systems conference MEPCON, Assuit University, Egypt.
Noureldeen, O. (2011). Low Voltage Ride through Strategies for SCIG Wind Turbines Interconnected Grid, International Journal of Electrical & Computer Sciences IJECS-IJENS Vol. 11 No: 02, Electrical Engineering Department, Faculty of Engineering, South Valley University, Qena, Egypte, 117502-6565 IJECS-IJENS.
Paulo Fischer, T., Hailian, X. (2005). Topic 7: Wind Farm in Weak Grids Compensated with STATCOM, KTH, KunglTekniskaHögskolan, EME departmentTeknikringen, 33-35, Stockholm, Sweden.
Review of Grid Codes, (October 2011). Wind Integration, International Experience, WP2.
Sedighizadeh, M., and Hosseini, M. (2010). Investigation and comparison of using SVC STATCOM and DBR's Impact on wind farm integration, International Journal of Engineering and Applied Sciences (IJEAS), Vol. 2, Issue 4, 38-54.
Teodorescu, R., Blaabjerg, F., Liserre, M., and Loh, P.C. (2006). Proportional-Resonant Controllers and Filters for Grid-Connected Voltage-Source Converters, Electric Power Applications, IEE Proceedings.
Tsili, M., and Papathanassiou, S., (2009). .A review of grid code technical requirements for wind farms, Renewable Power Generation, IET, Vol. 3, No. 3, pp. 308–332.
Wei, Q. (2007). Power Quality and Dynamic Performance Improvement of Wind Farms Using a STATCOM, Georgia Inst. of Technol., Atlanta Harley, and R.G. Published in: Power Electronics Specialists Conference.
Zhang, X.P., Rehtanz, C., and Pal, B., (2006). Flexible AC Transmission Systems: Modelling and Control, ISBN-13 978-3-540-30606-1, Springer-Verlag Berlin Heidelberg.

Received 25 July 2014; revised 24 November 2014

Deatils of authors

Mogamat-Fadiel Ahjum *BSc (Hons) (Physics) M Sc (Eng) (Sustainable Energy Eng.), Researcher, Energy Research Centre, University of Cape Town, Private Bag X3, Rondebosch, 7701, South Africa*
Tel: +27 21 650 2577
E-mail: mf.ahjum@uct.ac.za
Fadiel Ahjum is currently employed with the Energy Systems Analysis and Planning Group at the Energy Research Centre (ERC) since 2013. He is currently engaged in Water-Energy research utilising the TIMES modelling platform and contributes to the Group's annual Continuing Professional Development (CPD) energy systems modelling course. Other activities include ongoing refinement of the ERC's South African TIMES (SATIM) model – in particular the Synfuels and Industrial subsectors. Previous employment includes research and development in precision guided munitions at the Defence Science and Technology Organisation, Australia.

Mehdi Allagui *PhD student, High Engineering School of Tunis (ENSIT), Research at Electrical Systems Laboratory (LSE-ENIT)*
LR-SE-ENIT B.P 37 le Belvédère 1002 Tunis Tunisia
Tel: +216 52 842 062
E-mails: mehdieep@yahoo.fr and mehdi.allagui2@yahoo.fr
Mehdi Allagui was born in Tunis, Tunisia on March 1, 1982. He received (in 2005) his Master's degree from the Technical and Scientific High College of Tunis, and in 2009, his Master's from the same ESSTT, Tunisia. He is currently a teacher at the Technical College of Bizerte. Since 2010, he is a PhD student at ENSIT and prepared his PhD in Electrical Engineering and is part of the laboratory LSE-ENIT-electric system. He published 4 papers including 3 journal papers. His main fields of interest are the design, control and energy management of renewable energy systems.

Anthony Dane
Environmental Resources Management, 1st Floor, Building 32, The Woodlands Office Park, Woodlands Drive, Woodmead, 2148, Johannesburg, South Africa.
Tel: +27 76 636 6047
E-mail: Anthony.Dane@erm.com
Anthony Dane holds an M Com in Applied Economics (applications in development) from the University of Cape Town and a B Econ in Environmental Science and Economics from Rhodes University. Anthony has over six years of climate change and sustainability experience and has worked in the consulting sector, academia and the mining industry. He has deep skills and knowledge in strategy and policy development, greenhouse gas accounting (corporate footprint and national inventory development); climate change mitigation assessment; broader monitoring, reporting and verification (MRV); assessment of the socio-economic impacts of climate change mitigation actions; facilitation and complex decision-making; the energy-water nexus and general research.

Farzaneh Danesh
PhD candidate, Industrial Engineering, Tarbiat Modares University, Tehran, Iran
E-mail: farzaneh.daneshzand@yahoo.com
Farzaneh Daneshzand received the B.S. degree from Iran University of Science and Technology (IUST), in 2007 and an M.S. degree from Amirkabir University of Technology (Tehran Polytechnic), Iran, in 2009, both in industrial engineering. She is currently pursuing her PhD degree on energy planning systems in the Industrial Engineering Department of TarbiatModares University, Iran.

Thuli Dlamini
Cell: +27 (0)87 351 3057
E-mail: thulisile.dlamini@ipp-projects.co.za
Thuli Dlamini is a development economist, with a Master's Degree in Global Management and Development and currently pursuing an MPhil in Energy and Development Studies. Since 1994, she has worked in various capacities in the SADC region, particularly for regional organizations such as the SADC and SACU Secretariats in Botswana and Namibia. Currently, she is employed by the Department of Energy's IPP Office in the Economic Development Unit.

Basiru O Fatai *B Ed (Edu. Mgt/ Eco), M Sc (Eco)*
Doctoral Student at the Department of Economics, Faculty of the Social Sciences,
University of Ibadan, Nigeria.
Tel: +2348077944530
E-mail: bofatai@gmail.com
Basiru Fatai has a Master's degree in Economics, and is currently undertaking his PhD degree in Economics at the Department of Economics, University of Ibadan, Nigeria. He is the Research Assistant at the Trade Policy Research and Training Programme, Department of Economics, University of Ibadan.

Yang Han *PhD*
Department of Power Electronics, School of Mechanical, Electronic and Industrial Engineering, University of Electronic Science and Technology of China (UESTC),
No. 2006, Xiyuan Avenue, West Chengdu High-Tech Zone, Chengdu 611731, P. R. China
E-mail: hanyang_facts@hotmail.com
Dr Yang Han (S'08–M'10) received the PhD degree in Electrical Engineering from Shanghai JiaoTong University (SJTU), Shanghai, China, in 2010. He is currently a visiting scholar at the Department of Energy Technology, Aalborg University in Denmark. He is an Associate Professor with the University of Electronic Science and Technology of China, Chengdu, China. His research interests include smart grid control and analysis, grid-integration of renewable energy system, and power quality conditioners, voltage source inverters and multilevel converters for static var compensations (STATCOMs) and active power filters (APF) applications.

OthmanBk Hasnaoui *M Sc (Electrical systems) PhD (Electrical Eng.)*
Assistant Professor: Electrical Systems, Tunis National Engineering High School- University of Tunis; Electrical Systems Laboratory (LSE-ENIT)
PB 56 Montfleury, Tunis 1008, Tunisia
Tel: +216 98 363 242
Fax: +216 71 391 166
E-mail: othmanbk.hasnaoui@esstt.rnu.tn
OthmanBk Hasnaoui was born in 1955 in Tabarka, Tunisia. He received (in 1982) his M Sc degree from ENSET, Tunisia, and in 2010, his PhD degree from ENIT, Tunisia. Since September 1982, he has been with Tunis University, Tunis, where he is currently an Assistant Professor at the Electrical Engineering Department at Tunis National Engineering High School - University of Tunis and researcher at the Electrical Systems Laboratory (LSE-ENIT).
He is a regular reviewer of several conferences and journals. His main field of interest is the design, control and energy management of renewable energy systems: photovoltaic systems, large scale photovoltaic power plant, and electromagnetic compatibility.

Jennifer Patricia Holloway
Senior Statistician, Decision Support and Systems Analysis Research Group, Built Environment Unit, CSIR, PO Box 395, Pretoria, 0001, South Africa
Tel: 012 841 3305
E-mail: jhollowa@csir.co.za
Mrs Jennifer Holloway is Senior Statistician, Decision Support and Systems Analysis Research Group, Built Environment Unit, CSIR, Pretoria.

Tawanda Hove
Department of Mechanical Engineering, Faculty of Engineering, University of Zimbabwe, Harare, Zimbabwe
E-mail: Tawandahv@yahoo.co.uk
Tawanda Hove is a Senior Lecturer in the Renewable Energy Program, Department of Mechanical Engineering, University of Zimbabwe. He has accumulated a total of 26 years postgraduate experience, 18 years of which in university teaching and research in the areas of renewable energy, water engineering and project management. With background training in civil engineering, he has also worked a further 8 years as a civil/water/irrigation engineer for various governmental and non-governmental organisations. He has managed the successful implementation of several infrastructure development projects, implemented both in-house and contractor-based. He has published several articles in refereed international journals of note, and has also participated in contract research and consultancy related to solar energy system design, water supply infrastructure design and environmental impact assessment.

Rajangam Ilangovan
Assistant Professor, Department of Nanoscience and Technology, Alagappa University, Karaikudi, India
Rajangam Ilangovan is an Assistant Professor at Alagappa University, Karaikudi. He has completed his PhD in crystal growth and has 32 journal publications and 1 patent. He reviewed the Young Researcher award (IUMRS conference, I.I.Sc, Bangalore, India 1998), Young Scientist Award (ICCG-13 Conference, Doshisha University, Kyoto, Japan 2001), Science & Technology Agency (STA) Fellowship, Japan (2001-2003) through the Department of Science and Technology (DST), New Delhi, India .His area of interest include nanosensors, nanofluids, supercapacitors and Fe-RAM. He has 20 years of teaching and research experience.

Roula Inglesi-Lotz *B Com (Econ) M Com (Econ) PhD (Econ)*
Senior Lecturer, Department of Economics, University of Pretoria
Tukkiewerf Building, Office 1-13, University of Pretoria
Cnr Lynnwood and University Roads, Hatfield, 0083
Tel: +27 12 420 4504
Fax: +27 86 569 5811
Email: roula.inglesi-lotz@up.ac.za
Roula Inglesi-Lotz is an economist with particular interest in energy and environmental economics, economic growth and development as well as applications of time series and panel data econometrics. She completed her undergraduate studies at the University of Macedonia, Greece, and her Master's and PhD degrees at the University of Pretoria, South Africa. Currently, she is appointed as senior lecturer in the Department of Economics, University of Pretoria. Coordination of the Economics modules for first year students, supervision of postgraduate students and conducting research are included in her responsibilities. Since the beginning of her career, she has worked in numerous projects for various stakeholders such as Greenpeace, Eskom, the South African Department of Science and Technology, the World Intellectual Property Organisation (WIPO), WWF and others.

Vaibhav Jain
Department of Mechanical Engineering, National Institute of Technology, Kurukshetra, India
Flat no. 204, 3/126, Sector 5, Rajendra Nagar, Sahibabad-201005, Ghaziabad (Uttar Pradesh), India
Tel: +9198 68004700
E-mail: vaibhavursaathi@gmail.com
Mr Vaibhav Jain is research scholar at the National Institute of Technology, Kurukshetra. He received his B.E in Mechanical Engineering from VTU, Belgaum, in 2003, and his ME in Thermal Engineering from the University of Delhi, Delhi in 2009. He has published several papers in refereed journals and at international conferences. His area of interest is refrigeration and air conditioning.

S S Kachhwaha
Department of Mechanical Engineering, Pt. Deendayal Petroleum University, Gujarat, India
School of Technology, Pandit Deendayal Petroleum University, Raisan, District Gandhinagar - 382 007, Gujarat, India
Tel: +917 567622800
Email: Surendra.Singh@sot.pdpu.ac.in
Dr. S. S. Kachhwaha received his BE degree in Mechanical Engineering (1985) from M. B. M. Engineering College (University of Jodhpur) and his PhD in spray evaporative cooling from IIT, Delhi (1996). His research areas of interest are refrigeration and air conditioning, evaporative cooling, gas turbine cogeneration system, biodiesel and wind energy. He has published many papers in national and international journals. He has total teaching and research experience of 23 years.

Samantha Keen *M Phil*
Energy Research Centre, University of Cape Town, Private Bag, Rondebosch, 7701, South Africa
Tel: 021 650 2831
E-mail: samantha.keen@uct.ac.za
Samantha Keen is a researcher in the Energy, Environment and Climate Change Group, Energy Research Centre, University of Cape Town. In 2013, she completed a Master of Philosophy degree with her dissertation titled: The transport of pollutants over South Africa and atmospheric sulphur in Cape Town. She has four publications to her credit.

Renée Koen
Research Group Leader, Decision Support and Systems Analysis Research Group, Built Environment Unit, CSIR, PO Box 395, Pretoria, 0001, South Africa
Tel: 012 841 3045
Cell: 082 415 7880.
E-mail: rkoen@csir.co.za
Mrs Renée Koen is Research Group Leader, Decision Support and Systems Analysis Research Group, Built Environment Unit, CSIR, Pretoria, 0001. She is first author and author to whom all correspondence should be addressed.

M Kottaisamy
Professor, Department of Chemistry, Thiagarajar College of Engineering, Madurai, India
M Kottaisamy did his bachelor and master's degree in Chemistry and a PhD in Chemistry in the area of materials science. Since 1990, he is doing research in the area of developing materials for energy and environmental applications. Currently he is a professor in the Department of Chemistry, Thiagarajar College of Engineering, Madurai. He did his postdoc in the Opto-Smart laboratory, Shizuoka University, Japan. He worked as a young scientist in the Materials Science Research Centre, Indian Institute of Technology-Madras (IIT-Madras). He was awarded a young scientist fellowship by the Department of Science and Technology-SERC, Government of India for his research proposal on 'Development of phosphor converted white LEDs'.

Pieter J Krog *B Com (Hons) M Sc Energy and Sustainable Energy (Current).*
Master's student: Energy and Sustainable Development, Energy Research Centre, University of Cape Town, Upper Campus, Rondebosch
E-mail: pieterkrog@gmail.com

Pieter Krog is a final year master's student, studying toward the degree of Energy and Sustainable Development at the Energy Research Centre of Cape Town. His current research is focused on Sustainable Building Design. Pieter also acts as a consultant on various projects related to Energy and Climate Change. Pieter has an accounting undergraduate and postgraduate degree from the North West University, Potchefstroom Campus. After completing his accounting degrees, he spent several years in the private sector, specialising in auditing. After realising auditing wasn't his preferred field to work in, he commenced with his current master's programme in Energy and Sustainable Development. He hopes to someday be a leader in sustainable architecture. After completing his master's degree, he will commence with a bachelor of architecture at the University of Cape Town.

V Suresh Kumar *B Eng (EEE) M Eng (PS) PhD (PQ&H)*
Associate Professor: Electrical Engineering
Department Thiagarajar College of Engineering
Tiruparamkundaram, Madurai-625015,TamilNadu, India.
Tel: +91 452 2482240
Fax: +91 452 2482242
E-mail:vskeee@tce.edu
V Suresh Kumar graduated in Electrical & Electronics Engineering from Madurai Kamaraj University, India in 1994, and with a post-graduate qualification in Power Systems from the National Institute of Technology, Tiruchi, India in 1995. He then obtained his PhD in Power Quality & Harmonics from Madurai Kamaraj University in 2006. Dr. Suresh Kumar has carried out his post-doctoral research work at Northumbria University, Newcastle, UK (2010-2011). He has done four Sponsored Research Projects. He is a member of professional societies such as IEEE, IET, ISTE and Institution of Engineers India. He is an editor of publications for the International Journal on Renewable Energy Technology and International Journal of Soft Computing Applications in Engineering. He is a reviewer for IEEE Transactions on Industry Applications, IEE (IET) Transactions on Generation, Transmission & Distribution, International Journal of Energy Technology and Policy, International Journal of Global Energy Issues, and Korean Institute of Engineers.
Since 1997, he has been at the Faculty of Electrical and Electronics Engineering at Thiagarajar College of Engineering, Madurai, India, and currently works as an Associate Professor. He is an expert member in the All India Council for Technical Education AICTE, India. He has published 40 papers in national and international journals and conferences. His fields of interest include power quality and power electronics

Luxmore Madiye *B Tech (Mechanical Eng) M Sc (Renewable Energy) MZIE*
Department of Mechanical Engineering, Faculty of Engineering, University of Zimbabwe, PO Box MP 167, Mount Pleasant, Harare, Zimbabwe
E-mail: lmadiye@eng.uz.ac.zw
Luxmore Madiye has been a lecturer in the Department of Mechanical Engineering, University of Zimbabwe since 2006. He holds an MSc degree in Renewable Energy and B Tech (Hons.) in Mechanical Engineering. He previously worked in various capacities in the manufacturing and power generation industry since he graduated in 1993. His research interests are Renewable Energy and Power Plants.

Amos Madhlopa *M Sc (Eng) PhD*
Energy Research Centre, Department of Mechanical Engineering, University of Cape Town, Private Bag X3, Rondebosch 7701, Cape Town
Tel: +27 21650 3897,
E-mail: amos.madhlopa@uct.ac.za
Amos Madhlopa is in possession of a PhD in Mechanical Engineering and an MSc in Environmental Science, and has spent most of his working life at university institutions including the: Universities of Malawi and Strathclyde. At present, he is a Senior Researcher at the Energy Research Centre, University of Cape Town. His areas of interest include renewable energy technology development, energy efficiency, energy systems modelling, and rural energy provision.

Mascha Moorlach *M Sc (Building Engineering)*
Senior Research Officer: Energy Research Centre, Private Bag X3, Rondebosch, 7701, South Africa
Tel: +27 21 650 2825
Fax: +27 21 650 2830
E-mail: mascha.moorlach@uct.ac.za
Mascha Moorlach is a building engineer with a Master's degrees in physics from the built environment. Currently she is appointed as a Senior Research Officer at the Energy Research Centre at the University of Cape Town where she is part of the Energy Efficiency Group. She is also involved with measurement and verification for a diversity of energy efficient projects. She a board member of the Measurement and Verification Council of South Africa (MVCSA)

Downmore Musademba
Department of Fuels and Energy, School of Engineering Sciences and Technology, Chinhoyi University of Technology, Zimbabwe
E-mail: dmusademba@gmail.com
Downmore Musademba is a holder of an M Sc in Renewable Energy Engineering. He is a lead researcher in the following areas: base line and fea-

sibility studies, Evaluation of energy projects, Environmental impact assessments of Energy Projects, Economic Analysis of Energy Systems, and Renewable Energy & Energy Efficiency projects. He is currently Head of the Department of Fuels and Energy at Chinhoyi University of Technology, Zimbabwe.

Mohammad Reza Amin-Naseri

Associate Professor, Department of Industrial Engineering, Tarbiat Modares University, Tehran, Iran
E-mail: amin_nas@modares.ac.ir

Mohammad Reza Amin-Naseri is currently an associate professor of the Industrial Engineering Department at Tarbiat Modares University, Tehran, Iran. He received his PhD degree in Industrial and Systems Engineering from West Virginia University, WV, U.S.A., an M.S. degree in Operations Research from Western Michigan University, and a B.S. degree in Chemical and Petrochemical Engineering from Amir-Kabir University of Technology (Tehran Polytechnic). Dir. Amin-Naseri's research and teaching interests include optimization of various socio economic problems; especially energy planning and modelling, intelligent systems and their applications to forecasting and econometrics, meta-heuristics and their applications to various optimization problems.

Najmeh Neshat

PhD candidate, Industrial Engineering, Tarbiat Modares University, Tehran, Iran
E-mail: n.neshat@modares.ac.ir

Najmeh Neshat is an industrial engineer with a Master's degree in Industrial engineering from Sharif University of Technology. She is currently pursuing her PhD degree on energy planning systems in the Industrial Engineering Department of Tarbiat Modares University, Iran. Since 2005 she consulted to a variety of industry and public sectors in the fields of Industrial engineering and management. Neshat's research and teaching interests include energy systems planning and modelling, forecasting and econometrics, meta-heuristics and their applications to various optimization problems.

Arif M Ozgur *B Eng (Mechanical Eng) M Sc (Mechanical Eng) PhD (Mechanical Eng-Energy Division)*

Associate .Professor: Mechanical Engineering Department, Energy Division Dumlupinar University, Evliya Çelebi Campus, 43270, Kutahya, Turkey
Tel: +90 274 265 20 31 ext.:4102
Fax: +90 274 265 20 66
E-mail: arif.ozgur@dpu.edu.tr

Arif Ozgur is a mechanical engineer with a Master's degree and PhD in mechanical engineering. He has provided consulting services in energy investment to Turkish and European investors since 2005. He also has more than fifty national and international publications and has translated a book. Currently he is appointed as an associated professor at Dumlupinar University, Mechanical Engineering Department - Energy Division and he is also Vice Dean of the Engineering Faculty.

Sukumaran Lakshmi Priya

Sukumaran Lakshmi Priya has completed hers masters in materials science from TCE, Madurai. Her area of interest is nanofluids and their optical properties.

Gulshan Sachdeva

Department of Mechanical Engineering,, National Institute of Technology, Kurukshetra, 136119, Haryana, India
Tel. +919 812533221
Email: gulshansachdeva@nitkkr.ac.in

Dr. Gulshan Sachdeva did his BE from the National Institute of Technology, Kurukshetra in 2000. He completed his PhD in Computational Fluid Dynamics in 2010 from the same institution. His research areas are CFD, Refrigeration systems, Heat Transfer Enhancement. He has published many papers in International Journals. He is working as Assistant Professor in the Department of Mechanical Engineering at NIT, Kurukshetra.

G Sivasankar *B Eng (EEE) M Eng (PE &D)*

Assistant Professor: Electrical Engineering Department, Thiagarajar College of Engineering, Tiruparamkundaram, Madurai-625015, TamilNadu, India.
Tel: +91 452 2482240
Fax: +91 452 2482242
E-mail: g.sivasankar@live.in

G Sivasankar graduated in Electrical & Electronics Engineering from Madurai Kamaraj University, Madurai, India in 2002, and with a post-graduate qualification in Power Electronics and Drives from Anna University, Chennai, India in 2006. Since 2008, he has been at the Faculty of Electrical and Electronics Engineering at Thiagarajar College of Engineering, Tiruparamkundram, Madurai, India, and currently works as an Assistant Professor. From 2006 to 2008, he was at VIT University as Assistant Professor. He has published 10 papers in national and international conferences. His fields of interest include distributed generation, power quality, power electronics and drives.

Debbie Sparks *BSc (Hons) M Sc PhD (Cape Town)*

Senior Researcher: Energy Research Centre, University of Cape Town
Tel: +27 21 650 3753

Fax: +27 21 650 2825
E-mail: debbie.sparks@uct.ac.za
Dr Debbie Sparks is employed as a Senior Researcher at the Energy Research Centre, University of Cape Town. She works in the Energy, Environment and Climate Change Research Group, and is interested in climate adaptation issues and the nexus between water and energy. She is involved in teaching and co-ordinating the Energy and Climate Change Masters programme at the ERC. She also co-ordinates the mitigation component of the African Climate and Development Initiative's (ACDI) - Climate Change Adaptation and Mitigation Course.

Theodor Stewart *B Sc (Chem Eng) M Sc (Oper Res) PhD FRSSAf*
Professor Emeritus and Senior Research Scholar, Department of Statistical Sciences, University of Cape Town
Part-time Professor of Decision Science, Manchester Business School, University of Manchester
Tel: 021 650 3224
E-mail: theodor.stewart@uct.ac.za
Theodor Stewart trained initially in chemical engineering, and worked in that capacity in the mining and chemical industries from 1964-1971. He then joined the CSIR, Pretoria, where he moved into the field of operations research, with emphasis on problems of public sector planning, including defence, energy, water, fisheries and town planning. In 1984 he took up a chair in mathematical statistics (later to become statistical sciences) at UCT, with responsibility for developing OR activities there. His primary research interests are in the theory and applications of multiple criteria decision analysis (MCDA) and related areas of multiobjective optimization. He is Editor-in-Chief of the Journal of Multi-Criteria Decision Analysis, and has served as President of the International Society on Multiple Criteria Decision Making, and as Vice-President of the International Federation of Operational Research Societies. In 2013 he was awarded the Distinguished Service Medal of EURO (Association of Operational Research Societies in Europe).

A L Subramaniyan
Assistant Professor, Thiagarajar College of Engineering, Madurai, India
E-mail: alsubbu1@gmail.com
A.L. Subramaniyan holds a Bachelor's degree in Physics and a Master's degree in Solid state Physics from the University of Hyderabad. He has completed his Masters in Engineering with Materials Science specialisation from NIT, Trichy, India, and is currently pursuing his doctorate in Nanotechnology. His areas of interest include synthesis, characterisation and applications of nanofluids and nanosemiconductors. He is working as an assistant professor for the past 15 years and is currently employed with Thiagarajar College of Engineering, Madurai.

Lin Xu *PhD*
Sichuan Electric Power Research Institute, Sichuan Electric Power Company, State Grid Cooperation of China
No. 24, Qinghua Road, Qingyang District, 610072 Chengdu, China
E-mail: xulin198431@hotmail.com
Dr Lin Xu received the PhD degree in Electrical Engineering from Shanghai JiaoTong University (SJTU), Shanghai, China, in 2011. Currently, she is a Senior Engineer at Sichuan Electric Power Research Institute (EPRI), Chengdu, China. Her research interests include power system analysis and real-time digital simulator (RTDS), flexible AC transmission systems (FACTS), such as TCSCs, STATCOMs, and power quality conditioners (DVRs, APFs).

Index to Volume 25: February–November 2014

Authors / Title index

Subject index

Sponsored by the
Department of Science & Technology

This journal is accredited by the South African Department of Higher Education and Training for university subsidy purposes. It is abstracted and indexed in Environment Abstract, Index to South African Periodicals, and the Nexus Database System.

The journal has also been selected into the Science Citation Index Expanded by Thomson Reuters, and coverage begins from Volume 19 No 1. It is also on the Scientific Electronic Library Online (SciELO) SA platform and is managed by the Academy of Science of South Africa (ASSAf).

Annual subscriptions (four issues)
Individuals (Africa): R160 (single copy R51)
Individuals (beyond Africa): US$109 (single copy US$39)
Corporate (Africa): R321 (single copy R103)
Corporate (beyond Africa): US$218 (single copy US$77)

Cost includes VAT and airmail postage.
Cheques should be made payable to the University of Cape Town and sent to the address given below.

Enquiries may be directed to:
The Editor, Journal of Energy in Southern Africa,
Energy Research Centre, University of Cape Town,
Private Bag, Rondebosch 7701, South Africa
Tel: +27 (021) 650 3894 Fax: +27 (021) 650 2830
E-mail: Richard.Drummond@uct.ac.za

Website: www.erc.uct.ac.za

It is the policy of the Journal to publish papers covering the technical, economic, policy, environmental and social aspects of energy research and development carried out in, or relevant to, Southern Africa. Only previously unpublished work will be accepted; conference papers delivered but not published elsewhere are also welcomed. Short comments, not exceeding 500 words, on articles appearing in the Journal are invited. Relevant items of general interest, news, statistics, technical notes, reviews and research results will also be included, as will announcements of recent publications, reviews, conferences, seminars and meetings.

Those wishing to submit contributions should refer to the guidelines given on the inside back cover.